Durham University

Durham E-Theses

Estimations of Q from seismic Rayleigh waves

Burton, Paul W.

How to cite:

Burton, Paul W. (1973) *Estimations of Q from seismic Rayleigh waves*, Durham theses, Durham University. Available at Durham E-Theses Online: http://etheses.dur.ac.uk/9218/

Use policy

The full-text may be used and/or reproduced, and given to third parties in any format or medium, without prior permission or charge, for personal research or study, educational, or not-for-profit purposes provided that:

- a full bibliographic reference is made to the original source
- a link is made to the metadata record in Durham E-Theses
- the full-text is not changed in any way

The full-text must not be sold in any format or medium without the formal permission of the copyright holders.

Please consult the full Durham E-Theses policy for further details.

Academic Support Office, The Palatine Centre, Durham University, Stockton Road, Durham, DH1 3LE
e-mail: e-theses.admin@durham.ac.uk Tel: +44 0191 334 6107
http://etheses.dur.ac.uk

Estimations of Q from Seismic Rayleigh Waves

Paul W Burton B.A. (Cantab)

January 1973

DURHAM UNIVERSITY
SCIENCE
31 MAY 1973
SECTION
LIBRARY

This thesis is submitted for the degree of Ph.D. at the University of Durham and to the best of my knowledge no part of it has previously been submitted to this or any other university.

Paul W. Burton.

Paul W Burton
The Graduate Society
University of Durham

January 1973

ABSTRACT

The specific attenuation factor, Q_γ^{-1}, has been estimated from seismic Rayleigh waves in the frequency range 0.015-0.11 Hz. The 95% confidence limits determine a narrow region around all estimates.

The observational data consists of digitised Rayleigh wave traces from film chips of the long period vertical component instruments of the WWSSN stations. Events used are nuclear explosions in Novaya Zemlya, the Lop Nor region of China (Southern Sinkiang Province) and the Aleutian Islands.

The group velocity and spectral amplitudes are obtained for each seismogram using an improved "multiple filter technique". Q_γ^{-1} is estimated by a least squares regression fit to the subsequent amplitude-distance plots.

Values of Q_γ^{-1} are generally larger when determined from Novaya Zemlya (.004) than for the Lop Nor test site (.003). The largest values of Q_γ^{-1} (.009) are found at low frequencies (0.02 Hz), implying a zone of high dissipation in the upper mantle sampled by these frequencies alone.

The observed values of Q_γ^{-1} are directly inverted using an extended Monte-Carlo technique - "Hedgehog". This successfully inverted the data from Novaya Zemlya revealing a region of high dissipation coincident with the low velocity zone, although low velocity is not assumed. The inversion model shows $Q_\alpha^{-1} = .002$, $Q_\beta^{-1} = .0045$ for the uppermost 120 km and $Q_\alpha^{-1} = .007$, $Q_\beta^{-1} = .015$ ($Q_\alpha = 140$, $Q_\beta = 65$) in the absorption zone below 120 km.

ACKNOWLEDGEMENTS

Dr H I S Thirlaway and Professor M H P Bott have established a close liaison between the UKAEA Seismology Unit at Blacknest and the Department of Geology at the University of Durham. This liaison has allowed me to pursue these studies and write this thesis, and has given me the rare opportunity to see one objective from two viewpoints. I am very grateful to Dr H I S Thirlaway and Professor M H P Bott for giving me these opportunities.

Dr R E Long and Dr H I S Thirlaway supervised me for the three years. I am sincerely grateful to all the people who have helped me in many ways during this period, in particular I thank: Mr C Blamey, Mr A Douglas, Miss P K Eves, Mr E G Ford, Mr B L N Kennett and Mr J B Young.

My especial thanks are due to Mr P D Marshall who has tolerated all my questions and encouraged me with the answers and help at all times.

CONTENTS

Page

Too well I know these godlike ones.
They will that men believe on them,
and that doubt be held sin.

Friedrich Wilhelm Neitzche

INTRODUCTION

I.1 "Q"

The importance of Q is demonstrated by Knopoff's (1964) statement "Were it not for the intrinsic attenuation of sound in the earth's interior, the energy of earthquakes of the past would still reverberate through the interior of the earth today".

It is obvious that after an event has taken place the energy from it is gradually absorbed by the earth and converted into heat - this is a normal consequence of the non-elastic phenomenon of dissipative wave propagation. However the means and amounts of this dissipation are generally not known. The geophysicist is interested in knowing if certain areas of the earth are better or worse dissipators of seismic energy than others. Such information may throw light on the interior of the earth in terms of the chemistry and physics of materials and mechanisms at depth.

Any seismic wave is composed of a set of harmonics or a continuous range of frequencies (f). To quantify the amount of attenuation (dissipation) suffered by each harmonic we use the attenuation factor Q(f), or more sensibly we use the specific attenuation factor, Q^{-1}, because this is directly proportional to the amount of attenuation.

For a propagating monochromatic wave its attenuation may be described by an exponential function of the form:

$$D = \exp\left(\frac{-\omega}{2}\int_{t_1}^{t_2} \frac{dt}{Q}\right)$$

ω = angular frequency (radians/s)

t = travel time.

In terms of frequency, f, and assuming a phase velocity c we have

$$D = \exp\left(-\pi f \int_{x_1}^{x_2} \frac{dx}{cQ}\right)$$

$$= \exp\left(\frac{-\pi f X}{cQ}\right)$$

where X is the distance travelled.

DURHAM UNIVERSITY SCIENCE 31 MAY 1973 SECTION LIBRARY

In terms of a spatial attenuation coefficient, γ, we have the function $\exp(\gamma x)$ and so

$$\gamma = \frac{-\pi f}{cQ} \text{ km}^{-1}$$

If we were dealing with standing waves we would measure their amplitude at a point as it varies in time, essentially a damping factor of the form $\exp(\nu t)$ is determined. The Qs for the two possible types of experiment, Q_T for travelling or Q_s for standing waves, are not the same and Knopoff, Aki et al. (1964) have rigorously shown that

$$UQ_s = c\, Q_T$$

where U is the group velocity. In this work, unless specifically stated, Q_T is to be assumed.

From these equations it is clear that Q is dimensionless and a measure of the loss or attenuation per cycle of a wave, rather than a measure of loss with absolute distance as is the case for the attenuation coefficient γ. This is simply shown by expressing γ in terms of wavelength λ

$$\gamma = -Q^{-1} \frac{\pi}{\lambda} \text{ km}^{-1}$$

I.2 Q DETERMINATIONS IN THE LABORATORY

Observational data on Q usually falls into one of three categories:

1 Laboratory experiments on non earth materials

2 Laboratory experiments on earth materials

3 Experiments on the real earth

with the errors involved increasing from category to category.

For liquids Q^{-1} is found to be proportional to the frequency. Pinkerton (1947) plots $\frac{\gamma}{f^2}$ against frequency and the straight lines of zero slope which he obtains illustrate the result very well.

The attenuation coefficient, γ, for solids is usually found to be proportional to the frequency and hence values of Q^{-1} are frequency independent. This implies the theory of constancy of Q over all frequencies.

For example Peselnick and Zietz (1959) measured the Q of Solenhofen Limestone using compressional pulses in the frequency range 3-15 Mc/s and found it to be 110. More recent measurements by Mason and Kuo (1971) for Pennsylvania Slate over the frequency range .01-20 megahertz gave an approximately constant value.

The concept of constant Q is important because if it is accepted for the real earth then any deviation from "normal" Q will imply a change in substance, physical or chemical. But a distinction must be made between the Q of body waves and surface waves. Yamakawa and Sato (1964) state that body wave Q is a physical constant for a medium whereas surface wave Q depends on the physical properties and the structure of the medium. The Q of surface waves, like the velocity, may have an "apparent" frequency dependence simply due to the geometry of a layered structure.

Other people have investigated the joint problem of liquid and solid; Born (1941), has investigated sandstone with varying water contents. His pleasing results are that Q^{-1} becomes more frequency dependent as the water content increases. Q^{-1} is constant for the dry rock case, Figure I.1 is taken from Born's work.

The disadvantage of these experiments is that they are conducted at non-geophysical frequencies. We are really interested in the range .001 to 10 Hz.

I.3 Q MECHANISMS

Several mechanisms have been put forward to describe microscopic Q, and a good review paper is that of Jackson and Anderson (1970).

Some of the less successful mechanisms involve atomic diffusion and dislocation mechanisms. The better mechanisms seem to involve

1 partial melting

2 grain boundary relaxations and

3 a mechanism of "high temperature, internal friction background" (i.e. vacancy creation and diffusion) which obeys

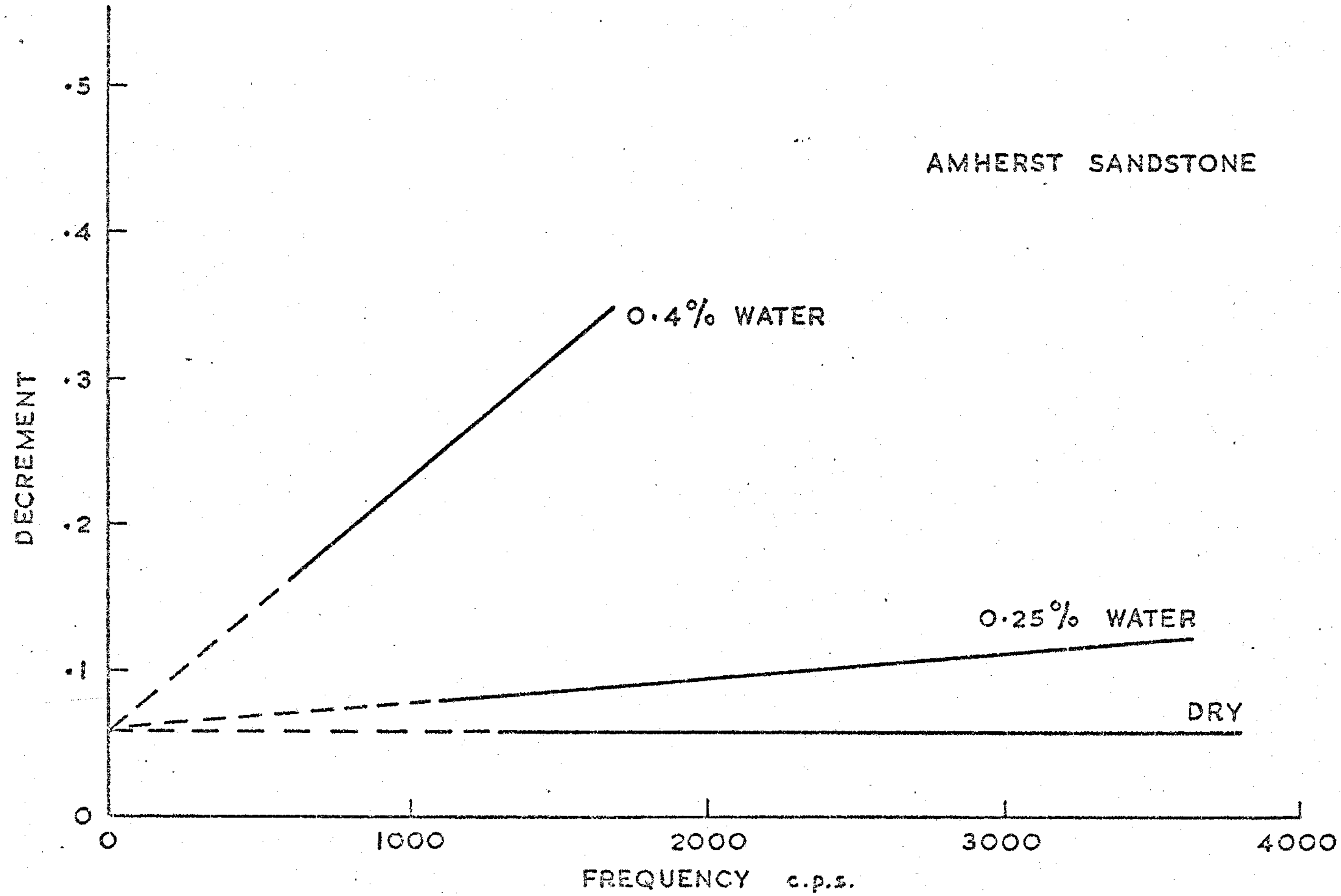

FIGURE I.1 SANDSTONE WITH VARYING AMOUNTS OF INTERSTITIAL WATER (BORN)
(LOG DECREMENT $\propto Q^{-1}$)

$$Q^{-1} = \frac{A}{f} \exp(-H/RT)$$

where H is the appropriate energy required for initiation and T is the absolute temperature. Note that for this mechanism $Q^{-1} \propto f^{-1}$.

Processes such as diffusion of dislocations and crystal point defects, fluid flow in pores and phase changes will act to relieve an applied stress - these are relaxation mechanisms. Energy is absorbed and then released during consecutive halves of a cycle and this energy transfer takes a finite relaxation time.

Zener (1948) has shown that if the rate of stress relief is proportional to stress for constant strain then each of the above processes creates an internal friction Q^{-1} of the form

$$Q^{-1} = \frac{M_u - M_R}{M_u} \quad \frac{f/f_p}{1+(f/f_p)^2}$$

M_u: "unrelaxed" elastic modulus

M_R: relaxed elastic modulus

f_p: constant of proportionality between stress and rate of stress relaxation.

If the mechanism is thermally activated then the relaxation times are pressure and temperature dependent. We would therefore expect the internal friction to vary with depth. Allowing for the effect of temperature on relaxation times alters the above expression for Q^{-1} to

$$Q^{-1} = \frac{M_u - M_R}{M_u} \quad \frac{\frac{f}{f_p} \exp(\frac{-H}{RT})}{1+(\frac{f}{f_p} \exp(\frac{-H}{RT}))^2}$$

However, it is not possible to state that one particular mechanism is entirely responsible for attenuation effects.

Also, a particular attenuation mechanism may be quite strongly frequency dependent - but if we consider a wide range of chemical and physical properties (for example grain and pore size within the earth) and a multi component, multi phase system then we may obtain a Q^{-1} which is only weakly frequency dependent. The earth's heterogeneity may average a Q mechanism to produce a predominantly frequency independent result.

I.4 Q DETERMINATIONS FROM THE REAL EARTH

Experimental measurements of Q for the real earth differ in their degree of directness and in the number of secondary effects which have to be considered e.g. reflection coefficients.

Body wave determinations of Q usually rely on the spectral ratios of two distinct seismic wave phases. If we take the spectral ratios for the phases (from the same event) P and the surface reflection pP for recordings at the same station then we have a Q_α dependent quantity. The difference between the two phases is caused mainly by the epicentre-hypocentre structure at the source and the loss of energy at the surface reflection. The surface reflection is an unwanted secondary effect which when taken into consideration is a source of error. Niazi (1971) used the technique to determine Q_α values for the upper mantle; his results have been criticised by Buchbinder (1972).

The phases PcP and P have been used to determine Q_α in the mantle. Ibrahim (1971) obtains the ratio PcP/P and chooses as the best Q values those which reduce the scatter in his data; the technique seems to be effectiv

The work of Kovach and Anderson (1964) produced values for Q_β using S waves reflected at the core mantle boundary; ScS, sScS, ScS_2, $sScS_2$ were observed and Q_β determined. The surface reflected waves allow distinct Q s to be determined for the upper and lower regions of the mantle, giving values of 200 and 2200 respectively.

Both of these last two methods assume coefficients of reflection and obtain Q indirectly by the comparison of two or more different phases of seismic energy. To determine the degree of attenuation directly it is necessary to observe the same wave at more than one point.

The surface waves from a large earthquake will travel round the earth several times before they are attenuated down to the noise level - hence they may be recorded more than once at the same station. The amplitude attenuation can then be easily measured from the two consecutive time series.

A disadvantage of this technique is the values of Q being determined for one very specific path. Kanamori (1970) made measurements for both Love and Rayleigh waves and found that Q differed considerably for differing great circle paths. His values for Rayleigh wave Q_γ are 180 ± 80 and for Love waves 110 ± 40, using Kurile Island earthquakes. A further disadvantage is that the period range is approximately 150-350 seconds, a range very much restricted to these large earthquakes. Such long periods are required for the method because shorter periods are attenuated rapidly with distance.

A different approach to the problem is given in the work of Carpenter and Marshall (1970). A nuclear explosion is used as the source of surface waves and assuming a circular radiation pattern the great circle technique need not be used. Instead, there are several recording stations around the event, but at different distances and a simple plot of amplitude against distance is obtained, which simply determines Q. This is discussed in more detail later.

A final important technique is the observation of the normal modes of oscillation of the earth. These are of long period and therefore contain information about the earth at depth. However such observations are made at two points in time, not space, and Q_s is determined for these standing waves.

All of these techniques have their particular difficulties. Body wave techniques involve the determination of reflection coefficients while surface wave measurements must necessarily lead to an inversion problem when a depth dependence for Q is required.

CHAPTER 1

1.1 The Amplitude of Rayleigh Waves

A general expression for the amplitude A(f) of a seismic Rayleigh wave (vertical component) in a layered medium is

$$A(f,r) = K.L(f,d).I(f).S(f).D(f,r).G(f,r) \qquad 1.1$$

f = frequency Hz

K = a constant

r = distance from source

L = amplitude response of layered medium (depth d)

I = instrument transfer function

S = source spectral function

D = absorption term

G = geometrical spreading correction.

This Rayleigh wave amplitude A(f) is expressed in the frequency domain (Toksoz, Ben-Menahem and Harkrider 1964); the amplitude A(t) observed on the seismogram is similar to the above expression except the terms are convolved and not multiplied.

Carpenter and Marshall considered the time domain problem for an expanding pressure pulse as source. Their work shows that for measurements of period, T, made directly from the seismogram that

$$A(T) = K' \, U(dU/dT)^{-1/2} \, (\Delta^{-1/2} \sin^{-1/2}\Delta) \, \exp\left(\frac{-\pi E\Delta}{QUT}\right) \qquad 1.2$$

where E is the radius of the earth and Δ the angular distance of travel. This may be rewritten as

$$A(T) = K'' \left[(E \sin \Delta)^{-1/2} \right] \left[U\left(E\Delta\frac{dU}{dT}\right)^{-1/2} \right] \exp\left(\frac{-\pi E\Delta}{QUT}\right) \qquad 1.3$$

where the term in $(E \sin \Delta)^{-1/2}$ takes account of geometrical spreading, and not $\Delta^{-1/2}\sin^{-1/2}\Delta$ implied by equation 1.2. The term $U(E\Delta\frac{dU}{dT})^{-1/2}$ arises because the stationary phase approximation has been used to determine the far field Rayleigh wave shape in the time domain from a frequency domain formulation. Their measurements were confined to the apparent period (the time between successive peaks) and the amplitude for that period, these are strictly time domain measurements.

1.2 The Time or Frequency Domain?

The question of relative merit of data representation in the time or frequency domain appears trivial (because both forms are just different representations of the same data), but it is important. There are definite advantages to be gained by working in the frequency domain.

We have to consider the effect of instrumentation. The instrumental response is inherently a frequency domain description. We may consider an input in the time domain to an instrumental "black box" filter and observe its output, but to appreciate the change in waveform, and correct for it, we require a set of magnifications at the different frequencies and the corresponding phase delays. Correction with these values is simple division, the alternative is a lengthy time domain deconvolution process.

Also, the apparent periods measured in the time domain are forced upon us by the individual record, and more likely than not, they are not directly comparable between one record and the next. Worse than this, when an apparent period is measured and a value assigned, say 15s, we are not certain how many periods are compounding to that waveform. A nominal value of 15s may easily cover the true range 12-19s. To correct for this partial dispersion it is necessary to apply the stationary phase correction, and to accept that the earth is not a perfect Fourier filter.

The stationary phase approximation generates a term for correcting amplitudes measured from a time series which is of the form

$$U.R^{-\frac{1}{2}} \left(\frac{dU}{dT}\right)^{-\frac{1}{2}} T^{-1} \qquad 1.4$$

where R is the distance travelled and equal to $E\Delta$. For a particular type of explosion, underground or atmospheric, this term is further modified in its T dependence and becomes in both cases

$$U.R^{-½} \left(\frac{dU}{dT}\right)^{-½} T^{-3/2} \qquad 1.5$$

As expected the correction is determined by the group velocity and period we are considering and the rate of change in that group velocity. Further, there is a distance term, $R^{-½}$, implying that the longer the path on the earth's surface then the greater will be the reduction in time domain amplitudes due to smearing by dispersion.

The meaning of term 1.5 is usually hidden and confused by introducing the geometrical spreading term, $(E \sin \Delta)^{-½}$ (for surface waves) at an earlier stage, and splitting the term into a geometrical and dispersive term

$$\left[U.R^{-½} \left(\frac{dU}{dT}\right)^{-½} T^{-3/2} \right] \left[(E \sin \Delta)^{-½} \right]$$

$$\equiv \left[E^{-1} \Delta^{-½} \sin^{-½} \Delta \right] \left[U.T^{-3/2} \left(\frac{dU}{dT}\right)^{-½} \right] \qquad 1.6$$

However, for the stationary phase correction to hold a condition to be fulfilled is (where k is wavenumber)

$$\frac{t\frac{d^3w}{dk^3}}{\left(t\frac{d^2w}{dk^2}\right)^{3/2}} < \varepsilon \qquad 1.7$$

and if this quantity does not converge to such a limit then the method is invalid (Båth, "Mathematical Aspects of Seismology", p.43). Such convergence is certainly in question near turning points of the dispersion curve, when $\frac{dU}{dk} = \frac{d^2w}{dk^2} = 0$. Examination of the averaged group velocity curves published by Oliver (1962), show three turning point regions for which $\frac{d^3w}{dk^3}$ is certainly non zero, the one of importance creating the Airy phase for periods around 18s. Thus, condition 1.7 need not hold and the Airy phase approximation (Pekeris (1948) considers 3rd order phase terms) may be more appropriate than the simple second order stationary phase approximation. The Airy phase has been shown to propagate with a different dependence on distance then the remainder of the Rayleigh wave (Ewing, Jardetzky and Press (1957), Pekeris (1948)), and has occasionally been regarded as a separate phase, Rg, although it is only part of the fundamental Rayleigh mode. The non-Airy phase Rayleigh mode has distance dependence R^{-1}, the Airy phase depends on $R^{-5/6}$. Increasing distance makes the Airy phase stand out from the rest of the mode, hence its mistaken identity on the seismogram as a unique phase Rg.

Even if the Airy phase is avoided (although it often contains most of the energy!) a set of values at different "apparent" periods for the dispersive term in 1.6 is still inadequate to correct amplitudes measured from the time series. At a particular apparent period the dispersive expression is a function of the type of path traversed by the wave train. Continental, mixed and oceanic paths assign widely different values to this expression because of the different dispersion characteristics. Application of the stationary phase approximation as a "path type" correction has been applied by some researchers, notably Marshall and Basham (1972) to redetermine M_s values. It is apparent that systematic errors will still remain because the individual epicentre-station path correction was replaced by an average, for example, all continental paths were averaged as one group type correction. It would be extremely laborious to determine this correction term for all paths and periods.

However, such path corrections are an unfortunate artifact of amplitude measurements made directly from the partially dispersed time-series representation of the data. A great advantage of working in the frequency domain is that dispersion expressions of the type in 1.6 simply disappear: this alternative is now considered.

1.3 Amplitudes in the Frequency Domain

Rayleigh waves which have propagated a large distance are of the form

$$f(t) = \int_{-\infty}^{\infty} S(\omega)\, f(k_\gamma)\, \exp\,[i(\omega t - k_\gamma R - \emptyset)\,]\, d\omega \qquad 1.8$$

where f(t) is an observed seismogram (ignoring the transducing and distorting instrument effects), $S(\omega)$ the spectrum of the generating force and k_γ the Rayleigh wave number. This integral could be approximated by the stationary phase approximation to give the direct observables A(T); the difficulties of this method are explained above. Alternatively the seismogram f(t) is Fourier analysed to give

$$A(f) = \int_{-\infty}^{\infty} f(t)\, \exp\,[-i2\pi ft]dt \qquad 1.9$$

This approach has only been possible since the advent of algorithms to simplify Fourier transform calculations, and large computers to carry out the calculations; the lack of these forced the use of previous techniques.

We have now returned to the simple form of equation 1.1

$$A(f,r) = K\, L(f,d).I(f).S(f).D(f,r).G(f,r)$$

with $G(f,r) = (E \sin \Delta)^{-½}$

$$D(f) = \exp(-\pi fE\Delta/cQ)$$

The assumption will be made that the amplitude response of the layered medium L(f,d) does not introduce a non circular radiation pattern. Also A(f,r) will be taken as instrument corrected, that is A(f,r)/I(f).

Therefore, the distance dependence of spectral amplitudes is

$$A(f,r) = K'(E \sin \Delta)^{-½} \exp(-\pi fE\Delta/cQ) \qquad 1.10$$

Brune (1962) has shown for surface waves that the group velocity U rather than phase velocity c ought to be used in the attenuation expression. Taking logs gives

$$\log_{10}\,[A(f,r)\,] + 0.5\, \log_{10}(E \sin \Delta) = -(Q^{-1})(\pi fE\Delta/U) + \log_{10}K'' \qquad 1.11$$

This is the amplitude-distance dependence expressed as a straight line with the general form "$y = Q^{-1}\, x + b$". The amplitudes are corrected for geometrical spreading and the "distance" term, $\pi fE\Delta/U$, condenses the true distance, frequency and group velocity dependence into one term. The slope of the line should give estimates of Q^{-1}, and the scatter of points an estimate of the errors involved.

It is worth noting that the dimensions of the Fourier spectra $A(f,r)$ are length x time e.g. microns seconds, but measurements made directly from the seismogram have the dimensions of length. This is because the Fourier amplitudes apply to a continuous function and are really spectral densities. If one Fourier spectral amplitude A (dimension LT) is assumed to cover the frequency interval Δf (dimension T^{-1}) then the product $A \times \Delta f$ may be related to the amplitudes as measured on the seismogram.

Also, the validity of the Fourier expansion should be verified for propagation on the surface of a globe. Brune et al. (1961) have carried out some work with this purpose in mind. The correct functions to be used in a series expansion for a spherical system are the Legendre polynomials. Brune et al. (1961) have shown that a Fourier expansion and a Legendre expansion are almost identical, except at the antipode, where there is a rapid phase advance of $\pi/2$ between the two systems. This implies Hilbert transformation of a waveform as it goes through an antipode: Brune et al. (1961) observed such a change in a model experiment they conducted. However, at other regions of the global surface the Fourier expansion is an excellent match to the Legendre. Since none of the surface waves used in this work were observed for propagation paths of greater length than π these antipodal considerations need not concern us.

1.4 Factors Necessary to Estimate Q^{-1}

From the discussion of equation 1.11 it is apparent that to estimate Q^{-1} it is necessary to measure the following

- $A(f,r)$: the Fourier spectral amplitudes for a range of distances.
- Δ: epicentre-station distance
- f: frequency
- U: group velocity

and an instrument correction for the spectral amplitudes.

The data used and the measurements taken are discussed in the next chapter.

CHAPTER 2

2.1 The Data

The records of some large nuclear explosions were chosen for analysis, these events are listed in Table 2.1 and Figure 2.1. The emphasis was on atmospheric explosions for the following reasons:

1. Atmospheric explosions have been of significantly greater yield than underground explosions and so a better signal-to-noise ratio will be expected for the available records.
2. Larger events, atmospheric explosions, are more efficient generators of low frequencies than are smaller events. A large event will therefore sample a greater depth of the earth.

One earthquake was examined for comparison purposes, this also appears in Table 2.1 and Figure 2.1. Earthquakes in general were not used, and explosions preferred, because:

1. Depth and Origin Time: for explosions the epicentre is usually constrained to zero depth thereby removing a source of error from the origin time. The origin time is vital for the determination of the wave train group velocities and usually it is more accurately known for explosions than for earthquakes.
2. Radiation patterns: for the method to be used it is important that equal or known quanta of radiation energy are emitted from the source in all directions. It is well known that earthquakes show various radiation patterns, determined by the phase concerned; and hence the energy emitted from an earthquake is a function of azimuth.

   It is here considered that such a radiation pattern is not sufficiently well known to be removed from the measurements, in the sense that geometrical spreading may be corrected for and removed. An explosion intrinsically radiates equal quanta

Region	Event Type	Date	Time GMT	Latitude	Longitude	Body Wave Magnitude m_b	Source of Information
Novaya Zemlya	Atmospheric	27. 9.62	08 03 16.4	74.3°N	52.4°E	5¼-5½ (Pal)	PDE No 76-62
Novaya Zemlya	Atmospheric	22.10.62	09 06 10.1	73.4°N	54.9°E	5-5¼(Pal)	PDE No 84-62
Novaya Zemlya	Atmospheric	24.12.62	11 11 42.0	73.6°N	57.5°E	Similar to 27.9.62	PDE No 103-62
Aleutian Islands (Longshot)	Underground	29.10.65	21 00 00.1	51.433°N	179.183°E	5.97	Marshall et al. 0-67/66
Lop Nor (China)	Atmospheric	17. 6.67	00 19 07.9	40.73°N	89.56°E	4.6(CGS)	PDE No 47-67
Novaya Zemlya	Underground	7.11.68	10 02 05.3	73.4°N	54.9°E	6.0(CGS)	PDE No 87-68
Lop Nor (China)	Atmospheric	29. 9.69	08 40 31.0	40.7°N	89.6°E	4.7	LASA Bulletin
Northern Easter Island	Earthquake	17. 6.67	00 56 29.4	4.5°S	104.73°W	4.8(CGS)	PDE No 41-67

Table 2.1 Event Time, Epicentre and Origin Time

EVENT EPICENTRIES AND THE WWSSN STATIONS USED

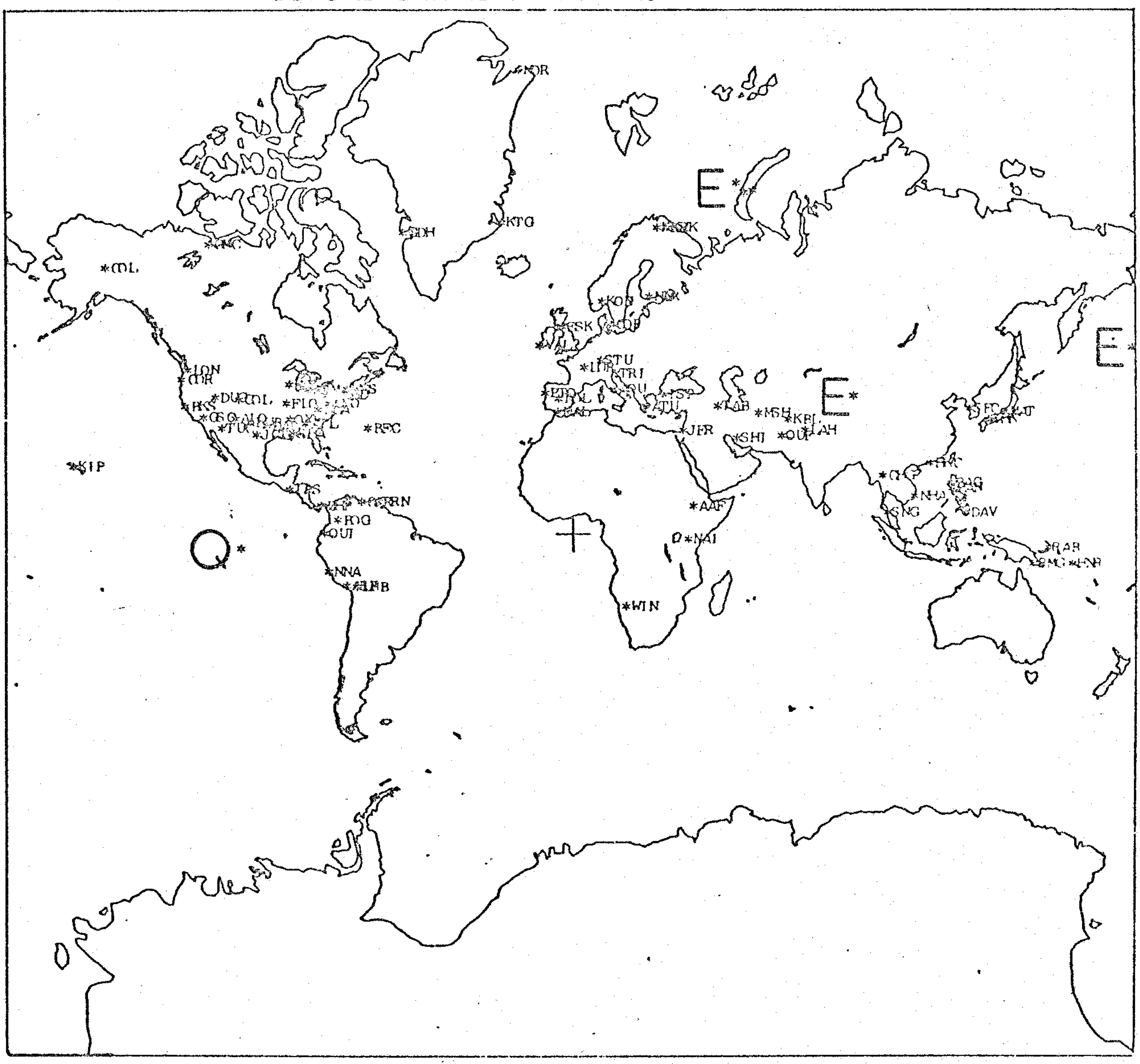

MERCATOR PROJECTION

ALL BEARINGS CORRECT AND ORTHOMORPHIC

FIGURE 2.1

in all azimuthal directions, that is if we ignore the lateral variations in geological structure and the specific attenuation factor Q^{-1}. Further, it would be impossible to distinguish between anomalous source effects and anomalous lateral variations of Q^{-1}.

3. Spectral content: Carpenter and Marshall (1970) have published the source spectrum for atmospheric explosions. It is approximately a constant, as expected, because intuitively it is the Fourier transform of an impulse in the time domain. In determining Q^{-1} as a function of frequency all frequencies are of equal interest, therefore it is pleasing to have all frequencies equally represented in the source spectrum.

A spectral source-layering term for underground explosions, $S_u(f).L_u(f,d)$, has been published (Marshall and Burton 1971) and this represents the product of the source spectrum with the amplitude response of the layered medium at the epicentre. This function can be seen to be monotonically decreasing for underground explosions, whereas the similar function for an earthquake has a minimum turning point (Marshall and Burton 1971 Figures 2 and 4), commonly referred to as a spectral hole. The hole in an earthquake spectrum is associated with the depth of the source interacting with the source mechanism (Douglas, Hudson and Khembhavi 1971) and therefore no explosion will exhibit such a phenomenon, for this reason, because they are near surface events. This smoothness of the underground spectral frequency content means that no particular group of frequencies in the spectrum will be particularly difficult to investigate because of suppression at the source.

It should be possible to determine the underground explosion source function, rather than the source-layering term, by applying the "Common Path" method to a large explosion and the subsequent cavity collapse.

The cavity collapse records from the large Cannikin event are of sufficient signal-to-noise ratio to encourage such an investigation.

With the events chosen because of the above reasons the available WWSSN film chip recordings for the long period, vertical component system were examined. The WWSSN gives good world coverage with standard instrumentation.

The records which were digitised are listed in Appendix 1. In all several hundred records were examined and about 200 of these were digitised. Many of the records examined were not digitised because of their poor quality, extremely poor signal-to-noise, "knitting" records, coincident events or simply because the relevant event was not found. Much of the data obtained from the WWSSN records are of excellent quality, especially the earlier data recorded with a fast drum speed.

The digitised records were sampled every 1.6s, determining a Nyquist frequency of 0.3125 Hz. The digitising was performed on an AGI film assessor which was especially suitable for WWSSN film chips. This machine steps along the time axis at equal increments, and the digitised amplitude coordinate was obtained by matching crosswires to the top side of the seismogram. Digitising started at a minute marker or at a known number of sample intervals before a prominent record feature and continued until the end of the record. Care was taken to omit any lateral refractions, or reflections of seismic energy and to avoid digitising the minute markers.

Measurements were taken from the individual record calibration pulses and instrument parameters noted, in accordance with the work of Espinosa, Sutton and Miller (1965). Appendix C describes the calculation of I(f) from these measurements.

To complete the initial data it is necessary to know the epicentral coordinates and the origin times for events. These are obtained from the PDE cards published by the USCGS. Also the coordinates of the WWSSN stations are required, these are published in the WWSSN handbook (1965).

2.2 Data Analysis

The data analysis falls into two main parts; the determination of the spectral Fourier amplitudes and the group velocities, followed by the estimations of Q^{-1} using a least squares technique.

Initial information was obtained using the program GEDESS (Young and Gibbs 1968). This program calculates the epicentre-station separation Δ^{o} and allows for the ellipticity of the earth. The program also calculates the estimated time of arrival of the Rayleigh 40s period wave (assuming a velocity of 3.97 km/s) from an epicentre to any recording station. This helped to find the correct event when other events occurred on the same record.

Spectral amplitudes and group velocities were obtained using the "Time Series Analysis Program" (TSAP) described in the attached report (Burton and Blamey 1972). This program was written in its present form especially for this work, its structure will be summarised briefly here and its advantages described later.

2.2.1 Spectral Amplitudes

The spectrum x(f) of a continuous time series x(t) is usually given as the Fourier Transform integral

$$x(f) = \int_{-\infty}^{\infty} x(t)\exp(-i2\pi ft)dt \qquad 2.1$$

Experimentally sampled data X(t) differs from x(t) in several respects. Because it is sampled data it is a discrete valued function rather than continuous, and so the transform integral is replaced by a summation and the values of f and t become discrete. Further, the range of integration cannot possibly be infinite. We obtain a function of the form

$$Z(f_j) = \sum_{n=0}^{N-1} X(t_n)\exp\left(\frac{-i2\pi jn}{N}\right) \qquad |j| < \frac{N}{2} \qquad 2.2$$

when there are N points in the time series. The increment dt is omitted because it is now only of use as a scaling factor. But it is important to include the scaling factor, which is the sampling interval, when converting to absolute values (Enochson and Otnes 1968).

If the value N is increased so that the new $N = 2^L$ (integer L) then expression 2.2 may be rapidly calculated using the Cooley-Tukey algorithm. It is the combined simplification caused by these algorithms and the availability of fast computers which make possible the treatment of data in the frequency domain.

The function $Z(f_j)$ in 2.2 is complex; it contains information about both amplitude and phase for the spectrum. This is discussed in detail by Burton and Blamey (1972).

The real and imaginary parts of the instrument transfer function, I(f), may easily be allowed for by complex division in the frequency domain.

The spectra obtained after allowing for instrumental distortions are filtered to remove very low frequencies, that is the fundamental and a few higher harmonics. Also the spectra are smoothed, simply averaging eight consecutive values to give a smoothed value, but moving along in steps of four values at a time.

Three seismograms illustrating the "raw" data are shown in Figure 2.2. The records at Malaga and Kongsberg have good signal-to-noise; the one for Kap Tobin is very noisy. The amplitude spectra for these seismograms after correcting for the instrument transfer function, removal of low frequencies and smoothing are shown in Figures 2.3-2.5. The Malaga spectrum is excellent data. The spectra for the Kongsberg and Kap Tobin records show some of the possible sources or elimination of errors.

The spectral values for Kongsberg have two distinct holes at frequencies 0.05 and 0.075 Hz. Such spectral holes are not a common occurrence but will obviously influence the Q^{-1} values and broaden the confidence limits around these frequencies. These holes probably result

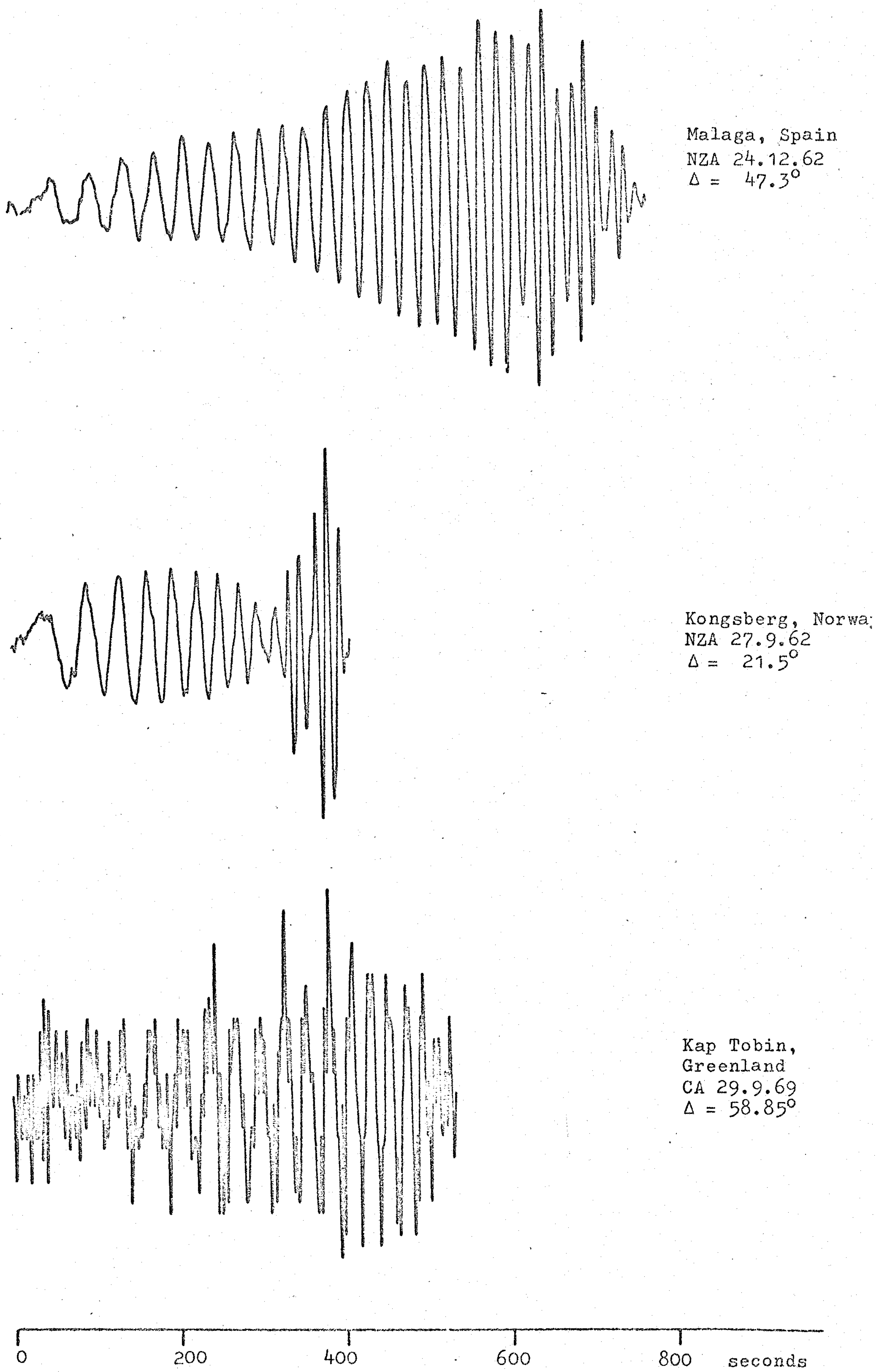

FIGURE 2.2 Three Typical Seismograms

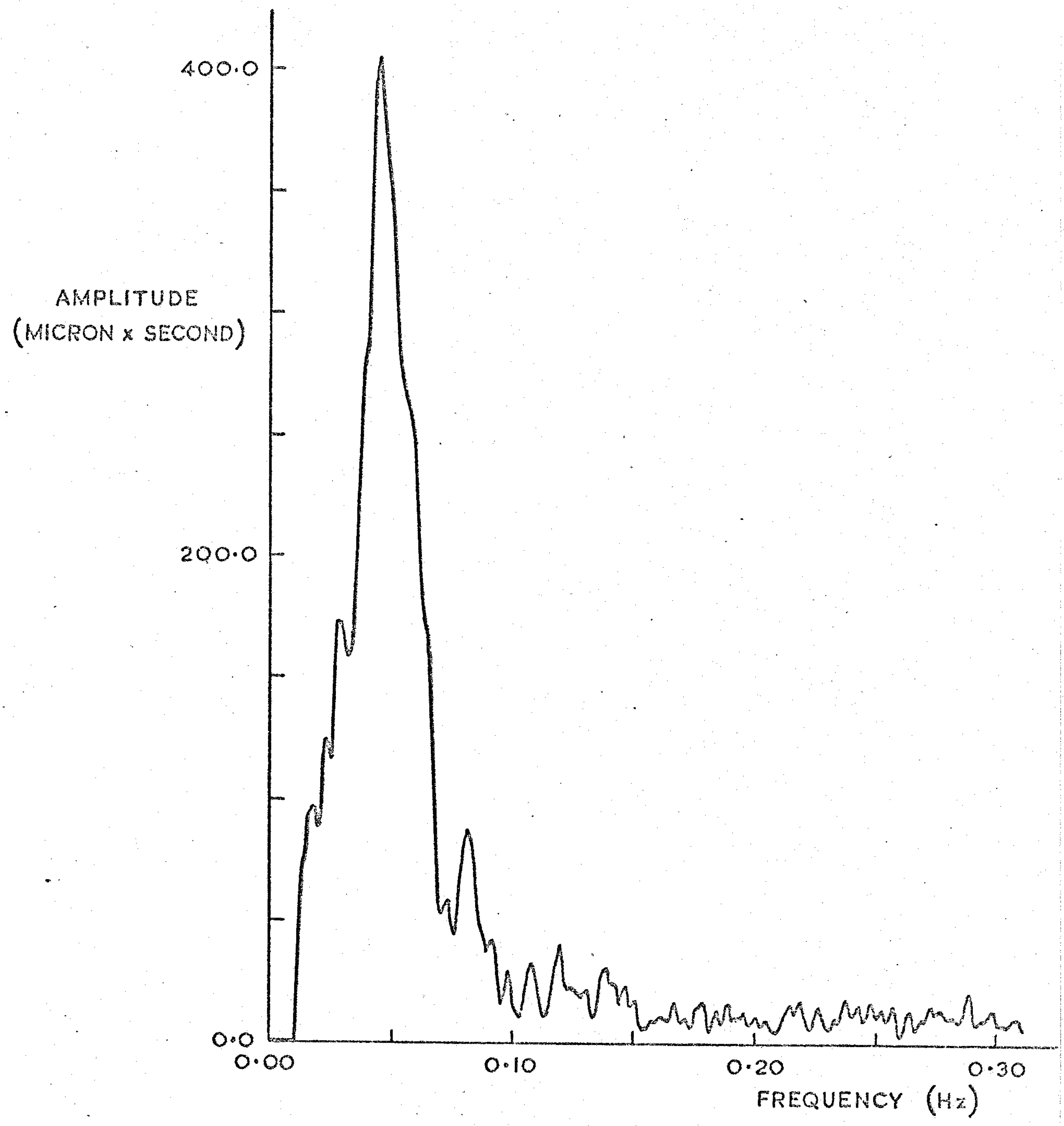

FIGURE 2.3 SPECTRAL AMPLITUDES FROM MALAGA SEISMOGRAM
(EVENT: ATMOSPHERIC EXPLOSION,
NOVAYA ZEMLYA, 24th DECEMBER 1962,
DISTANCE ≃ 5260 km)

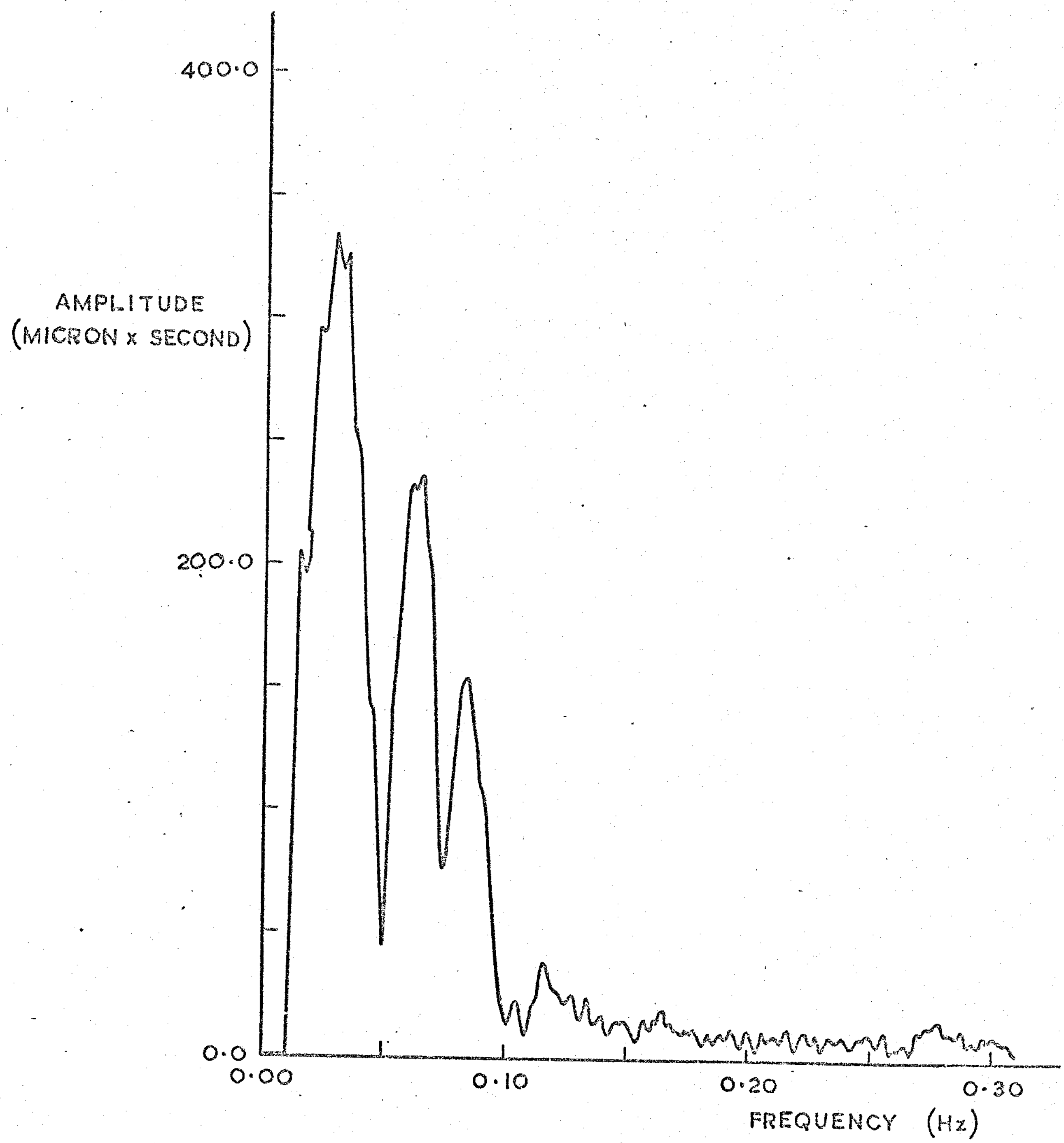

FIGURE 2.4 SPECTRAL AMPLITUDES FROM KONGSBERG SEISMOGRAM
(EVENT: ATMOSPHERIC EXPLOSION,
NOVAYA ZEMLYA, 27th SEPTEMBER 1962,
DISTANCE ≈ 2391 km)

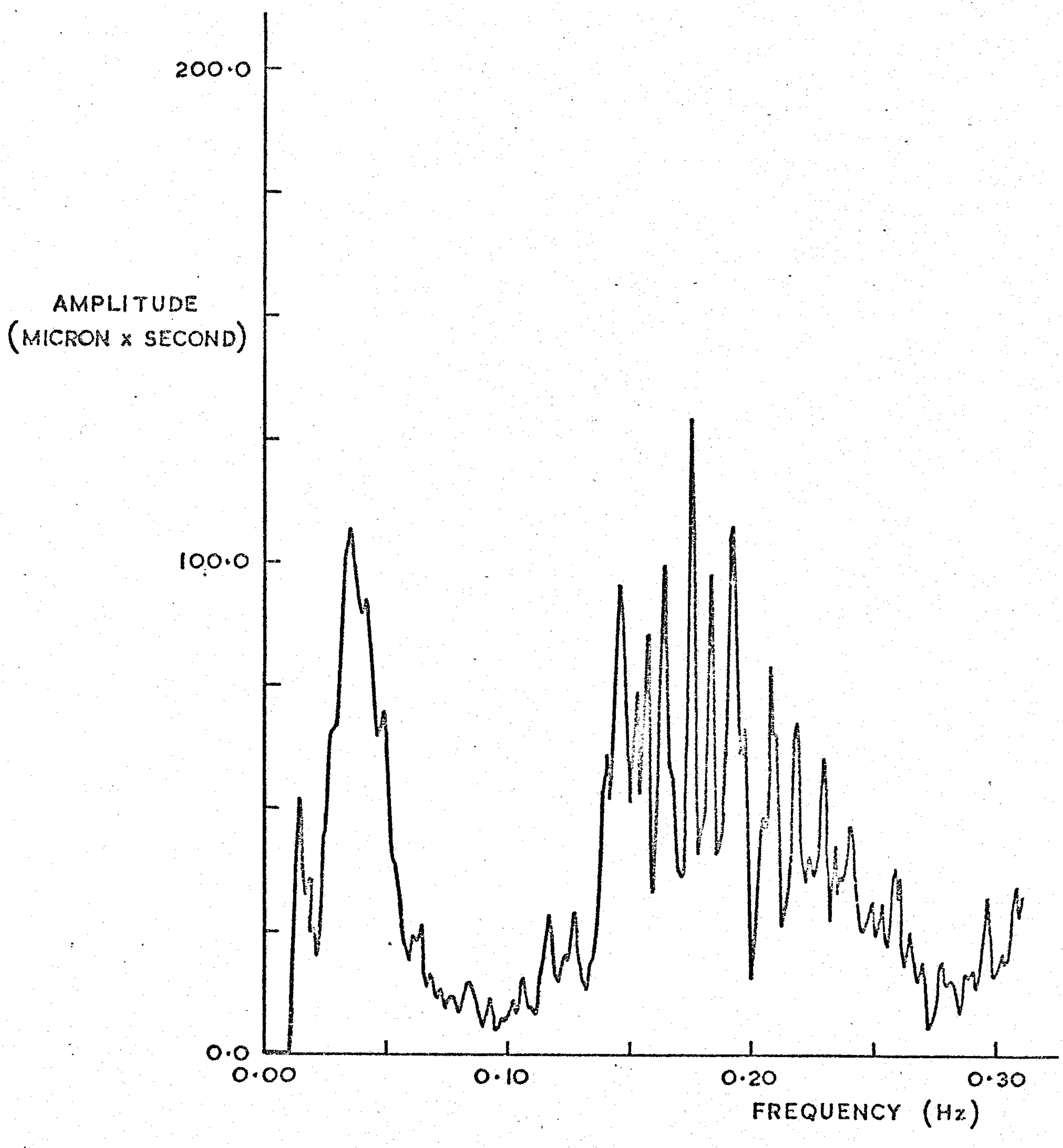

FIGURE 2.5 SPECTRAL AMPLITUDES FROM KAP TOBIN SEISMOGRAM (EVENT: ATMOSPHERIC EXPLOSION, S. SINKIANG PROV., CHINA, 29th SEPTEMBER 1969, DISTANCE = 6544 km)

from multipathing between Novaya Zemlya and Kongsberg, causing destructive wave interference at these particular frequencies.

The spectrum of the very noisy Kap Tobin record is surprisingly good for the frequency range of interest, up to 0.1 Hz. The signal spectrum has obviously been separated from the noise, there is a pronounced microseism peak in the range 0.15-0.25 Hz. It is quite apparent that poor signal-to-noise in the time domain does not necessarily imply poor signal-to-noise in the frequency domain. The Kap Tobin record also shows evidence of low frequency barometric noise around 0.017 Hz, but this is described later.

These three seismograms illustrate the data ideal along with factors which will subsequently contribute to the experimental errors.

2.2.2 Group Velocity

The group velocities for the frequencies required were determined for each record using the multiple filtering technique of Dziewonski, Block and Landisman (1969). The technique used differs from that of Dziewonski et al. in one important respect, for this work the group velocities were determined at exact Fourier harmonics to eliminate frequency errors. The method and the reasons for doing this are described later.

Dziewonski's method uses the formulation of Goodman (1960) who investigated the determination of instantaneous amplitude and phase for a dispersed time series. It is not sufficient to filter a seismogram for a set of specific frequencies because the filter output will also be an oscillating signal and its maximum point will therefore be difficult to determine. Goodman (1960) assigned a non-oscillating instantaneous amplitude and phase, $R(t)$ and $\phi(t)$, to a signal $A(t)$ by using the analytic signal definition

$$R(t)\, e^{i\phi(t)} = A(t) - iH(t) \qquad 2.3$$

where ideally $H(t)$ is the Hilbert transform of $A(t)$ and

$$R(t) = [A^2(t) + H^2(t)]^{1/2} \qquad 2.4$$

If the frequency domain filter response to a seismogram is a(f) then also required is the quadrature filter response h(f). The quadrature filtering is simply the Hilbert transform (H) of the filter response a(f), this simply means that the filter response a(f) is advanced by $\pi/2$ giving h(f).

The spectrum of 2.3 may be approximated by the form

$$\left[\frac{1}{-g(f)} \quad \frac{g(f)}{|g(f)|^2}\right] a(f) \qquad 2.5$$

which improves in efficiency as $g(f) \rightarrow i$ (Goodman 1960). However since the work of Goodman modern fast Fourier transform (F) techniques make such approximation negligible and the Hilbert transform may easily be found because

$$F\,H\,(A(t)) = i \text{ sign } (f)\, F(A(t)) \qquad 2.6$$

Equation 2.4 gives a non-oscillating signal waveform from which the discrete instantaneous amplitudes R(t) may be determined. Figure 2.6 illustrates group velocity determination at the filter frequency 0.033 Hz for an atmospheric explosion at Novaya Zemlya (NZA 24.12.62) recorded at Kongsberg. The relation between the instantaneous amplitudes R(t) and the group velocity or group arrival time is easily seen. The figures 6, 7 and 8 of Burton and Blamey (1972) show that the process may be extended to determine group arrival times and the consequent group velocities for a range of frequencies.

2.3 Reduction of Errors

Of the many possible sources of error in the analysis of the time series several could be reduced, whilst others had to be accepted.

2.3.1 Spectral Amplitude Measurements

It was first decided that all spectral amplitudes would be determined for the same frequency values for the Fourier Harmonics, irrespective of the record length. Since all records were increased in length to satisfy the relation $N=2^L$ this was simply a matter of choosing a consistent value for L (L=11 was chosen) and so all records were increased to 2048 points and the Fourier Harmonics are therefore

FIGURE 2.6 A Group Velocity Determination from the Instantaneous Amplitudes at the Filter Frequency 0.033 Hz.

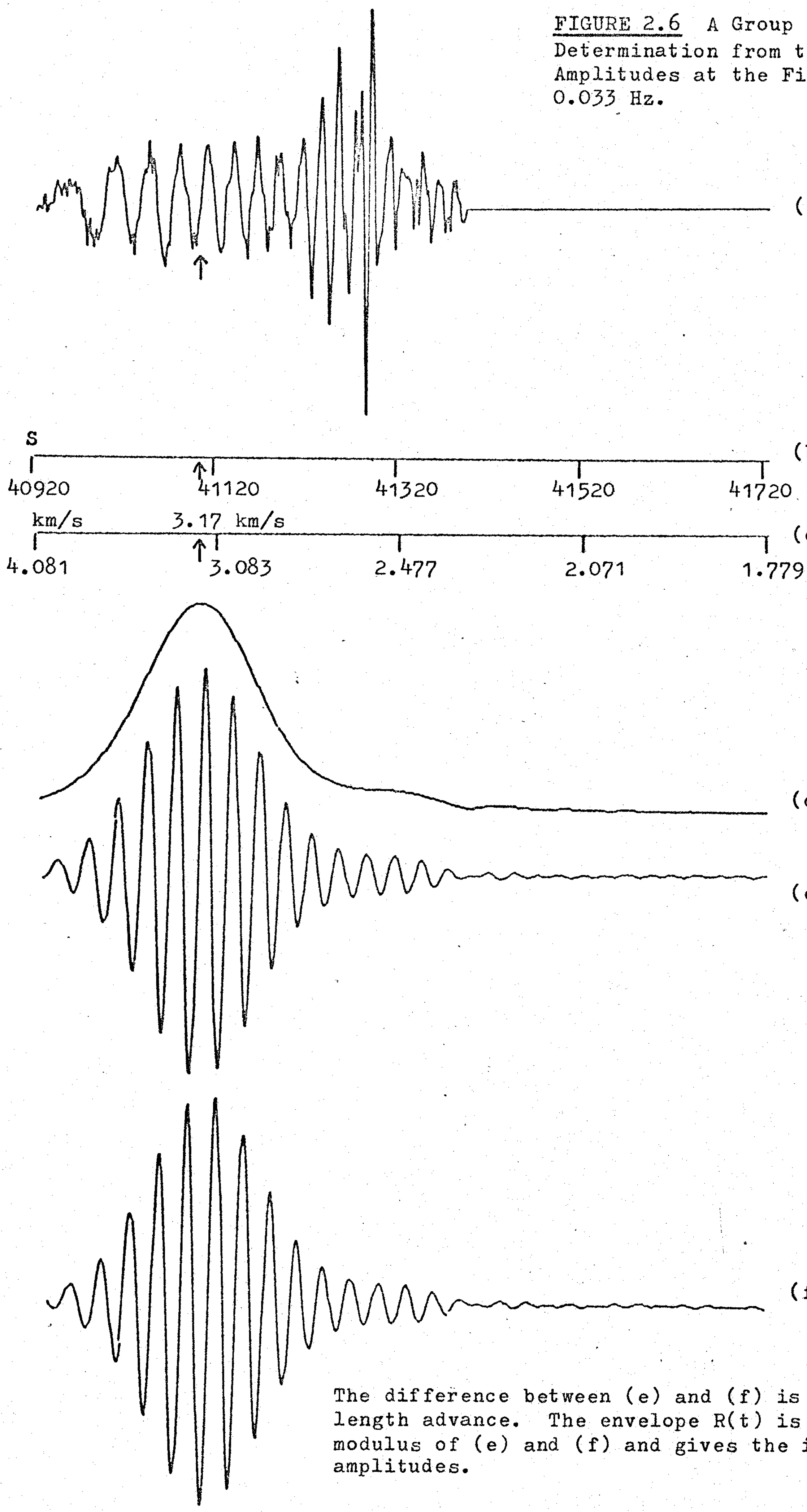

(a) The seismogram

(b) its arrival time scale and

(c) the related velocity scale

(d) The envelope, R(t), of the filter response to the seismogram

(e) the filter response, A(t), to the seismogram and

(f) the Hilbert transform, H(t), of A(t).

The difference between (e) and (f) is a quarter wavelength advance. The envelope R(t) is formed from the modulus of (e) and (f) and gives the instantaneous amplitudes.

$$f_j = \frac{f_{NYQ} \times j}{N/2} \qquad 2.7$$

The sampling interval used is 1.6s and so the Nyquist frequency is

$$f_{NYQ} = \frac{1}{3.2} \text{ Hz}$$

$$= 0.31250 \text{ Hz}$$

the fundamental Fourier Harmonic is

$$\Delta f = \frac{f_{NYQ}}{N/2}$$

$$\sim 0.00305 \text{ Hz}$$

and the Fourier Harmonic series is

$$f_j = j \times \Delta f \qquad (0 < j \leqslant N/2) \qquad 2.8$$

Amplitude measurements at these frequencies may be in error because of

1 Digitising errors

2 Digitising excess record

3 The instrument correction

4 Noise

5 Higher modes

6 Fourier analysis preferred to Legendre polynomial.

1 <u>Digitising Errors</u>

The first type of digitising error is caused simply by the machine resolution. The machine used, an AGI Film Assessor, displayed the x and y coordinates to four significant figures. The last figure (one assessor unit) resolved 10^{-5}m on the film chip. The factor between a film chip and the original seismogram is an eight fold reduction and so

1 assessor unit (a.u.) $\equiv 8.10^{-5}$m of original seismogram

Any y coordinate was usually repeatable to better than ± 4 a.u. or 3.10^{-4}m of original seismogram. An absolute random digitising error of $\pm$ 0.3 10^{-5}m for the original sized seismogram is good and no attempt was made to improve this resolution.

However, an attempt was made to minimise the introduction of high frequencies caused by motion of the digitiser between digits during hand digitising. The introduction of these high frequencies is demonstrated in a paper by Bogert et al. (1962). The crosswires were always traced along the top side of the seismogram line, this arbitrary decision prevents the digitising trace oscillating within the thickness of the seismogram line.

The first digit was always set to read 5000 a.u. so that the digitised trace was on a pedestal. Whenever possible the seismogram was orientated so that the last digit would be the same as the first, to eliminate a step effect at the end of the record. During the program processing the digitised time series was depedestalled by removing the mean. Also the series was cosine tapered at each end to ensure a smooth junction between the trace and baseline and avoid spurious high frequency content.

Occasionally a mispunch would occur during digitising and the most significant figure would be omitted. If such a trace was Fourier analysed then the "spike" caused in this way would dominate the spectral content. So all traces were graphed out before processing by TSAP, and these glitches removed.

2 Digitising Excess Record

Any excess of digitised record is only obvious in the time domain display (with an exception to be discussed later) and can be dealt with when the digitised trace is first graphed out. Any excess record will alter the Fourier harmonic amplitudes at the frequencies it contains, this is normally the higher frequencies because they occur at the end of the dispersed record. Lateral refractions may be identified by matching the separation between crossovers for a later part of the time trace with an earlier section. Such lateral refractions must be removed because they have not travelled by the direct path from epicentre to receiver.

3 <u>The Instrument Correction</u> (Described in Appendix C)

The instrument corrections used assigned a small, but finite, value for magnification at the low frequencies (less than .01 Hz) whereas the peak magnification might be several hundred times larger. A nuclear explosion does not usually produce such low frequencies. But for the uncompensated WWSSN seismometer the barometric noise amplitude is proportional to the square of the period. It was found that these small amplitudes at low frequencies, when divided by a very small magnification as instrument correction, dominated the event itself. On reverse transforming to the time domain, all that could be seen was a large amplitude low frequency component with a tiny seismogram superimposed onto it! So all frequencies lower than 0.0125 Hz were filtered out.

4 <u>Noise</u>

The enhancement of low frequency noise, and its removal, has been described above. The frequency range of interest is about 0.014-0.1 Hz and any higher frequencies are omitted. An explosion does not produce energy which propagates for large distances with frequencies much greater than 0.1 Hz, so the seismic noise peak at about 0.12 Hz is omitted. Fourier analysis of the trace does separate out the signal from this noise peak as is shown by Figure 2.2 and Figure 2.5 (seismogram and spectrum). The frequencies of interest stand out as a separate peak and are clearly distinguished from the noise peak, thus eliminating this systematic source of noise.

Random noise in the useful frequency range cannot be distinguished, but a useful frequency range for a particular signal spectrum may be obtained by considering signal-to-noise in the entire range. For example in Figure 2.5 it is apparent that .015 to .09 Hz is good. A particularly noisy station may show a noise spectrum generating ground motion of the order of microns, this may fluctuate down to $m\mu$ in a short time (Brune and Oliver 1959).

5 Higher Modes

It is assumed in this analysis that only the fundamental Rayleigh mode is analysed, no reason was found to doubt this. If higher modes were present they would disturb the spectral values at high frequencies. No coherent high frequency energy was ever found superimposed onto the seismograms, and no high frequency dispersion branches were found in the group velocity determinations. The assumption that Fourier analysis was analysis of the fundamental mode always appears to be valid.

6 Fourier Analysis Preferred to Legendre Polynomials

This has already been described. Because none of the Rayleigh waves used pass through an antipode the Fourier representation is excellent. If the waves did pass through an antipode only the phase properties would be incorrect, and this has no bearing on the present analysis.

At this stage of the processing, when the time series has been depedestalled, cosine tapered, increased to 2^L points and Fourier analysed, it is possible to improve the spectrum by smoothing. Smoothing is especially valid because the spectrum is greatly overdetermined. A typical record of length 500 points (about 13 minutes) has been increased to 2048 points. The spectrum therefore has four times as many frequency points or harmonics than are required to uniquely determine it. (Assuming that the time series does not contain any frequencies greater than the Nyquist.) A reasonable smoothing would decrease the number of harmonics by a factor of four. The smoothing chosen compounds eight values at a time, but steps along the frequency harmonics four at a time. The smoothed spectrum is now less erratic for noisy signals. The smoothing operation is also designed so that the new frequency values generated still correspond to the old exact Fourier harmonics, with a step of $4 \times \Delta f$ between each smoothed value.

The number of harmonics filtered out at low frequencies is 41 (due to the long period noise and instrument response previously mentioned) and so the available frequency harmonics which are non-zero are $42\Delta f$ up to the Nyquist. However all the frequency harmonics, from the zero DC component onwards are smoothed as described above. The harmonics available after smoothing are

$$4\Delta f, 8\Delta f \text{ - - - - - } \text{Nyquist.}$$

But spectral values up to $41\Delta f$ have been set to zero and so the first smoothed harmonic which is not contaminated by this filtering is $48\Delta f$; the smoothed, uncontaminated harmonics now available are

$$48\Delta f,\ 52\Delta f \text{ - - - - - } \text{Nyquist}$$

and those selected to be punched out from the computer processing are $48\Delta f$-$360\Delta f$. There are 79 values in this frequency range 0.015-0.110 Hz. It later appears that this choice of upper frequency content is perhaps over optimistic; and is often seriously contaminated by noise.

2.3.2 The Frequencies of Spectral Amplitudes and Group Velocities

In this section a modification to the technique of Dziewonski et al. is described, which was thought to be desirable in general, and necessary in this particular study.

The paper by Dziewonski, Bloch and Landisman (1969) describes their "multiple filter technique". The points of interest here are

1 The seismogram $x(t)$ is Fourier transformed producing

2 the complex array $Z(\omega)$ at

3 the Fourier harmonics ω_j.

4 Centre frequencies for group velocity determination are selected according to a rule of the type

$$\omega_{c,n-1}/\omega_{c,n} = k \tag{2.9}$$

5 A range of group arrival times, τ_m, is selected

$$\tau_m = \frac{\text{DISTANCE}}{V_m}$$

6 Filters of constant Q (ratio of peak frequency to bandwidth) are formed, the filter or frequency window centred at ω_n is

$$W_n(\omega) = \exp\left[- \alpha \left(\frac{\omega - \omega_{c,n}}{\omega_{c,n}}\right)^2 \right]$$

where the constant α determines roll-off.

There are two separate frequency arrays. The values of the Fourier harmonics are directly determined by the number of points in the time series and the sample interval, as before

$$\omega_j = j \times \Delta\omega \qquad 0 < j \quad N/2$$

with
$$\Delta\omega = \frac{\omega_{NYQ}}{N/2}$$

and ω is angular frequency.

Centre frequencies are chosen according to $\omega_{c,n-1}/\omega_{c,n} = k$; and so it is unlikely for these centre frequencies to correspond to an exact harmonic. For the Dziewonski technique the harmonic nearest to a given $\omega_{c,n}$ is chosen to replace $\omega_{c,n}$ in all computation. Dziewonski et al. (1969) stated that "the maximum deviation of the harmonics from the array frequencies was always less than 1.5 per cent".

The rule for selection of centre frequencies makes the interval between these frequencies a function of frequency since

$$\Delta\omega_{c,n} = \omega_{c,n} - \omega_{c,n-1}$$

$$\Delta\omega_{c,n} = \omega_{c,n}\,(1-k)$$

and the smallest interval occurs at the lowest frequency.

To ensure that two centre frequencies for group velocity determination are replaced by different Fourier harmonics (if this is not done then the same group velocity will be assigned) we must have

$$\Delta\omega_{c,n} > \Delta\omega$$

$$\therefore \quad \omega_{c,n}\,(1-k) > \frac{\omega_{NYQ}}{N/2}$$

Assuming the values:

$$\omega_{c,n} = 2\pi \times 0.01 \text{ rad s}^{-1}$$

$$k = 0.95$$

$$\omega_{NYQ} = 2\pi \times 0.5 \text{ rad s}^{-1}$$

gives $N > 2000$

To ensure that the low centre frequencies, and therefore group velocities, are distinct we have a necessary lower limit on the record length.

Further, we may wish to improve the condition that the error introduced by replacing a centre frequency by a harmonic is less than 1%.

$$\frac{\omega_{c,n} - \omega_j}{\omega_{c,n}} < 0.01$$

The greatest possible error in the offset from a filter centre frequency to a harmonic is $\frac{1}{2}\Delta\omega$, the best it can be is right; averaging out at $\frac{1}{4}\Delta\omega$. So on average $\omega_{c,n} - \omega_j = \frac{1}{4}\Delta\omega$ and we have

$$\frac{\frac{1}{4}\Delta\omega}{\omega_{c,n}} < 0.01$$

$$\frac{\omega_{NYQ}}{2N\omega_{c,n}} < 0.01$$

$$N > \frac{50\omega_{NYQ}}{\omega_{c,n}}$$

and using the previous values for ω_{NYQ} and $\omega_{c,n}$

$$N > \frac{50.2\pi 0.5}{2\pi.0.01}$$

$$\therefore \quad N > 2500$$

Even applying these conditions to the above values we find the ratio of the average error in a filter frequency to the gap between filter frequencies is

$$\text{ratio} = \frac{\Delta\omega}{4\Delta\omega_{c,n}}$$

$$\therefore \text{ratio} = 1/5$$

and so this resolution is not too good.

This discrepancy between the harmonic frequencies at which spectral amplitudes are determined, and the filter frequencies for determining group velocities, may influence any investigation of Q^{-1} as a function of frequency because Q^{-1} is determined using amplitudes and velocities presumed determined at the same frequency. This situation may be altered quite easily.

First, it is apparent that angular frequency may be replaced by frequency in all the above calculations so that ω_j becomes f_j, which is a more familiar quantity.

If the selection equation 2.9 is changed to

$$f_{c,n} - f_{c,n-1} = k'$$

then by careful choice of $f_{c,1}$ and k' it is possible to match all the centre frequencies to exact Fourier harmonics. Then, the above limitations are removed, and there is no discrepancy between spectral and group velocity frequencies. We have a frequency selection rule of the form

$$f_{j,n} - f_{j,n-1} = k'' \Delta f$$

where Δf is the fundamental. The equation finally used was

$$f_{j,n} - f_{j,n-1} = 8\Delta f$$

and the value selected for $f_{j,1}$ was $48\Delta f$ because this exactly corresponds to the first smoothed harmonic frequency of interest (see before). Selecting $8\Delta f$ as the interval ensured that a group velocity was determined at every other frequency for which a spectral amplitude had been calculated, giving 40 values in the required frequency range. Because the interval chosen is an even number of Δfs simple linear interpolation exactly half way between two adjacent group velocity values generates the other 39 values required.

This process gives exactly matching smoothed spectral amplitudes and group velocities, without any frequency errors, by careful choice of the smoothing operation and selection of the filter centre frequencies as exact harmonics.

2.3.3 Group Velocity Errors

Errors in simple velocity determination are of the form

$$\frac{\delta U}{U} = \frac{\delta\Delta}{\Delta} - \frac{\delta t}{t}$$

The angular distance, Δ, is accurately known (Young and Gibbs, GEDESS, 1968) and errors are confined to measurements of the group arrival time. Values of the group arrival time must be within the time span of the digitised seismogram, however, times assigned to individual samples may be in error for two reasons:

1 It has been assumed that the digitising machine increment between samples remains constant and

2 the reduction of seismograms to film chips (x8) is exact and no photographic "shrinkage" takes place.

The first assumption was checked for systematic variations. There are two time scales in use on film chips, they are 3.10^{-3}m representing 48s and 3.10^{-3}m representing 96s. Because 1 assessor unit represents 10^{-5}m of film the digitising increments used were 10 a.u. and 5 a.u., both representing a 1.6s sample interval. A typical 10 minute record is therefore about 3750 a.u. or 1875 a.u. long. After digitising such a record and returning to the starting point the starting point reading was never found to differ by more than 3 a.u. from its original value, showing remarkable consistency in the long term average sample interval. Any random variations in the sample length were not evident when the digitised series was graphed out and so are ignored.

Photographic reduction proves not to be exact. When the digitising of a record started exactly on the leading edge of a minute marker then the number of samples in the first three minutes was noted. Assuming the sample interval is 1.6s (it has been shown to be at least constant above) then about 112.5 samples would be expected. The number of samples required would occasionally differ by 2 from this figure. Because the mechanical sample interval is certainly constant this implies that the time scales differ because of inexact reduction, by about 1%.

It is possible to exactly determine the time sample interval by digitising between two minute markers, counting the number of samples, and hence deducing the interval (DELA). This would lead to an independent value of DELA for each seismogram, the accuracy being that of the mechanical sample interval. This was not done because the value of DELA determines the subsequent Fourier harmonics for a record and it was desirable to have matching harmonics for all records. To simplify the analysis this error of about 1% was tolerated, rather than eliminated as was possible.

Consequently, errors in the group arrival time increase with record length and this a effects high frequencies more than low frequencies (because low frequencies usually arrive first). Considering a wave with travel time 30 minutes (about 60°) to the first sample, and of length 10 minutes, errors in the group velocity at the latter end of the record are

$$\frac{\delta U}{U} \sim \frac{6}{40.60} \times 100\% = 0.25\%$$

This effect is obviously very small and worth accepting to obtain the matching Fourier harmonics.

A much larger error may be introduced by bursts of noise. The seismic noise around 0.1 Hz is important in this respect. A dispersed Rayleigh signal may contain energy around 0.1 Hz, usually at the latter end of the signal, but noise energy at the same frequency may be superimposed randomly on the record. The noise energy may be greater than the modal propagated energy and the program technique has no means of distinguishing the two. Because the program searches to find when the most energy (of a particular frequency) arrives, and then assigns a group arrival time to that peak (see Burton and Blamey 1972) the corresponding group velocities may be in considerable error.

Such errors are not serious because obviously if the local noise amplitude is greater than the propagated wave amplitude then the spectral Fourier amplitude can no longer be regarded as a Rayleigh fundamental mode amplitude. These values of amplitude can only be used to determine Q^{-1} if the noise may be corrected for at each recording station. When these errors occur the signal-to-noise ratio for the frequency domain must be worse than 1:1.

2.3.4 Redetermination of the End of the Signal

It has already been stated that if the record is digitised beyond the end of the true signal then this excess signal will contribute erroneously to the signal spectral amplitudes, usually at the higher frequencies. Once a group velocity curve has been obtained then it is possible to redetermine the end of the signal. Essentially noise is removed which has an apparent velocity less than the slowest determined group velocity, U_s km/s. There are four velocities of interest here for a digitised signal. The velocity to the first sample is V_F, to the last sample V_L (noting that the number of samples has been increased to 2^L) and the velocity to the last true digit before increasing to 2^L is V_{ED}. Their relative sizes are $V_F > U_S > V_{ED} > V_L$; ideally U_s is close to V_{ED} so that little extra record is present to introduce spurious spectral content. The instantaneous amplitudes R(t) described in section 2.2.2 are stored in a matrix, the E matrix, as a function of both velocity and filter frequency. Instantaneous amplitudes for a particular frequency form one column of the E matrix, and subsequent columns store R(t) for further frequencies. The maximum of the entire matrix is set to 99 dB and all other values are normalised relative to this maximum. The seismogram of Figure 2.7 recorded at Lahore (Pakistan) produces the E matrix, contoured at 5 dB intervals, shown in Figure 2.8. Velocities V_F, U_s, V_{ED} and V_L are easily identified on this figure. Everything represented on the contour plot, or in the E matrix, with velocity < 2.26 km/s is meaningless in terms of real data and represents rounding error. Therefore in the region of 2.26 km/s the contour lines are closely packed and parallel to the x axis - because there is a discontinuity between genuine time domain content and very low level time domain content outside the observed length of the signal time range. The dB jump in the E matrix representation is about 30 dB.

The minimum value of group velocity is about 2.80 km/s. This particular value is chosen because it is slower than the velocity of the highest frequency analysed and this velocity is several dBs down from the ridge followed by the group velocity curve. The region between 2.80 and 2.26 km/s, for all frequencies, can only represent noise; it is non propagating energy or lateral refractions. Ideally this region should not exist, and so the arrival time corresponding to $U_s = 2.80$ km/s is calculated and the digitised record truncated to this new length. Figure 2.7 shows the alteration in seismogram length and Figure 2.9 the contour plot for the new E matrix.

Where possible this process was applied to all seismograms, to improve the spectral amplitudes (by lowering their noise content). However this method cannot improve the seismogram for velocities within the true signal range, and only helps to isolate the pure signal.

2.4 Amplitude-Distance Plots and Estimations of Q

For each event the data are now in the form of fundamental Rayleigh mode amplitudes (approximated to by Fourier amplitudes) and group velocities as functions of frequency for a set of stations at varying distances from the epicentre.

Every block of station data is essentially amplitude and group velocity as a function of frequency at fixed Δ, this has to be manipulated

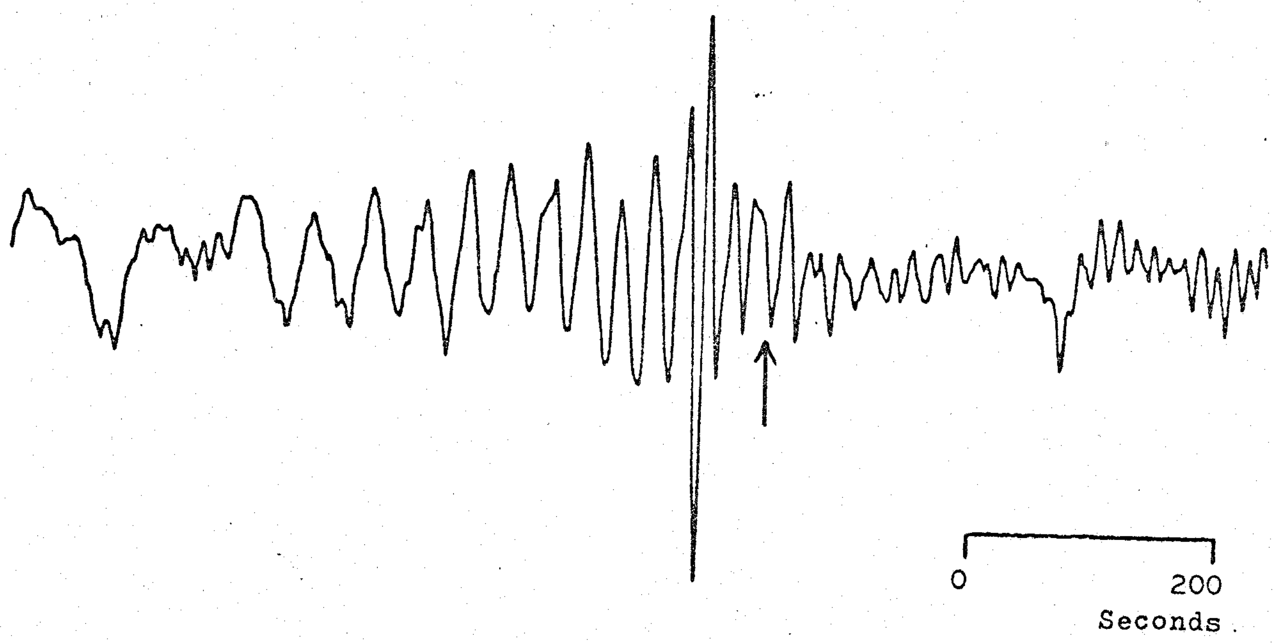

FIGURE 2.7 The Lahore Seismogram for the Atmospheric Explosion NZA 24/12/62 ($\Delta = 43^{\circ}$) The Redetermined Record End is Marked by the Arrow.

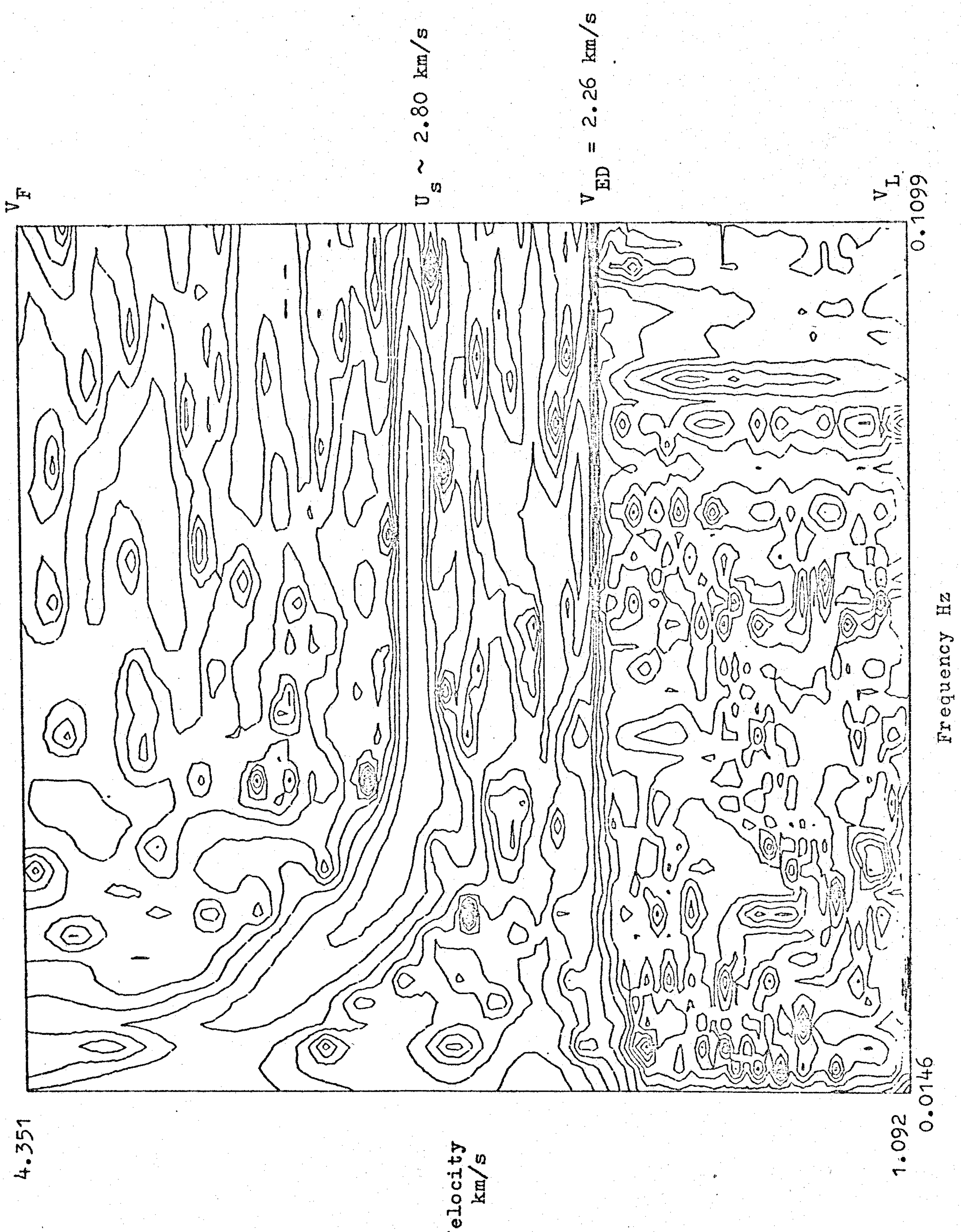

FIGURE 2.8 The Contoured E Matrix for the Full Length Lahore Seismogram.

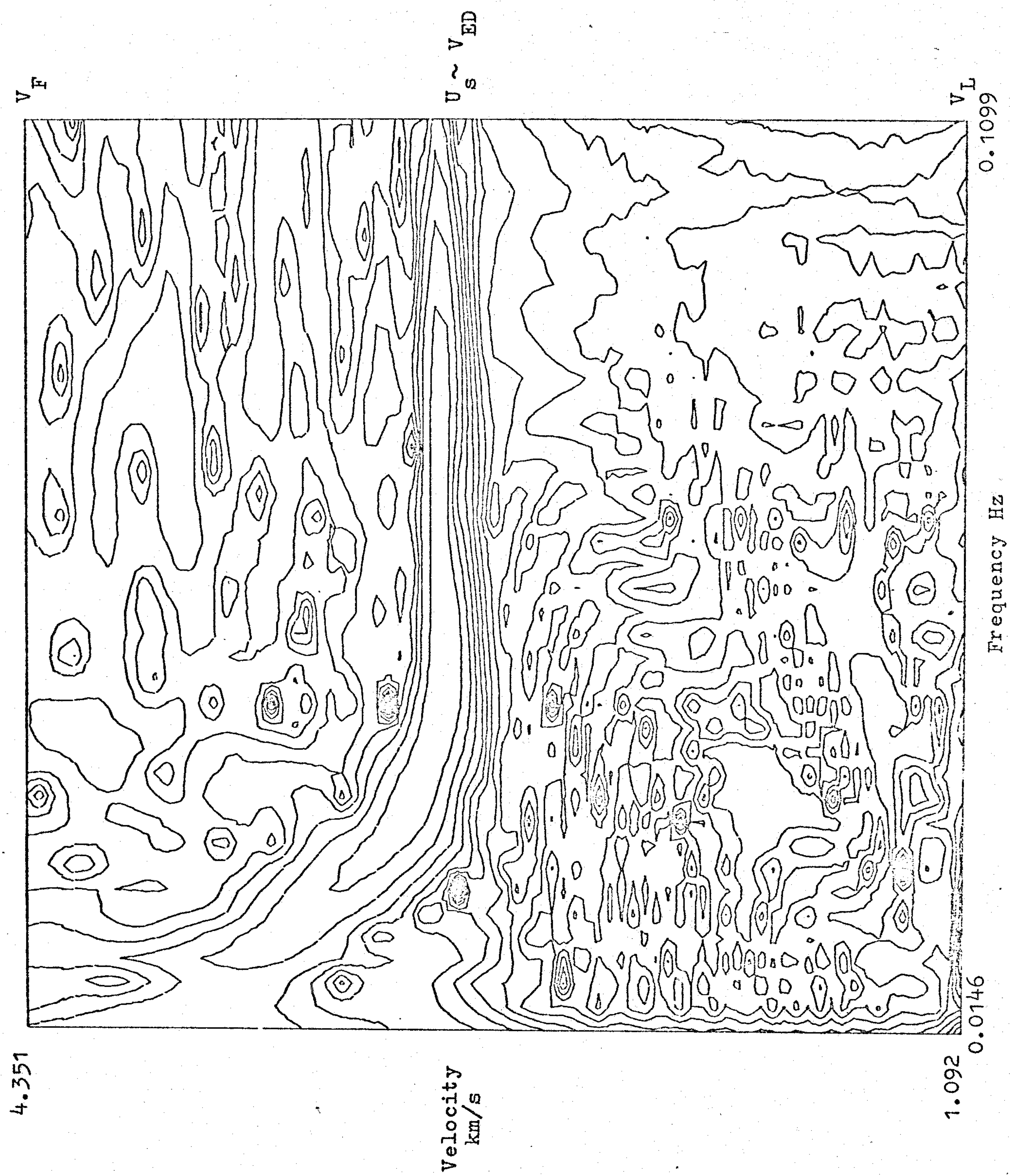

Figure 2.9 The Contoured E Matrix After Redetermining the End of the Lahore Seismogram.

into the form amplitude and group velocity as a function of Δ at fixed frequency, so that spatial Q may be determined. The required plot is given by equation 1.11 as

$$\log_{10}(A(f,r)) + 0.5 \log_{10}(E \sin \Delta) = -(Q^{-1})(\pi f E \Delta / U(f,r)) + \text{const} \qquad 2.10$$

where the left hand side is plotted as ordinate and $\pi f E \Delta / U$ as abscissa. The slope of the best line through these points estimates Q^{-1}. Note that it is inverse Q, not Q, which is physically estimated; the more natural and useful quantity of Q^{-1} will be used.

Appendix G contains the program AVD which performs this data manipulation, geometrical spreading correction and estimation of Q^{-1}. From a measure of the scatter of the data points about the best line confidence limits for Q^{-1} are also determined.

2.5 The Best Line

2.5.1 Average Q^{-1}

Simple linear least squares regression was found to be a very close approach to the best line fit, and is thus used. The program AVD contains a subroutine which determines regression coefficients and hence Q^{-1} and the confidence limits.

The basic assumption for this regression is that the ordinate alone contains errors. The present data are a good approximation to this, the errors in amplitude measurements being far greater than for group velocity.

This is easily demonstrated by considering surface wave magnitudes. An underground explosion, MILROW, has average surface wave magnitude determined by the USCGS as $M_s = 5.0$. Using the formula

$$M_s = \log_{10} Y + 2.0 \qquad 2.11$$

gives the yield Y kton as 1000 kton. The event is large and good signal-to-noise is generally to be expected. M_s values are calculated from formulae of the type

$$M_s = \log A(T) + B(\Delta) \qquad 2.12$$

where $B(\Delta)$ is a distance correction term. Ideally an event gives the same M_s value wherever it is recorded, with good signal-to-noise the scatter should be small and attributable to 10% errors in instrument magnification and hence in the amplitude A. The recording at Blacknest of MILROW gave $M_s = 4.52$, an apparent deviation from the mean magnitude of 10% (Marshall, Corbishley and Gibbs 1970). This would imply an error in A of 300%, obviously this is not so. In some way the path between MILROW and Blacknest is anomalous, the measured amplitude is in error by about 10% but is anomalous by a much greater margin.

But <u>average</u> Q^{-1} is being estimated. A reasonably accurate measurement of amplitude at a station may have a large anomaly margin from the expected value. For least squares fitting purposes such anomalous deviations must be regarded as "errors", and as shown above of the order of 10% errors. Also, because the average is sought, any extremely anomalous values must be subjectively rejected, this was done rarely. If many events at the same site had been used it would have been possible to isolate these anomaly margins as station path corrections.

Errors in the ordinate are possibly 10% whilst about 0.25% in the group velocity. The ratio of errors between the two axes is 40:1, this is possibly optimistic but an order of magnitude certainly prevails. Simple linear regression is therefore a good approximation to the best line. A more sophisticated regression fitting is described in Appendix D, and the errors in reducing this to the present case are discussed there.

It is worth noting that the abscissa term also contains the variables Δ and f, errors in the abscissa will compound to form

$$\frac{\delta''x''}{''x''} = \frac{\delta\Delta}{\Delta} + \frac{\delta f}{f} - \frac{\delta U}{U}.$$

Ignoring $\delta\Delta$ leaves δf and δU, the importance of ensuring that group velocity and amplitude are measured at the same exact frequencies is again apparent.

A typical plot of amplitude/distance at frequency 0.0525 Hz

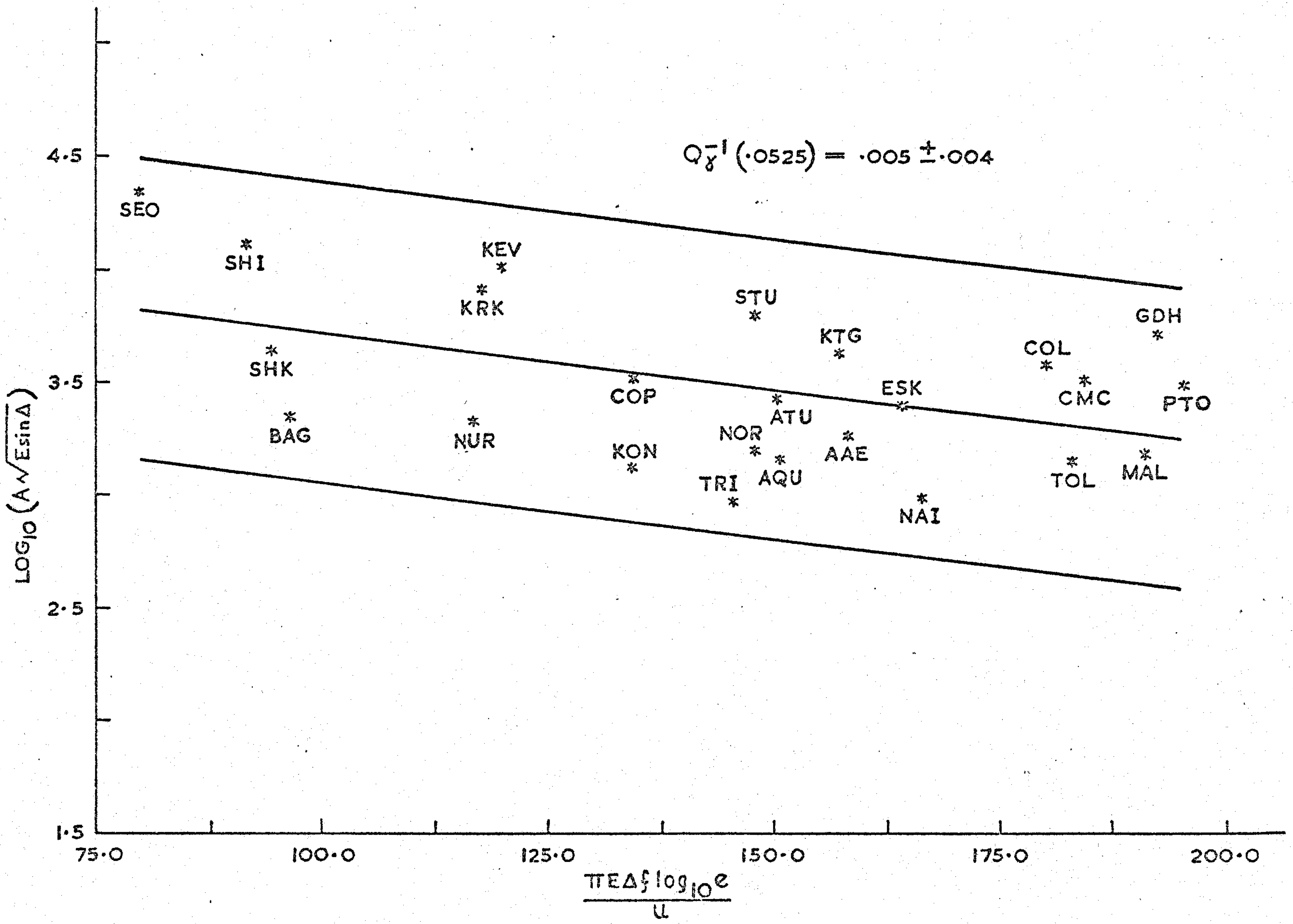

FIGURE 2.10 AN AMPLITUDE – DISTANCE PLOT FOR AN ATMOSPHERIC EXPLOSION AT S. SINKIANG PROV., CHINA (17th JUNE 1967. FREQUENCY = 0·0525 Hz. THE REGRESSION LINE AND 95% SCATTER ARE MARKED)

is shown in Figure 2.10, this gave a value of Q_{γ}^{-1} = .005 $\pm$ .004, with 95% confidence limits. Student's t for this line is 2.62, significant at the 98% level, implying that there is good correlation between the ordinate and abscissa, this reasserts that a line is a good curve to fit to this data. (The correlation coefficient = -.49.)

Figure 2.10 also shows the deviation of the individual data points from the least squares line, these deviations are in agreement with the preceding argument concerning the variation of M_s values.

2.5.2 Assumptions for Linear Regression

Using linear regression with one independent variable assumes that the ordinate, y_{ij}, is a normal deviate distributed about a mean μ_i which is of the form $\alpha + \beta\ (x_i - x)$ with variance σ_i^2, and all variances are equal (Miller and Kahn 1962).

To test normality it would be necessary to have n_i values of the amplitude (for one frequency) at each station, this would require a series of similar explosions detonated at the same site. This cannot be tested when n_i is small as in this study, further, the explosions are all different and unrepeatable events. To test for equal variances it would be necessary to apply Bartlett's test, again impossible when n_i is small.

The assumption of linearity is adequately tested by calculation of the correlation coefficient and Student's t for each line.

2.6 Summary

This chapter has described the data used and its analysis to produce spectral amplitudes and group velocities for the fundamental Rayleigh mode, both for varying frequency and distance. The data was then manipulated to produce arrays of amplitude against distance at a frequency. The slope of the best line (chosen to be linear regression with one independent variable) through these data points is the required estimation of Q^{-1}.

CHAPTER 3

3.1 The Estimations of $Q_\gamma^{-1}(f)$

The techniques described in the previous chapter were used to produce values of Q_γ^{-1} as a function of frequency. This was done for each of the nuclear explosions listed in Table 2.1 and one earthquake for comparison purposes. The 95% confidence limits around each $Q_\gamma^{-1}(f)$ value were also calculated. Values of $Q_\gamma^{-1}(f)$ and confidence limits are obtained from the best line fit to the amplitude/distance plot for a particular frequency, the program AVD performs this operation and it is described elsewhere. The results of this process are shown in the eight figures, 3.1-3.8, and listed in Appendix B.

Figure 3.8 shows the Q_γ^{-1} values obtained using eleven station recordings of an earthquake. As expected these results are very poor, and obviously this method is not applicable to an earthquake. The major reason for this is the radiation pattern which earthquakes usually possess. Also, earthquakes must necessarily occur in an anomalous environment; the local Q at source is probably laterally very inhomogeneous. Confidence limits are therefore very broad for the earthquake.

Nine recordings of the 80 kton "LONGSHOT" underground nuclear explosion (Marshall et al. 1966) were used to obtain Figure 3.7. Broad confidence limits are again apparent, especially at low frequencies, but these results are an improvement over the earthquake and use fewer stations. Broader confidence limits at the lower frequencies are to be expected because an underground explosion contributes more energy to the higher frequencies. However, in general these results are again poor probably because "LONGSHOT" occurred in another anomalous region - an island arc - where lateral inhomogeneities in Q are to be expected. The paper of Barazangi et al. (1972) well illustrates the unusual Q variations to be expected in such anomalous regions.

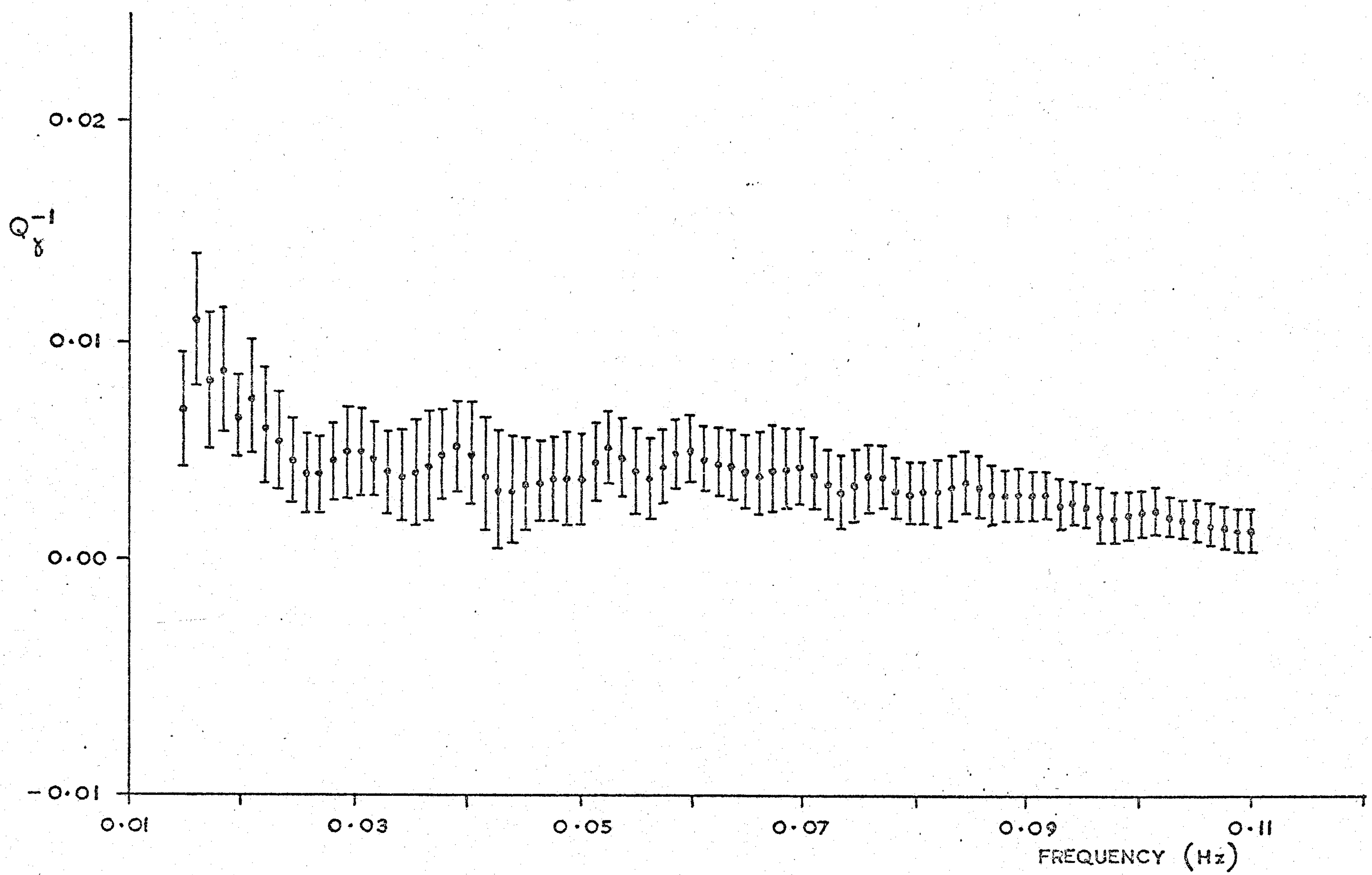

FIGURE 3.1 Q_γ^{-1} AND 95 P.C. CONFIDENCE LIMITS ESTIMATED USING 28 RECORDINGS OF THE ATMOSPHERIC EXPLOSION IN NOVAYA ZEMLYA, 27th SEPTEMBER 1962

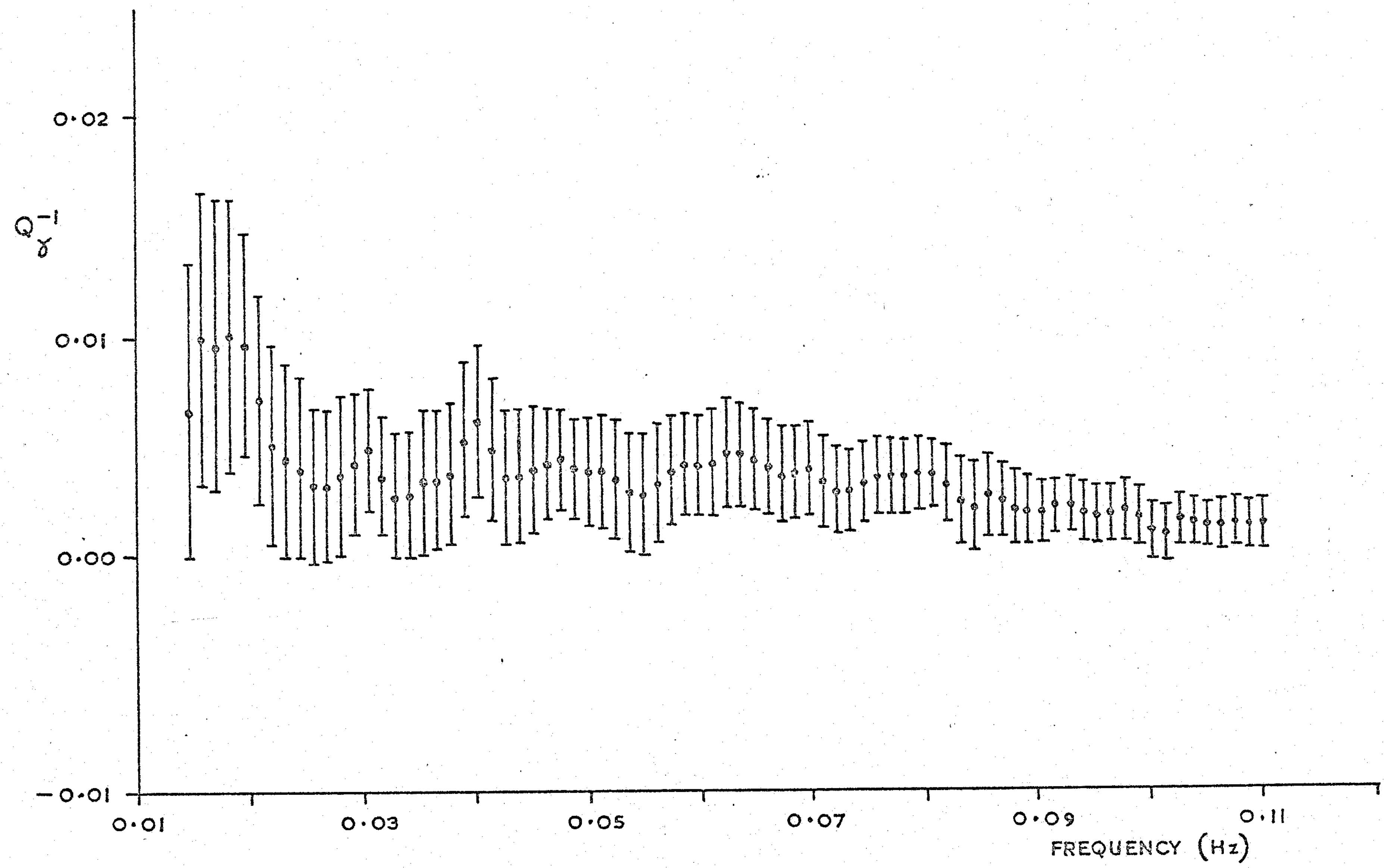

FIGURE 3.2 Q_γ^{-1} AND 95 P.C. CONFIDENCE LIMITS ESTIMATED USING 27 RECORDINGS OF THE ATMOSPHERIC EXPLOSION IN NOVAYA ZEMLYA, 22nd OCTOBER 1962

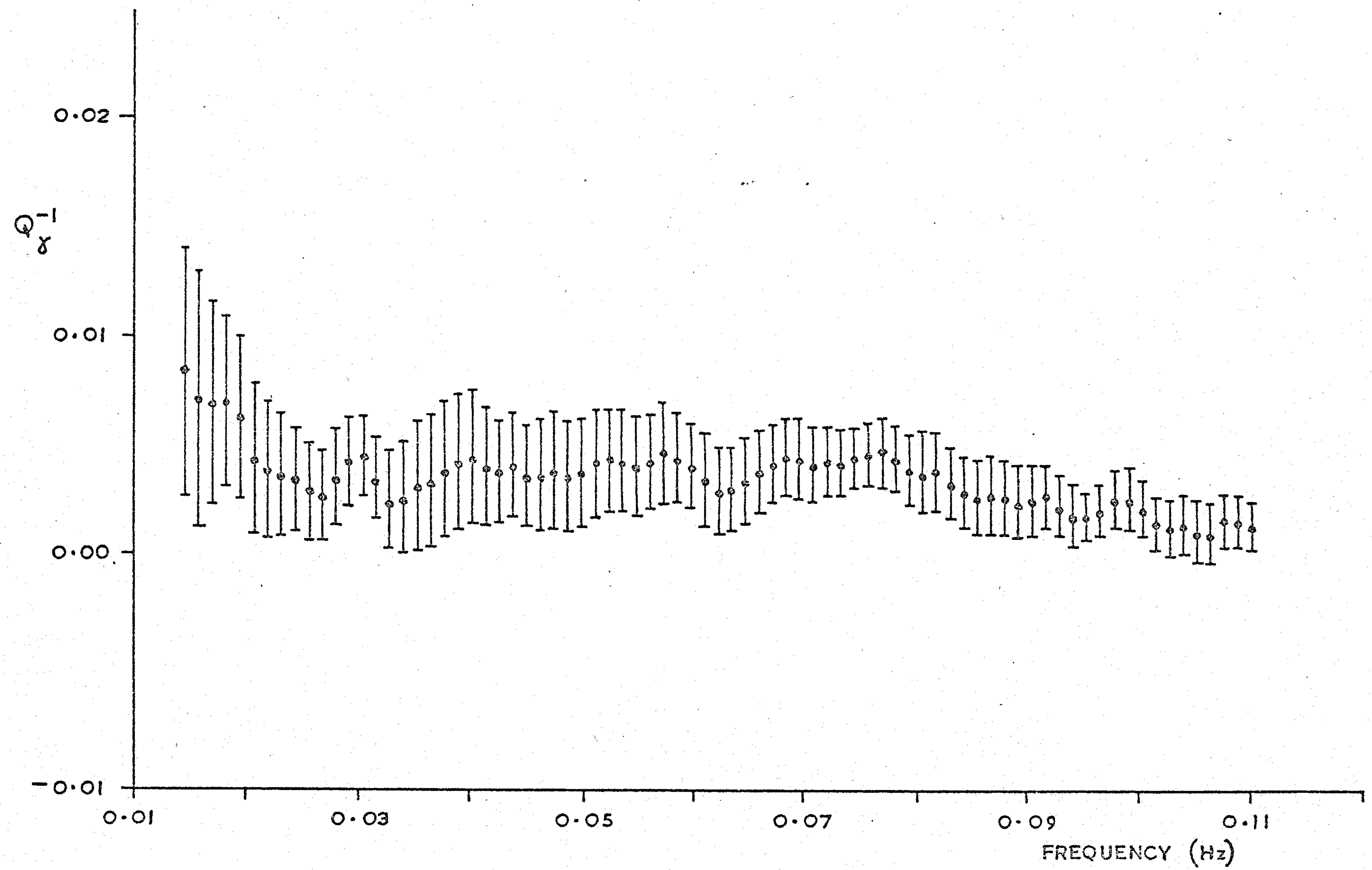

FIGURE 3.3 Q_γ^{-1} AND 95 P.C. CONFIDENCE LIMITS ESTIMATED USING 26 RECORDINGS OF THE ATMOSPHERIC EXPLOSION IN NOVAYA ZEMLYA, 24th DECEMBER 1962

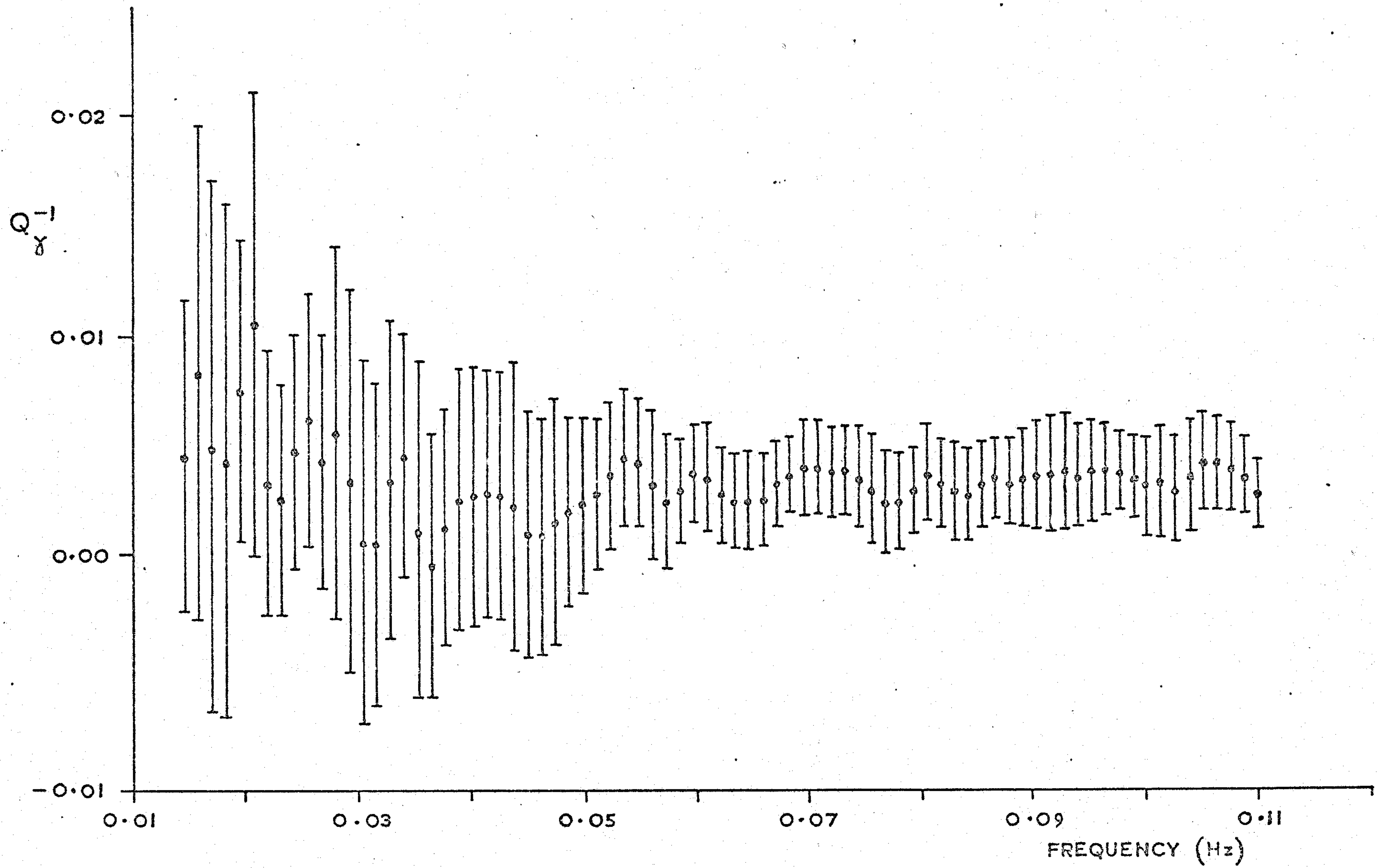

FIGURE 3.4 Q_γ^{-1} AND 95 P.C. CONFIDENCE LIMITS ESTIMATED USING 18 RECORDINGS OF THE UNDERGROUND EXPLOSION IN NOVAYA ZEMLYA, 7th NOVEMBER 1968

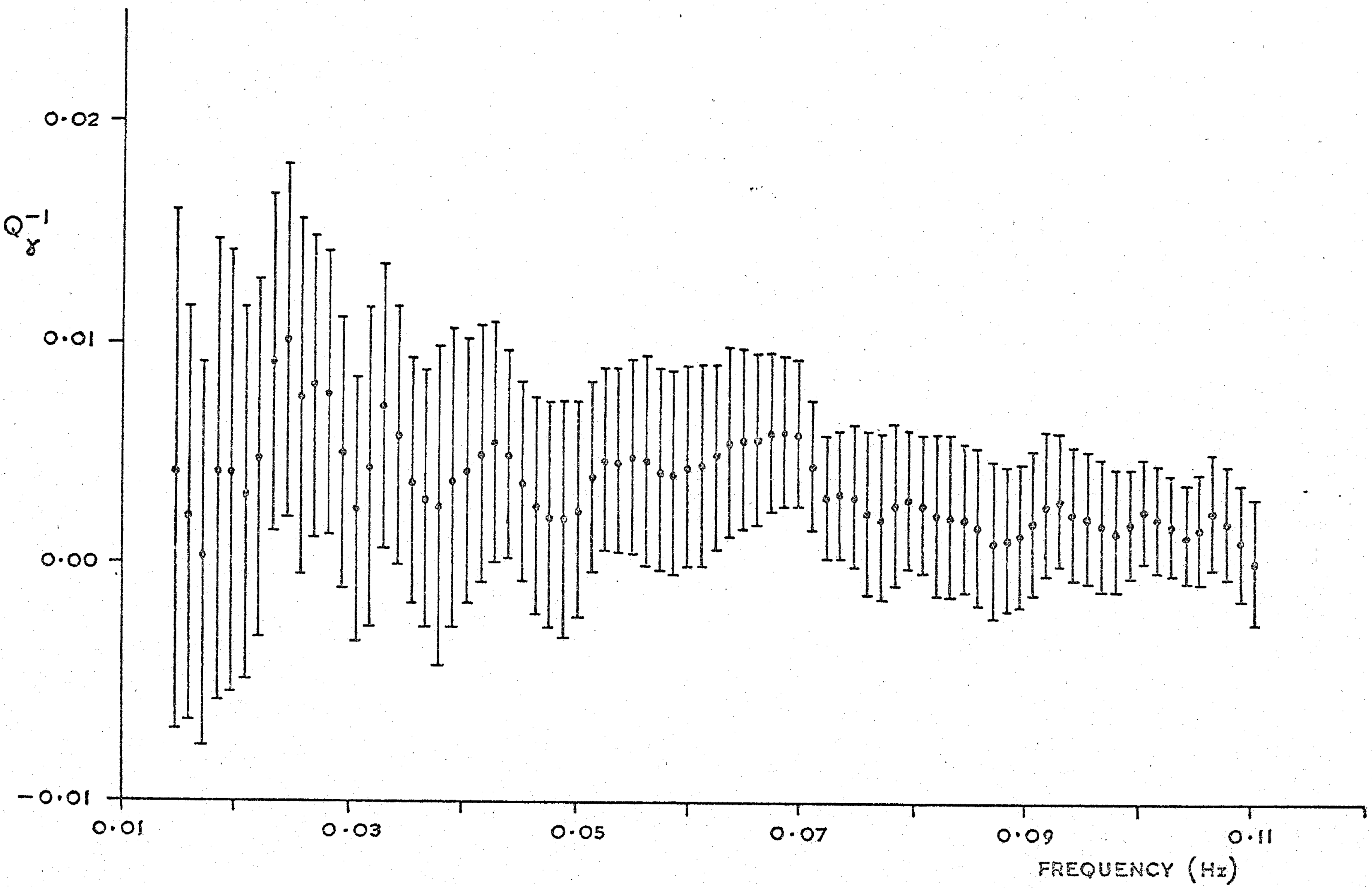

FIGURE 3.5 Q_γ^{-1} AND 95 P.C. CONFIDENCE LIMITS ESTIMATED USING 24 RECORDING OF THE ATMOSPHERIC EXPLOSION IN SOUTHERN SINKIANG PROV., CHINA, 17th JUNE 1967

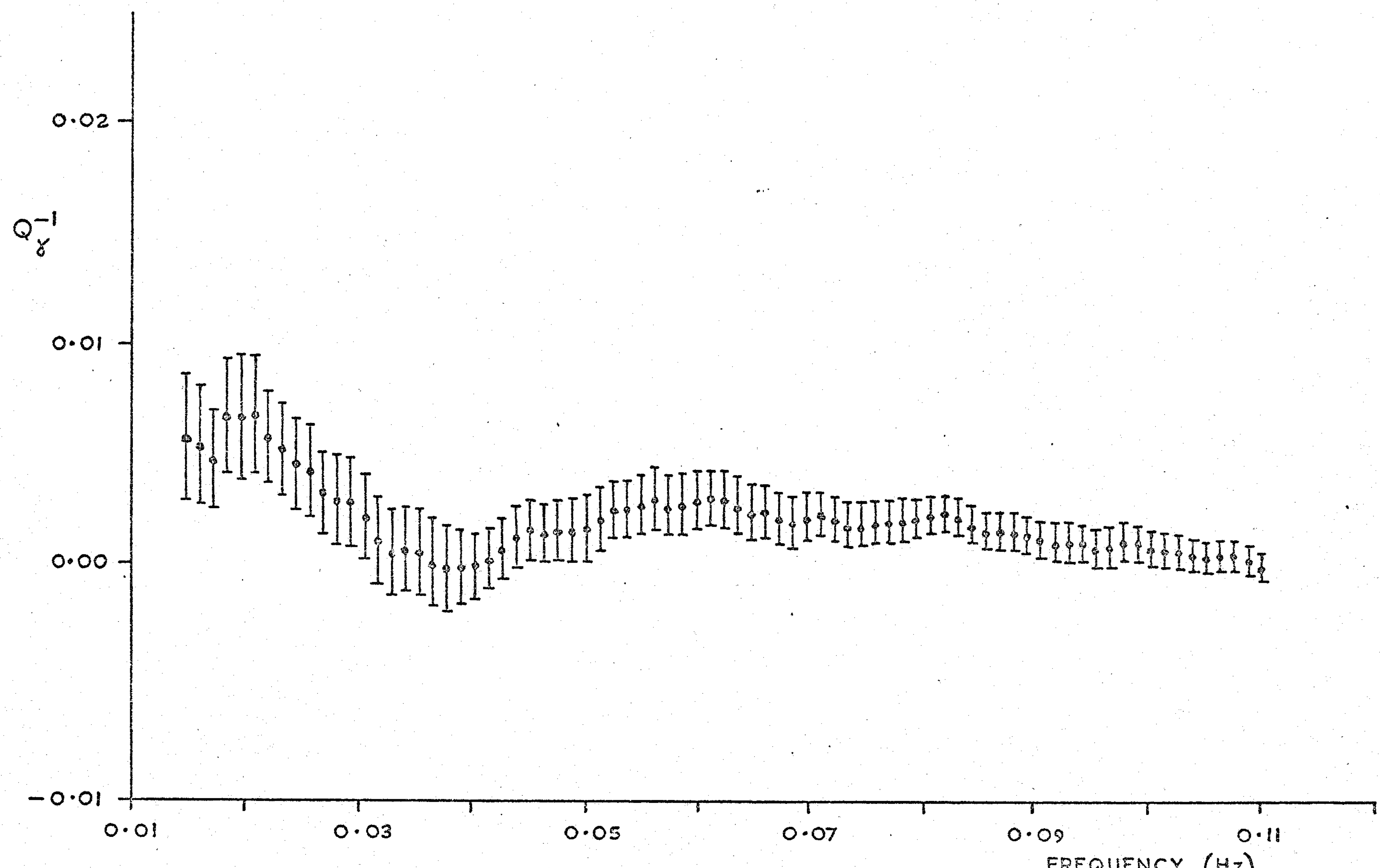

FIGURE 3.6 Q_γ^{-1} AND 95 P.C. CONFIDENCE LIMITS ESTIMATED USING 39 RECORDINGS OF THE ATMOSPHERIC EXPLOSION IN SOUTHERN SINKIANG PROV., CHINA, 29th SEPTEMBER 1969

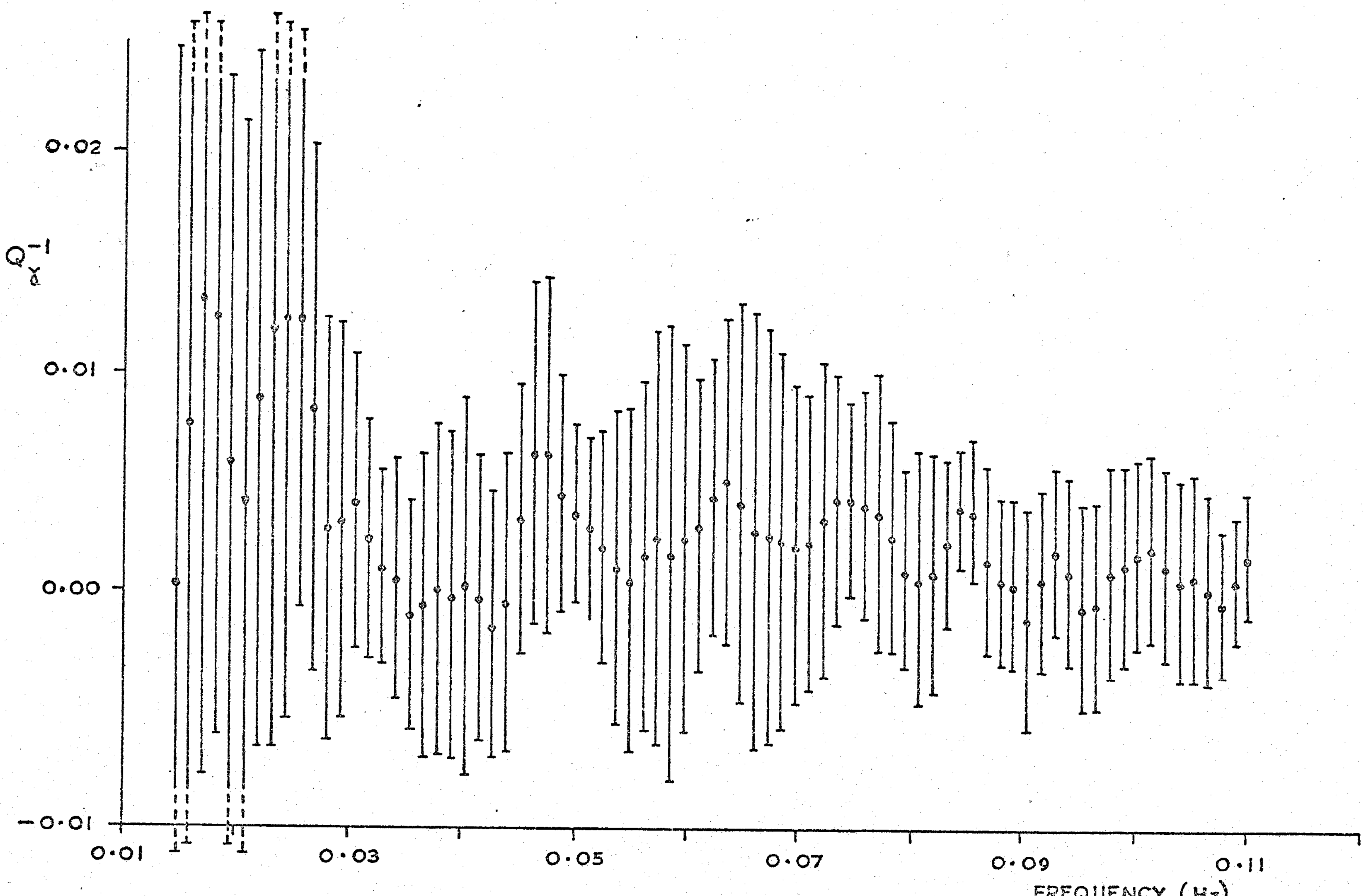

FIGURE 3.7 Q_{γ}^{-1} AND 95 P.C. CONFIDENCE LIMITS ESTIMATED USING 9 RECORDINGS OF THE UNDERGROUND EXPLOSION "LONGSHOT", ALEUTIAN ISLANDS, 29th OCTOBER 1965

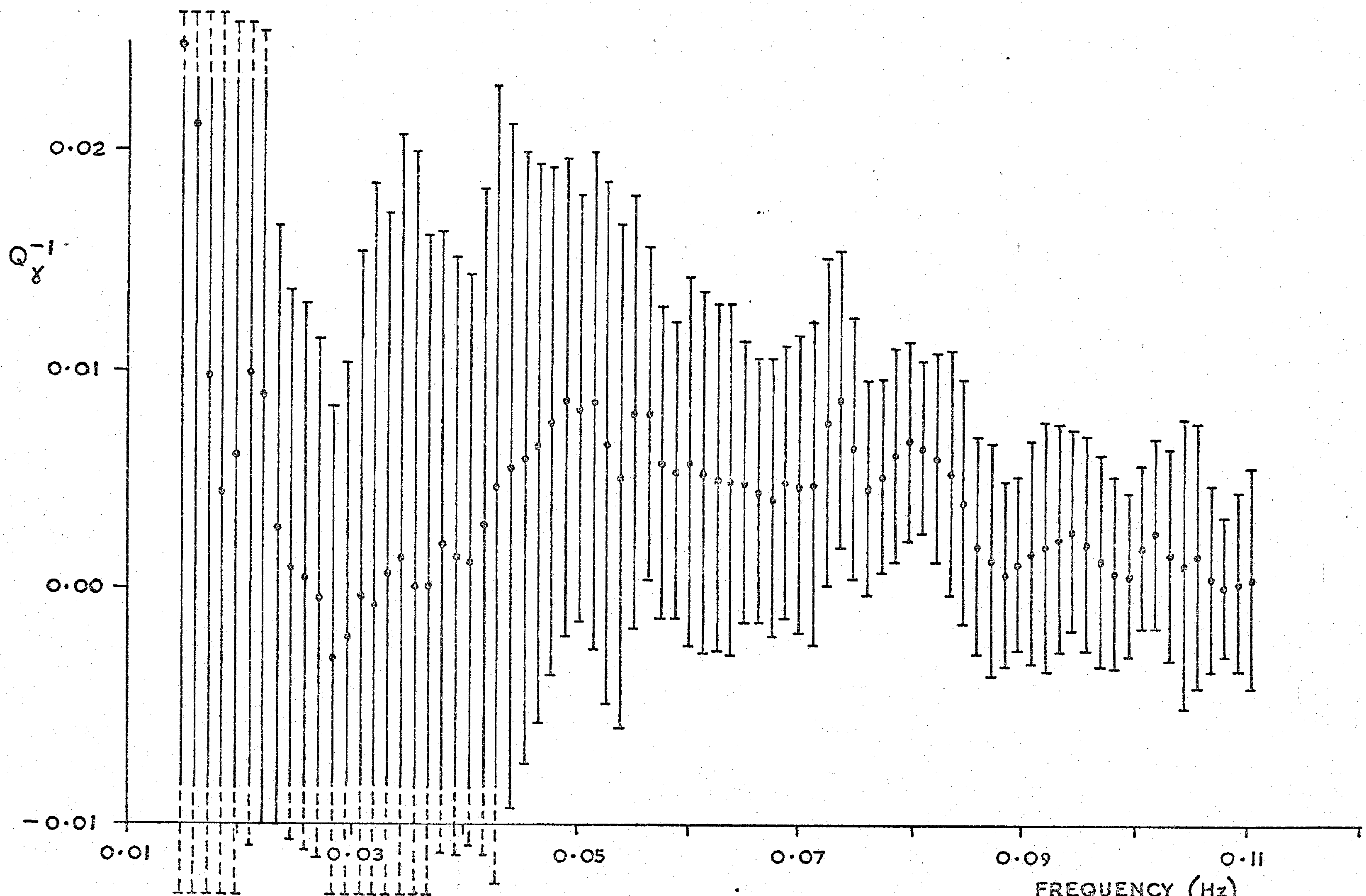

FIGURE 3.8 POOR RESULTS FOR Q_γ^{-1} USING 11 RECORDINGS OF AN EARTHQUAKE

Figures 3.1-3.6 show well determined $Q_\gamma^{-1}(f)$ values. These improvements have resulted for several reasons. Several station recordings of each event were used, the explosions occurred in "normal" regions and large explosions with good signal-to-noise were chosen.

It is worth noting that the stations SNG, CHG, JER and IST were omitted from the atmospheric explosion in China, 17/6/67, because they consistently plotted low on amplitude-distance plots, for example Figure 3.9. This implies anomalously highly attenuating paths to these stations, or incorrect instrument responses. All of these paths are influenced by the tectonically active Himalayas, presumably a region of particularly high Q_γ^{-1} has been traversed.

3.2 The Influence of Noise

3.2.1 Low Frequency Noise

The underground explosion at Novaya Zemlya shows the expected broader confidence limits at low frequencies, which improve for higher frequencies. Signal-to-noise was generally poorer for this event than the others, because underground contained explosions are generally smaller than uncontained atmospheric explosions.

It is generally true for all the events that the confidence limits broaden at the low frequencies. There are two factors contributing to this. The spectrum predicted by Carpenter and Marshall (1970) for an atmospheric explosion is about 7 db down from its peak value at frequency 0.02 Hz; also this corresponds to the region of instrument response roll-off for the vertical component, LP system, of the WWSSN, and so little propagation energy will be recorded by the seismogram from the event. Further these WWSSN instruments are barometrically uncompensated for atmospheric variations, and barometric noise is proportional to the period squared.

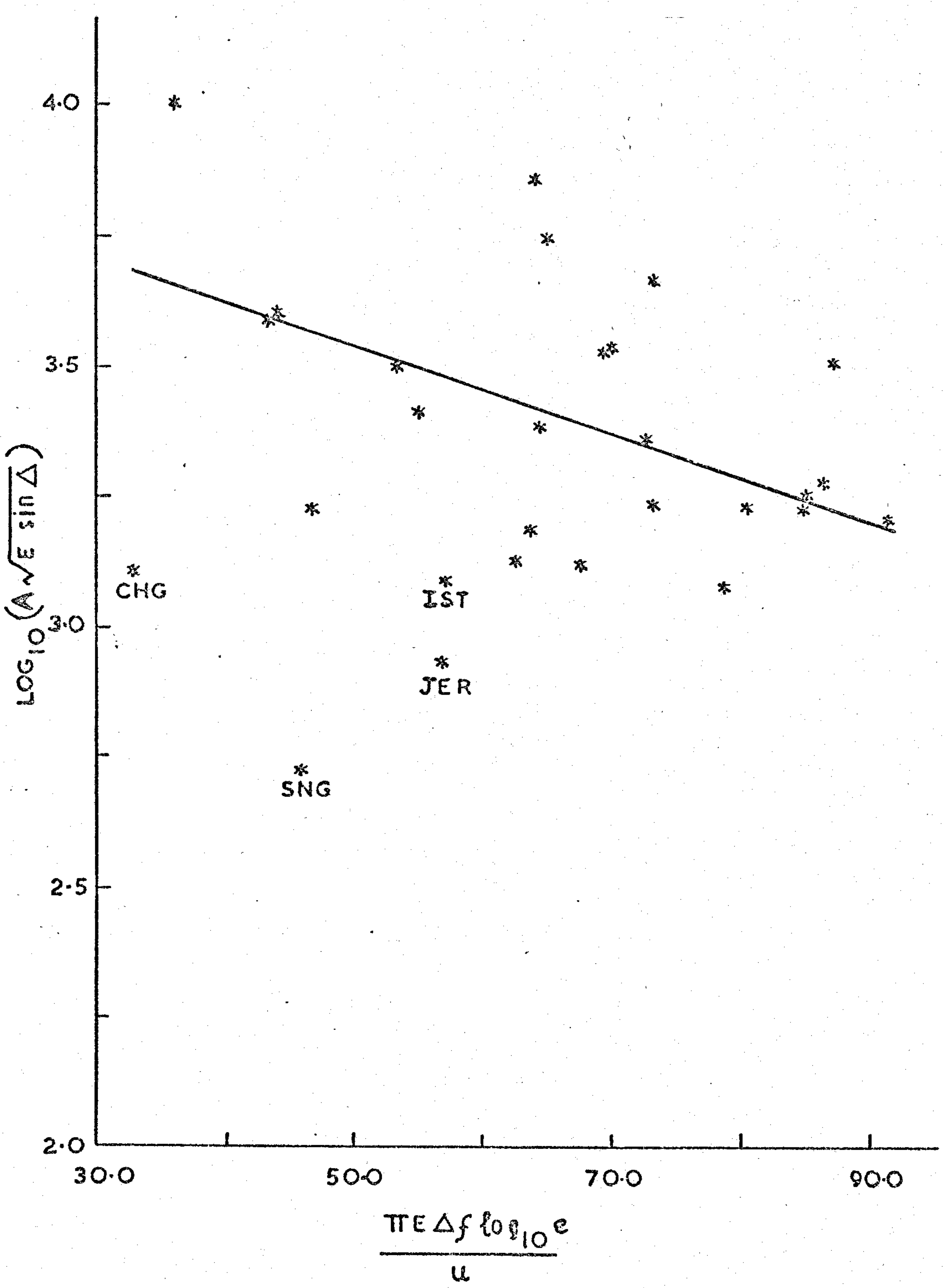

FIGURE 3.9 THE STATIONS CHG, SNG, IST, JER CONSISTENTLY PLOTTED LOW FOR THE EVENT CA 17/6/67
(FREQUENCY = ·0281 Hz, Q_γ^{-1} = ·008 ± ·006 for 24 STATIONS)

The net result is that long period energy propagated from an explosion is recorded at a low magnification and is contaminated by local barometric noise producing a broadening of the confidence limits at this end of the spectrum.

3.2.2 High Frequency Noise

For high frequencies the confidence limits narrow to a remarkable extent. Also, for the atmospheric explosions $Q_{\gamma}^{-1}(f)$ tends to zero for these high frequencies. This seems to imply that included in the spectral estimates of the Rayleigh fundamental mode is a large amount of non-propagating energy, local station noise. Brune and Oliver (1959) have presented information demonstrating the existence of a long period noise peak around 8s period, and this noise peak will extend into and contaminate the high frequencies in this work. What has been plotted on the amplitude/distance graphs at high frequencies is the amplitude of the propagating fundamental Rayleigh mode plus local noise superimposed onto a geometrical spreading term (which generally increases with distance). The net result is a set of roughly similar values, decreasing very slowly with distance and implying little attenuation ($Q_{\gamma}^{-1} \rightarrow 0$). This result for the atmospheric explosions is contradicted by the one underground explosion (Novaya Zemlya) of Figure 3.4 which shows reasonable attenuation at high frequencies, $Q_{\gamma}^{-1} = 0.004$. This is simply because the underground explosion does generate propagating energy of high frequencies, whereas the atmospheric explosions contain very little energy at high frequencies in comparison to the local non-propagating noise. This raises the problem how much real data is contained in the results for each event; up to what frequency may it be assumed that the energy recorded has been propagated from the event and a value of spatial Q_{γ}^{-1} may be assigned?

Three separate items of information were used to determine the highest useful frequency contained by each seismogram. For each seismogram the graphs of unwound spectral phase, spectral amplitudes and the group velocity curve were required. An example of a typical seismogram is shown in Figure 3.10, recorded at Kevo from the atmospheric explosion of September 29 1969 at S Sinkiang Province, China. This seismogram shows the low frequencies arriving first, but contaminated by the superposition of high frequency noise creating a typical signal-to-noise problem. Further along the record an Airy phase is seen with an obvious high frequency content. The Figures 3.11-3.13 show spectral phase, spectral amplitudes and the group velocity curve obtained from the Kevo seismogram. The highest useful frequency contained by the seismogram is now obtained as follows:

3.2.2.1 Spectral Phase and the Highest Signal Frequency

Figure 3.11 shows unwound spectral phase, that is, the phase is not allowed to oscillate between $-\pi$ and $+\pi$ but is made continuous. The subroutine DRUM (Robinson 1966) given by Burton and Blamey (1972) performs this operation. This phase curve would be perfectly smooth for a pure, noiseless signal. Figure 3.11 is smooth up to frequency 0.125 Hz where a small perturbation may be seen, this is the threshold of noise onset in the frequency domain for this signal. The perturbation marks the onset of random energy.

3.2.2.2 Spectral Amplitude and the Highest Signal Frequency

Spectral amplitudes are shown in Figure 3.12. This graph shows a distinct minimum at 0.125 Hz which divides the spectrum into the two expected regions of signal and noise. Obviously the choice of this particular point is more arbitrary than for the phase perturbation, but it does give a good estimate of the highest available frequency in the signal.

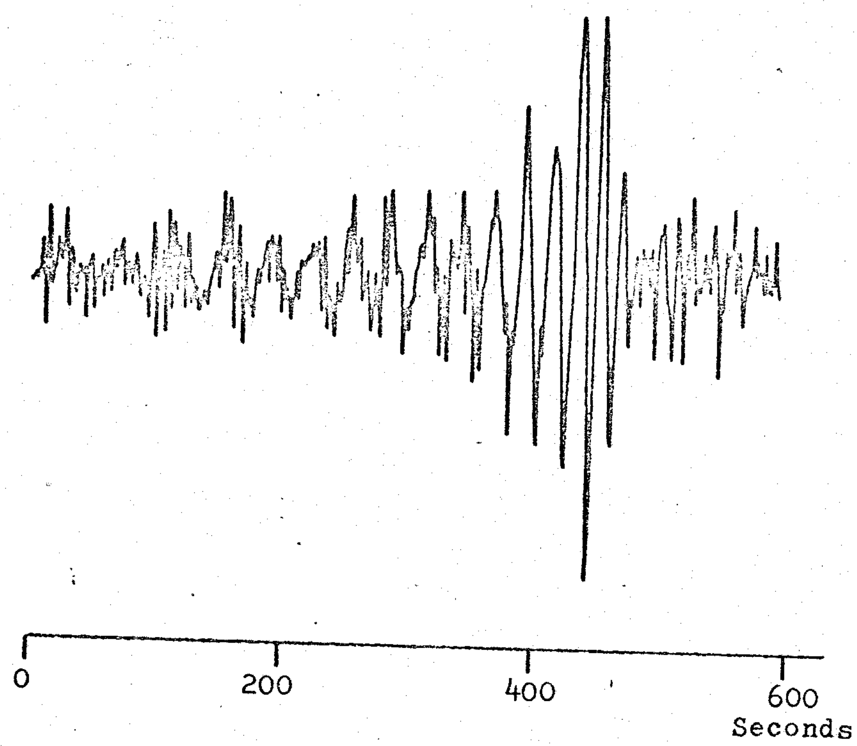

FIGURE 3.10

A Seismogram Recorded at Kevo, Finland (from an Atmospheric Explosion At S Sinkiang Prov, China, 29 September 1969. Distance = 4783 km).

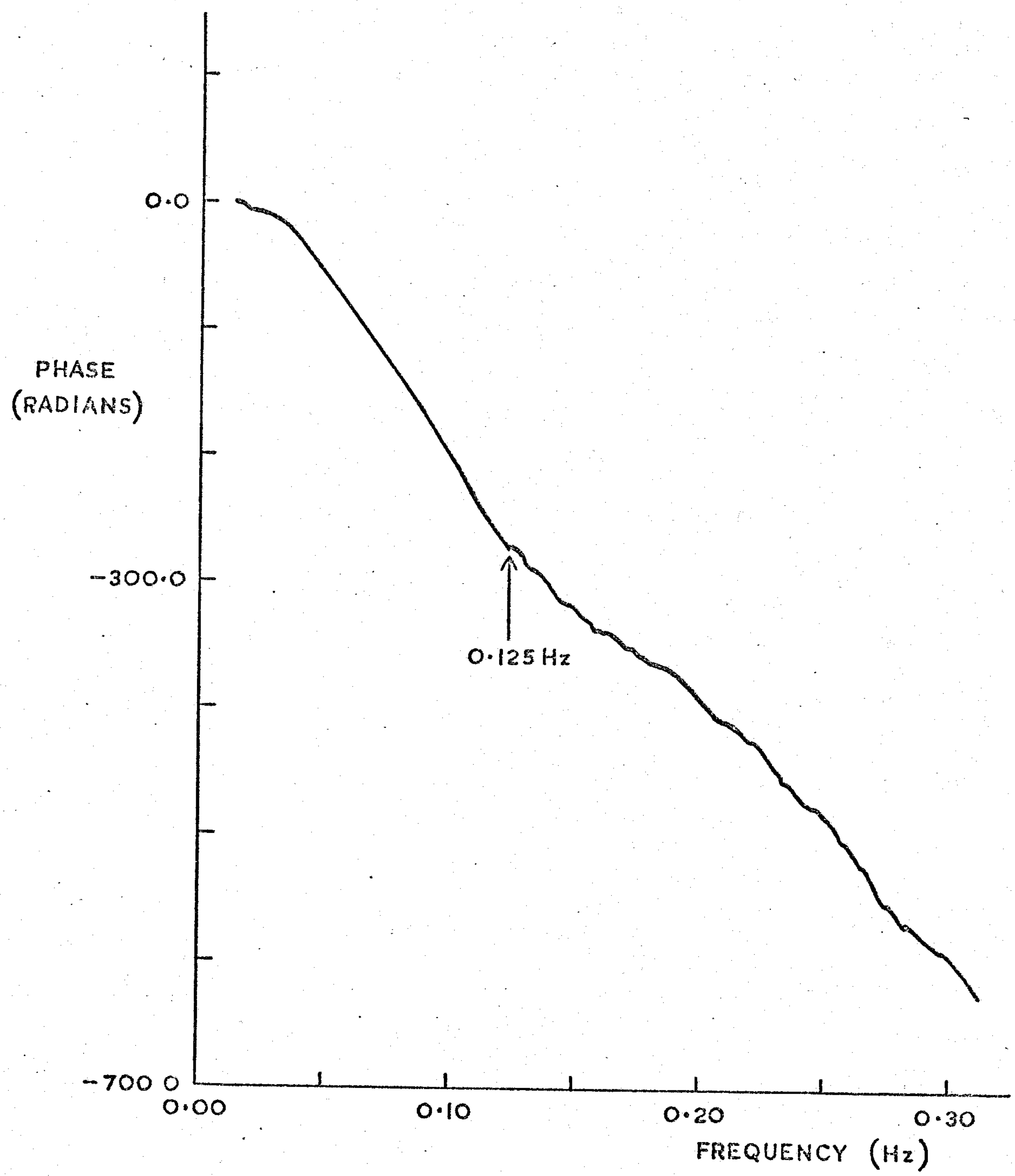

FIGURE 3.11 SPECTRAL PHASE ("UNWOUND PHASE") FOR THE KEVO SEISMOGRA
(NOTE THE PERTURBATION AT 0·125 Hz)

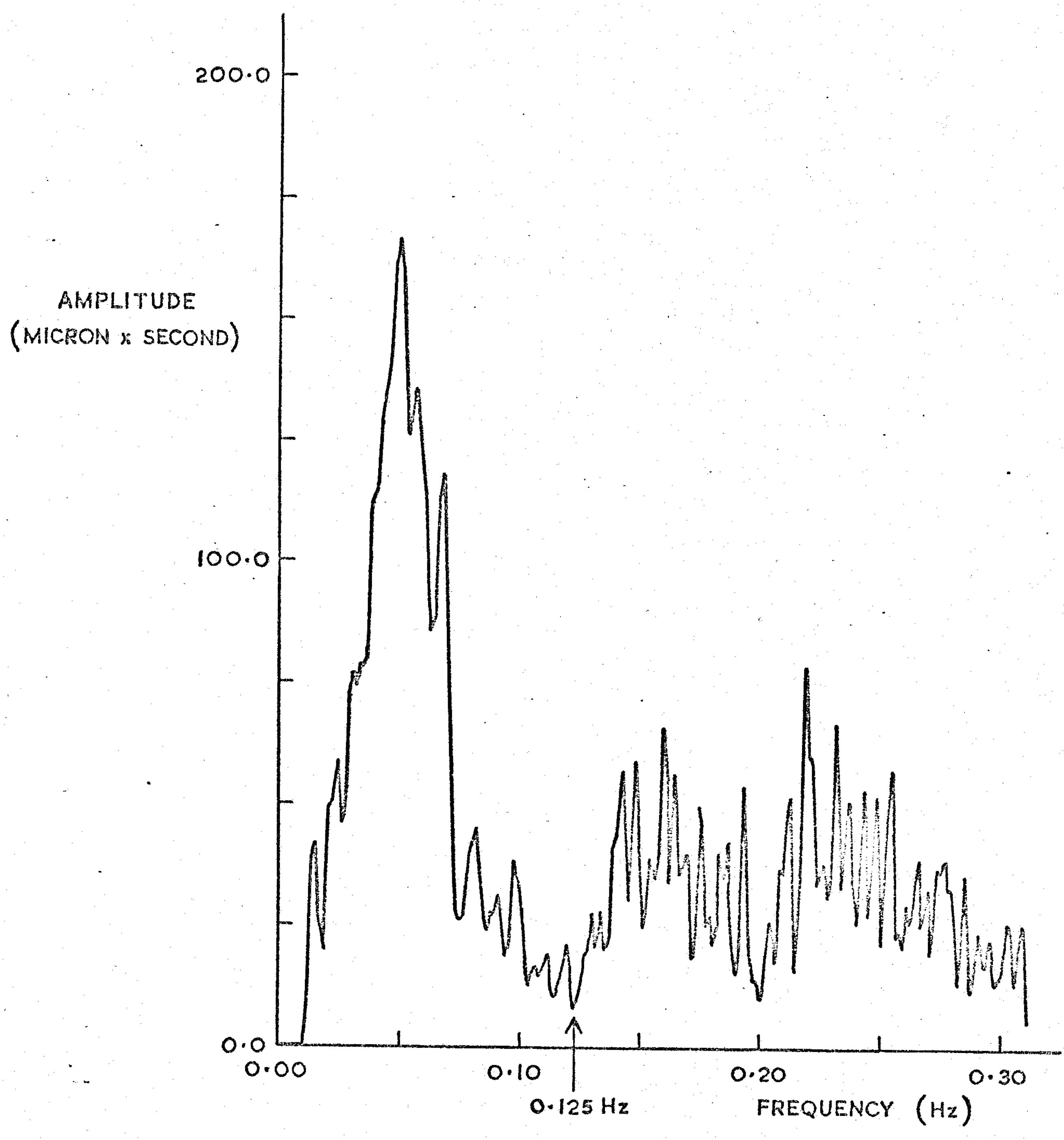

FIGURE 3.12 SPECTRAL AMPLITUDES FOR THE KEVO SEISMOGRAM (NOTE THE SIGNAL-NOISE SEPARATION AT 0·125 Hz)

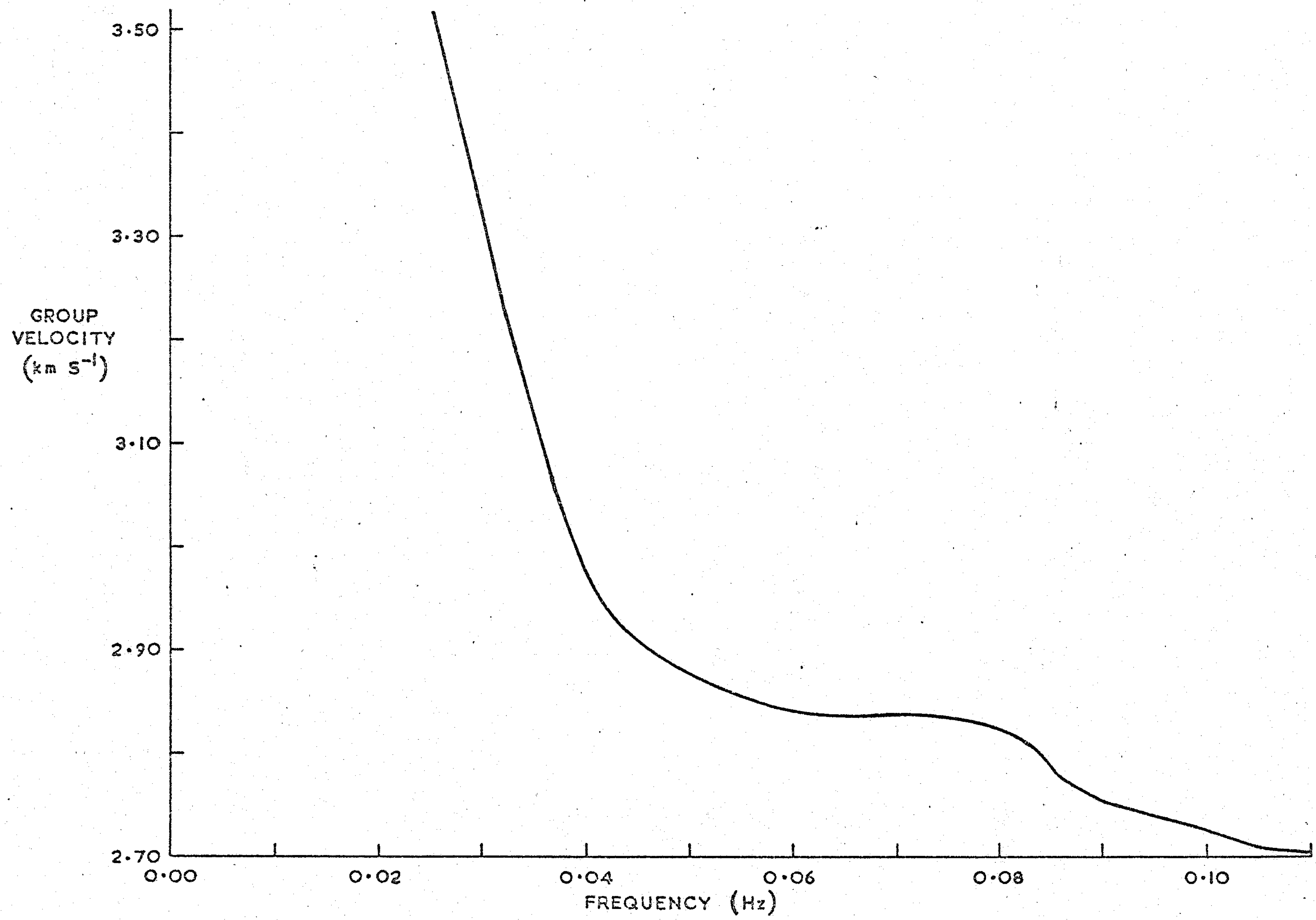

FIGURE 3.13 THE GROUP VELOCITY CURVE FOR THE KEVO SEISMOGRAM

3.2.2.3 Group Velocity and the Highest Signal Frequency

Figure 3.13 shows a perfectly good group velocity curve for the Kevo record. This is expected because the highest frequency has been demonstrated to be 0.125 Hz and so a representation which only goes to 0.11 Hz should be noise free. The frequency 0.11 Hz had been chosen as the highest frequency to be analysed and so this particular signal is good for processing in the entire frequency range of interest.

It has already been shown (section 2.3.3) that the group velocity curve will only contain spurious values at a particular frequency if the signal-to-noise ratio is worse than 1:1. This is a weak test to determine the highest frequency present in the signal, whereas the phase test will be shown to be far more restrictive.

These three measurements were made for all the seismograms. For the phase and amplitude curves a grid, drawn onto a transparent overlay, was used to give accurate measurements; this made the phase measurements especially accurate. A summary of the results obtained is in Table 3.1. If a higher frequency greater than 0.11 Hz was obtained from any measurement then it was subsequently set to 0.11 Hz to form the average for a particular event because this is the highest frequency to be used. The abbreviations A, U and Q mean atmospheric or underground explosion or earthquake, and NZ represents Novaya Zemlya, C, explosions in China etc. The term 3NZA is the average for the three atmospheric explosions at Novaya Zemlya.

Table 3.1 shows that the phase measurement is the most restrictive determination of the highest frequency, it always assigns a lower value than either of the other two methods.

Also note that as expected the underground explosion at Novaya Zemlya goes to higher frequencies than the atmospheric explosions at this site. Using the highest frequency obtained from phase measurements for the three atmospheric explosions, 3NZA, gives .0761$\pm$.0217 Hz and for the underground explosion, NZU, .0977$\pm$.0145 Hz. The validity of the average, 3NZA, is demonstrated later. If it is assumed that all events have the same highest frequency then these values are two samples from the same population, this hypothesis may be tested by calculating "Student's t" for the difference between the two means. The value of "t" obtained is 3.997 which for 95 degrees of freedom is significant at the 99.99% level. The comparable "t" values for the columns headed Amplitude, Group Velocity and Average Result are 5.489, 2.744, 4.147 and are significant at 99.99, 99.9, 99.99% levels respectively. The relatively high frequency content of the underground bomb is confirmed; the importance of this will be seen later.

3.3 Statistical Comparison of the $Q_\gamma^{-1}(f)$ values

Two types of comparison of the $Q_\gamma^{-1}(f)$ data are required. The first comparison uses a single event and takes a Q_γ^{-1} value at a particular frequency and compares it to the Q_γ^{-1} values at all the other frequencies, the process cycles through all the frequencies in turn. This essentially tests to see if $Q_\gamma^{-1}(f)$ is frequency dependent, albeit a pseudo dependence on frequency.

The second type of comparison is between two events. The Q_γ^{-1} are compared between the two events at corresponding frequencies, to determine if the values obtained are statistically different.

The values of Q_γ^{-1} have been determined using linear regression which assumed a line of the type

$$Y = Q_\gamma^{-1} X + b \qquad 3.1$$

Event	Number of Stations	1. Phase	2. Amplitude	3. Group Velocity	Average Result
NZA 27. 9.62	28	.0736±.0189	.0763±.0046	.0843±.0200	.0782±.0164
NZA 22.10.62	27	.0794±.0188	.0841±.0190	.0867±.0180	.0828±.0190
NZA 24.12.62	26	.0754±.0256	.0779±.0228	.0812±.0342	.0798±.0285
NZU 7.11.68	18	.0977±.0145	.1032±.0109	.1018±.0157	.1029±.0142
CA 17. 6.67	24	.0846±.0211	.0956±.0151	.0942±.0173	.0910±.0184
CA 29. 9.69	39	.0797±.0186	.0831±.0178	.0830±.0158	.0818±.0177
3NZA Average	81	.0761±.0217	.0794±.0175	.0841±.0254	.0803±.0219
2CA Average	63	.0816±.0199	.0879±.0171	.0873±.0166	.0853±.0181
5A Average	144	.0785±.0209	.0831±.0173	.0855±.0220	.0825±.0202
LONGSHOT "L"	9	.0711±.0105	.0756±.0106	.0789±.0135	.0761±.0123
EARTHQUAKE "Q"	11	.0836±.0145	.0923±.0156	.0846±.0107	.0846±.0101

Table 3.1 The highest useful signal frequencies Hz determined using

1 Spectral phase,

2 Spectral amplitudes and

3 The group velocity curve.

where Y and X are amplitude and distance terms, Q_{γ}^{-1} and b the line gradient and intercept. A data set of n pairs of observables, (x_{1i}, y_{1i}), approximates to 3.1 but is scattered about it. The confidence limits on Q_{γ}^{-1} values are one instance of this scatter. A second data set, (x_{2i}, y_{2i}), will again be of the form 3.1. Whether the two data sets are from different events, but at the same frequency, or from the same event but at different frequencies does not matter - the problem is to compare two regression lines. The theory described by Brownlee (1965, p349---) has been incorporated into the programs CNL and C2L (Appendices E and G) to perform the comparisons in the two cases.

The first test performed is Fisher's F test on the ratio of the residual variances about the two regression lines. This test indicates if both lines are samples from the same parent population, and if this test is failed (Not from the same population) then no more tests are conducted. The second test takes the two values of gradient, that is $Q_{\gamma}^{-1}|_1$ and $Q_{\gamma}^{-1}|_2$, assumes they are equal, and then calculates a statistic to check this hypothesis. All tests are performed at the 95% confidence level. In all cases failure of a test is indicated by 0, success by 1, and a 2 indicates that a test has not been performed.

3.3.1 Q_{γ}^{-1} as a Function of Frequency

The tests on each event to investigate the regression coefficients as a function of frequency produce a 79 x 79 triangular matrix (79 frequencies were analysed). A typical result sheet for the F test is shown in Figure 3.14 and this was conducted on the event NZA 24/12/62.

The simple representation of Figure 3.14 quickly produces an important result. The data distinctly divides into two populations. There is a low frequency population for .0354 Hz and below, and a high frequency population beyond this point. Each population forms a distinct triangle, divided by a rectangular area for which no further tests may be performed because the variances of the two populations are unequal.

NOVAYA ZEMLYA 24/12/62 ATMOSPHERIC 26 STATIONS

F TEST MATRIX

```
Frequency
0.01465  2
0.01587  12
0.01709  112
0.01831  1112
0.01953  11112
0.02075  111112
0.02197  1011112
0.02319  10111112
0.02441  000111112
0.02563  0001111112
0.02686  00011111112
0.02808  001111111112
0.02930  0001111111112
0.03052  00011111111112
0.03174  001111111111112
0.03296  1111111111111112
0.03418  11111110000000012
0.03540  111000000000000012
0.03662  1110000000000000112
0.03784  11000000000000001112
0.03906  010000000000000011112
0.04028  0100000000000000011112
0.04150  11000000000000001111112
0.04272  111000000000000011111112
0.04395  1110000000000000111111112
0.04517  11100000000000001111111112
0.04639  010000000000000001111111112
0.04761  0000000000000000011111111112
0.04883  01000000000000000111111111112
0.05005  000000000000000001111111111112
0.05127  0000000000000000011111111111112
0.05249  00000000000000000111111111111112
0.05371  000000000000000001111111111111112
0.05493  0000000000000000011111111111111112
0.05615  00000000000000000111111111111111112
0.05737  000000000000000001111111111111111112
0.05859  0100000000000000011111111111111111112
0.05981  01000000000000000111111111111111111112
0.06104  000000000000000001111111111111111111112
0.06226  0000000000000000011111111111111111111112
0.06348  01000000000000000111111111111111111111112
0.06470  010000000000000001111111111111111111111112
0.06592  0100000000000000011111111111111111111111112
0.06714  01000000000000000111111111111111111111111112
0.06836  010000000000000001111111111111111111111111112
0.06958  0100000000000000011111111111111111111111111112
0.07080  01000000000000000111111111111111111111111111112
0.07202  110000000000000001111111111111111111111111111112
0.07324  1110000000000000011111111111111111111111111111112
0.07446  11100000000000000111111111111111111111111111111112
0.07568  111000000000000001111111111111111111111111111111112
0.07690  0100000000000000011111111111111111111111111111111112
0.07813  11000000000000000111111111111111111111111111111111112
0.07935  010000000000000001111111111111111111111111111111111112
0.08057  0000000000000000011111011111111111111111111111111011112
0.08179  00000000000000000111111111111111111111111111111111111112
0.08301  010000000000000001111111111111111111111111111111111111112
0.08423  0100000000000000011111111111111111111111111111111111111112
0.08545  00000000000000000111111111111111111111111111111111111111112
0.08667  0000000000000000011110111111111111111111111111111110111111112
0.08789  0000000000000000011111111111111111111111111111111101111111112
0.08911  00000000000000000111111111111111111111111111111111111111111112
0.09033  000000000000000001111111111111111111111111111111111111111111112
0.09155  0100000000000000011111111111111111111111111111111111111111111112
0.09277  01000000000000000111111111111111111111111111111111111111111111112
0.09399  010000000000000001111111111111111111111111111111111111111111111112
0.09521  1110000000000000011111111111111111111111111111111111110111101111112
0.09644  11100000000000000111111111111111111111111111111111111111111111111112
0.09766  010000000000000001111111111111111111111111111111111111111111111111112
0.09888  0000000000000000011111111111111111111111111111111111111111111111111112
0.10010  01000000000000000111111111111111111111111111111111111111111111111111112
0.10132  010000000000000001111111111111111111111111111111111111111111111111111112
0.10254  0100000000000000011111111111111111111111111111111111111111111111111111112
0.10376  00000000000000000111111111111111111111111111111111111111111111111111111112
0.10498  000000000000000001111011111111111111111111111111111011111111111111101111111 2
0.10620  0000000000000000011110111111111111111111111111111110111111111111111011111111 2
0.10742  00000000000000000111111111111111111111111111111111111111111111111111111111112
0.10864  000000000000000001111111111111111111111111111111111111111111111111111111111112
0.10986  0100000000000000011111111111111111111111111111111111111111111111111111111111112
```

FIGURE 3.14

Results of Inter-Frequency "F" Tests for NZA 24/12/62 (0 Indicates Test Failed, 1 Test Passed, 2 Test not Conducted).

It is worth noting Scheffe's (1964) observations concerning the effects of non-normality on the variance ratio. If non-normality is present, specified by finite kurtosis, then confidence levels are affected. But inequality of variances has little effect on inferences about means if the degrees of freedom are equal for the two variances, although inferences about variances will be seriously affected. However, explanations other than non-normality seem more likely for the two apparent regions.

It will later be seen that a Rayleigh wave frequency, .0354 Hz, correspondsto an approximate depth of penetration, 110 kms. This corresponds to the expected geophysical change from lithosphere to asthenosphere, where lateral variations in Q_{γ}^{-1} may be widespread. Such variations would influence the variance of any estimate of Q_{γ}^{-1}. Also, a subsequent inversion of this $Q_{\gamma}^{-1}(f)$ data shows the presence of a high Q^{-1} layer, which is only sampled by the low frequency population.

Instrumental roll-off and the lack of barometric compensation in the WWSSN seismometers also exacerbate the signal-to-noise problem at low frequencies, and must lead to increased variance for these Q_{γ}^{-1} estimates.

The second test, comparing the individual Q_{γ}^{-1} values or gradients, shows that the values in each population are comparable within that population, but where the F test had failed no comparisons were made.

For this event it therefore appears that two regions of Q_{γ}^{-1}, in terms of frequency, have been observed. From Figure 3.1 it is apparent that the low frequency population is of higher Q_{γ}^{-1}, and experiences greater attenuation.

A similar division was found for the other events of importance. The frequency at which the division occurred for each atmospheric explosion, the major events, is listed below.

Event	Highest Frequency of Low Frequency Population
NZA 24.12.62	.03418 Hz
NZA 27. 9.62	.03418 Hz
NZA 22.10.62	.03540 Hz
CA 17. 6.67	.03662 Hz
CA 29. 9.69	.03418 Hz

The mean frequency for this table indicates population division at 0.035 Hz.

3.3.2 $Q_\gamma^{-1}(f)$ Compared Between Events

It is necessary to compare the $Q_\gamma^{-1}(f)$ data between separate events at corresponding frequencies, it may then be possible to pool the data from such events and improve the results. The program used to carry out this comparison is C2L, it follows the testing procedure already described. Comparison of the events NZA 24.12.62 and NZA 27.9.62 produces the results shown in Figure 3.15. Columns headed NFTEST, NATEST give the result of the F test and then the gradient comparison test. If the gradients are comparable, statistically equal, a pooled gradient and confidence limits are also formed (otherwise this column is set to zero). The number of frequencies within the valid range for which the F test failed when comparing two events is summarised for several events in Table 3.2.

The data was then pooled to form the following averages. The three atmospheric explosions at Novaya Zemlya were averaged forming 3NZA, the two explosions in China formed 2CA. Finally, all the atmospheric explosions were combined giving 5A. The figures 3.16 and 3.17 show the individual $Q_\gamma^{-1}(f)$ values, without confidence limits, for the atmospheric explosions at Novaya Zemlya and in China. Trends for the three NZA events are very similar and are reflected in the average 3NZA (Figure 3.16). The two events in China differ considerably around .038 Hz, this is probably due to the poor signal-to-noise for CA 17.6.67, but the average 2CA (Figure 3.18) follows the general trends of CA 29.9.69 which has good signal-to-noise. (The combined

NOVAYA ZEMLYA 24/12/62 ATMOSPHERIC 26 STATIONS
NOVAYA ZEMLYA 27/9/62 ATMOSPHERIC 28 STATIONS

	FREQUENCY	A1	A2	NFTEST	NATEST	NBTEST	NEW GRADIENT & LIMITS	
1	0.014650	-0.006798	-0.007155	1	1	0	-0.007526	0.002349
2	0.015870	-0.007606	-0.011179	0	2	2	0.0	0.0
3	0.017090	-0.007411	-0.008450	1	1	1	-0.008048	0.002496
4	0.018310	-0.007482	-0.008911	1	1	1	-0.008276	0.002200
5	0.019530	-0.006757	-0.006889	1	1	1	-0.006844	0.001735
6	0.020750	-0.004940	-0.007746	1	1	1	-0.006530	0.001976
7	0.021970	-0.004392	-0.006434	1	1	1	-0.005516	0.001889
8	0.023190	-0.004219	-0.005805	1	1	1	-0.005095	0.001653
9	0.024410	-0.003979	-0.004909	1	1	1	-0.004494	0.001403
10	0.025630	-0.003459	-0.004341	1	1	1	-0.003947	0.001330
11	0.026860	-0.003263	-0.004299	1	1	1	-0.003838	0.001267
12	0.028080	-0.004081	-0.004891	1	1	1	-0.004529	0.001303
13	0.029300	-0.004781	-0.005258	1	1	1	-0.005044	0.001370
14	0.030520	-0.005037	-0.005312	1	1	1	-0.005188	0.001247
15	0.031740	-0.004022	-0.004977	1	1	1	-0.004541	0.001172
16	0.032960	-0.003025	-0.004398	1	1	1	-0.003775	0.001370
17	0.034180	-0.003187	-0.004248	1	1	1	-0.003770	0.001536
18	0.035400	-0.003660	-0.004395	1	1	1	-0.004064	0.001776
19	0.036620	-0.003874	-0.004672	1	1	1	-0.004311	0.001829
20	0.037840	-0.004399	-0.005147	1	1	1	-0.004814	0.001684
21	0.039060	-0.004735	-0.005539	1	1	1	-0.005187	0.001692
22	0.040280	-0.004937	-0.005208	1	1	1	-0.005088	0.001765
23	0.041500	-0.004552	-0.004286	1	1	1	-0.004404	0.001740
24	0.042720	-0.004305	-0.003582	1	1	1	-0.003901	0.001697
25	0.043950	-0.004591	-0.003603	1	1	1	-0.004038	0.001606
26	0.045170	-0.004112	-0.003844	1	1	1	-0.003963	0.001462
27	0.046390	-0.004099	-0.003987	1	1	1	-0.004037	0.001435
28	0.047610	-0.004354	-0.004095	1	1	1	-0.004210	0.001530
29	0.048830	-0.004083	-0.004138	1	1	1	-0.004114	0.001543
30	0.050050	-0.004221	-0.004108	1	1	1	-0.004159	0.001513
31	0.051270	-0.004639	-0.004851	1	1	1	-0.004753	0.001408
32	0.052490	-0.004761	-0.005472	1	1	0	-0.005145	0.001321
33	0.053710	-0.004757	-0.005052	1	1	0	-0.004916	0.001367
34	0.054930	-0.004523	-0.004450	1	1	0	-0.004483	0.001390
35	0.056150	-0.004723	-0.004146	1	1	0	-0.004403	0.001330
36	0.057370	-0.005093	-0.004643	1	1	1	-0.004843	0.001318
37	0.058590	-0.004906	-0.005268	1	1	0	-0.005109	0.001193
38	0.059810	-0.004521	-0.005422	1	1	0	-0.005029	0.001129
39	0.061040	-0.003889	-0.005039	1	1	1	-0.004542	0.001166
40	0.062260	-0.003380	-0.004859	1	1	1	-0.004198	0.001176
41	0.063480	-0.003461	-0.004709	1	1	1	-0.004137	0.001168
42	0.064700	-0.003834	-0.004408	1	1	1	-0.004153	0.001184
43	0.065920	-0.004250	-0.004336	1	1	1	-0.004299	0.001257
44	0.067140	-0.004632	-0.004528	1	1	1	-0.004573	0.001267
45	0.068360	-0.004874	-0.004538	1	1	1	-0.004685	0.001209
46	0.069580	-0.004804	-0.004643	1	1	1	-0.004715	0.001183
47	0.070800	-0.004520	-0.004341	1	1	0	-0.004422	0.001134
48	0.072020	-0.004682	-0.003830	1	1	0	-0.004206	0.001060
49	0.073240	-0.004629	-0.003528	1	1	0	-0.004011	0.001080
50	0.074460	-0.004836	-0.003797	1	1	1	-0.004264	0.001020
51	0.075680	-0.004959	-0.004130	1	1	1	-0.004504	0.001017
52	0.076900	-0.005080	-0.004209	1	1	1	-0.004601	0.001016
53	0.078130	-0.004810	-0.003680	1	1	1	-0.004186	0.000954
54	0.079350	-0.004269	-0.003494	1	1	1	-0.003850	0.000983
55	0.080570	-0.004215	-0.003529	1	1	1	-0.003850	0.001084
56	0.081790	-0.004215	-0.003455	1	1	1	-0.003807	0.001110
57	0.083010	-0.003691	-0.003706	1	1	1	-0.003699	0.001032
58	0.084230	-0.003290	-0.003984	1	1	1	-0.003668	0.001000
59	0.085450	-0.003076	-0.003760	1	1	1	-0.003452	0.001044
60	0.086670	-0.003169	-0.003389	1	1	1	-0.003291	0.001030
61	0.087890	-0.003053	-0.003372	1	1	1	-0.003232	0.000967
62	0.089110	-0.002819	-0.003396	1	1	1	-0.003144	0.000949
63	0.090330	-0.002892	-0.003380	1	1	1	-0.003167	0.000902
64	0.091550	-0.003086	-0.003405	1	1	1	-0.003262	0.000835
65	0.092770	-0.002656	-0.003059	1	1	1	-0.002874	0.000827
66	0.093990	-0.002216	-0.003054	1	1	0	-0.002670	0.000790
67	0.095210	-0.002147	-0.002968	1	1	0	-0.002593	0.000711
68	0.096440	-0.002488	-0.002532	1	1	0	-0.002512	0.000794
69	0.097660	-0.002951	-0.002403	1	1	1	-0.002651	0.000827
70	0.098880	-0.002947	-0.002500	1	1	1	-0.002700	0.000837
71	0.100100	-0.002529	-0.002616	1	1	0	-0.002577	0.000779
72	0.101320	-0.001845	-0.002691	1	1	0	-0.002312	0.000755
73	0.102540	-0.001661	-0.002460	1	1	0	-0.002102	0.000720
74	0.103760	-0.001771	-0.002346	1	1	0	-0.002088	0.000737
75	0.104980	-0.001538	-0.002269	1	1	1	-0.001941	0.000798
76	0.106200	-0.001441	-0.002107	1	1	1	-0.001805	0.000789
77	0.107420	-0.001975	-0.001995	1	1	1	-0.001986	0.000718
78	0.108640	-0.001926	-0.001835	1	1	1	-0.001877	0.000716
79	0.109860	-0.001746	-0.001839	1	1	0	-0.001796	0.000696

FIGURE 3.15 Comparison of Regression Values for NZA 24/12/62 and NZA 27/9/62 at Each Frequency.

	NZA 24.12.62	NZA 27. 9.62	NZA 22.10.62	CA 17. 6.67	CA 29. 9.69	NZU 7.11.68
NZA 24.12.62	-					
NZA 27. 9.62	1	-				
NZA 22.10.62	6	11	-			
CA 17. 6.67	7	13	1	-		
CA 29. 9.69	8	16	1	1	-	
NZU 7.11.68	25	27	24	23	20	-

Table 3.2 The number of frequencies at which the F test fails for comparison of two events. The underground explosion NZU 7.11.68 differs from the atmospheric explosions.

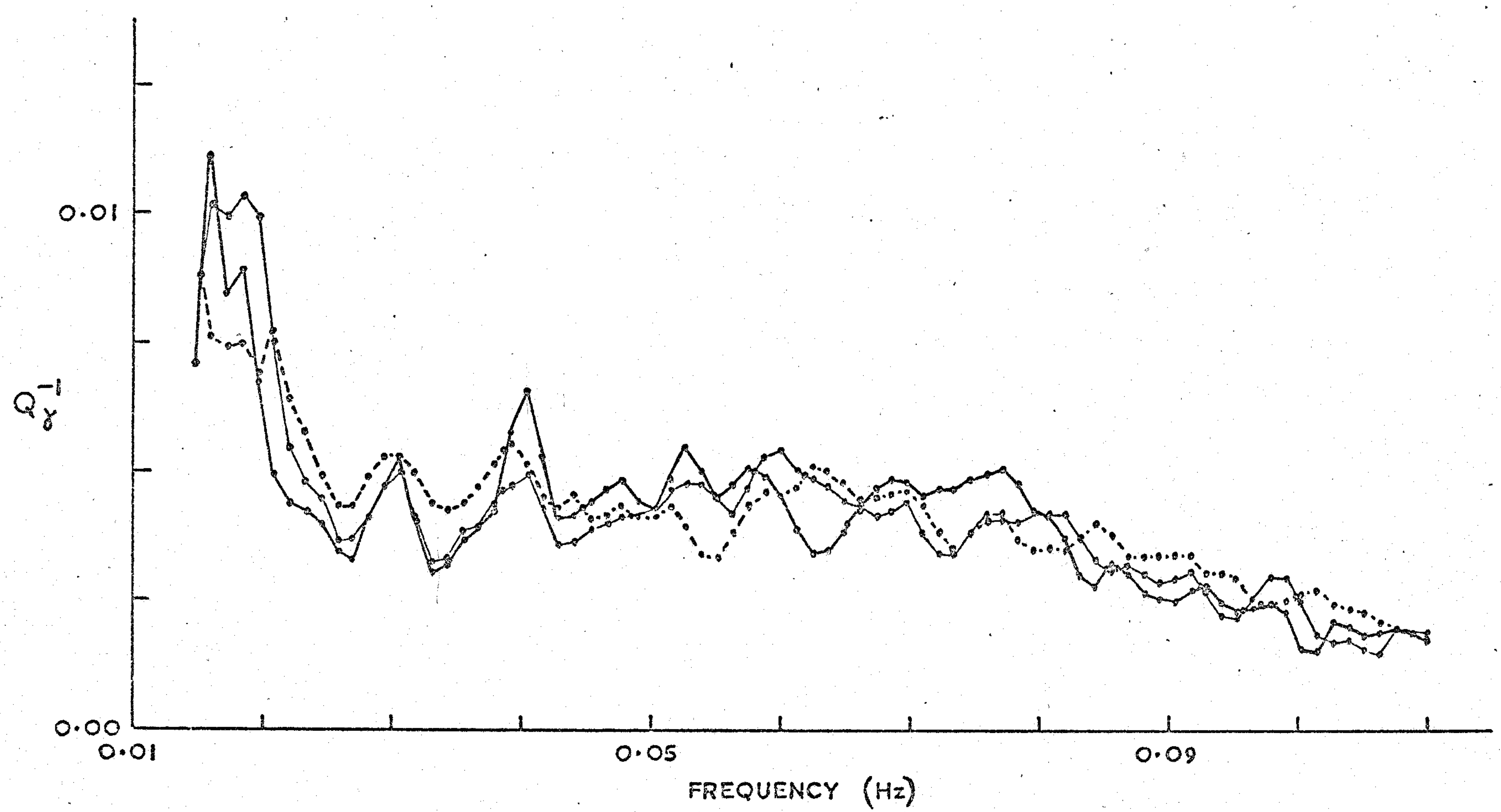

FIGURE 3.16 ESTIMATES OF Q_γ^{-1} FOR THE THREE ATMOSPHERIC EXPLOSIONS AT NOVAYA ZEMLYA

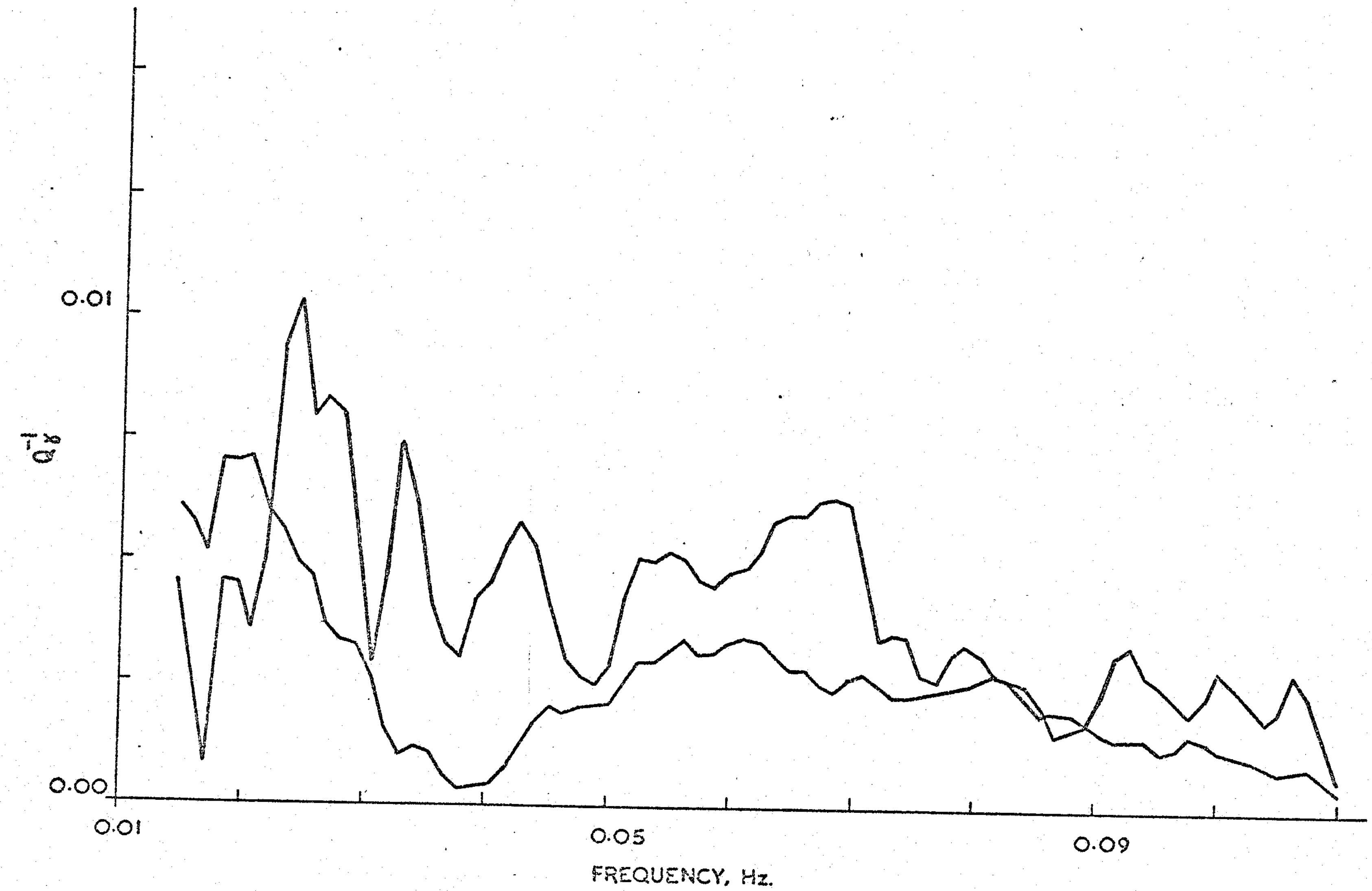

FIGURE 3.17 ESTIMATES OF Q_γ^{-1} FOR THE TWO ATMOSPHERIC EXPLOSIONS IN CHINA (S. SINKIANG PROV.)

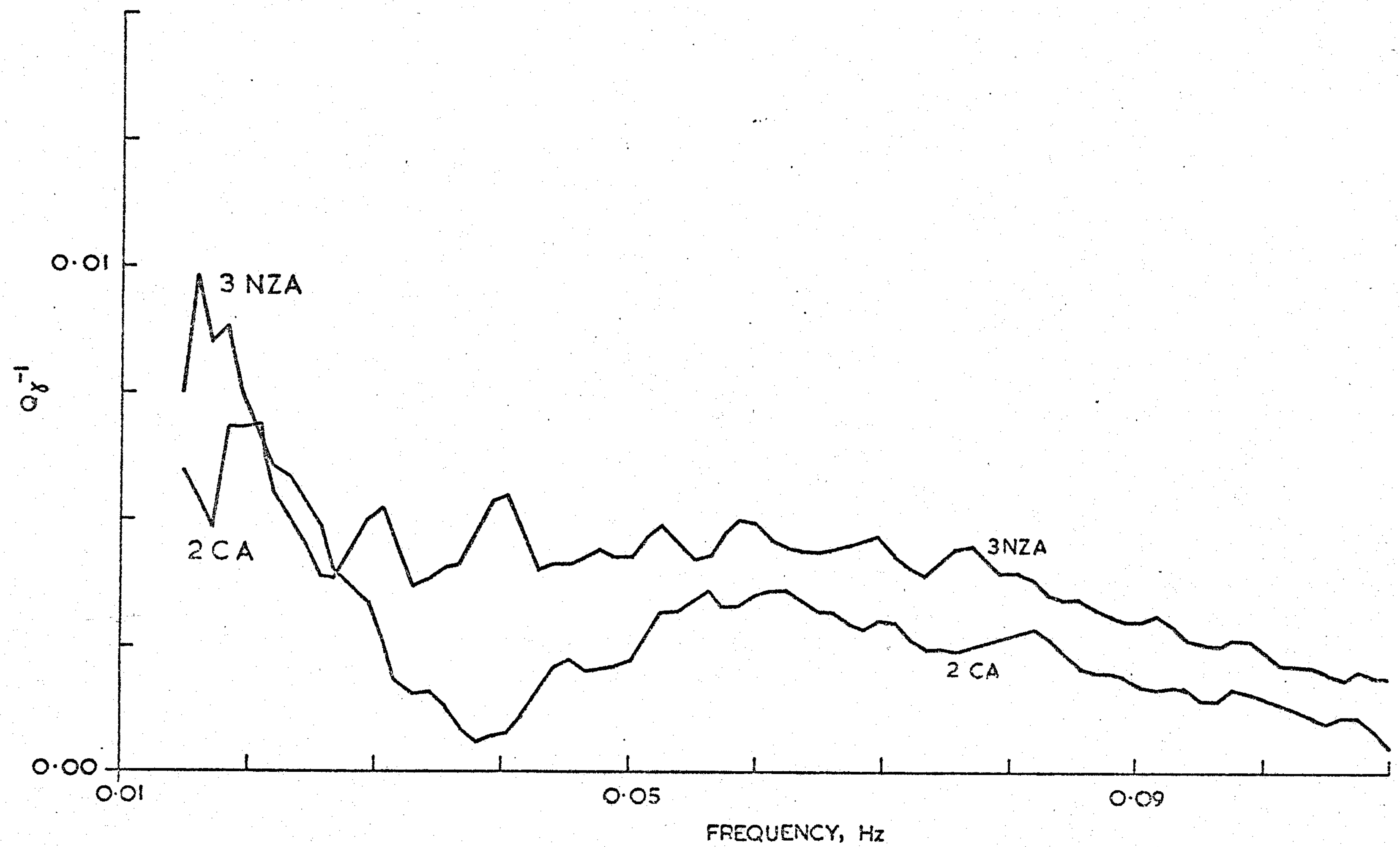

FIGURE 3.18 AVERAGE Q_γ^{-1} ESTIMATES FOR TWO SETS OF ATMOSPHERIC EXPLOSIONS: 1) THREE IN NOVAYA ZEMLYA (3NZA) AND 2) TWO IN CHINA (2CA)

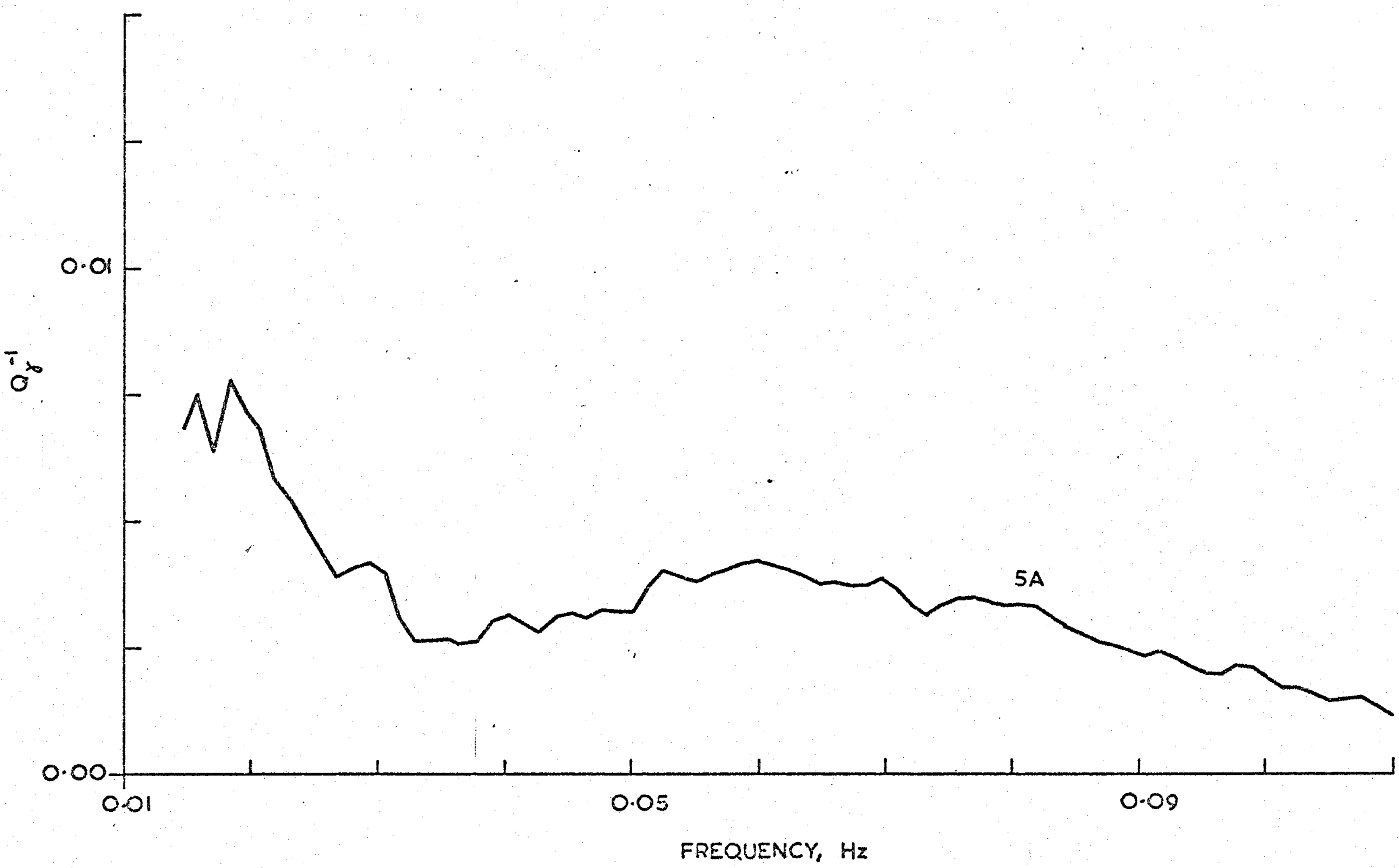

FIGURE 3.19 AVERAGE Q_γ^{-1} ESTIMATED USING FIVE ATMOSPHERIC EXPLOSIONS, THREE IN NOVAYA ZEMLYA (3NZA) AND TWO IN CHINA (2CA)

average for the five atmospheric explosionsis shown in Figure 3.19.) The averages 3NZA, 2CA and 5A with their appropriate 95% confidence limits are shown in Figures 3.20-3.22.

3.4 Average $Q_{\gamma}^{-1}(f)$ Values

3.4.1 Q_{γ}^{-1} at Low Frequencies

The figures for 3NZA, 2CA and 5A still persist in showing high Q_{γ}^{-1} at low frequencies. This will later be interpreted as a layer of greater attenuation at depth.

Broader confidence limits are still apparent at low frequencies, but this does not necessarily mean that these results are poorer, instead it is informative. Two populations may have the same mean, but with different variances, one population is "broader" than the other. Samples from the broader population will contain a wider range of values and so the confidence limits on the calculated mean will be wider than for the other population. Low frequencies penetrate deeper into the earth than high frequencies, presumably sampling a wider range of Q^{-1} values. Also the depth to which low frequencies penetrate may be expected to contain lateral inhomogeneities. Both effects broaden the confidence limits and simultaneously increase their interpretational use!

3.4.2 Q_{γ}^{-1} at High Frequencies

The tendency at high frequencies is for Q_{γ}^{-1} to trend towards zero. This has already been explained in terms of the propagational frequency content for each explosion. However, figure 3.23 shows an interestir comparison between the atmospheric average 3NZA and the underground explosion NZU 7/11/68. For NZU the erratic behaviour of the mean and the very broad confidence limits (Figure 3.4) at low frequencies indicates little low frequency energy content, but for high frequencies the situation has obviously improved. From Table 3.1 we expect NZU to contain useful propagating energy up to about 0.10 Hz, while 3NZA will contain energy up to 0.08 Hz. The curves for 3NZA and NZU start to diverge for frequencies around

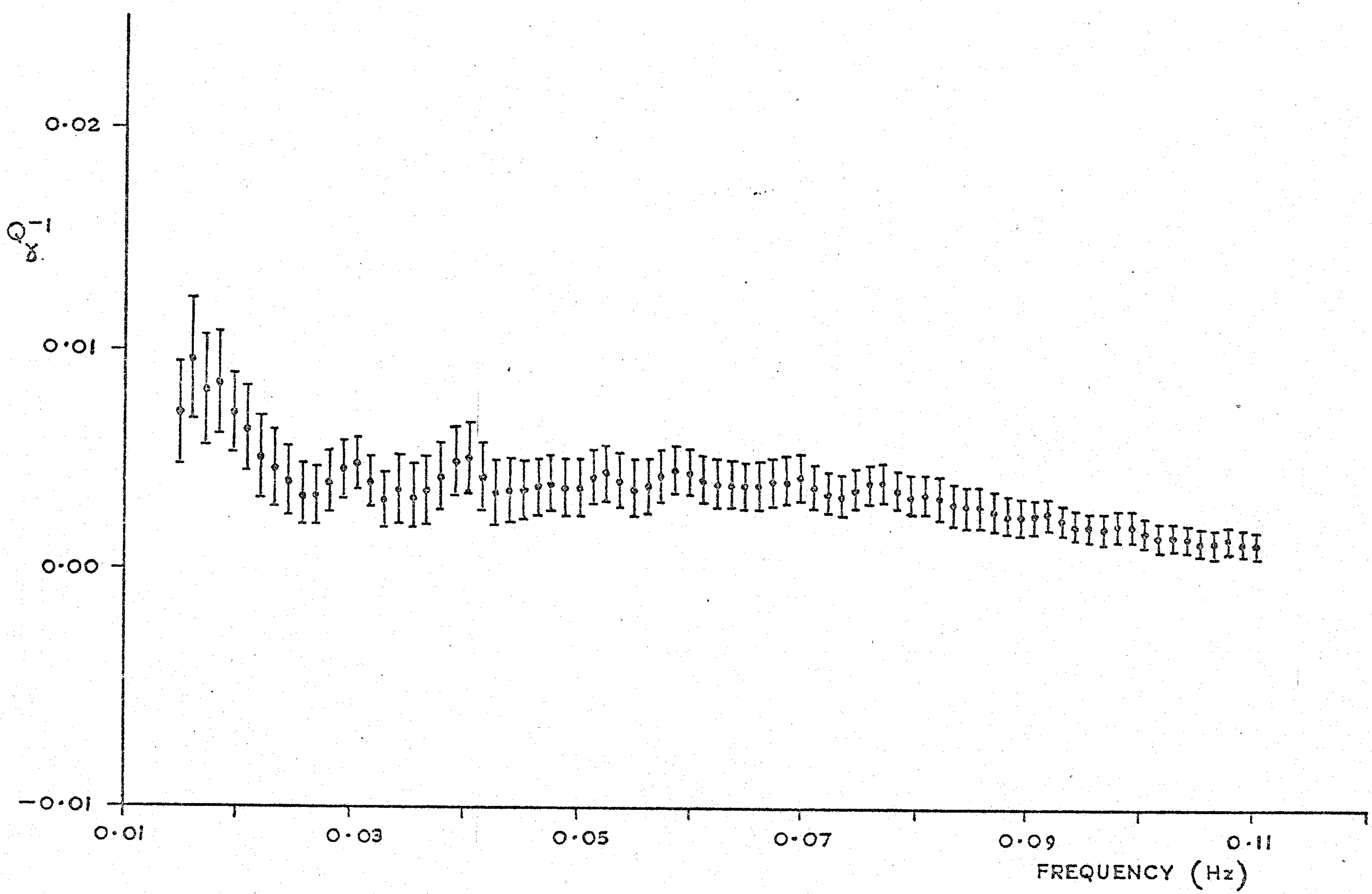

FIGURE 3.20 Q_γ^{-1} AND 95 P.C. CONFIDENCE LIMITS ESTIMATED USING THE 3 ATMOSPHERIC EXPLOSIONS IN NOVAYA ZEMLYA

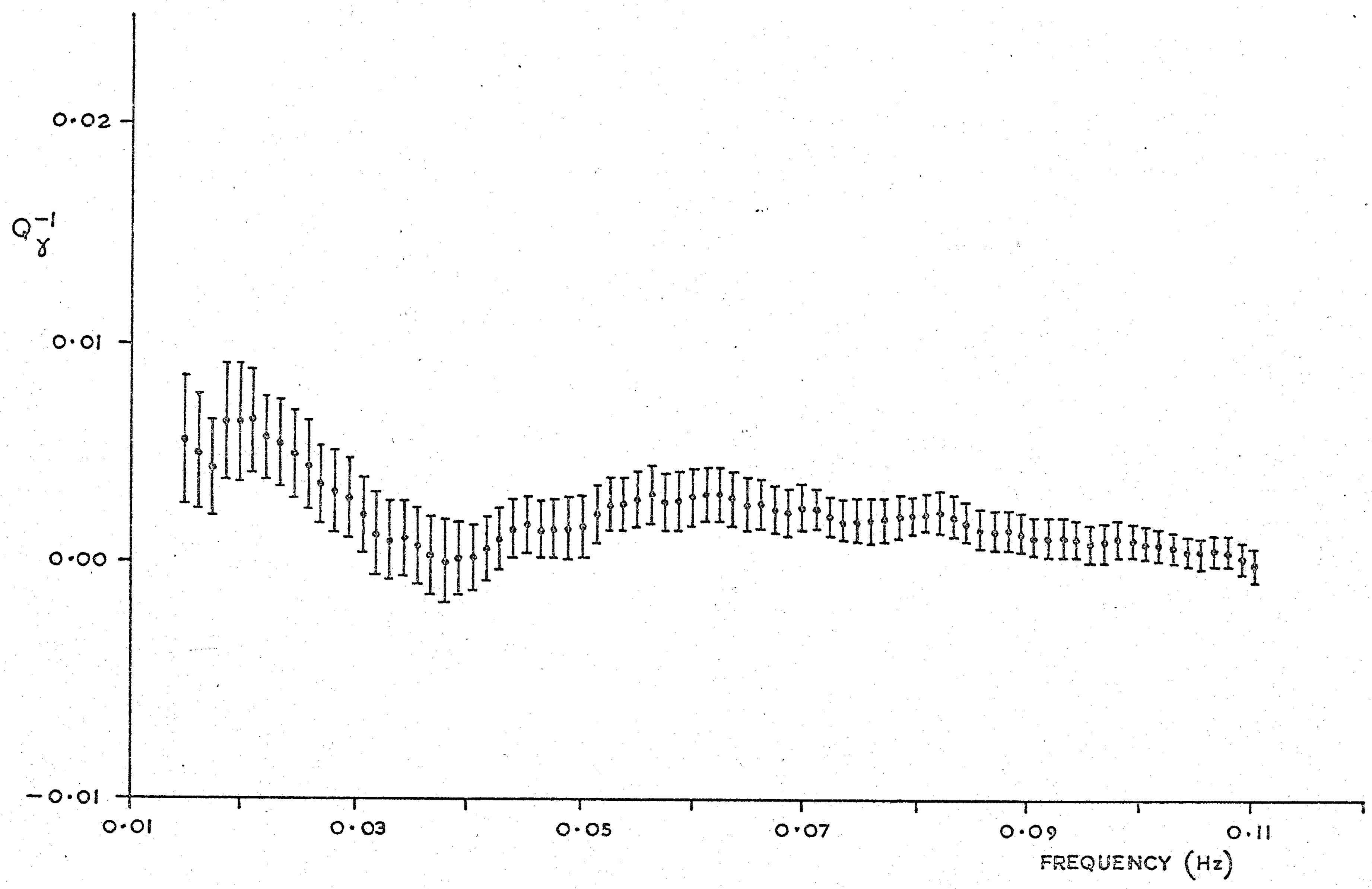

FIGURE 3.21 Q_γ^{-1} AND 95 P.C. CONFIDENCE LIMITS ESTIMATED USING THE 2 ATMOSPHERIC EXPLOSIONS IN SOUTHERN SINKIANG PROV., CHINA

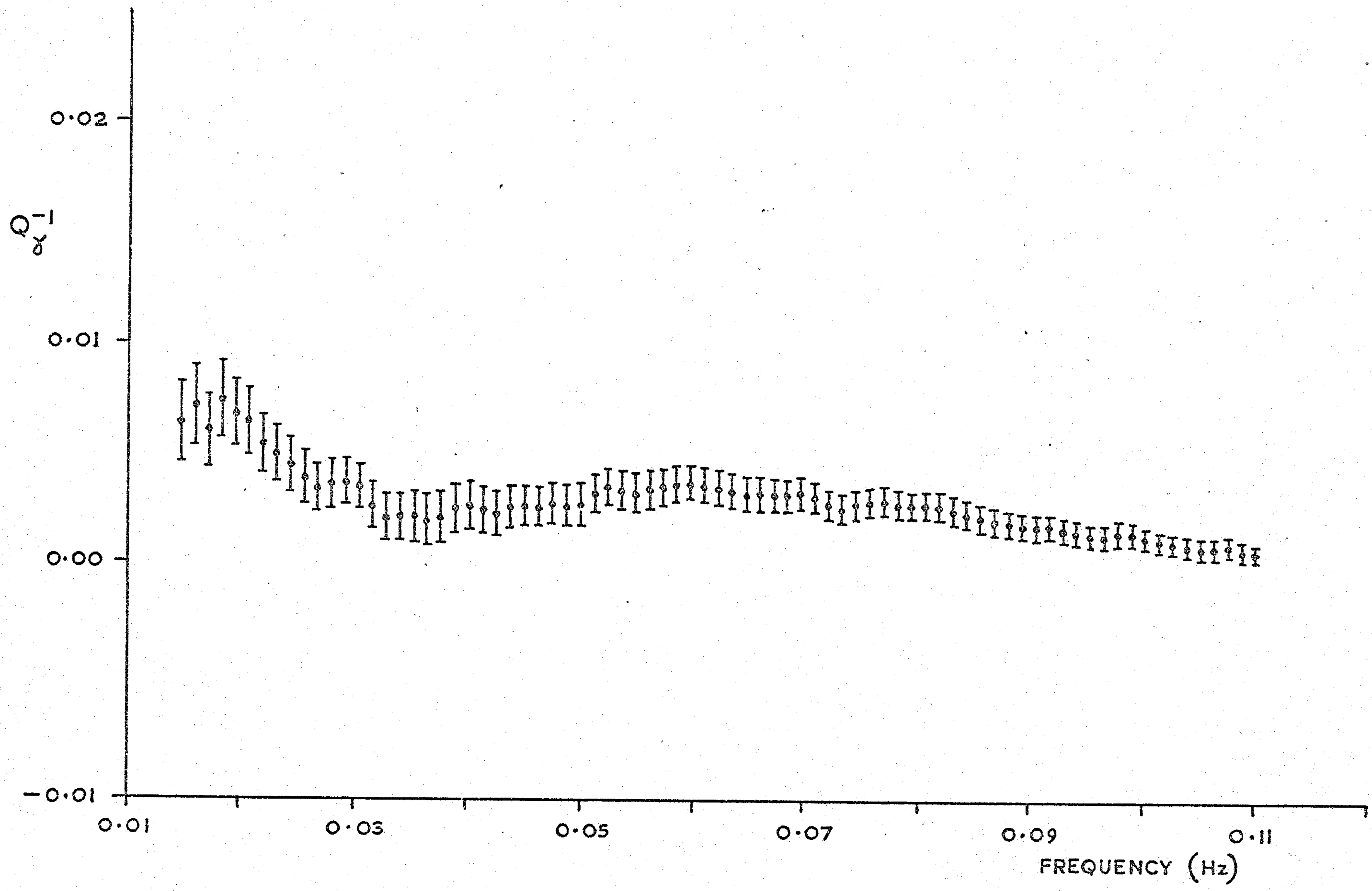

FIGURE 3.22 Q_{γ}^{-1} AND 95 P.C. CONFIDENCE LIMITS ESTIMATED USING THE 5 ATMOSPHERIC EXPLOSIONS, 3 IN NOVAYA ZEMLYA AND 2 IN CHINA

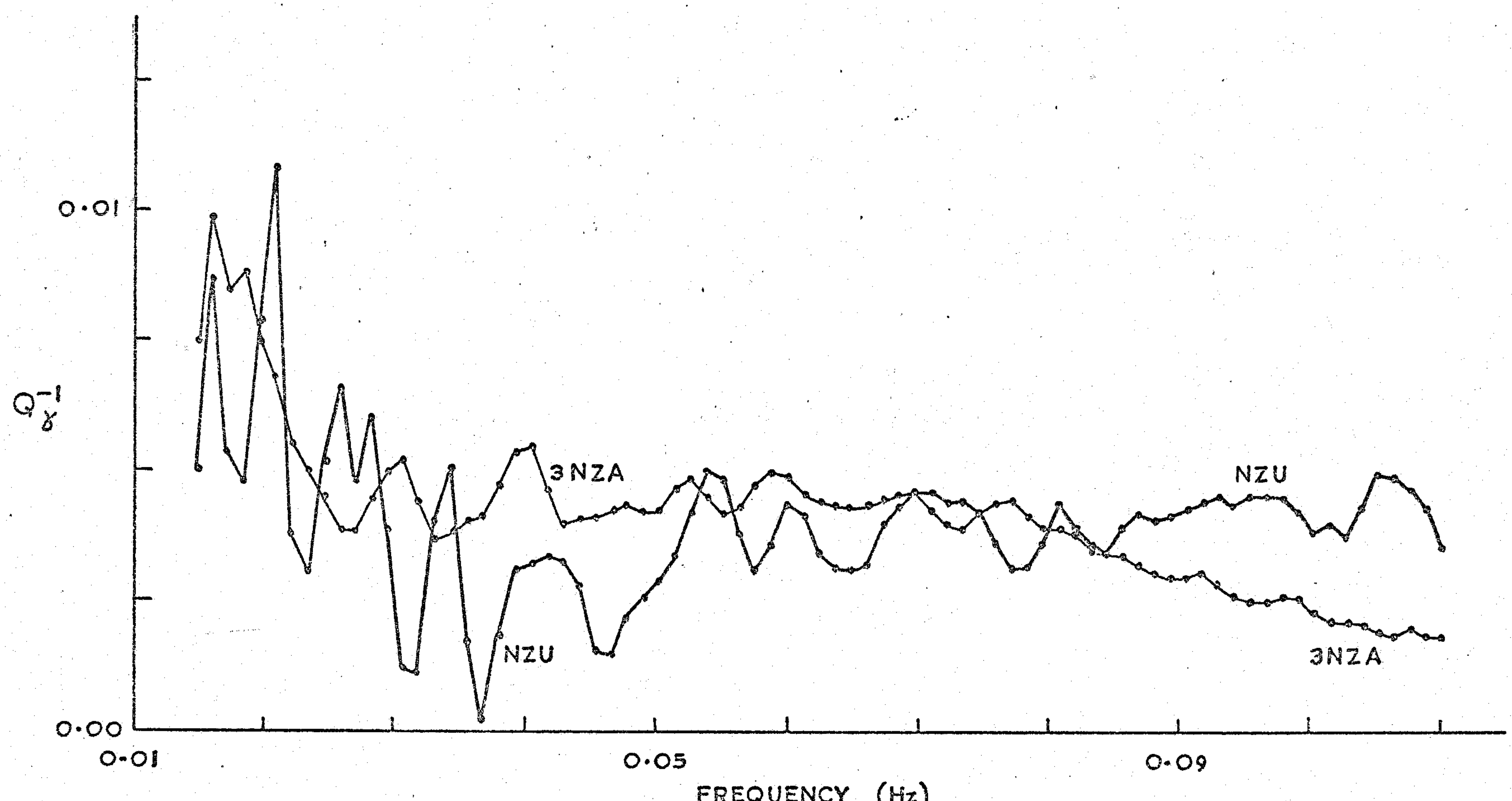

FIGURE 3.23 AVERAGE Q_{γ}^{-1} FOR THE THREE ATMOSPHERIC EXPLOSIONS COMPARED TO Q_{γ}^{-1} FOR THE UNDERGROUND EXPLOSION AT NOVAYA ZEMLYA

0.08 Hz, 3NZA trends towards zero while NZU gives a reasonable attenuation value, $Q_{\gamma}^{-1} \sim 0.004$. For frequencies greater than 0.08 Hz the underground explosion NZU is probably a better estimator of Q_{γ}^{-1} than 3NZA, simply because it does contain high frequency propagating energy.

3.5 Summary

The estimated values of $Q_{\gamma}^{-1}(f)$ have been presented for each event analysed, along with 95% confidence limits. The data for the separate atmospheric explosions has been combined to form improved averages. In all cases the highest useful frequency of propagating energy has been determined.

In general the $Q_{\gamma}^{-1}(f)$ values determined from Novaya Zemlya are greater than the equivalent values obtained from the explosions in China. In all cases the attenuation is greater at low frequencies, implying an attenuating layer at depth. It is now necessary to invert the $Q_{\gamma}^{-1}(f)$ data from a function of frequency for surface waves into a variation with depth, determining Q_{α}^{-1} and Q_{β}^{-1} for compressional and shear bodily waves.

CHAPTER 4

4.1 A Theoretical Formulation for the Dissipation and Dispersion of Rayleigh Waves

For the future purpose of inverting the experimental Q_{γ}^{-1} data it is necessary to describe the evaluation of the dissipation parameter by theoretical means. This will also throw light on Q^{-1} as an important earth parameter.

Any expression for the amplitude of a surface wave at angular frequency ω will contain the wave propagation term

$$\exp\left[i(\omega t - \underline{k} \cdot \underline{r})\right] \tag{4.1}$$

where $\underline{k}$ is the wave number vector and $\underline{r}$ the distance. Assuming isotropy this becomes

$$\exp\left[i(\omega t - kr)\right] \tag{4.2}$$

If dissipation is present then k is complex, if dissipation is small amplitudes may be calculated, using complex k, as if dissipation was not present. The wave number k becomes*

$$k(\omega) = k_o(\omega) + \delta k(\omega) \tag{4.3}$$

where k_o is the wave number in the elastic case and is pure real, and $\delta k(\omega)$ is complex.

---

*This representation for the wave number was shown to me by J Hudson. This differs from the work of Anderson, Ben-Menahem and Archambeau (1965) who use $k = k_1 + ik_2$, viscoelasticity only introducing an imaginary term for dissipation. Allowing $\delta k(\omega)$ to be complex leads to causally related information about dissipation and dispersion, the relation is obtained by Futterman's methods (1962).

The term $\delta k(\omega)$ may be written

$$\delta k(\omega) = \emptyset(\omega) + i\gamma(\omega) \qquad 4.4$$

and the term 4.2 becomes

$$\exp\left[i(\omega t - \emptyset(\omega)r)\right] \exp\left[\gamma(\omega)r\right] \qquad 4.5$$

As expected $\gamma(\omega)$ determines spatial attenuation, which we hope to prove negative, whilst $\emptyset(\omega)$ is a phase term, and $\gamma(\omega)$ may be rewritten as

$$\gamma(\omega) = -\omega/2Q_{\gamma}(\omega)U(\omega) \qquad 4.6$$

Group velocity, U, is used for surface waves; the argument is given by Brune (1962) and Knopoff et al. (1964).

The wave number $k_o(\omega)$ is obtained as solution to the surface wave equation which involves the earth parameters α_o and β_o (compressional and shear velocities). For the elastic half space case this characteristic equation is

$$\left(2 - \frac{C_o^2}{\beta_o^2}\right) - 4\left(1 - \frac{C_o^2}{\alpha_o^2}\right)^{1/2}\left(1 - \frac{C_o^2}{\beta_o^2}\right)^{1/2} = 0 \quad \text{(Bullen 1965)} \qquad 4.7$$

C_o is the velocity of the surface waves, and this may be represented by

$$F_o(k_o, \omega, \alpha_o, \beta_o) = 0 \qquad 4.8$$

because $k_o(\omega) = \frac{\omega}{C_o}$. When dissipation occurs the visco-elastic wave number k is the solution of

$$F(k, \omega, \alpha, \beta) = 0 \qquad 4.9$$

where k, α, β are all complex and α, β are of the form

$$\alpha(\omega) = \alpha_o + \delta\alpha(\omega) \qquad 4.10$$

If we now assume a plane N layered earth model where h_l denotes the thickness of the lth layer then identity 4.9 becomes

$$F(k, \omega, h_l, \alpha_l, \beta_l) = 0 \qquad 4.11$$

and adapting a statement by Anderson, Ben-Menahem and Archambeau (1965), $\delta k(\omega)$ is given by the partial derivative summation

$$\delta k(\omega) = \sum_{l=1}^{N} \left[\frac{\partial k_o}{\partial \alpha_{ol}} \delta \alpha_l + \frac{\partial k_o}{\partial \beta_{ol}} \delta \beta_l \right] \qquad 4.12$$

In the work of Anderson et al. $\delta\alpha_l$, $\delta\beta_l$ are pure imaginary, here they are complex.

The wave number k_o may be determined by applying equation 4.8 to a layered structure, that is solving

$$F_o(k_o, \omega, h_l, \alpha_{ol}, \beta_{ol}) = 0 \qquad 4.13$$

The solution for k_o is obviously of the form $k_o(\omega, h_l, \alpha_{ol}, \beta_{ol})$ and so the derivatives in 4.12 are of the form

$$\frac{\partial k_o(\omega, h_l, \alpha_{ol}, \beta_{ol})}{\partial \alpha_{ol}} \qquad 4.14$$

The Thomson-Haskell matrix formulation (Thomson 1950, Haskell 1953, 1964) for surface waves on a layered structure will later be used to obtain solutions for k_o for a chosen layered model. The program, written by A Douglas, was adapted to produce the derivatives of equation 4.14 by solving equation 4.13 for k_{oj+} and k_{oj-} by using $\alpha_{oj}+d\alpha_o$ followed by $\alpha_{oj}-d\alpha_o$ and then perturbing the parameters of each layer in turn and re-solving

$$F_o(k_{oj\pm}, \omega, h_l, \alpha_{ol} \pm \delta_{lj} d\alpha_o, \beta_{ol}) = 0 \qquad 4.15$$

The small increment $d\alpha_o$ is added to α_{oj} only (and j eventually runs from 1 to N, perturbing each layer in turn) and the new wave number k_{oj+} obtained. The required derivative is then approximated by

$$\left.\frac{\partial k_o}{\partial \alpha_{ol}}\right|_{\substack{l=j \\ \omega}} = \left.\frac{k_{oj+} - k_{oj-}}{2d\alpha_o}\right|_{\omega} \qquad 4.16$$

Because $k_o(\omega) = \frac{\omega}{\alpha_o(\omega)}$ a small positive change in $\alpha_o(\omega)$ produces a small negative change in $k_o(\omega)$; the derivatives are always negative.

The derivatives with respect to β are obtained in a similar manner, and they too are all negative.

Equation 4.12 may be written in full as

$$R(\delta k(\omega)) = \emptyset(\omega) = \sum_{l=1}^{N} \left[\frac{\partial k_o}{\partial \alpha_{ol}} R(\delta \alpha_l) + \frac{\partial k_o}{\partial \beta_{ol}} R(\delta \beta_l) \right] \Bigg|_{\omega} \tag{4.17a}$$

$$I(\delta k(\omega)) = \gamma(\omega) = \sum_{l=1}^{N} \left[\frac{\partial k_o}{\partial \alpha_{ol}} I(\delta \alpha_l) + \frac{\partial k_o}{\partial \beta_{ol}} I(\delta \beta_l) \right] \Bigg|_{\omega} \tag{4.17b}$$

By considering small changes in the body wave velocity α_{ol} it may be shown that (Appendix F)

$$I(\delta \alpha_l) = \frac{Q_{\alpha l}^{-1} \alpha_{ol}}{2} \tag{4.18a}$$

$$I(\delta \beta_l) = \frac{Q_{\beta l}^{-1} \beta_{ol}}{2} \tag{4.18b}$$

here $Q_{\alpha l}^{-1}$, $Q_{\beta l}^{-1}$ are specific attenuation factors for bodily waves. The equations 4.18 allow us to express the attenuation coefficient $\gamma(\omega)$ of equation 4.17b in terms of physically obtainable quantities, which was our major objective.

Further, the R and I parts of $\delta\alpha_l$, $\delta\beta_l$ are causally related and the treatment described by Futterman (1962) may be applied. The dissipative effects $(I(\delta \alpha_l))$ are related to the dispersive effects $(R(\delta \alpha_l))$ and applying Futterman's results gives (See Appendix F)

$$R(\delta \alpha_l) = \frac{\alpha_{ol}}{\pi} Q_{\alpha l}^{-1} \ln {}^{\omega}/{\omega_o} = \frac{2}{\pi} I(\delta \alpha_l) \ln {}^{\omega}/{\omega_o} \tag{4.19a}$$

$$R(\delta \beta_l) = \frac{\beta_{ol}}{\pi} Q_{\beta l}^{-1} \ln {}^{\omega}/{\omega_o} = \frac{2}{\pi} I(\delta \beta_l) \ln {}^{\omega}/{\omega_o} \tag{4.19b}$$

where ω_o, as Kolsky (1956) would have it, is a "disposable constant".

Therefore substituting in 4.17 we have

$$\emptyset(\omega) = \frac{2}{\pi} \ln \left(\frac{\omega}{\omega_o}\right) \gamma(\omega) \tag{4.20a}$$

$$\gamma(\omega) = \sum_{l=1}^{N} \left[\frac{\partial k_o}{\partial \alpha_{ol}} \frac{Q_{\alpha l}^{-1}}{2} \alpha_{ol} + \frac{\partial k_o}{\partial \beta_{ol}} \frac{Q_{\beta l}^{-1}}{2} \beta_{ol} \right] \tag{4.20b}$$

$$\delta k(\omega) = \gamma(\omega) \left(\frac{2}{\pi} \ln {}^{\omega}/{\omega_o} + i\right) \tag{4.21}$$

Using knowledge of the specific attenuation factor (body waves), the velocity of body waves and the derivatives $\frac{\partial k_o}{\partial \alpha_{ol}}$ the attenuation coefficient $\gamma(\omega)$ may be calculated for a layered structure. As expected the attenuation coefficient is negative, directly determined by the sign of the derivatives which are always negative. Further, if the group velocity for the model is known then Q_γ^{-1} may easily be calculated from $\gamma(\omega)$, by 4.6

$$Q^{-1}(\omega) = \frac{-2U(\omega)\gamma(\omega)}{\omega} \qquad 4.22$$

The Thomson-Haskell method determines the phase velocity dispersion for the model, the group velocity dispersion is easily obtained from this by using the usual equation

$$U(\omega) = \frac{d\omega}{dk} = C + k\frac{dc}{dk} \qquad 4.23$$

We may take the argument further and calculate the change in the Rayleigh wave phase velocity caused by dispersion linked, as above, with the dissipation.

A change in the wavenumber of $-\delta k$ is linked with a change $+\delta c$ in the Rayleigh velocity C_o

$$k_o - \delta k(\omega) = \frac{\omega}{C_o + \delta C(\omega)} \qquad 4.24$$

and because

$$k_o = \frac{\omega}{C_o}$$

$$\delta k(\omega) = \frac{\omega}{C_o} - \frac{\omega}{C_o + \delta C(\omega)}$$

$$\therefore \quad \delta k(\omega) \sim -\frac{\omega\delta C(\omega)}{C_o^2} \qquad 4.25$$

Taking the real parts and rearranging gives

$$\delta C(\omega) = -\frac{C_o^2}{\omega}\,\phi(\omega)$$

$$\therefore \quad \delta C(\omega) = -\frac{C_o^2}{\omega}\,\gamma(\omega)\,\frac{2}{\pi}\ln {}^{\omega}/_{\omega_o}$$

$$\therefore \quad C(\omega) = C_o(1 - \frac{C_o}{\omega}\,\gamma(\omega)\,\frac{2}{\pi}\ln\frac{\omega}{\omega_o})$$

$$\therefore \quad C(\omega) = C_o(1 + \frac{Q_\gamma^{-1}}{\pi}\,\frac{C_o}{U(\omega)}\,\ln\frac{\omega}{\omega_o}) \qquad 4.26$$

This equation is similar to a solution given by Kolsky (1956) for compressional waves in a rod

$$C(\omega) = C_o(1 + \frac{\tan\delta}{\pi} \ln \frac{\omega}{\omega_o}) \qquad 4.27$$

where $\tan\delta$ may be read as Q_α^{-1}. The group velocity appears in equation 4.26 because the energy of surface waves travels with this velocity rather than the phase velocity, and so is required in the attenuation expression 4.6. This second type of dispersion is a geometrical effect which occurs for surface waves because longer periods reach to greater depths within the earth than shorter periods, therefore sampling a different velocity structure. Because a different velocity structure is sampled a different Rayleigh wave velocity results for each frequency. This does not occur for body waves because all frequencies follow the same path, unless scattered in a frequency dependent manner. So for body waves the phase and group velocities (hence the energy velocity for these seismic frequencies) are almost identical, the difference is caused by dispersion linked to dissipation which is a small effect. If surface waves were not dispersed by geometrical means (as calculated by the Thomson-Haskell technique) then equation 4.26 would reduce to a form equivalent to 4.27.

It is usual to calculate Rayleigh wave geometrical dispersion using Thomson-Haskell matrices with frequency independent body wave velocities. If frequency dependent body wave velocities are used, and attenuation is allowed for, (essentially solving equation 4.11) the resulting Rayleigh wave dispersion curve has been shown to differ by 1% from the simpler model (Carpenter and Davies 1966). In this study derivatives of the $\frac{\partial k_o}{\partial \alpha_o}$ type were obtained using the simple elastic Thomson-Haskell formulation and then the attenuation coefficient calculated from equation 4.20b. Obviously there are some feedback errors in this process because the derivative expressed in 4.14 should really include attenuation and be of the form

$$\frac{\partial k(\omega, h_1, \alpha_1, \beta_1, Q_{\alpha 1}^{-1})}{\partial \alpha_1} \qquad 4.27$$

Such considerations were ignored. Also the possibility that the attenuation frequency relation (equation 4.6) is not linear is ignored, that is relations of the form $\gamma(\omega) \propto \omega^P$ (P not necessarily integer) which are considered advantageous by Strick (1967) are not considered, because the advantages gained are largely in the theoretical presentation of the attenuation mechanism.

4.2 The Attenuation of Rayleigh Waves on a Half Space

Before any attempt is made to invert the observed Q_γ^{-1} data into an attenuation-depth model involving Q_α^{-1}, Q_β^{-1} by using equations 4.20b and 4.22 for $\gamma(\omega)$ as a function of Q_α^{-1}, Q_β^{-1} and Q_γ^{-1} as a function of $\gamma(\omega)$ respectively, it would be useful to obtain a simple, if approximate, relation of the form $Q_\gamma^{-1} \sim f(Q_\alpha^{-1}, Q_\beta^{-1})$. With such an approximate equation it would be possible to estimate the range of values for Q_α^{-1}, Q_β^{-1} which ought to be considered for inversion purposes.

Equation 4.7 gives the characteristic equation for a Rayleigh wave in a perfectly elastic half space, this equation has the physical solution

$$c_o = 0.98\ \beta_o \qquad 4.28$$

Obviously dispersion does not occur with such a model. For a homogeneous viscoelastic half space an expression was obtained by Press and Healy (1957) relating the Rayleigh wave attenuation to Poisson's ratio, Q_α^{-1}, Q_β^{-1} only. Press and Healy obtained their expression by allowing the velocities in the characteristic equation 4.7 to become complex, their expression is quite complicated but following Anderson et al. (1965) it may be written as

$$Q_\gamma^{-1} = m\ Q_\alpha^{-1} + (1-m) Q_\beta^{-1} \qquad 4.29$$

where m is a complicated function of Poisson's ratio.

However, a much simpler equation may be obtained using the equation 4.20b for $\gamma(\omega)$. Rewriting equation 4.20b for a half-space immediately gives

$$\gamma(\omega) = \frac{\partial k}{\partial \alpha} \frac{Q_{\alpha}^{-1}\alpha}{2} + \frac{\partial k}{\partial \beta} \frac{Q_{\beta}^{-1}\beta}{2} \qquad 4.30$$

and assuming a Poisson solid ($\alpha=\sqrt{3}\beta$)

$$\gamma(\omega) = \frac{\partial k}{\partial \beta} \frac{\beta}{2} (Q_{\alpha}^{-1} + Q_{\beta}^{-1}) \qquad 4.31$$

Ignoring the dispersive effects of viscoelasticity implies equation 4.28 which will be written, for simplicity of manipulation, in the form

$$C_o = n\beta \qquad 4.32$$

$$\therefore \quad k = \frac{\omega}{n\beta}$$

$$\therefore \quad \frac{\partial k}{\partial \beta} = \frac{-\omega}{n\beta^2} + \frac{1}{n\beta}\frac{\partial \omega}{\partial \beta} \qquad 4.33$$

Now assuming that $\frac{\partial \omega}{\partial \beta} = 0$, that is non dispersive body waves (which is experimentally true!) gives

$$\frac{\partial k}{\partial \beta} = \frac{-\omega}{n\beta^2} \qquad 4.34$$

therefore

$$\gamma(\omega) = \frac{-\omega}{n\beta} \frac{1}{2} (Q_{\alpha}^{-1} + Q_{\beta}^{-1}) \qquad 4.35$$

which leads to

$$Q_{\gamma}^{-1} = Q_{\alpha}^{-1} + Q_{\beta}^{-1} \qquad 4.36$$

Before this equation is used it is worthwhile calculating the partial derivatives $\frac{\partial k_o}{\partial \alpha_{ol}}$, $\frac{\partial k_o}{\partial \beta_{ol}}$ to show the limitations of this equation.

4.3 Partial Derivatives for Inversion Purposes

As has already been described the partial derivatives were obtained by using the Thomson-Haskell procedure to solve a layered structure for the wavenumber k_{oj+}, then perturbing the velocity α_{oj} in the jth layer, and re-solving for k_{oj-}; hence $\left.\frac{\partial k_o}{\partial \alpha_{oj}}\right|_{\omega}$ and similarly $\left.\frac{\partial k_o}{\partial \beta_{oj}}\right|_{\omega}$ may be calculated for a range of ω. An alternative procedure would be to use the surface wave energy equation described by Jeffreys (1961) and this has been done by Takeuchi, Dorman and Sato (1969) to perform numerical inversion of surface wave data.

The velocity depth model assumed from which the derivatives were calculated is listed in Table 4.1. This is a simple six layered continental type model, chosen because most of the propagation paths used in this work are largely of continental type. The model is also illustrated in Figure 4.1, and its characteristic group velocity curve in Figure 4.2.

The partial derivatives of the wavenumber, k_o, with respect to both body wave velocities for the six layers are shown in Figures 4.3 and 4.4, as functions of frequency. It is immediately apparent that for a given layer (value of l) $\frac{\partial k_o}{\partial \beta_{ol}}$ is an order of magnitude larger than $\frac{\partial k_o}{\partial \alpha_{ol}}$.

This implies, referring to equation 4.20b for the attenuation coefficient $\gamma(\omega)$, attenuation of shear waves has a greater contribution to $\gamma(\omega)$ for surface waves than does compressional wave attenuation. (Of course assuming Q_α^{-1}, Q_β^{-1} are of the same order.) The further implication is

$$\frac{\partial Q_\gamma^{-1}}{\partial Q_\beta^{-1}} > \frac{\partial Q_\gamma^{-1}}{\partial Q_\alpha^{-1}} \qquad 4.37$$

which is born out by the observations of Anderson et al. (1965).

Two more comments are worth noting about the way the derivatives change with frequency and as a function of layer depth. The derivatives show a pronounced negative minimum at a particular frequency, the deeper the layer the lower the frequency. This quality is retained even for the derivatives of deep layers with respect to compressional wave velocity, Figure 4.5 for $\frac{\partial k_o}{\partial \alpha_{04}}$ shows this well. This variation is again expected because Rayleigh waves of different frequencies spread their energy through the layers to different extents. High frequencies are concentrated in the upper layers and only influence the derivatives for the upper layers. Conversely the derivative values for high frequencies in the lower layers are zero; there is no high frequency energy in the lower layers. Kolsky has shown in "Stress waves in solids" (1953) that at a depth of one wave-

Thickness of Layer h_1 km	P-Wave Velocity α_1 km s^{-1}	S-Wave Velocity β_1 km s^{-1}	$\frac{3}{4}\left(\frac{\alpha_1}{\beta_1}\right)^2$ $(=Q_{\alpha 1}^{-1} / Q_{\beta 1}^{-1})$
14.0	6.10	3.50	2.29
22.0	6.50	3.72	2.29
22.0	8.06	4.40	2.51
10.0	8.08	4.46	2.51
55.0	8.121	4.45	2.51
∞	8.50	4.96	2.19

Table 4.1 Assumed Velocity-Depth Model

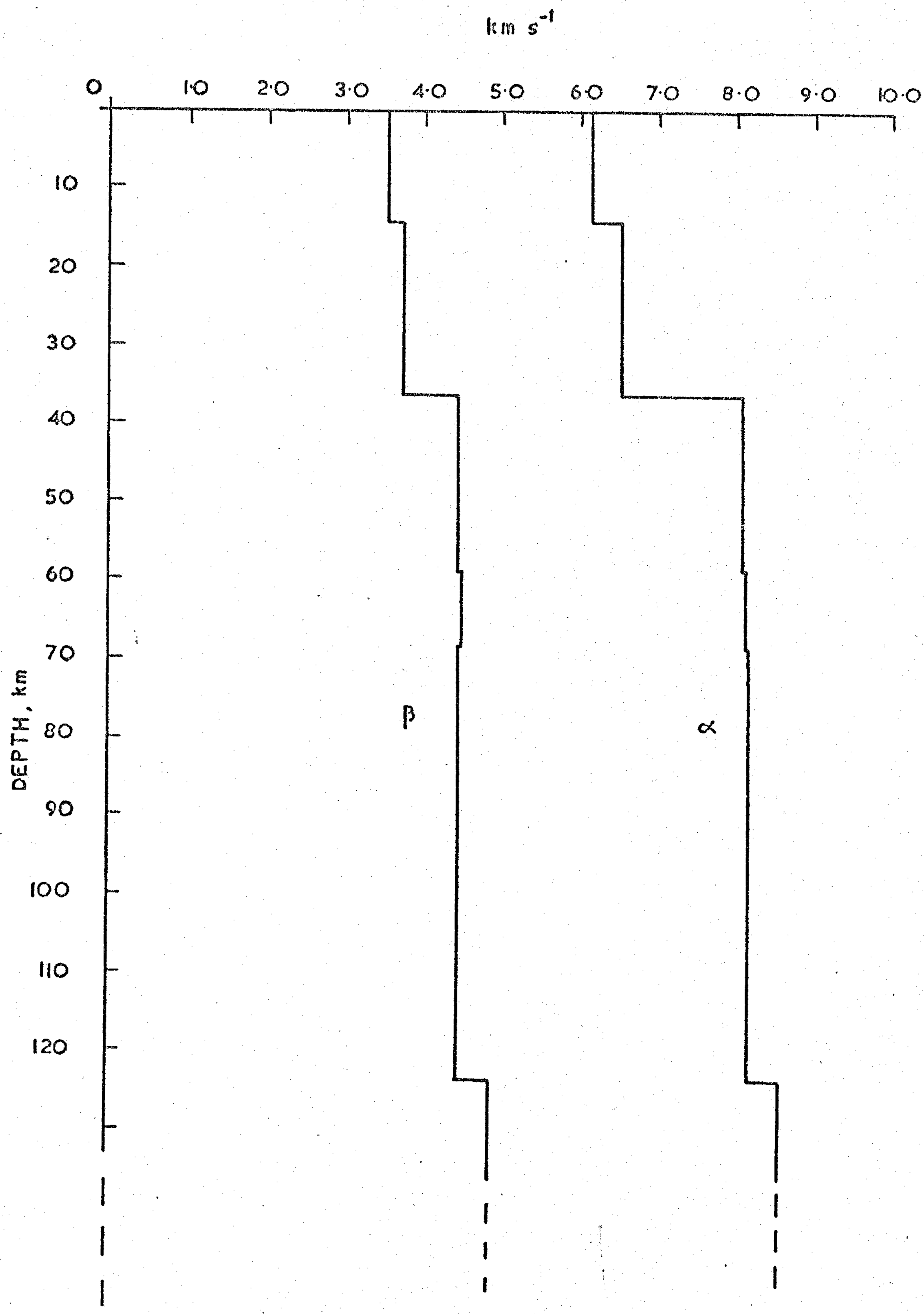

FIGURE 4.1 THE VELOCITY—DEPTH MODEL ASSUMED FOR INVERSION PURPOSES

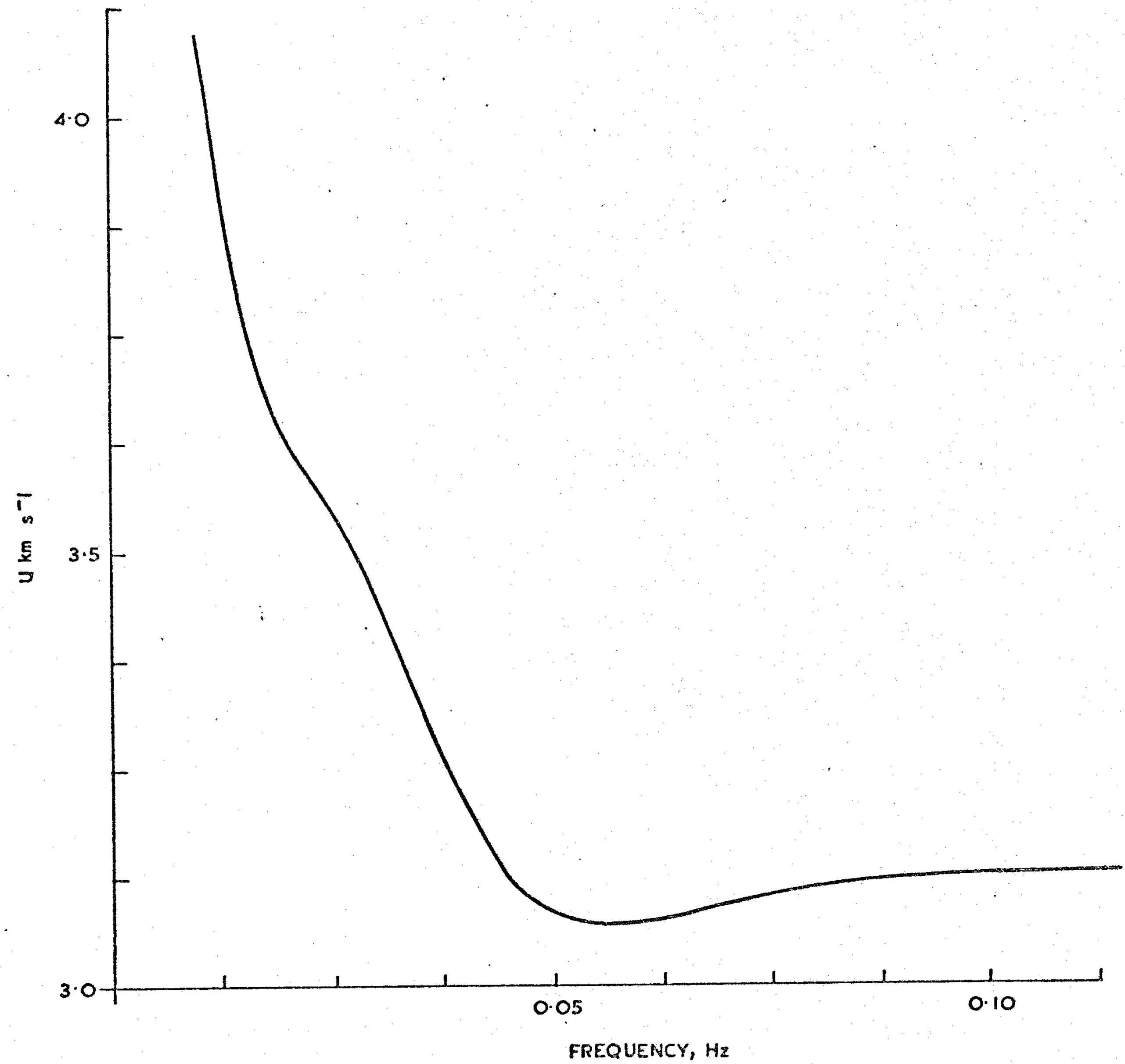

FIGURE 4.2 THE GROUP VELOCITY DISPERSION CURVE (U) FOR THE ASSUMED VELOCITY-DEPTH MODEL

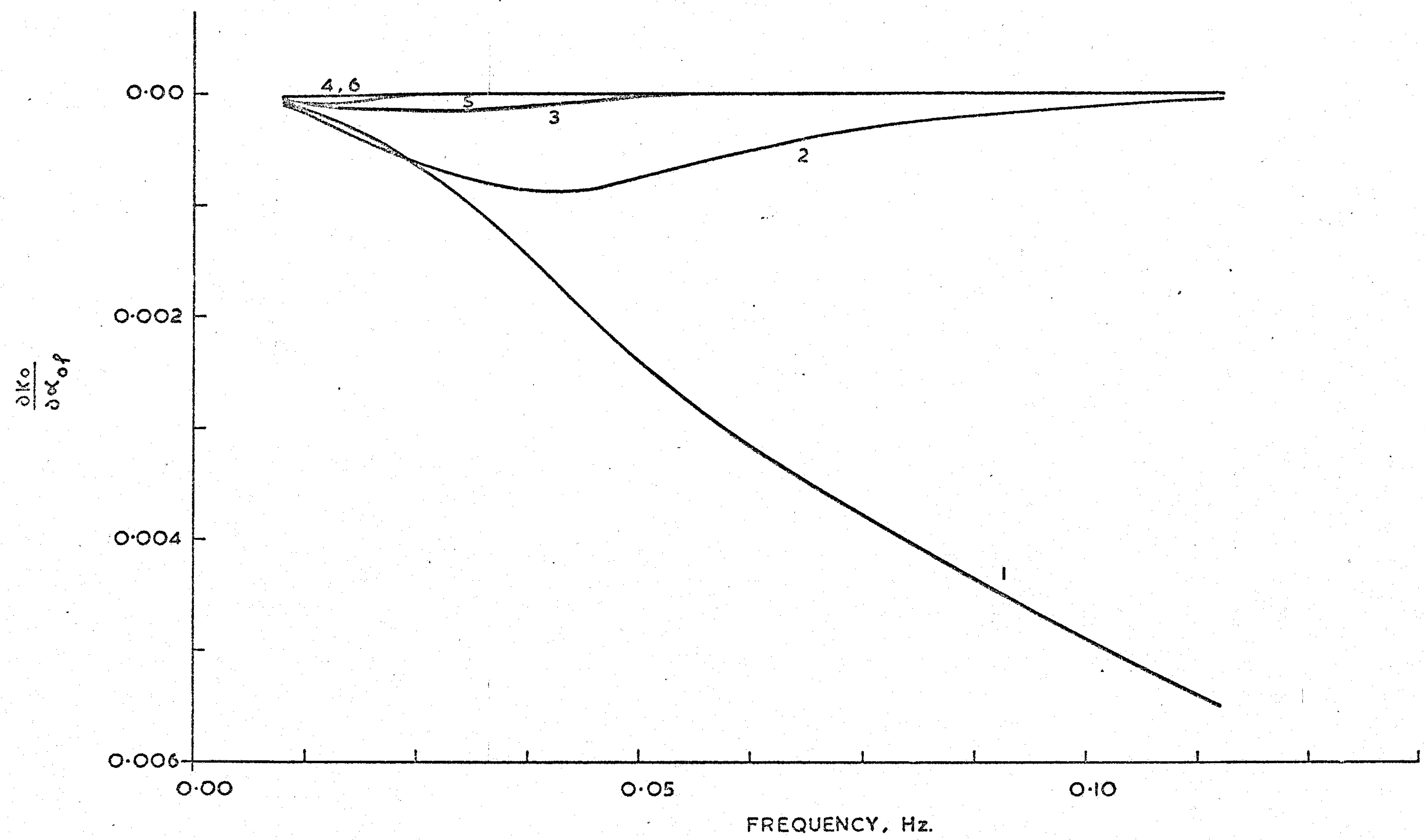

FIGURE 4.3 DERIVATIVES $\frac{\partial K_o}{\partial \alpha_{o\ell}}$ FOR THE SIX LAYERED VELOCITY-DEPTH MODEL (LAYERS, ℓ, MARKED 1 TO 6)

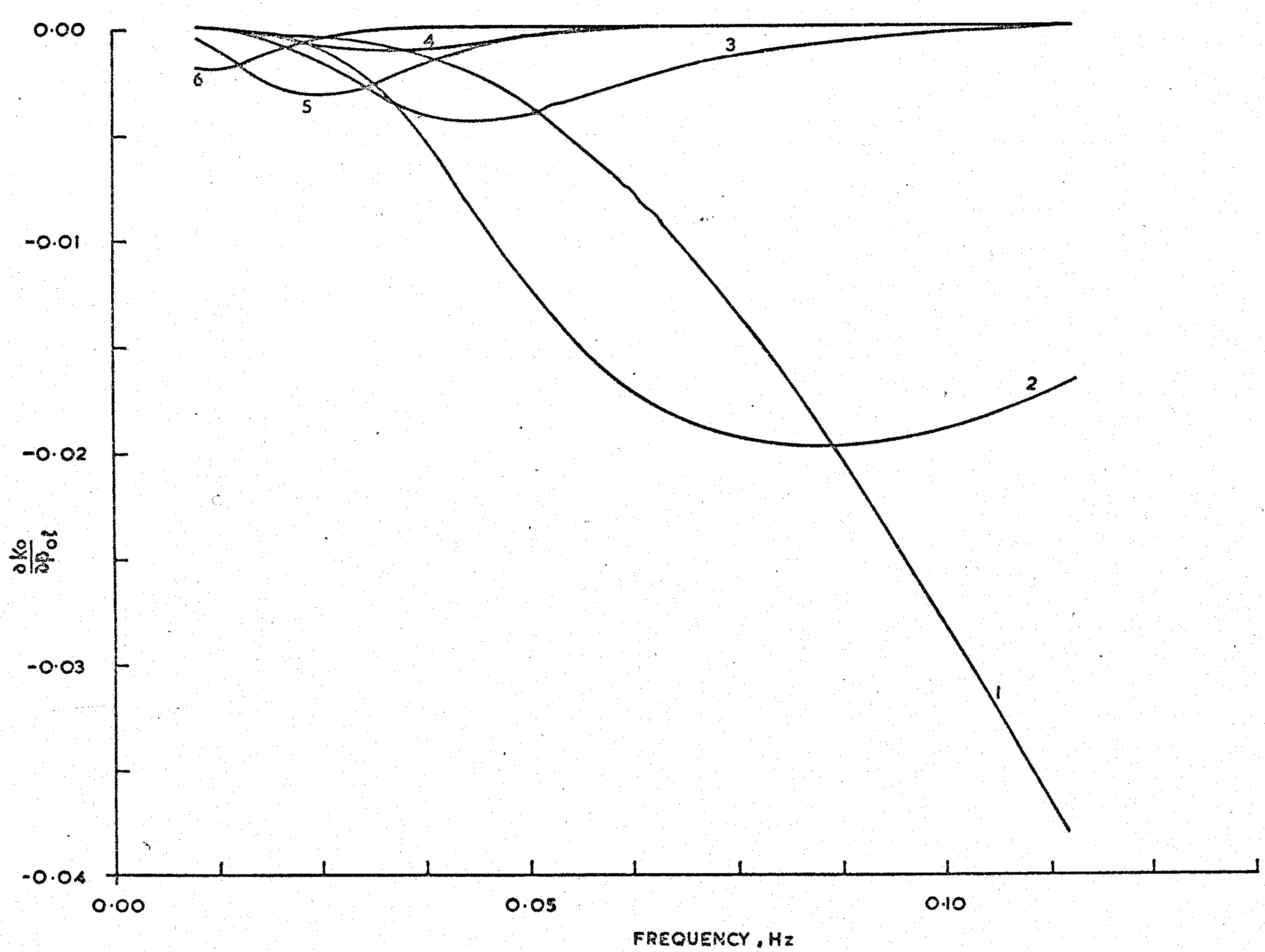

FIGURE 4.4 DERIVATIVES $\frac{\partial K_o}{\partial \beta_{o\ell}}$ FOR THE SIX LAYERED VELOCITY–DEPTH MODEL (LAYERS, ℓ, MARKED 1 TO 6)

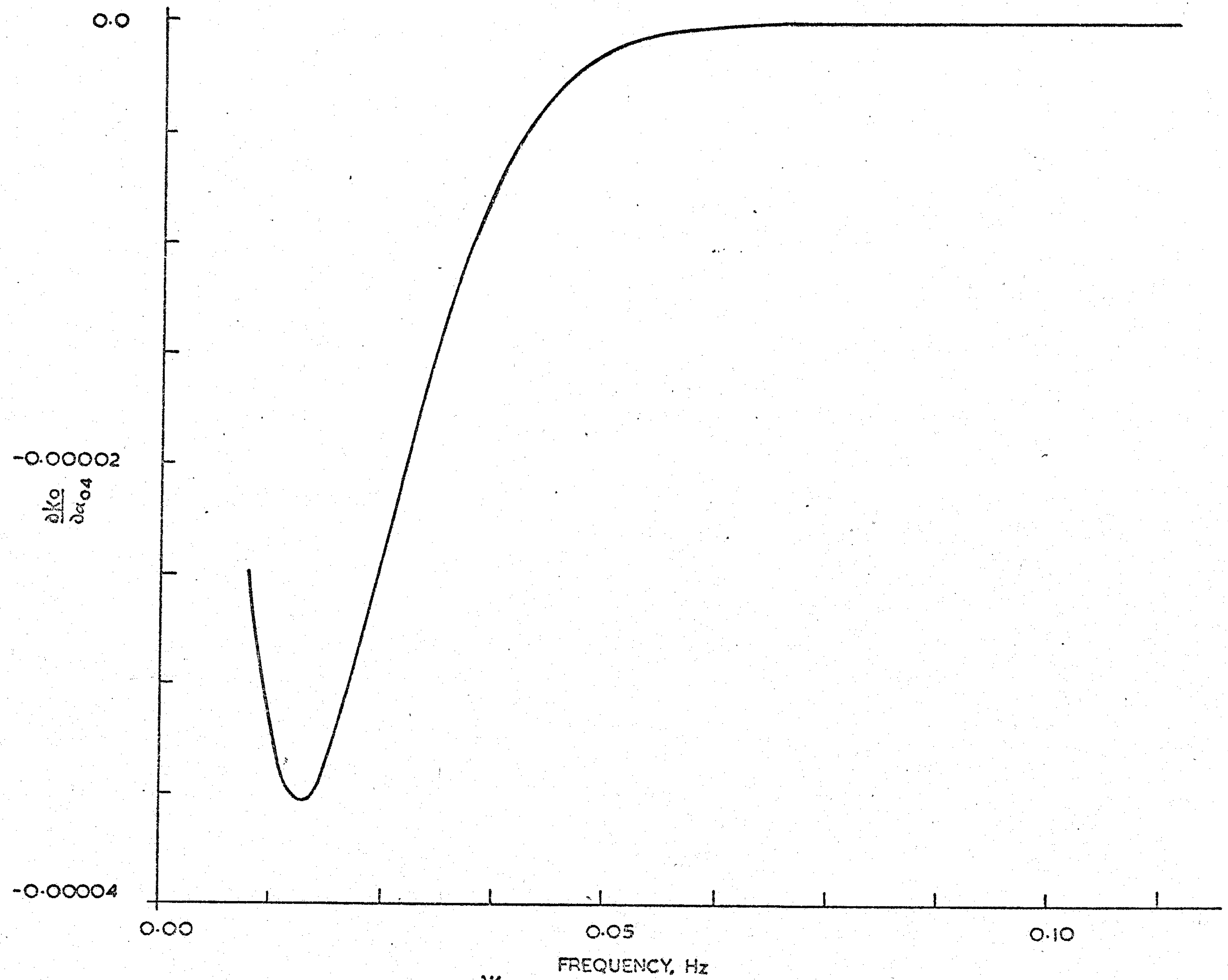

FIGURE 4.5 THE DERIVATIVE $\frac{\partial K_0}{\partial \alpha_{04}}$ FOR THE SIX LAYERED VELOCITY-DEPTH MODEL.

length into an homogeneous halfspace the vertical amplitude of motion has fallen to 0.19 of its value at the surface. For example a Rayleigh wave period 60s at a depth of 250 km is propagating with about 20% of its surface vertical amplitude. This depth value is regarded as the extreme limit of penetration of the waves used in this study; this is an obvious limit to the inversion range of depth.

The second comment arises because the deeper layer derivatives are much smaller than for shallower layers. For an homogeneous half space the shallower depths therefore have greater effect on the summation for $\gamma(\omega)$. For inversion over all frequencies into a depth model the upper layers are better resolved (because they are more heavily weighted by the derivatives). This is later of importance when direct "Hedgehog" inversion is used.

To summarise, the two sets of derivatives should be regarded as two dimensional weights varying with frequency and depth. When an attenuation model is postulated which varies with depth, the derivatives weight the model, shaping it and forming a result which may be compared to the observed.

4.4 Simple Qualitative Inversion of the $Q_\gamma^{-1}(f)$ Data

Using the assumed velocity-depth structure, and the related partial derivatives, makes it possible to invert $Q_\gamma^{-1}(f)$ into an attenuation model of Q_α^{-1}, Q_β^{-1} with depth. For the six layered attenuation structure to be used this requires twelve independent values of $Q_{\alpha,\beta}^{-1}$. It is desirable to reduce this number to six by assuming a simple relationship between Q_α^{-1} and Q_β^{-1} for all layers. Anderson et al. (1965) and Kanamori (1970) have suggested the adhoc relations

$$Q_\beta^{-1} = 2.25\, Q_\alpha^{-1} \qquad 4.37\ \text{C1}$$

$$Q_\beta^{-1} = Q_\alpha^{-1} \qquad 4.38\ \text{C2}$$

Burton and Kennet (1972) suggest using

$$Q_\beta^{-1} = \tfrac{3}{4} \left(\frac{\alpha}{\beta}\right)^2 Q_\alpha^{-1} \qquad 4.39\ \text{C3}$$

because this has a physical interpretation: no attenuation attributable to the bulk modulus. The values of ¾ $(\frac{\alpha_1}{\beta_1})^2$ and hence the ratio $\frac{Q^{-1}_{\beta 1}}{Q^{-1}_{\alpha 1}}$ are listed in Table 4.1.

Not forgetting the influence the partial derivatives have on the calculation of $Q^{-1}_{\alpha}(f)$ for the real earth we may now take equation 4.36 further. Using the condition, C1, $Q^{-1}_{\beta} = 2.25\, Q^{-1}_{\alpha}$ gives

$$Q^{-1}_{\gamma} = 3.25\, Q^{-1}_{\alpha} \qquad 4.40$$

A very simple qualitative inversion is now possible. The figures 3.1 to 3.6, and in particular 3.18 and 3.19 for average $Q^{-1}_{\gamma}(f)$, show that $Q^{-1}_{\gamma}(f)$ for higher frequencies is about 0.003 but for lower frequencies it may reach 0.009. Using the approximation of 4.40 this gives

Depth	Q^{-1}_{α}	Q^{-1}_{β}	Q^{-1}_{γ}	Frequency
Shallow	0.001	0.002	0.003	High
Deep	0.003	0.007	0.009	Low

Obviously the tentative conclusion is a region of greater attenuation at depth, which is only sampled by the penetrating low frequencies. The partial derivatives have been ignored in the above approximations, but the way in which they weight the deeper layers (previously described) will make larger values of Q^{-1} at depth difficult to resolve.

4.5 Model Inversion of the $Q^{-1}_{\gamma}(f)$ data

It is possible to attempt inversion by trial and error. A model may be postulated, guided by the simple qualitative inversion above, and the $Q^{-1}_{\gamma}(f)$ it would generate may be calculated. It was decided to model Q^{-1}_{α} because this parameter is more abundant in the literature than Q^{-1}_{β}.

The computer program QRALEY (Appendix G) was written to calculate $Q^{-1}_{\gamma}(f)$ for any postulated model of Q^{-1}_{α} with depth and any simple relationship between Q^{-1}_{α} and Q^{-1}_{β} may be used in this program.

A simple model (M1) was found which approximates the curve shape for the $Q^{-1}_{\gamma}(f)$ values averaged for five atmospheric explosions shown in Figure 3.19, that is the model generates roughly constant Q_γ^{-1} in the frequency range 0.03-0.09 Hz and Q_γ^{-1} increases for lower frequencies. This model shows a high value, $Q_\alpha^{-1} = 0.008$, for the deepest layer.

Model M1 was compared to four other models. All five models are listed in Table 4.2. The models attributed to Teng, Anderson et al. and Kanamori have been adapted (to fit the layers in this study) from the Q_α values listed in Ibrahim's (1971) paper. The model M2 represents a simple decrease of attenuation with depth, this phenomenon might be expected due to increased compaction of material with depth. The control model M1 is regarded as a reasonable picture of the observed data. All five models were compared for the three conditional equations between Q_α^{-1} and Q_β^{-1} specified by equations 4.37-4.39. The results are shown in Figures 4.6-4.8.

The models of Kanamori and M2 are untenable for all three conditions. Decreasing attenuation at low frequencies is found by M2, while the Kanamori values are too large. Teng's model is unsuitable given conditions C1 and C3 but using $Q_\alpha^{-1} = Q_\beta^{-1}$ it is a possible model, although the onset of increasing Q_γ^{-1} at low frequencies occurs at too high a frequency (0.05 Hz). Anderson's model has possibilities but the peak at low frequencies, rather than a smooth increase of Q_γ^{-1}, tends to make it unacceptable.

4.6 Conclusions

An expression has been obtained from which the specific attenuation factor $Q_\gamma^{-1}(f)$ for Rayleigh waves may be calculated.

For the calculation of $Q_\gamma^{-1}(f)$ it is necessary to assume a velocity-depth structure, for which partial derivatives of the type $\frac{\partial k_o}{\partial \alpha_{o1}}$ are calculated. An attenuation model for Q_α^{-1} with depth is then postulated, and a condition of the type $Q_{\beta 1}^{-1} = ¾ \left(\frac{\alpha_1}{\beta_1}\right)^2 Q_{\alpha 1}^{-1}$ assumed. The derivatives are regarded as weights which shape the attenuation model, forming a surface wave $Q_\gamma^{-1}(f)$ from body wave $Q_{\alpha,\beta}^{-1}(h)$.

Thickness of Layer	Model 1	Model 2	Teng		Anderson et al.		Kanamori	
h km	Q_α^{-1}	Q_α^{-1}	Q_α	Q_α^{-1}	Q_α	Q_α^{-1}	Q_α	Q_α^{-1}
14.0	.0025	.0045	450	.00222	1012	.00099	450	.00222
22.0	.0025	.0040	450	.00222	1012	.00099	450	.00222
22.0	.0025	.0035	255	.00392	135	.00741	60	.01667
10.0	.0045	.0030	68	.01471	135	.00741	60	.01667
55.0	.0015	.0025	95	.01053	195	.00513	87	.01149
∞	.0080	.0020	100	.01000	260	.00385	120	.00833

Table 4.2 Attenuation models for Q_α^{-1} as a function of depth. (The model types attributed to Teng, Anderson et al. and Kanamori are adapted from the Q_α values listed by Ibrahim (1971).)

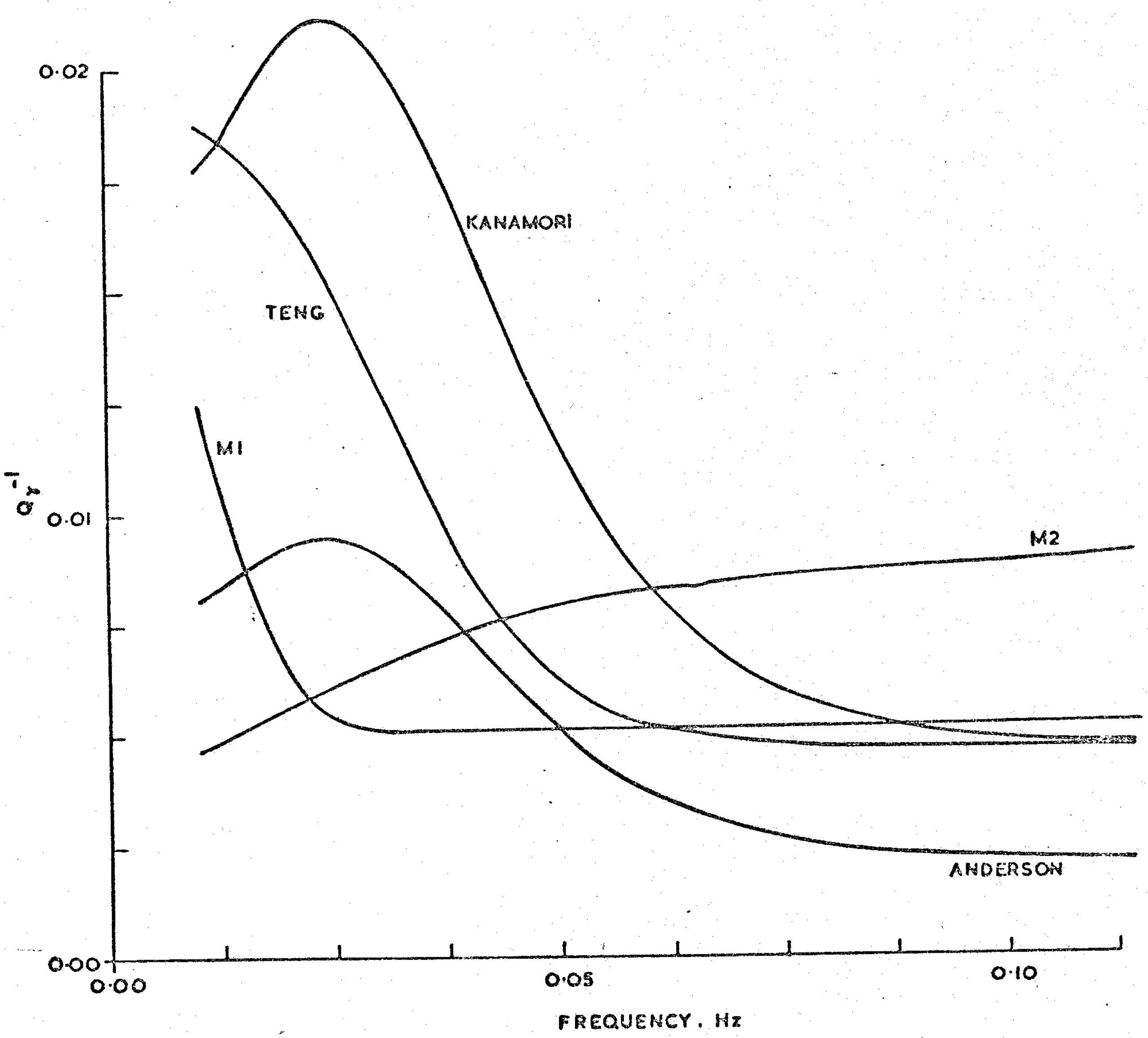

FIGURE 4.6 THEORETICAL RAYLEIGH WAVE Q_γ^{-1} FOR MODELS USING $Q_\beta^{-1} = 2{\cdot}25\, Q_\alpha^{-1}$

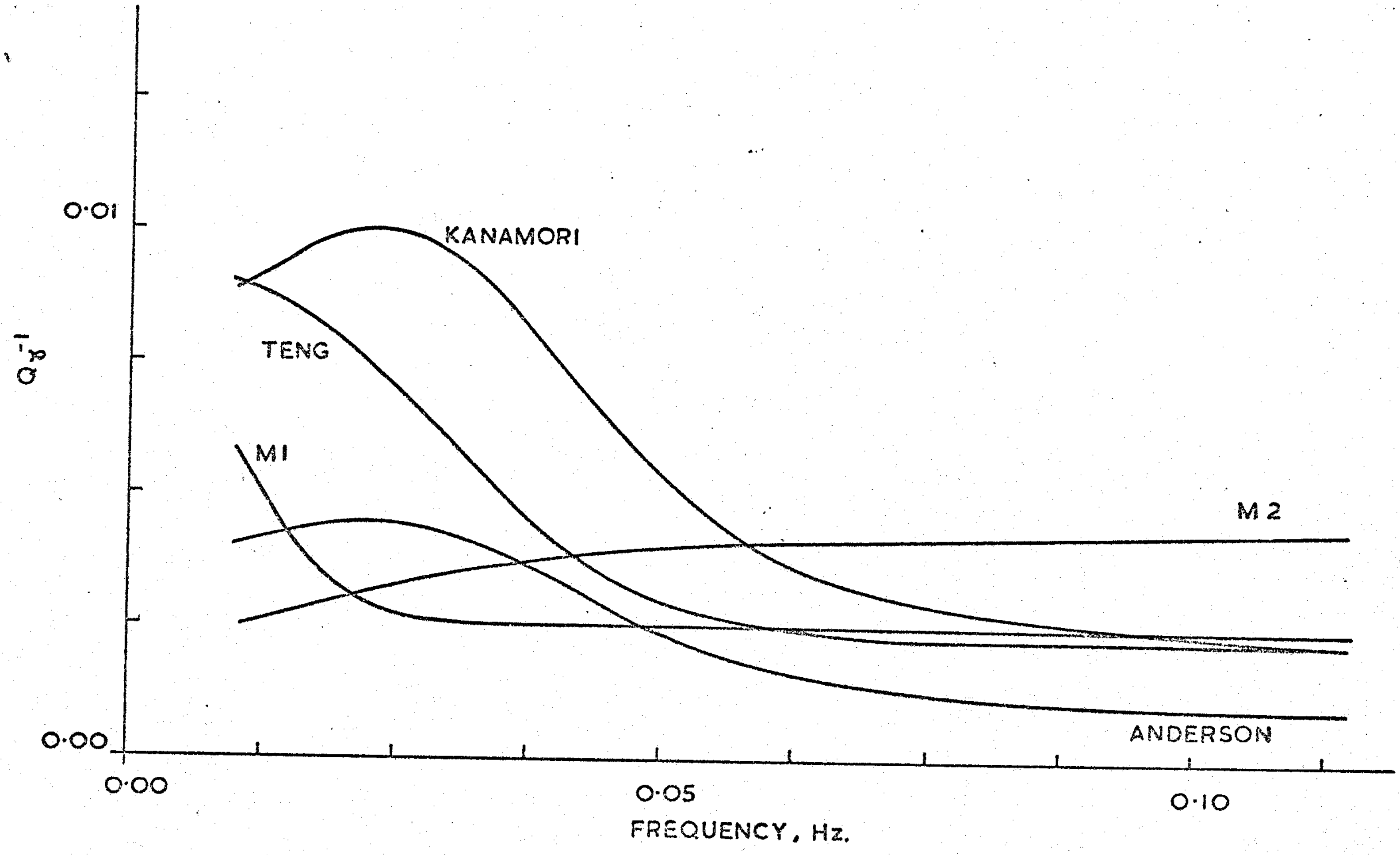

FIGURE 4.7 THEORETICAL RAYLEIGH WAVE Q_γ^{-1} FOR MODELS USING $Q_\beta^{-1} = Q_\alpha^{-1}$

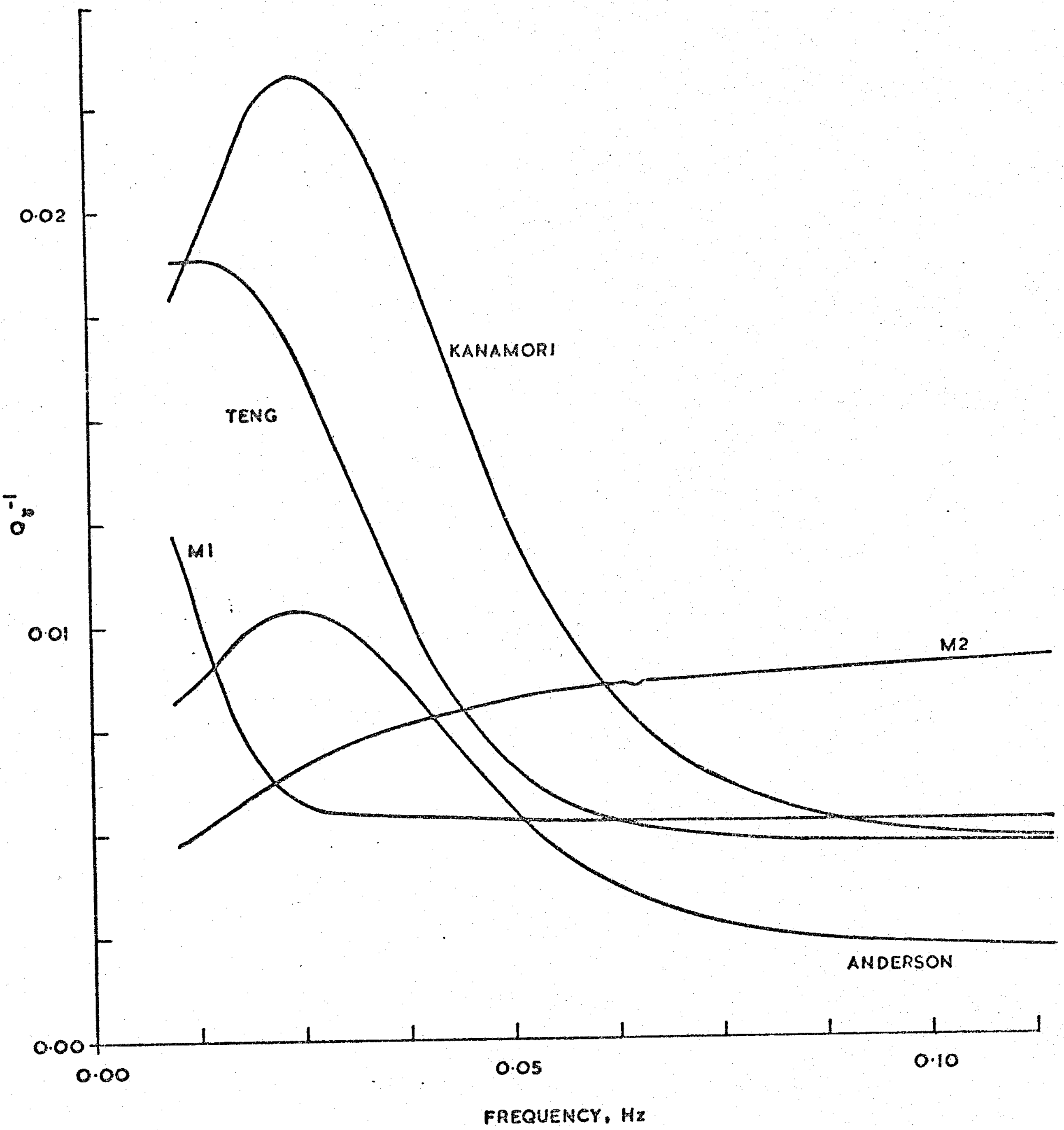

FIGURE 4.8 THEORETICAL RAYLEIGH WAVE Q_γ^{-1} FOR MODELS USING $Q_\beta^{-1} = \frac{3}{4}\left(\frac{\alpha}{\beta}\right)^2 Q_\alpha^{-1}$

A model M1 was found which approximates to the observed data. This model was compared to four other models, all of which were found to possess very individual characteristics. The model M1 was the best match to the data and condition C3

$$Q_{\beta}^{-1} = \tfrac{3}{4} \left(\frac{\alpha}{\beta}\right)^2 Q_{\alpha}^{-1}$$

was retained because it has physical meaning.

However trial and error model fitting of this nature is very inadequate because it gives little idea about the model accuracy. It is not possible to say by how much an individual layer in the model may be perturbed before the resulting $Q_{\gamma}^{-1}(f)$ is incompatible with that observed. Also the accuracy of the observed data, expressed by the 95% confidence limits of figures 3.20 to 3.22 has been entirely ignored. A direct method of inversion, using this additional information, is desirable.

CHAPTER 5

5.1 'Hedgehog' - Direct Inversion

5.1.1 Introduction

Many data inversions - the matching of a particular depth dependent model to observed data at the surface of the earth - produce simple line models. The inversion attempts to show a simple one-to-one correspondence between surface results and depth dependent variables. This would only be possible for the present data if the inherent variability in the Q_{γ}^{-1} data, expressed by the confidence limits, was neglected. Any inversion of Q_{γ}^{-1} must produce a plot of Q_{α}^{-1}, varying with depth, and with a range of Q_{α}^{-1} values for any depth. It is important to realise that errors alone need not explain a range of Q_{α}^{-1} at a particular depth; it is realistic to expect a laterally inhomogeneous earth. The narrow confidence limits obtained in Chapter 3 have geophysical meaning and do not just contain experimental errors.

To invert the Q_{γ}^{-1} surface wave data it is necessary to postulate models in some form of Q space. "The difference between $Q=\infty$ and $Q=1450$ is not significant at present, since one is in fact comparing reciprocals of these quantities." This was stated by Knopoff (1969) and succintly explains why all models considered here are in inverse Q space.

5.1.2 "Hedgehog"

Any depth model in Q^{-1} space may be used to postulate Q_{γ}^{-1} at the surface by using the equations in Chapter 4. Once the postulated values for the surface have been obtained then a comparison may be made with the surface observed data.

It is necessary to distinguish between experimentally observed data and theoretically calculated values. The symbols $Q_{\gamma o}^{-1}$ and Q_{γ}^{-1}, for observed and theoretical values respectively, make this distinction, and as a function of frequency $Q_{\gamma o}^{-1}(f_i)$ will become $Q_{\gamma oi}^{-1}$. (i=1 ... NFA).

The goodness of fit for a particular model, compared to the observed data, may be quantitatively defined using the equations

$$\left| \frac{Q^{-1}_{\gamma i} - Q^{-1}_{\gamma oi}}{\Delta Q^{-1}_{\gamma oi}} \right| = a' \qquad i=1 \qquad NFA \qquad 5.1$$

$$\left[\frac{1}{NFA} \sum_{i=1}^{NFA} \left(\frac{Q^{-1}_{\gamma i} - Q^{-1}_{\gamma oi}}{\Delta Q^{-1}_{\gamma oi}} \right)^2 \right]^{\frac{1}{2}} = \sigma' \qquad 5.2$$

The quantity $\Delta Q^{-1}_{\gamma oi}$ relates to the confidence limits determined for each value of the observable $Q^{-1}_{\gamma oi}$. If a' and σ' are arbitrarily set to values a and σ and an inequality imposed on equations 5.1 and 5.2, then these equations either accept or reject a particular model (Burton and Kennett 1972).

The Monte-Carlo technique may be used to generate random models and equations 5.1, 5.2 used to select the acceptable ones. However, this shows no unity in the inversion models. Nor does it indicate, except by the density of acceptable models in Q^{-1} - depth space, any breadth of fit for a particular depth.

The Hedgehog program, once a good model has been found by Monte-Carlo in continuous valued Q^{-1} space, then moves onto a mesh or network of discrete values in Q^{-1} space. If the knot it has moved to is acceptable then all adjacent knots are tested until a boundary between good and bad models is reached. In this way the program determines a region of connected inversion solutions to the observed data and creates an area of fit rather than individual points. After completing one region the program returns to the Monte-Carlo technique to look for further solutions and regions outside those already found, until the entire region of search has been exhausted or sufficient models tested. The region of search is chosen by imposing geophysically realistic values on the Q^{-1} space for each layer of the model.

The values of $\Delta Q^{-1}_{\gamma oi}$ calculated in Chapter 3 are the 95% confidence limits on $Q^{-1}_{\gamma oi}$, and values were determined for 79 frequencies. Altering a and σ changes the precision to which a model must fit the experimental data. If a=1.0 then models must lie within the 95% confidence limits. For other confidence levels the value of a depends upon the degrees of freedom for that particular event.

A typical Hedgehog network N1 used in this work is shown in Table 5.1. The values of δQ^{-1} are used to increment from Q^{-1}_{LOW} to Q^{-1}_{HIGH}. In all cases Q^{-1}_{LOW} was chosen as zero. It is possible to improve resolution of the inversion model by choosing a fine net, this presents problems because a fine net implies many knots and therefore many models to be tested. Monte-Carlo type inversion is only possible because the computation time involved in calculating $Q^{-1}_{\gamma i}$ and testing against $Q^{-1}_{\gamma oi}$ is minimal, 1000 models can be tested in 4 seconds. On one occasion a quarter million models were tested by the program in 15 minutes, however this did not facilitate inversion, because it also rejected the quarter million models! The precision to which the models fit the data, and the fineness of the net creating the models must be compatible.

5.2 Inversion

5.2.1 The General Model

The six layered velocity-depth model and partial derivatives of Chapter 4 are used. The relation

$$Q^{-1}_{\beta l} = \tfrac{3}{4}\left(\frac{\alpha_l}{\beta_l}\right)^2 Q^{-1}_{\alpha l} \qquad l=1\ldots6 \qquad 5.3$$

is used for the six layers to reduce the number of Q^{-1} variables to six.

Inversion was attempted for three sets of $Q^{-1}_{\gamma oi}$ data:

1 <u>3NZA</u> The average formed from the three atmospheric explosions at Novaya Zemlya (Figure 3.18).

2 <u>2CA</u> The average from the two atmospheric explosions at S Sinkiang Prov. China (Figure 3.18).

3 <u>5A</u> The average of all five atmospheric explosions (Figure 3.19

The underground explosion was not included in 3NZA because it has been shown to be a different statistical population (Chapter 3). Table 3.1 shows

Table 5.1 HEDGEHOG NETS

(Q_α^{-1} Parameter Space)

N1

Layer	Q_α^{-1} LOW	Q_α^{-1} HIGH	δQ^{-1}
1	0.0	0.01	.001
2	"	0.008	"
3	"	0.008	"
4	"	0.01	"
5	"	0.01	"
6	"	0.02	0.002

N2

Layer	Q_α^{-1} LOW	Q_α^{-1} HIGH	δQ^{-1}
1	0.0	.0105	.0015
2	"	.0075	"
3	"	"	"
4	"	.0105	"
5	"	.006	.001
6	"	.02	.002

N3

Layer	Q_α^{-1} LOW	Q_α^{-1} HIGH	δQ^{-1}
1	0.0	0.008	0.002
2	"	"	"
3	"	0.014	0.003
4	"	0.016	"
5	"	"	"
6	"	0.02	0.004

N4

Layer	Q_α^{-1} LOW	Q_α^{-1} HIGH	δQ^{-1}
1	0.0	.005	.002
2	"	"	"
3	"	.01	.003
4	"	"	"
5	"	.016	.004
6	"	.02	.005

N5

Layer	Q_α^{-1} LOW	Q_α^{-1} HIGH	δQ^{-1}
1	0.0	.008	.004
2	"	.008	.004
3	"	.012	.006
4	"	.012	.006
5	"	.005	.002
6	"	.020	.010

that these data sets only contain useful information up to a certain highest frequency. The frequency range used and therefore the number of $Q^{-1}_{\gamma oi}$ values for each group is

$Q^{-1}_{\gamma oi}$ Data Set	Number of Stations	Frequency Range Hz	Number of $Q^{-1}_{\gamma oi}$ Values
3NZA	81	.0147-.0806	55
2CA	63	.0147-.0855	59
5A	144	.0147-.0830	57

For two reasons the removal of higher frequencies is beneficial for direct inversion. The depth of penetration for surface waves depends on wavelength. Therefore high frequencies will only contain information about the upper layers of the earth, whereas low frequencies contain information about both the upper layers and greater depths. Further, the shape of the weighting derivatives $\frac{\partial k_o}{\partial \alpha_{ol}}$, $\frac{\partial k_o}{\partial \beta_{ol}}$ (see Figures 4.3, 4.4) used to calculate theoretical $Q^{-1}_{\gamma i}$ for the models, would heavily bias the resolution towards the upper layers, because of the large derivative values at high frequencies. Figure 5.1 for the major derivative $\frac{\partial k_o}{\partial \beta_{ol}}$ up to frequency .0623 Hz, shows more equal weighting for the various layers. To include high frequencies is to weight the inversion model towards the upper layers, at the expense of resolution at depth. A spread of energy throughout all layers is required for good inversion.

5.2.2 Inversion of 3NZA

The models were tested against the data for several levels of precision, also different nets were used to improve and confirm the results. The range of figures 5.2-5.5 show the inversion models, found using net N1, for different confidence levels on the observed data.

Figure 5.2 accepted models fitting within 90% confidence limits, a narrow band of fit, using a = 0.833. Only two Monte-Carlo models, and no Hedgehog connected region, are obtained out of the 80,000 random models

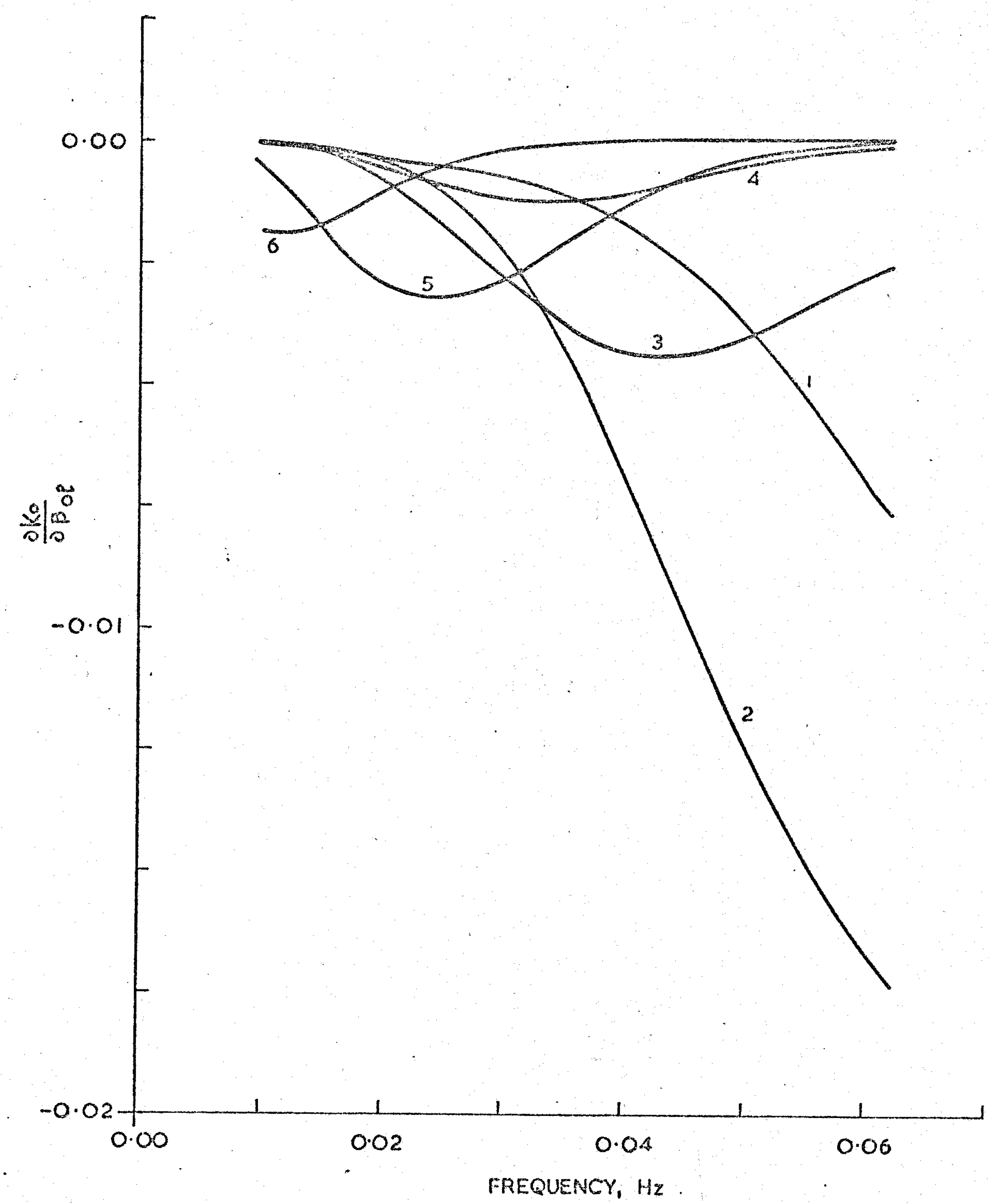

FIGURE 5.1 DERIVATIVES $\frac{\partial K_o}{\partial \beta_{o\ell}}$ FOR 'HEDGEHOG' INVERSION

tested.

Two independent regions of fit are found using N1 and 95% confidence limits, these are shown in Figures 5.3 and 5.4. A fit to very broad confidence limits, 99%, was tried using nets N1 and N2. This produces Figures 5.5 and 5.6; execution of the program was finished in each case before the entire region had been delineated because far too many solution knots were being found to be of any use. The Hedgehog regions of Figures 5.3 and 5.4 represent the best inversion of the data from the Novaya Zemlya atmospheric explosions.

Three solutions, chosen as typical examples from the two Hedgehog regions, are shown in Figure 5.7. Table 5.2 lists the three models. All these models show a layer of high attenuation in the upper mantle, as did Burton and Kennett using one event. This again supports the theory of a highly attenuating zone corresponding to the Gutenberg low velocity zone, without assuming any such low velocity during model fitting.

Table 5.2 Three Typical Solutions for 3NZA

Layer	Model A		Model B		Model C		Depth to Layer Base km
	Q_α^{-1}	Q_β^{-1}	Q_α^{-1}	Q_β^{-1}	Q_α^{-1}	Q_β^{-1}	
1	.002	.00456	.001	.00228	.002	.00456	14
2	.002	.00458	.003	.00687	.002	.00458	36
3	.002	.00503	.001	.00252	.002	.00503	58
4	.002	.00501	.001	.00251	.006	.01504	68
5	.002	.00500	.003	.00749	.001	.0025	123
6	.008	.01762	.006	.01322	.008	.01762	∞

Model A shows the upper 120 km to be of uniform low attenuation material, overlying the zone of high absorption. Model C shows a similar distribution but with a strongly attenuating perturbation around 70 km. This type of model was generally characteristic of the second Hedgehog region shown in Figure 5.4.

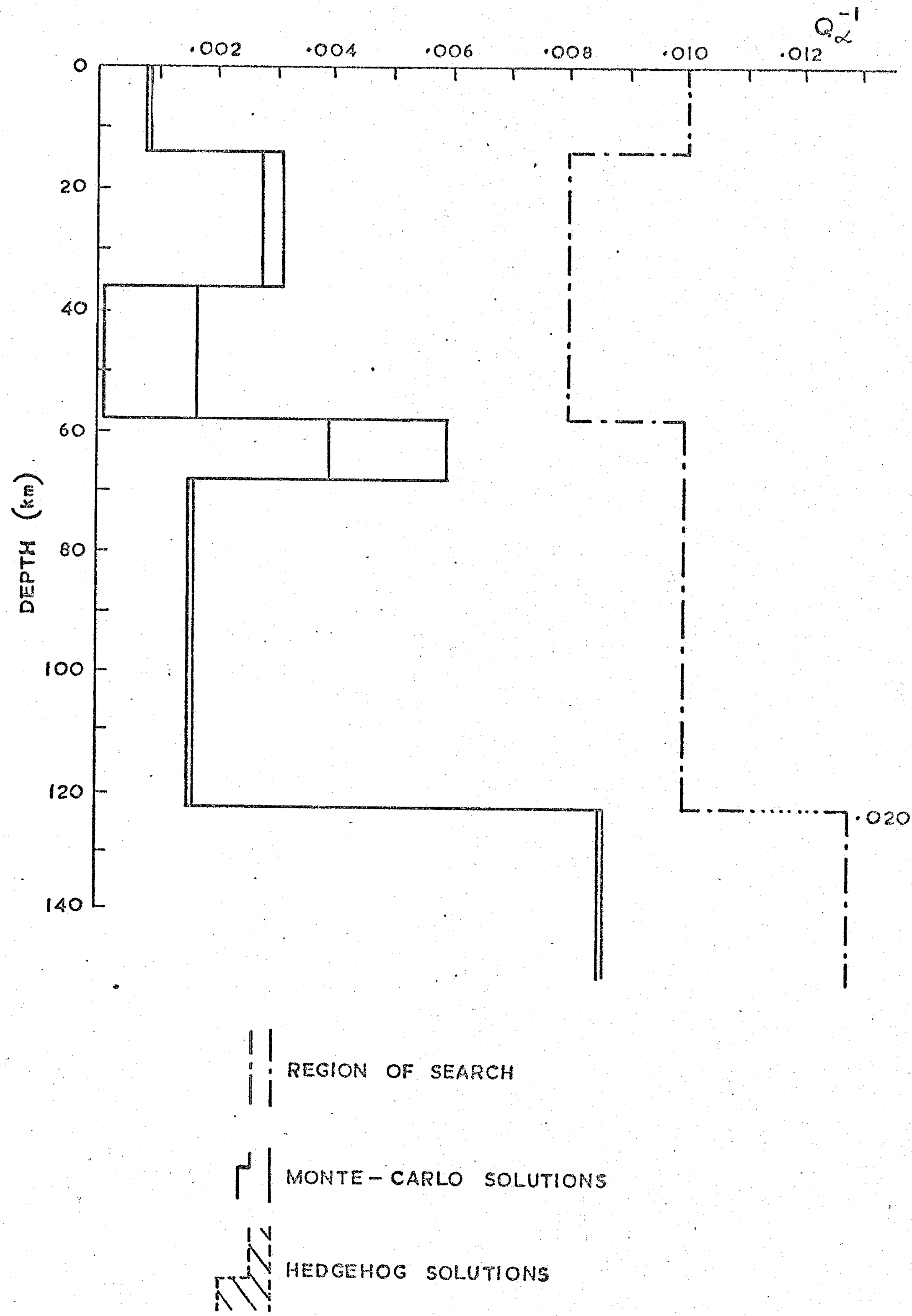

FIGURE 5.2 INVERSION OF THE AVERAGED NOVAYA ZEMLYA DATA (3NZA) (90% CONFIDENCE LIMITS AND NET NI)

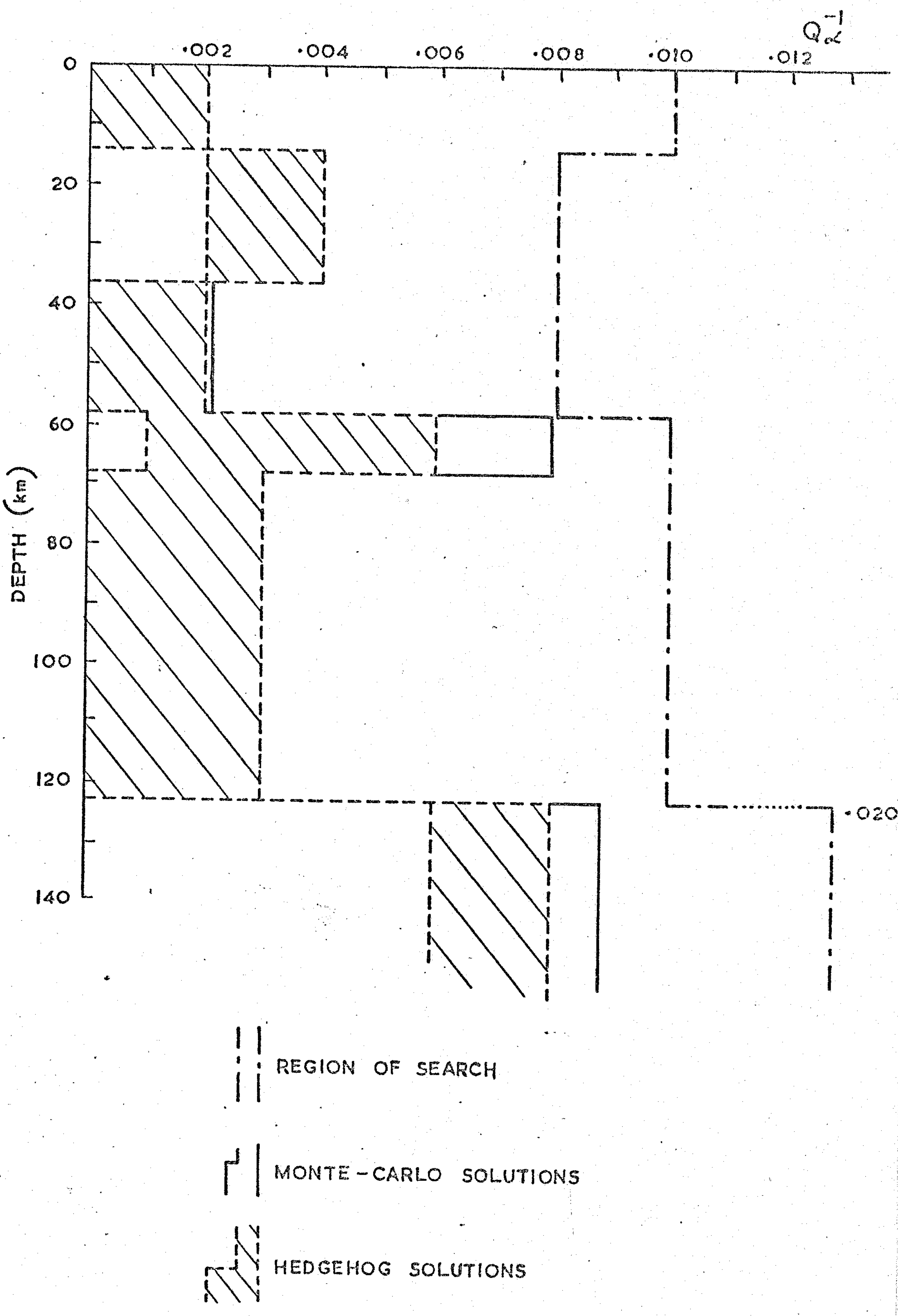

FIGURE 5.3 THE FIRST HEDGEHOG SOLUTION FOR 3NZA
(95% CONFIDENCE LIMITS AND NET NI)

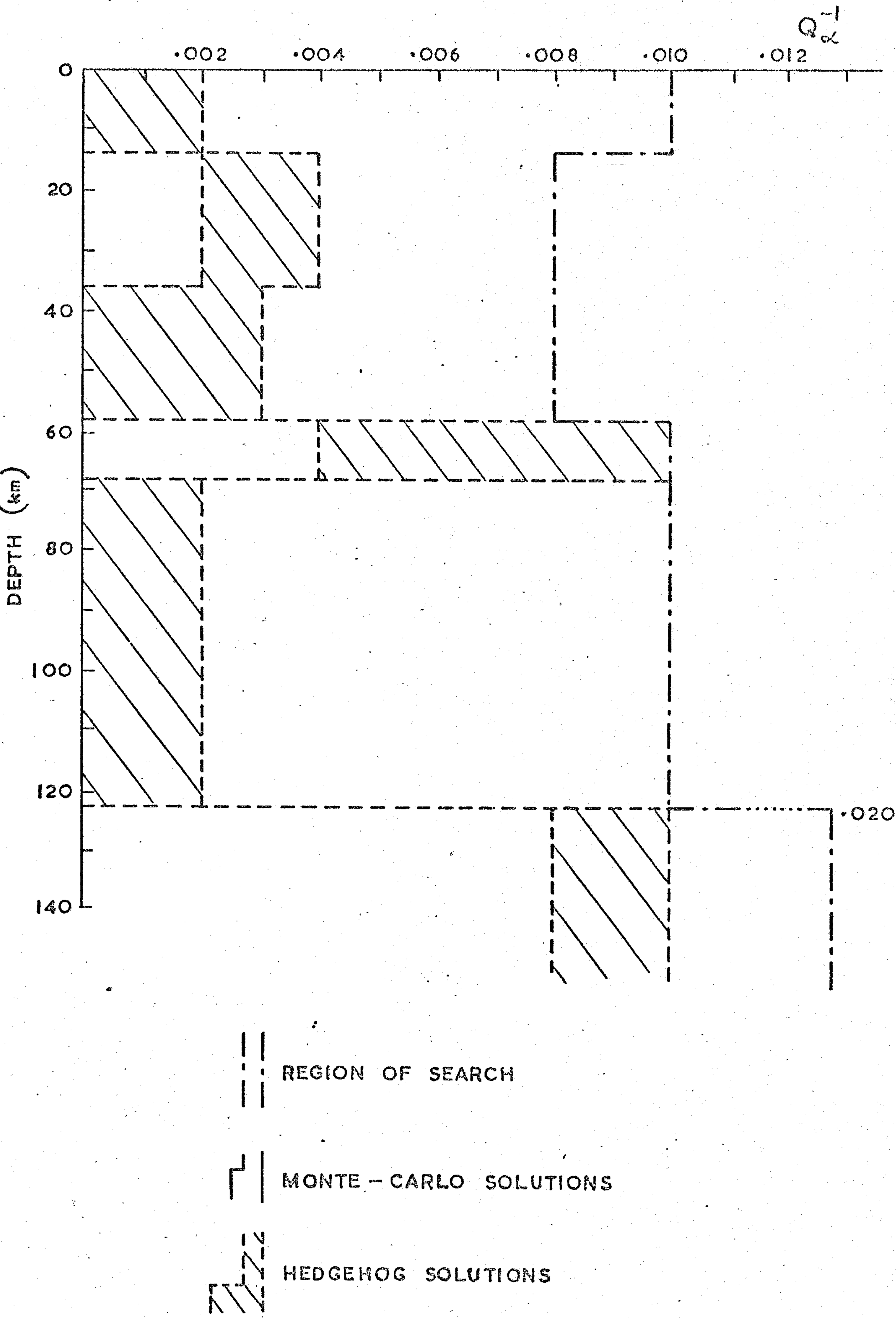

FIGURE 5.4 THE SECOND HEDGEHOG SOLUTION FOR 3NZA (95% CONFIDENCE LIMITS AND NET NI)

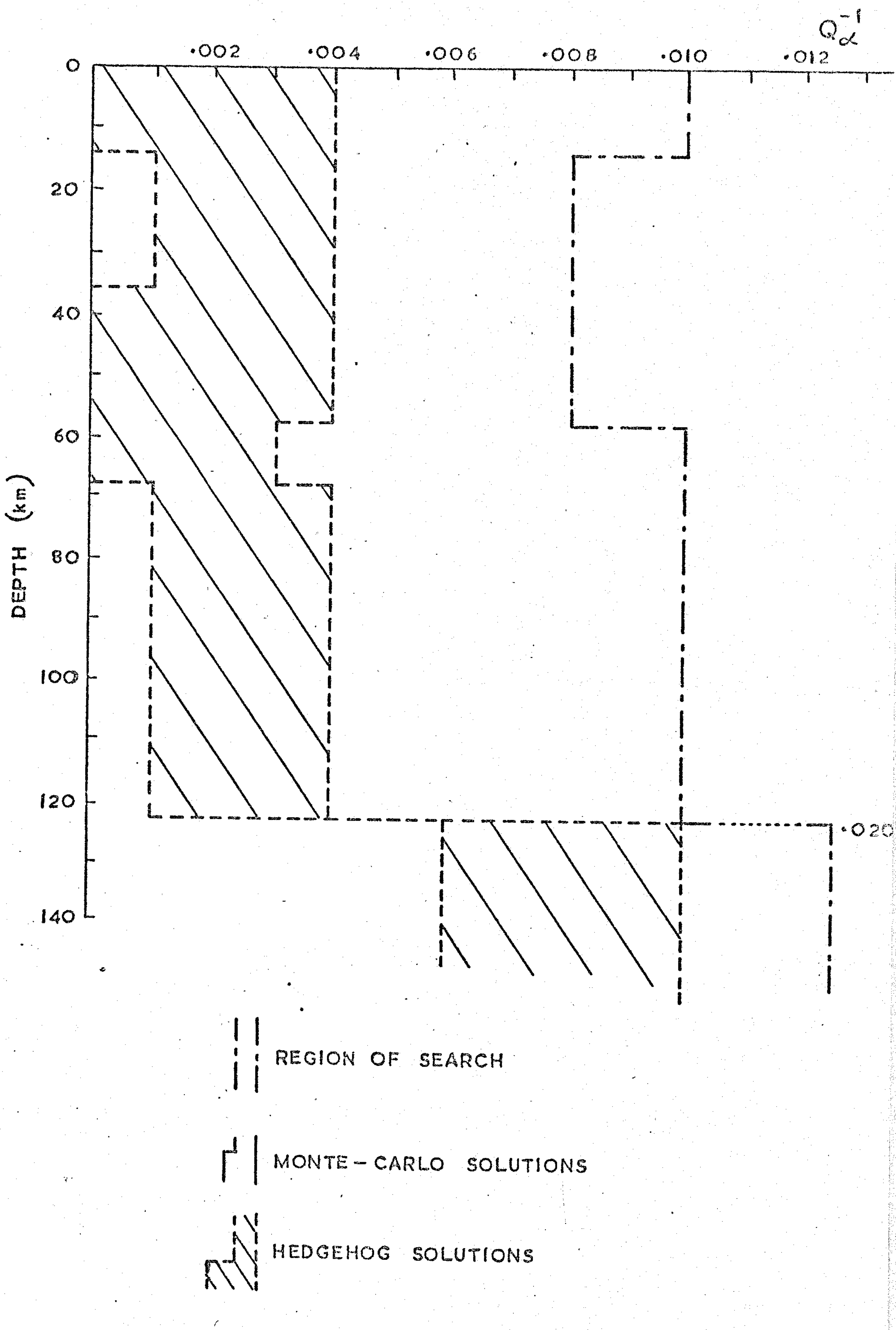

FIGURE 5.5 ATTEMPTED INVERSION OF 3NZA
(99% CONFIDENCE LIMITS AND NET NI)

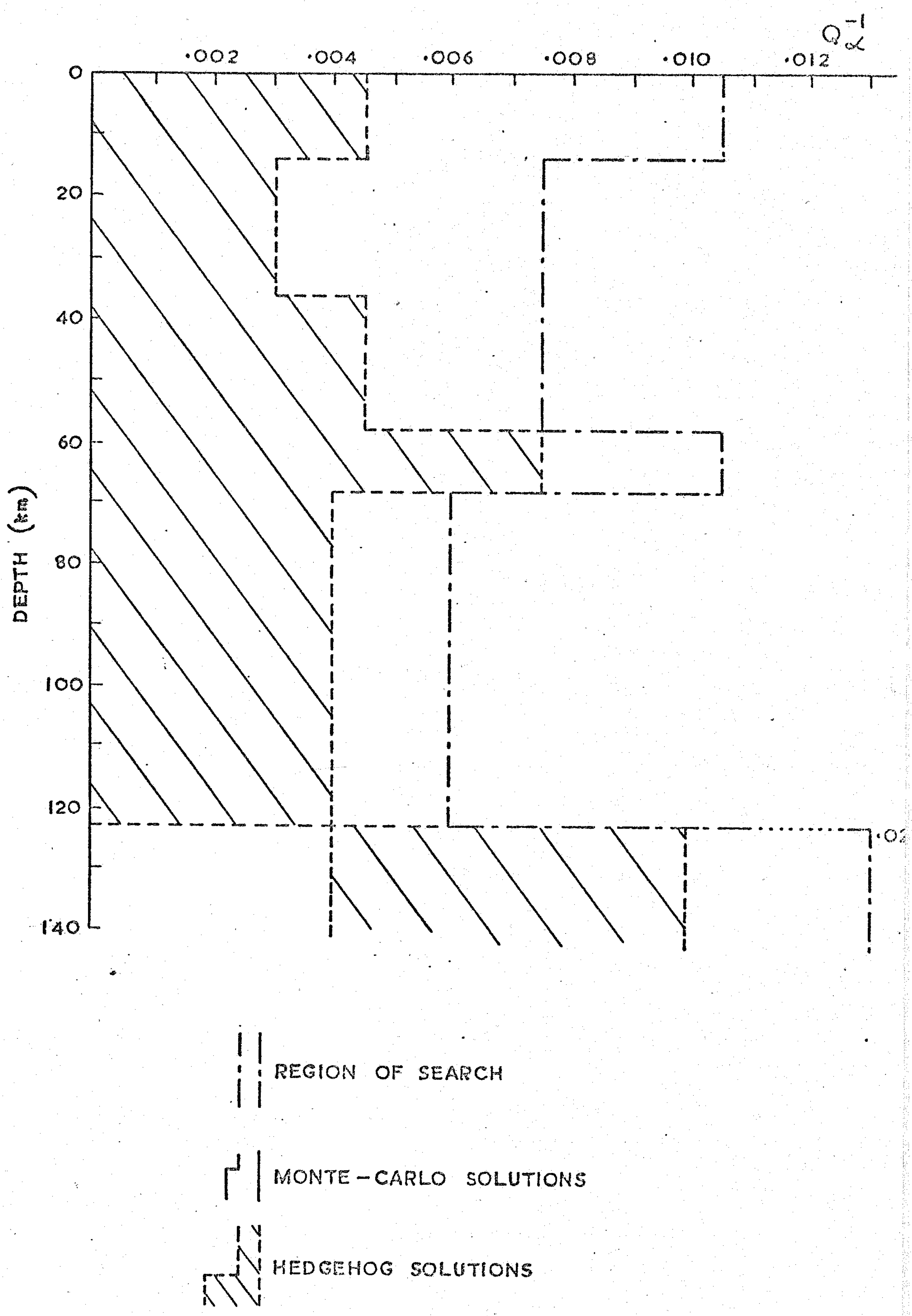

FIGURE 5.6 ATTEMPTED INVERSION OF 3NZA
(99% CONFIDENCE LIMITS AND NET N2)

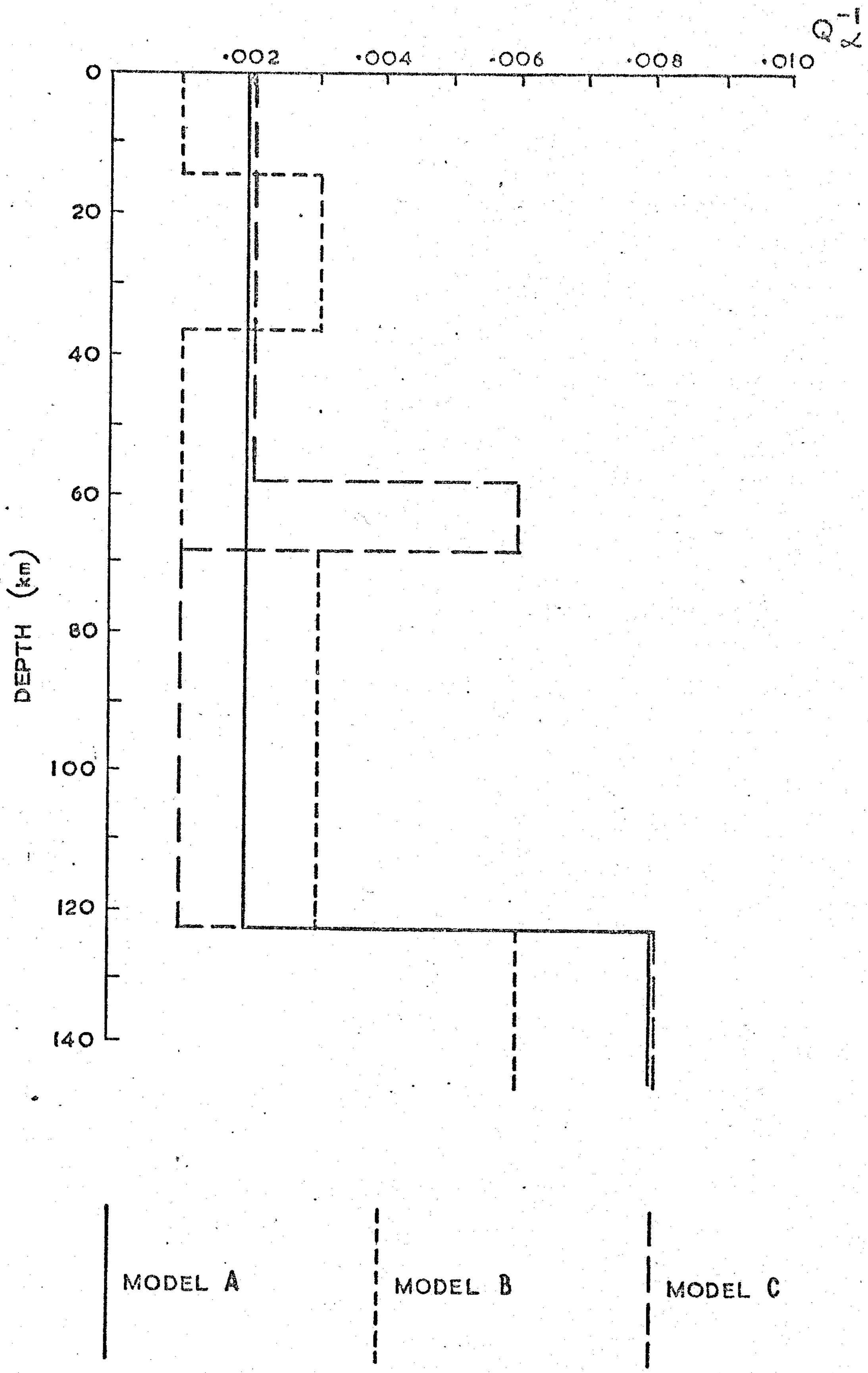

FIGURE 5.7 THREE TYPICAL INVERSION SOLUTIONS FOR 3 NZA

The other model, B, shows a more gradual onset of the absorption zone below 70 km. Also, Model B shows a region of slight absorption around 30 km depth. This region is influenced by the combined effects of the Conrad and Mohorovicic discontinuities. Apart from any real changes of Q^{-1} in these regions a discontinuity will tend to increase the value of observed Q^{-1}. Any discontinuity will scatter and diffract energy, increasing the path length, and therefore magnifying the effectiveness of any spatial Q^{-1}. Such effects cannot be separated from the truly dissipative characteristic of the materials and must be included in these estimates. Model B shows a crust and uppermost mantle well suited to the propagation of seismic energy, overlying a region below 70 km of increasing dissipation until a "zone of low Q" is reached.

Burton and Kennett resolved a separate Hedgehog region which showed a zone of very high Q between 15 and 70 kms depth, this is because the region of search was described in Q rather than Q^{-1} space. Comparing the following sequencies of values explains this.

Q space	Q	100	300	500	700	900	1100
Q^{-1} space	Q^{-1}	.01	.008	.006	.004	.002	0
Equivalent Q	Q	100	125	167	250	500	∞

Models in Q space give better resolution at the high Q end of the range; however the step from Q=100 to Q=500 is far more significant than from 500 to 1100 and is not sufficiently well resolved. Because the attenuation factor per wavelength is πQ^{-1} models should preferably be in Q^{-1} space. This procedure more accurately describes the physical phenomenon of dissipation.

5.2.3 Inversion of 2CA and 5A

The inversion of these two data sets produced much poorer results than for 3NZA. Using the net N3 and 50% confidence limits for 2CA produced Figure 5.8, N4 and 40% confidence limits for 5A produced Figure 5.9. In

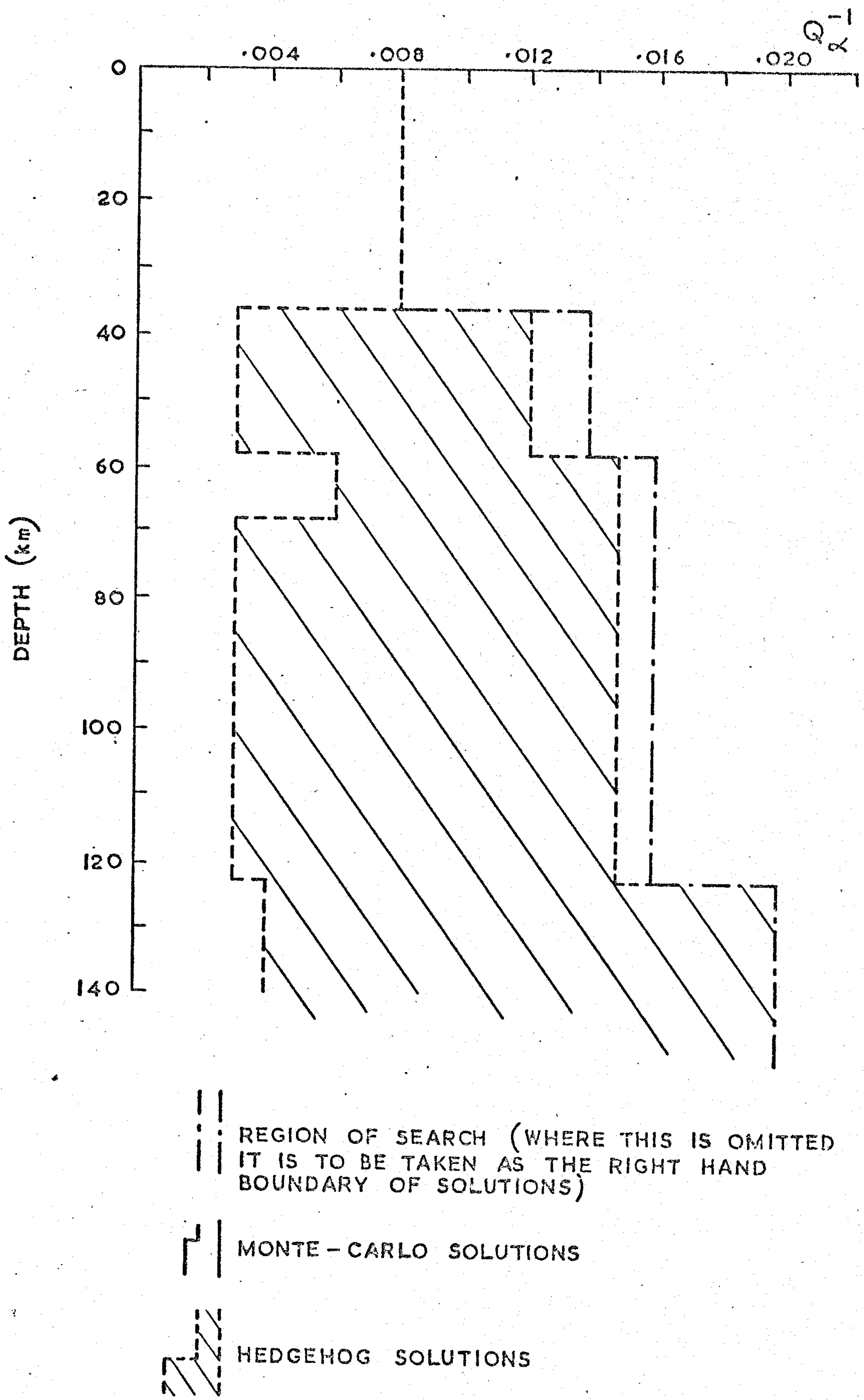

FIGURE 5.8 ATTEMPTED INVERSION OF THE AVERAGED SOUTHERN SINKIANG DATA (2CA) (50% CONFIDENCE LIMITS AND NET N3)

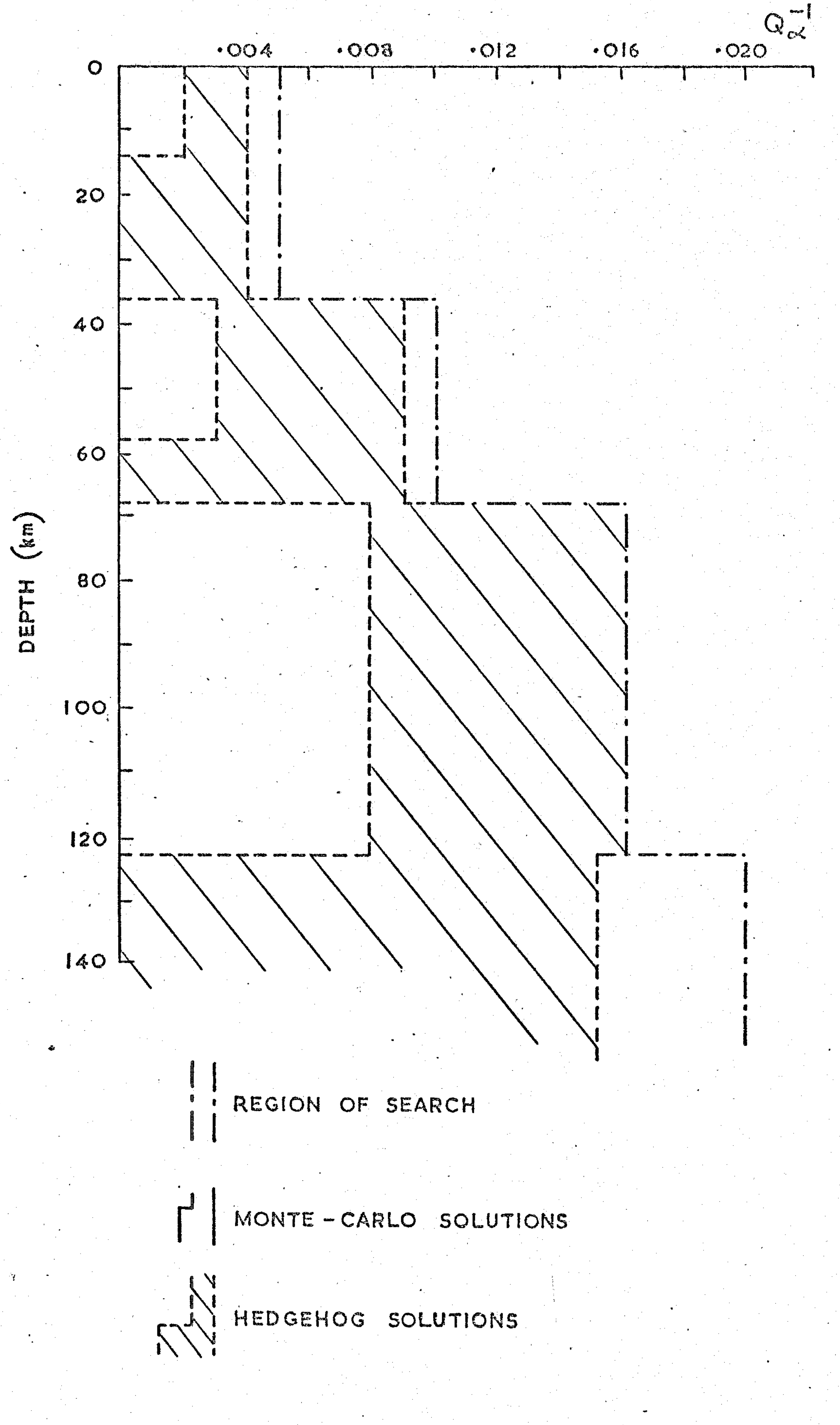

FIGURE 5.9 ATTEMPTED INVERSION OF THE AVERAGED ATMOSPHERIC EXPLOSION DATA (5A) (40% CONFIDENCE LIMITS AND NET N4)

both cases the entire region was not obtained because too many adequate knots were discovered before completion of the region. However, using 42.5% and 30% confidence limits for 2CA and 5A respectively, produced no solutions.

The conclusion is that the region of search and the nets used are inadequate to perform suitable inversion. Examination of Figure 3.18 for average $Q_{\gamma o}^{-1}$ from the two explosions in China provides an explanation. There is a minimum point around .038 Hz implying a region of very little dissipation. The minimum covers the frequency range .03-.05 Hz, outside this range normal values of $Q_{\gamma o}^{-1}$ are obtained. The rule has already been stated that the depth of penetration at a frequency corresponds to a wavelength, because the wave amplitude has fallen to 20% its surface value. This gives a range of depth penetration of about 80-130 kms. Frequencies higher than .05 Hz only penetrate to 80 km, and return normal values of $Q_{\gamma o}^{-1}$. The lower frequencies which sample all zones of the earth above 130 km, return anomalously low values of $Q_{\gamma o}^{-1}$. Obviously layer 5 of the inversion model (68-123 km) must consist of very low Q^{-1}. The nets N3 and N4 have not placed a sufficient constraint on the Hedgehog search in layer 5, and have allowed unrealistically large values of Q^{-1} for these depths to dominate the inversion. Further the lower frequencies, less than .03 Hz, which sample all depths of the model must be sampling very high Q^{-1} below 130 km to produce the $Q_{\gamma o}^{-1}$ values of Figure 3.18.

A further inversion was attempted using the net N5. This net restricts the Q^{-1} of layer 5 to a maximum value 0.005, also this net is coarser than those previously used. Inversion of 2C using 49.8% confidence limits produced Figure 5.10, and 33.2% confidence limits on 5A produced Figure 5.11. Some improvements are obtained but the picture is still unsatisfactory and the Hedgehog region ill defined. When the data from Southern Sinkiang is introduced we are led to the conclusion that the general model of section 5.2.1 must be questioned.

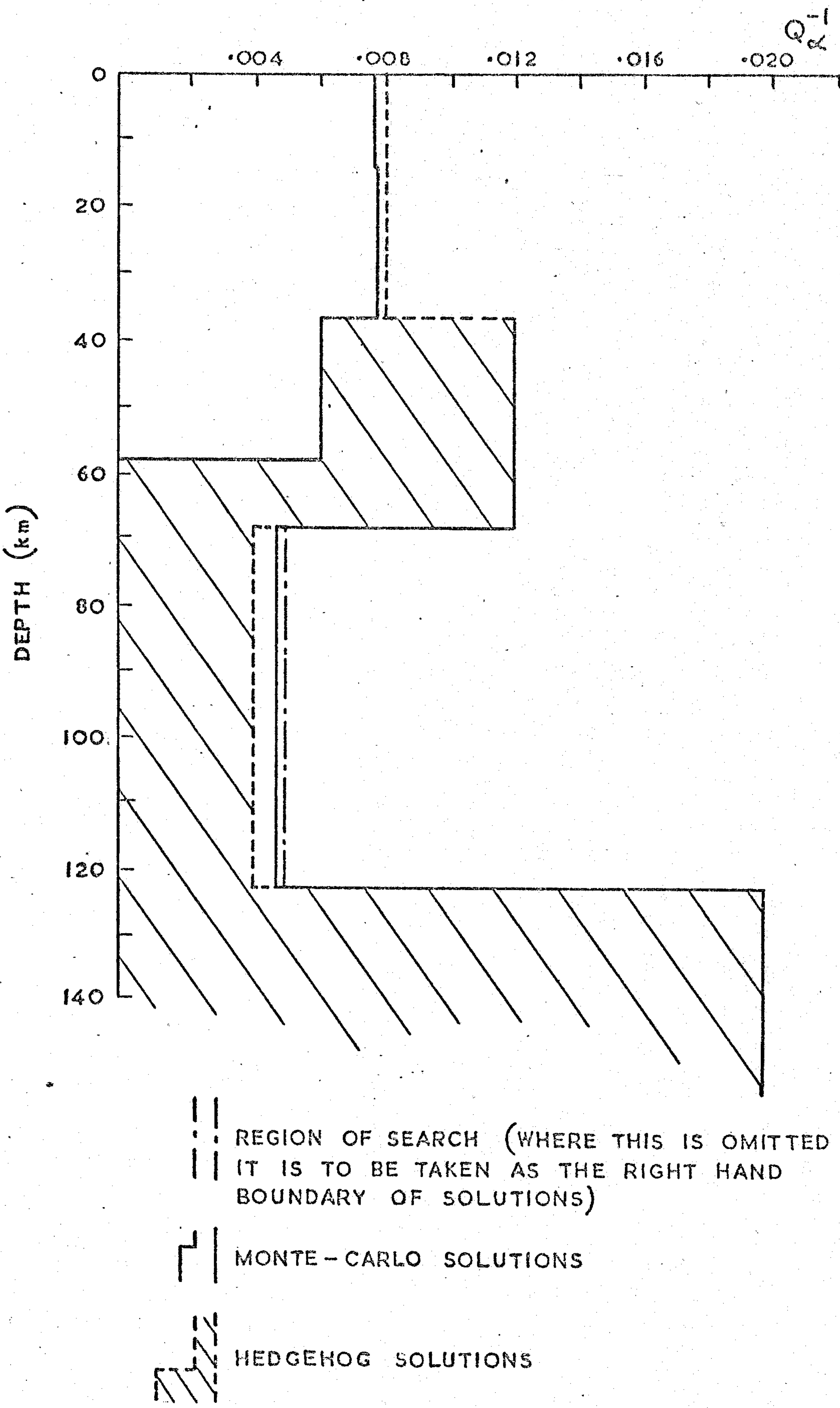

FIGURE 5.10 THE HEDGEHOG SOLUTION FOR 2CA (49·0% CONFIDENCE LIMITS AND NET N5)

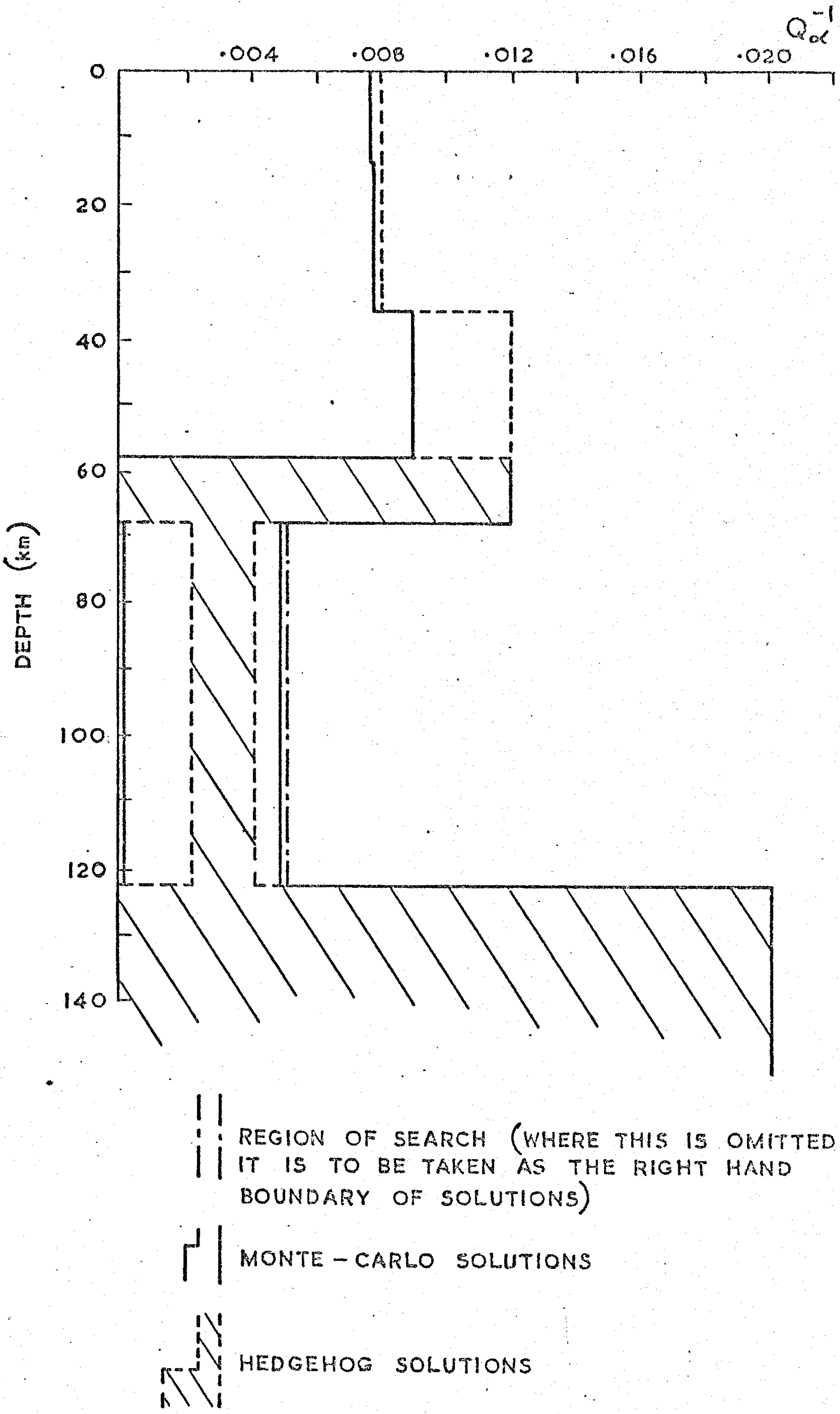

FIGURE 5.11 THE HEDGEHOG SOLUTION FOR 5A
(33·2% CONFIDENCE LIMITS AND NET N5)

Local variations of the crustal thickness and lateral heterogeneity introduced by the Himalayas will influence the inversion. The paths from Southern Sinkiang to CHG, SNG, JER and IST have already been omitted due to particularly anomalous behaviour. So it is possible that the velocity-depth model (Figure 4.1) is inappropriate for the general region of the propagation paths around Southern Sinkiang. Also the assumed relation of Q_α^{-1} to Q_β^{-1} (equation 5.3) is another limitation on the general inversion technique which may be inadequate for this region.

A future inversion which varies the parameters which are here fixed may well provide the solution.

5.3 Interpretation

Backus and Gilbert (1968) point out that the resolving power of any gross earth data is limited. The uncertainty of an earth parameter for a layered model will increase if an attempt is made to increase the depth resolution by using thinner layers. The delta-type resolution functions of Backus and Gilbert were calculated by Der et al. (1970) for the determination of shear velocity in the crust and upper mantle from surface wave observations. Der et al. concluded that a five layered model for the upper 130 km of the earth gave acceptable resolution and eliminated instability due to an excessive number of layers - the inversion model used here also has five layers and data obtained from the fundamental Rayleigh wave mode. Inclusion of a thin fourth layer (10 km) in the present inversion illustrates certain aspects of this resolution problem. The Hedgehog solutions of figures 5.3 and 5.4 show that the Q_α^{-1} values in the fourth layer are the most uncertain, whereas Q_α^{-1} is comparatively well resolved in the remaining thicker layers. With this resolution in mind it is possible to consider the implications of the Q^{-1} values in the various layers.

The major features of the three typical solutions for 3NZA (Figure 5.7) have already been described, but certain details of these models may not be adequately resolved. High Q^{-1} around 60 km in model C is uncertain, as is the distinction between models A and B. All of the models show clearly resolved high values for Q^{-1} at depth, and model A may be regarded as the general continental Q^{-1} model which excludes any excessive detail. The inversion has provided substantial evidence for a zone of dissipation below about 120 km. If the usually accepted low velocity zone (Press 1970a) had been included the resolution of the discontinuity in Q^{-1} would have been further enhanced.

Press (1970b) failed to find low density associated with low shear velocity in the earth, and concluded that high density (3.5 gm/cc) was the rule over substantial intervals between depths of 70 km and 370 km. Both incipient melting of the rocks and interstitial water content may provide an explanation for a zone of low Q and low velocity associated with high density. The results of Born, illustrated in the introduction, show that a very small percentage of interstitial water occurring as a free phase in the rock causes a significant increase in the decrement (decrement is proportional to Q^{-1}). Incipient melting will have a similar effect. Spetzler and Anderson (1968) examined the NaCl-H_2O binary system and found that α, β, Q_α and Q_β vary slowly as the eutectic temperature is approached from below, and then suddenly drop at the eutectic by 9.5%, 13.5%, 48% and 37% respectively (1% NaCl). The shape of the liquid inclusions determines the amount of melt necessary to obtain the required velocities, 0.1% melt maybe sufficient and this would have a negligible effect on density.

If the oceanic geotherm is assumed, melting is not possible above 90 km (Anderson and Sammis 1970) unless water is present to reduce the solidus melting temperature. The continental geotherm gives much smaller temperatures at corresponding depths (approximately 250°C less) and therefore implies the solidus temperature is only reached at a greater depth. Lambert and Wyllie (1970a, b) have investigated a peridotite mantle model with 0.1% by weight of water and came to the conclusion that the "beginning of melting should occur at about 60 km for normal oceanic geothermal gradients, and at about 110 km for normal shield geotherms".

Mineralogical variations may cause a low velocity zone but incipient melting is Green and Ringwood's (1970) preferred explanation. The region of anomalously high dissipation which is here found to start at the expected lithosphere-asthenosphere junction, combined with a low velocity zone, makes it difficult to conceive of an alternative explanation to incipient melting and interstitial water content. This lends support to Ringwood's (1969) concepts of the composition of the crust and upper mantle.

Ringwood's pyrolite model for the upper mantle in continental regions proposes a zone of dunite-peridotite over pyrolite, the transition occurring around 100-200 km. Partial melting causes the lower melting-point components to segregate upwards, and this is obviously influenced by variations of temperature with depth. Variations in seismic velocity may occur because of these chemical and physical zoning effects. However, these effects are not sufficient to explain the large shear wave velocity variations, and negative velocity gradients, which occur for the low velocity zone.

Incipient melting would cause a low velocity zone. However at depths of 100 km the pressure causes the degree of pyrolite melt to be very sensitive to temperature, and therefore unstable magmas might result. Water may stabilise this mechanism. A small quantity of water (0.1%) will lower the melting point and make it diffuse. A mechanism with a diffuse melting point is stable because a large temperature variation will only cause a small change in the degree of partial melt. Such a zone of incipient melting explains the anomalous dissipation found by the inversion for depths around 120 km, and why it may occur in conjunction with a low velocity zone.

CHAPTER 6

Concluding Comments

The inverse problem of seismology has been described by many people (Keilis-Borok and Yanovskaja 1967) but it is still very topical. Some measure of motion at the surface of the earth is obtained, the motion presumably caused by a particular source, and the problem is to obtain the variation within the earth of the elastic parameters k and μ (bulk modulus and rigidity), the density ρ and the dissipation constant Q. These are the four fundamental quantities of seismology. From these the velocities of bodily waves (P and S) may be determined and related to travel times on the seismogram. An understanding of the often ignored second axis of the seismogram, amplitudes, requires knowledge of the attenuation constant Q and the generating source. However, velocities and density are often known to a few per cent whereas Q is rarely known so well - but it is still an equally fundamental and intrinsic property of rocks which influences the propagation of seismic waves as characterised by the seismogram. For example dynamic damping (Q) allows us to calculate amplitude variation with distance from the source as a function of frequency. On the other hand static properties of rocks exemplified by creep also relate to the internal friction Q (Lomnitz 1957), and creep is very important on the geophysical time scale in regions of large tectonic stress - plate subduction zones are an obvious example. Further, a quantitative knowledge of the Q causing amplitude-distance variation by damping would help us to estimate source functions of various events and perhaps thereby elucidate the source mechanism. Source elucidation is important to seismology because such knowledge is necessary for earthquake prediction and control, and it is directly relevant to the earthquake-explosion discrimination problem.

Heterogeneity of the earth is also of great importance and this has appeared in several ways in this work. The average values of Q_{γ}^{-1} for the atmospheric explosions in Novaya Zemlya and China both show larger values of Q_{γ}^{-1} at the lower frequencies, implying vertical heterogeneity in the form of a strongly dissipative layer at depth. Such a zone of "low Q" may be caused by incipient melting stabilised by the presence of small quantities of water, this is congruous with Ringwood's (1969) ideas concerning the low velocity zone of continental regions at the corresponding depth. Also the attenuation of Rayleigh waves for those propagation paths radiating from Novaya Zemlya is greater for all frequencies than for the paths investigated for the explosions in Southern Sinkiang Province, an example of lateral variation. Further, the attenuation-depth models attributable to several authors appear to be very dependent on the data source or region used.

The existence of a widespread low Q zone has wider implications in general geophysics. If plate theory is to be accepted then a discontinuity between the mobile lithosphere and the asthenosphere is a necessary prerequisite. A discontinuity caused by incipient melting, which implies low shear stress, would facilitate sliding motion. This discontinuity would be expected at different depths for oceanic and shield environments because the geothermal gradients differ. Kanamori (1970) has used surface wave phase velocity data to show that the major difference between the oceanic and shield environments must lie within the upper 200 km. Using the definition that the lithosphere ends where the shear velocity drops below 4.5 km/sec has led to thickness estimates of about 70 km for the suboceanic lithosphere and twice as much for the subshield lithosphere (Kanamori and Press 1970, Press 1970a). The discontinuity in Q around the depth of 120 km is perhaps a clear estimate of the thickness of the lithosphere under continental regions.

There is scope for extending the present technique into other regions where the all important assumption of the radially symmetric explosion source function would be equally useful. The French test site in the Pacific now gives the opportunity to determine oceanic Q^{-1} and the thickness of the suboceanic lithosphere. The large underground explosion CANNIKIN is of sufficient yield (5 Mt) to give records with good signal-to-noise. CANNIKIN is ideally situated in the Aleutian Island Arc to investigate the lateral variations of Q^{-1} both parallel and perpendicular to the arc and over oceanic and continental paths. Such data should be useful for the understanding of tectonic processes occurring at arcs.

It is also apparent that the lateral variations indicated by this work, and the extremities of the low Q zone, need resolving in greater detail. Perhaps body waves will provide this resolution. Frasier and Filson (1972) have determined P Wave Q_α and obtained distinctly different results for different paths. Douglas et al. (1972) have shown the effects of anomalous dissipation manifest in particular seismogram records. Douglas et al. also state that with a knowledge of tQ_p^{-1} (travel time t and Q_p^{-1} the average Q^{-1} for a particular path) the source function of explosions and earthquakes may be estimated; the difficulty is tQ_p^{-1} is not usually known. It is difficult to estimate the source function itself, but a simple source parameter is available as the surface wave magnitude scale M_s. The amplitude A(T) of a surface wave at period T is measured in the time domain directly from the seismogram and used in estimating M_s. The M_s values are influenced by several phenomena; two of major importance are the nature of the source spectrum generating the waves and heterogeneity of the earth experienced by those waves. Obviously there will be considerable differences between earthquake and explosion spectra (Marshall 1970). Regional variations in surface wave amplitudes have also been demonstrated by Marshall and Basham (1972). These variations were mainly attributed to dispersion effects in the different paths sampled and so they introduced a strictly time domain path correction term P(T) to compensate the M_s values between different regions. A term allowing for geometrical spreading and dissipation with distance must also be included. Marshall and Basham used near surface events and measured A(T) from the most prominent period in the record which would therefore be around 20s, and so their distance dependent term could assume a constant value of 300 for Q. But deep focus earthquakes appear very rich in long periods and this work has shown that Q_γ^{-1} increases for frequencies around 0.02 Hz (50s). A direct use of the Q_γ^{-1} values found here would be to adapt a magnitude scale for deep focus earthquakes to include a dissipation correction term dependent on the frequency.

The attenuation of bodily waves needs further research. More investigations are required into the relationship between Q_α^{-1} and Q_β^{-1} using P and S waves. This is difficult because for a given frequency the wavelength of S waves is much shorter than for P waves, and therefore even if spatial Q^{-1} is the same for both, S will be attenuated far more with distance than P.

In this chapter an attempt has been made to indicate the general significance of the results obtained relative to earth structure. However the general need and usefulness of increased knowledge of Q^{-1} in many fields of research is still very much apparent.

APPENDIX A

The WWSSN Recording Stations Used for Each Event

All the WWSSN stations used for each event are listed. For an event the distance between each recording station and the hypocentre is expressed in degrees, radians and kilometres. These angular distances, Δ^{o}, were calculated using the program GEDESS (Young and Gibbs, 1968).

The geometrical spreading term used to correct the amplitudes at each station is also listed. The term is $(E \sin \Delta)^{\frac{1}{2}}$ where E, the radius of the earth, is taken to be 6371 km.

The maps in Figures A.1 to A.4 show the distribution of recording stations around each event.

A list is included expanding the station abbreviations for all the WWSSN stations used. This list also indicates the region where the station is sited.

NOVAYA ZEMLYA 27/9/62 ATMOSPHERIC 28 STATIONS

NSTAT = 28 NFA = 79 NFL = 40. T = 2.056

STATION	DATA NO.	DELTAD	DELTAR	DISTANCE(KMS)	SQRT(E*SIN(DELTAR))
ALQ/0007	C005	70.10	1.2235	7794.8	77.40
AUU/0010	C027	36.60	0.6388	4069.7	61.63
ARE/0011	C029	114.60	2.0001	12742.9	76.11
BEC/0015	C035	65.90	1.1502	7327.7	76.26
BHP/0017	C037	91.80	1.6022	10207.7	79.80
BKS/0018	C039	68.10	1.1886	7572.4	76.88
BLA/0019	C041	64.40	1.1240	7160.9	75.80
BOG/0021	C043	94.80	1.6546	10541.3	79.68
CAR/0024	C045	87.50	1.5272	9729.6	79.78
COR/0030	C049	61.40	1.0716	6827.4	74.79
DAL/0032	C051	71.20	1.2427	7917.1	77.66
HNR/0048	C057	103.70	1.8099	11530.9	78.67
LON/0058	C061	59.20	1.0332	6582.7	73.98
LPB/0060	C063	113.90	1.9879	12665.1	76.32
LUB/0063	C065	71.00	1.2392	7894.8	77.61
PMG/0086	C073	100.30	1.7506	11152.8	79.17
QUE/0092	C017	44.80	0.7819	4981.5	67.00
RAB/0094	C075	96.70	1.6877	10752.5	79.55
TOL/0115	C013	43.10	0.7522	4792.5	65.98
TRN/0118	C077	86.10	1.5027	9573.9	79.73
COP/0029	C047	24.30	0.4241	2702.0	51.20
GOL/0043	C055	65.30	1.1397	7261.0	76.08
IST/0050	C009	35.10	0.6126	3902.9	60.53
KEV/0052	C059	9.00	0.1571	1000.8	31.57
KON/0055	C001	21.50	0.3752	2390.7	48.32
MOS/0067	C067	58.50	1.0210	6504.9	73.70
NUR/0081	C071	17.20	0.3002	1912.6	43.40
WES/0123	C079	57.70	1.0071	6415.9	73.38

NOVAYA ZEMLYA 22/10/62 ATMOSPHERIC 27 STATIONS

NSTAT = 27 NFA = 79 NFL = 40 T = 2.060

STATION	DATA NO.	DELTAD	DELTAR	DISTANCE(KMS)	SQRT(E*SIN(DELTAR))
ARE/0011	C031	115.70	2.0193	12865.2	75.77
BAG/0014	C081	67.50	1.1781	7505.7	76.72
BEC/0015	C083	67.00	1.1694	7450.1	76.58
BHP/0017	C085	92.90	1.6214	10330.0	79.77
BLA/0019	C089	65.60	1.1449	7294.4	76.17
BOG/0021	C091	95.90	1.6738	10663.6	79.61
CAR/0024	C093	88.60	1.5464	9851.9	79.81
DAL/0032	C097	72.30	1.2619	8039.4	77.91
DUG/0036	C099	66.40	1.1589	7383.3	76.41
GOL/0043	C101	66.40	1.1589	7383.3	76.41
LON/0058	C103	60.10	1.0489	6682.8	74.32
LPB/0060	C104	114.90	2.0054	12776.3	76.02
LUB/0063	C105	72.10	1.2584	8017.1	77.86
MAL/0065	C106	46.50	0.8116	5170.6	67.98
MAN/0066	C107	69.30	1.2095	7705.8	77.20
MOS/0067	C108	59.60	1.0402	6627.2	74.13
NHA/0076	C109	68.60	1.1973	7628.0	77.02
NUR/0081	C110	17.20	0.3002	1912.6	43.40
GSC/0085	C111	71.40	1.2462	7939.3	77.71
PMG/0086	C112	99.60	1.7383	11075.0	79.26
QUE/0092	C113	43.70	0.7627	4859.2	66.34
SCP/0101	C114	61.60	1.0751	6849.0	74.86
WES/0123	C115	58.80	1.0263	6538.3	73.82
ALQ/0007	C021	71.20	1.2427	7917.1	77.66
BKS/0018	C087	69.00	1.2043	7672.4	77.12
COP/0029	C095	24.60	0.4294	2735.4	51.50
KON/0055	C102	21.90	0.3822	2435.2	48.75

NOVAYA ZEMLYA 24/12/62 ATMOSPHERIC 26 STATIONS

NSTAT = 26 NFA = 79 NFL = 40 T = 2.064

STATION	DATA NO.	DELTAD	DELTAR	DISTANCE(KMS)	SQRT(E*SIN(DELTAR))
AAE/0001	0025	63.50	1.1083	7060.9	75.51
ALQ/0007	0023	71.20	1.2427	7917.1	77.66
ARE/0011	0033	116.20	2.0281	12920.8	75.61
BEC/0015	0116	67.50	1.1781	7505.7	76.72
BHP/0017	0117	93.30	1.6264	10374.5	79.75
BKS/0018	0118	68.80	1.2008	7650.2	77.07
BLA/0019	0119	65.90	1.1502	7327.7	76.26
GDH/0040	0122	30.70	0.5358	3413.7	57.03
GOL/0043	0123	66.40	1.1589	7383.3	76.41
IST/0050	0125	35.30	0.6161	3925.2	60.68
KON/0055	0126	22.70	0.3962	2524.1	49.58
LPB/0060	0129	115.50	2.0159	12843.0	75.83
LPS/0061	0130	89.70	1.5656	9974.2	79.82
LUB/0063	0131	72.20	1.2601	8028.3	77.88
MAL/0065	0132	47.30	0.8255	5259.5	68.43
TUL/0115	0136	44.20	0.7714	4914.8	66.65
TFN/0118	0137	87.60	1.5289	9740.7	79.78
VAL/0121	0138	35.00	0.6109	3891.8	60.45
WIN/0124	0139	99.50	1.7366	11063.9	79.27
CAR/0024	0120	89.10	1.5551	9907.5	79.81
LAH/0056	0127	43.00	0.7505	4781.4	65.92
LON/0058	0128	59.90	1.0455	6660.6	74.24
MOS/0067	0133	59.90	1.0455	6660.6	74.24
QUE/0052	0135	43.80	0.7645	4870.3	66.41
COP/0029	0121	25.30	0.4416	2813.2	52.18
HNR/0048	0124	102.50	1.7890	11397.5	78.87

NOVAYA ZEMLYA 7/11/68 UNDERGROUND 18 STATIONS

NSTAT = 18 NFA = 79 NFL = 40 T = 2.120

STATION	DATA NO.	DELTAD	DELTAR	DISTANCE(KMS)	SQRT(E*SIN(DELTAR))
ATL/0012	0143	69.93	1.2205	7775.9	77.36
BAG/0014	0144	67.51	1.1783	7506.8	76.72
BLA/0019	0145	65.57	1.1444	7291.0	76.16
CFG/0026	0146	59.85	1.0446	6655.0	74.22
COP/0029	0147	24.57	0.4288	2732.1	51.47
ESK/0038	0148	29.23	0.5102	3250.2	55.78
FLO/0039	0149	65.60	1.1449	7294.4	76.17
HKC/0045	0150	60.17	1.0502	6690.6	74.34
IST/0050	0152	34.70	0.6056	3858.5	60.22
JER/0051	0151	42.91	0.7489	4771.4	65.86
KON/0055	0153	21.90	0.3822	2435.2	48.75
MAT/0064	0154	53.51	0.9339	5950.0	71.57
NSH/0071	0155	37.24	0.6500	4140.9	62.09
OXF/0083	0156	69.67	1.2160	7746.9	77.29
SHI/0104	0158	43.84	0.7652	4874.8	66.43
STU/0109	0159	31.68	0.5529	3522.7	57.84
TAB/0110	0160	35.66	0.6224	3965.2	60.94
LOR/0126	0161	34.47	0.6016	3832.9	60.05

CHINKY 11/6/67 24 STATIONS

NSTAT = 24 NFA = 79 NFL = 40 T = 2.070

STATION	DATA NO.	DELTAD	DELTAR	DISTANCE(KMS)	SQRT(E*SIN(DELTAR))
KRK/0222	1000	42.00	0.7330	4670.2	65.29
TOL/0115	1006	67.81	1.1835	7540.1	76.81
SHK/0114	1007	34.41	0.6006	3826.2	60.00
STU/0109	1008	55.18	0.9631	6135.7	72.32
SHI/0104	1009	32.04	0.5592	3562.7	58.14
KTG/0100	1012	58.85	1.0271	6543.8	73.84
PTO/0091	1014	69.89	1.2198	7771.4	77.35
NUR/0081	1018	43.63	0.7615	4851.4	66.30
ESK/0038	1033	59.22	1.0336	6585.0	73.98
ATU/0013	1040	49.95	0.8718	5554.2	69.83
TRI/0117	1005	53.57	0.9350	5956.7	71.60
SLO/0102	1011	29.01	0.5063	3225.8	55.58
NOR/0079	1019	52.33	0.9133	5818.8	71.01
NAI/0074	1021	63.56	1.1093	7067.5	75.53
MAL/0065	1023	69.88	1.2196	7770.3	77.34
KON/0055	1025	51.18	0.8933	5690.9	70.45
KEV/0052	1027	43.05	0.7514	4786.9	65.95
GOH/0040	1031	67.04	1.1701	7454.5	76.59
COP/0029	1035	50.88	0.8880	5657.6	70.30
COL/0028	1036	65.62	1.1453	7296.6	76.18
CMC/0027	1037	70.19	1.2250	7804.8	77.42
BAG/0014	1039	36.10	0.6301	4014.1	61.27
AQU/0010	1041	55.22	0.9638	6140.2	72.34
AAE/0001	1042	54.86	0.9575	6100.1	72.18

SNG/0068	1022	34.81	0.6075	3870.7	60.31
CHG/0026	1038	23.27	0.4061	2587.5	50.17
JER/0051	1028	44.17	0.7709	4911.5	66.63
IST/0050	1029	44.99	0.7852	5002.7	67.11

CHINKY 29/9/65 39 STATIONS

NSTAT = 39 NFA = 79 NFL = 40 T = 2.026

STATION	DATA NO.	DELTAD	DELTAR	DISTANCE(KMS)	SQRT(E*SIN(DELTAR))
AAE/0001	1043	54.86	0.9575	6100.1	72.18
AAM/0002	1044	97.16	1.6958	10803.7	79.51
ALQ/0007	1045	103.29	1.8027	11485.3	78.74
ARE/0011	1047	150.82	2.6323	16770.4	55.73
ATL/0012	1048	106.02	1.8504	11788.9	78.25
ATU/0013	1049	49.95	0.8718	5554.2	69.83
BEC/0015	1051	103.50	1.8064	11508.7	78.71
BKS/0018	1052	96.55	1.6851	10735.9	79.56
BLA/0019	1053	101.93	1.7790	11334.1	78.95
CAR/0024	1055	124.62	2.1750	13857.1	72.41
COR/0030	1058	90.10	1.5725	10018.7	79.82
DAV/0033	1059	46.35	0.8090	5153.9	67.90
DUG/0036	1061	96.94	1.6919	10779.2	79.53
FLO/0039	1062	100.88	1.7607	11217.3	79.10
GDH/0040	1063	67.04	1.1701	7454.5	76.59
GEO/0041	1064	99.85	1.7427	11102.8	79.23
IST/0050	1066	44.99	0.7852	5002.7	67.11
JER/0051	1067	44.17	0.7709	4911.5	66.63
KEV/0052	1068	43.05	0.7514	4786.9	65.95
MAT/0064	1072	37.82	0.6601	4205.4	62.50
NAI/0074	1074	63.56	1.1093	7067.5	75.53
KTG/0100	1077	58.85	1.0271	6543.8	73.84
TOL/0115	1080	67.81	1.1835	7540.1	76.81
TRI/0117	1081	53.57	0.9350	5956.7	71.60
AQU/0010	1046	55.22	0.9638	6140.2	72.34
BAG/0014	1050	36.10	0.6301	4014.1	61.27
BOG/0021	1054	132.47	2.3120	14730.0	68.55
CHG/0026	1056	23.27	0.4061	2587.5	50.17
COL/0028	1057	65.62	1.1453	7296.6	76.18
JCT/0035	1060	108.64	1.8961	12080.2	77.70
HKC/0045	1065	27.69	0.4833	3079.0	54.41
LAH/0056	1069	15.33	0.2676	1704.6	41.04
KBL/0057	1070	17.39	0.3035	1933.7	43.64
LON/0058	1071	88.54	1.5453	9845.2	79.81
MAN/0066	1073	37.73	0.6585	4195.4	62.44
NOR/0079	1075	52.33	0.9133	5818.8	71.01
QUE/0092	1076	21.17	0.3695	2354.0	47.97
STU/0109	1078	55.18	0.9631	6135.7	72.32
TAB/0110	1079	33.30	0.5812	3702.8	59.14

ALEUTIAN ISLANDS 29/1C/65 LCNG SHCT 9 STATICNS

NSTAT = 5 NFA = 79 NFL = 40 T = 2.365

STATION	DATA NC.	DELTAC	DELTAR	DISTANCE(KMS)	SORT(E*SIN(DELTAR))
BLA/CC19	2CC1	67.70	1.1816	7527.9	76.78
CMC/0027	20C2	35.00	0.6109	3891.8	60.45
COL/0028	2CC3	21.69	0.3786	2411.8	48.52
FLO/0039	20C4	61.13	1.0669	6797.3	74.69
HNR/0048	20C5	62.86	1.0971	6989.7	75.30
MAT/0064	2CC6	32.55	0.5681	3619.4	58.55
NOR/0C79	20C7	46.94	0.8193	5219.5	68.23
OGD/0082	20C8	67.77	1.1828	7535.7	76.79
PMG/0086	20C9	66.61	1.1626	7406.7	76.47

QUAKE, 17/6/67 11 STATICNS

NSTAT = 11 NFA = 79 NFU = 40 T = 2.260

STATION	DATA NO.	DELTAD	DELTAR	DISTANCE(KMS)	SORT(E*SIN(DELTAR))
SHA/0103	1010	38.41	0.6704	4271.0	62.91
QUI/0093	1013	26.59	0.4641	2956.7	53.40
GSC/0085	1015	41.19	0.7189	4580.1	64.77
OXF/0083	1016	41.39	0.7224	4602.4	64.90
NNA/0078	1020	28.53	0.4979	3172.4	55.16
KIP/0053	1026	58.22	1.0161	6473.8	73.59
GEO/0041	1030	50.17	0.8756	5578.6	69.95
FLO/0039	1032	45.08	0.7868	5012.7	67.17
DUG/0036	1034	45.10	0.7871	5014.9	67.18
TRN/0118	1004	45.66	0.7969	5077.2	67.50
TUC/0119	1003	37.06	0.6468	4120.9	61.96

Figure A.1

TITLE NOVAYA ZEMLYA 27/09/62 ATMOSPHERIC 28 STATIONS
CENTRE LATITUDE 74.4000°N
CENTRE LONGITUDE 52.4000°E
RADIAL DISTANCE 120.0000°

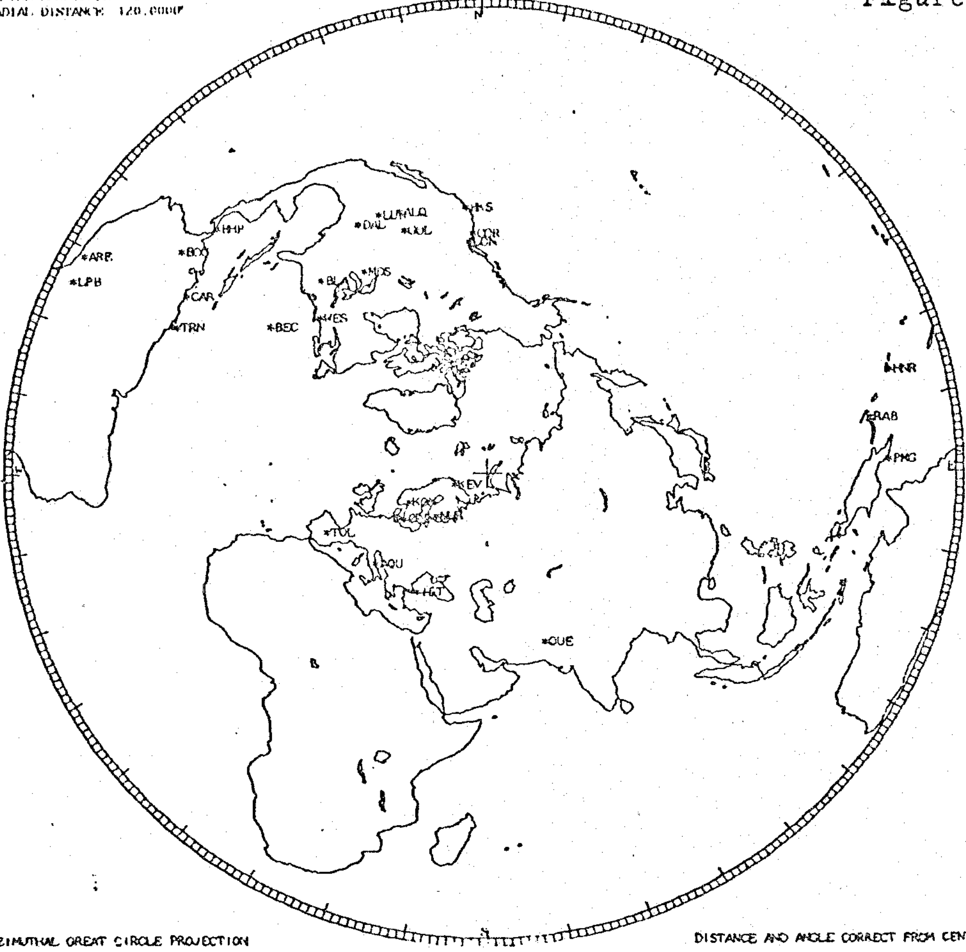

AZIMUTHAL GREAT CIRCLE PROJECTION

DISTANCE AND ANGLE CORRECT FROM CENTRE

TITLE NOVAYA ZEMLYA 22/10/62 ATMOSPHERIC 27 STATIONS
CENTRE LATITUDE 73.4000°N
CENTRE LONGITUDE 54.9000°E
RADIAL DISTANCE 120.0000°

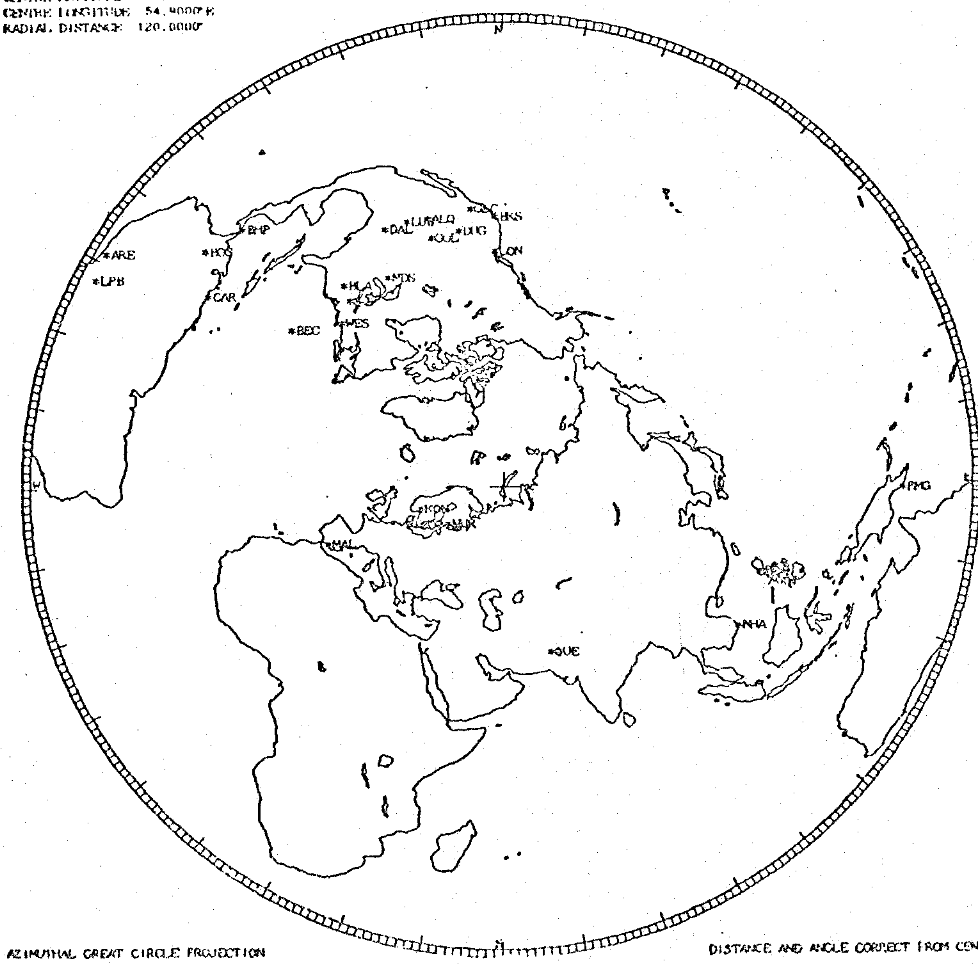

AZIMUTHAL GREAT CIRCLE PROJECTION

DISTANCE AND ANGLE CORRECT FROM CENTRE

Figure A.2

TITLE NOVAYA ZEMLYA 24/12/62 ATMOSPHERIC 26 STATIONS
CENTRE LATITUDE 74.6000N
CENTRE LONGITUDE 57.5000E
RADIAL DISTANCE 120.0000

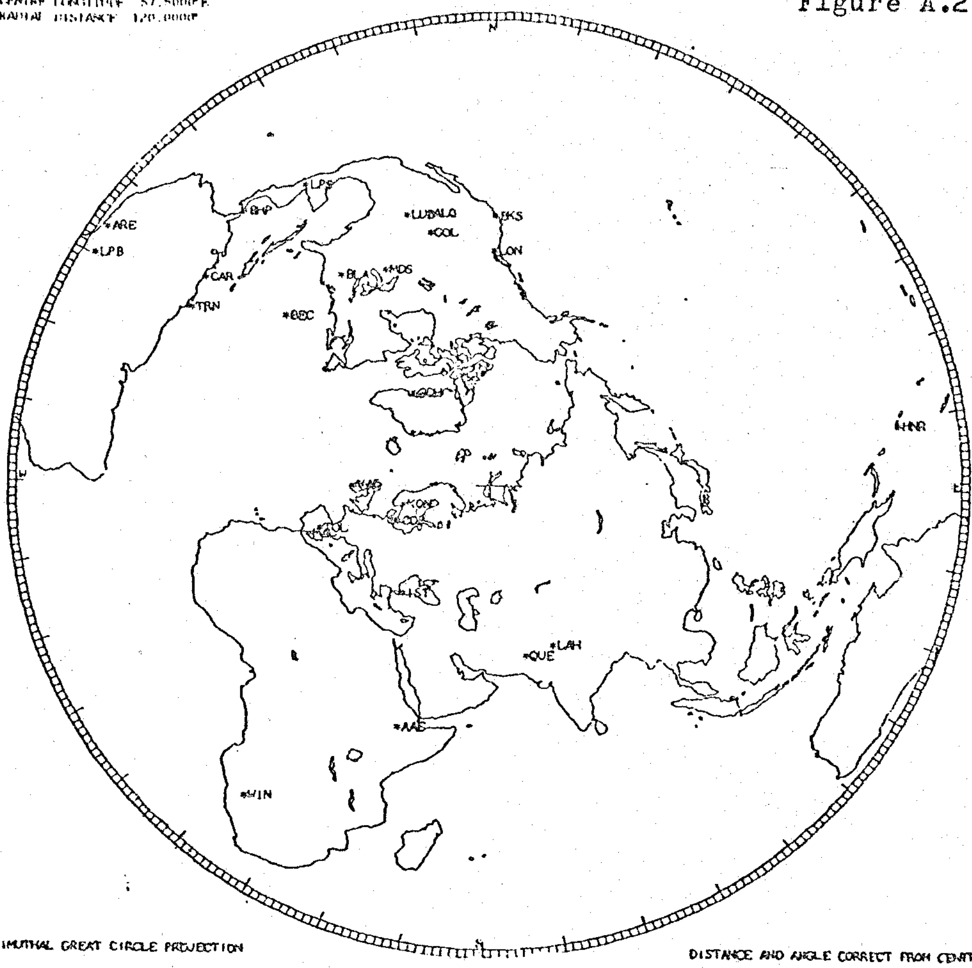

AZIMUTHAL GREAT CIRCLE PROJECTION

DISTANCE AND ANGLE CORRECT FROM CENTRE

TITLE NOVAYA ZEMLYA 7/11/68 UNDERGROUND 18 STATIONS (16 USED)
CENTRE LATITUDE 74.4000N
CENTRE LONGITUDE 54.9000E
RADIAL DISTANCE 70.0000

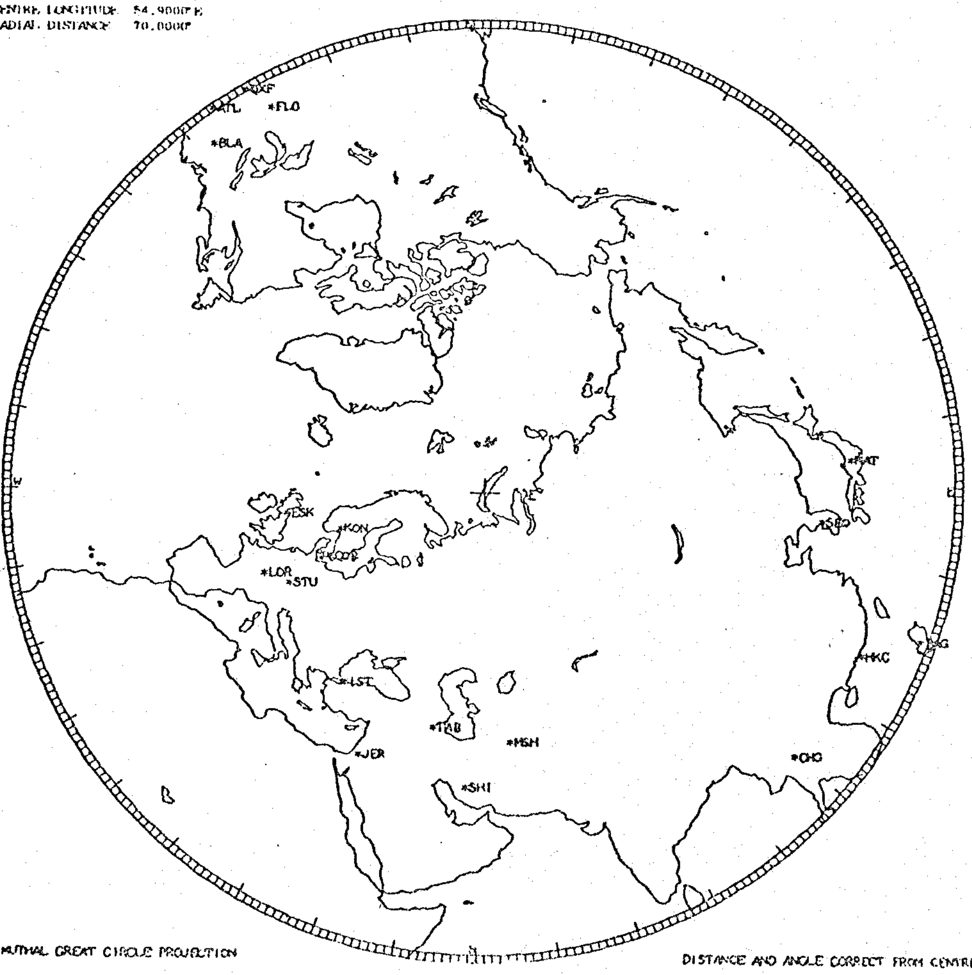

AZIMUTHAL GREAT CIRCLE PROJECTION

DISTANCE AND ANGLE CORRECT FROM CENTRE

Figure A.3

TITLE S.SINKIANG PROV. CHINA 17/06/67 ATMOSPHERIC 28 STATIONS (24 USED)
CENTRE LATITUDE 40.7000 N
CENTRE LONGITUDE 89.6000 E
RADIAL DISTANCE 70.0000

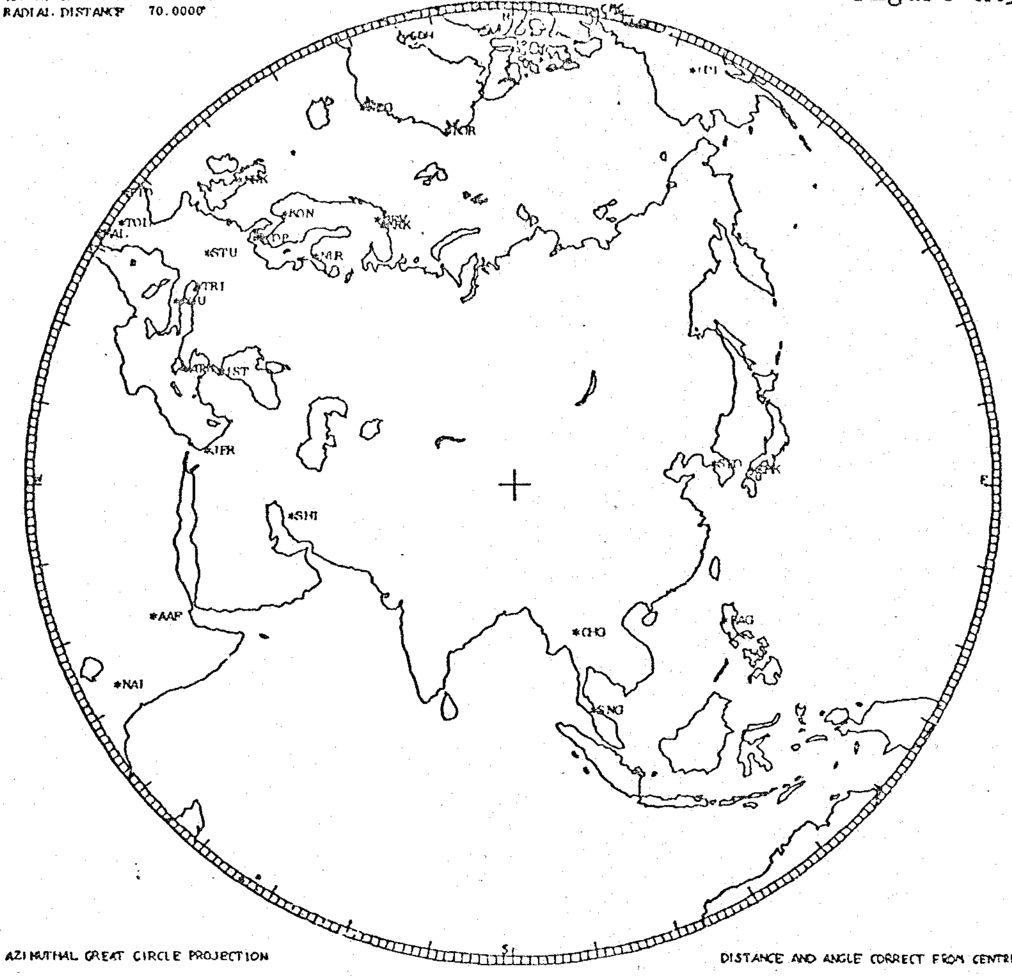

AZIMUTHAL GREAT CIRCLE PROJECTION

DISTANCE AND ANGLE CORRECT FROM CENTRE

TITLE S.SINKIANG PROV. CHINA 29/09/69 ATMOSPHERIC 39 STATIONS
CENTRE LATITUDE 40.7000 N
CENTRE LONGITUDE 89.6000 E
RADIAL DISTANCE 160.0000

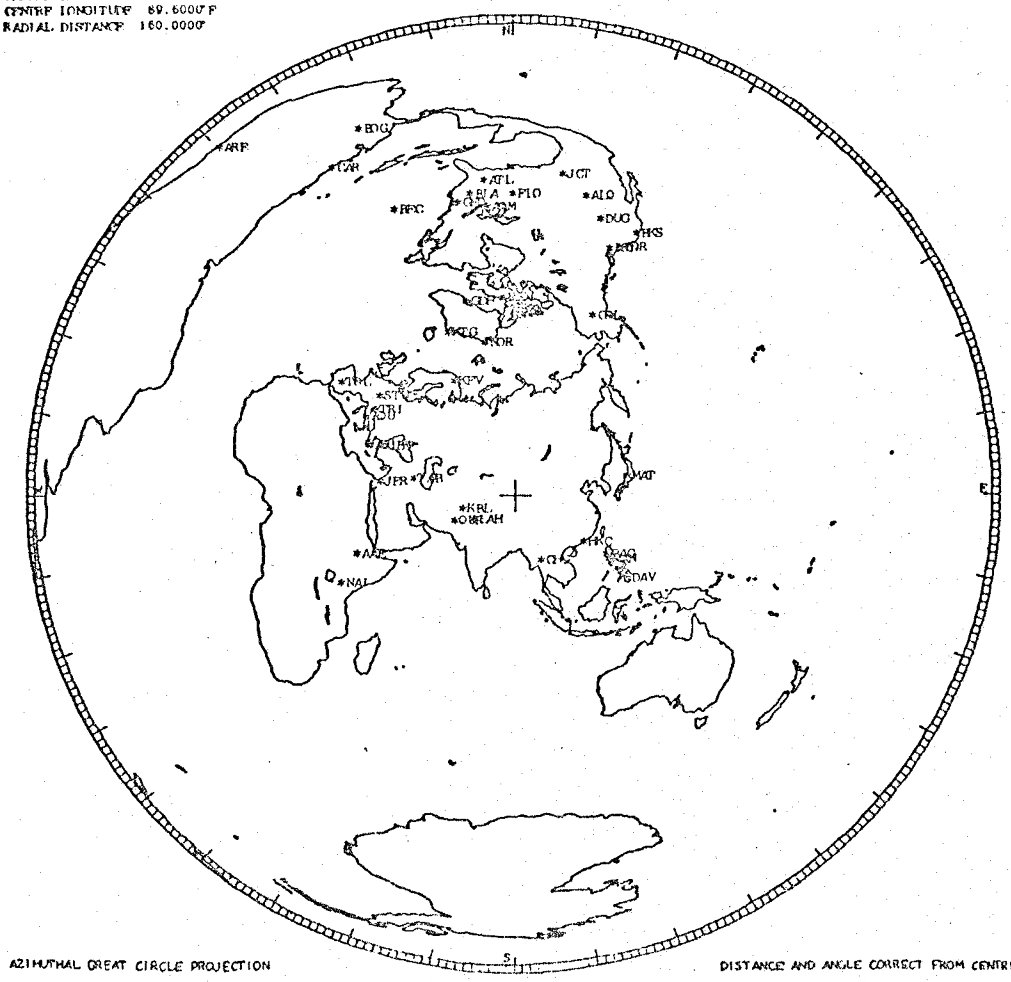

AZIMUTHAL GREAT CIRCLE PROJECTION

DISTANCE AND ANGLE CORRECT FROM CENTRE

Figure A.4

TITLE ALEUTIAN ISLANDS 29/10/65 UNDERGROUND 9 STATIONS (LONGSHOT)
CENTRE LATITUDE 51.4360°N
CENTRE LONGITUDE 179.1800°E
RADIAL DISTANCE 120.0000°

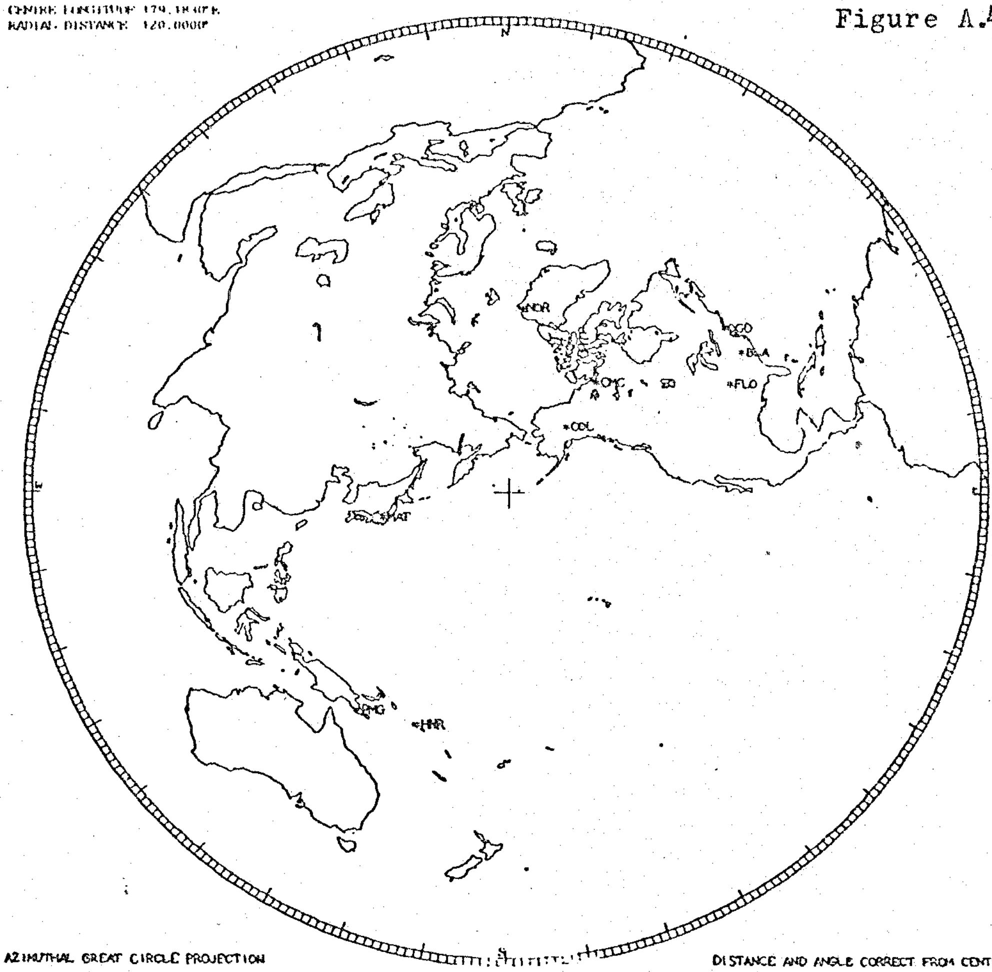

AZIMUTHAL GREAT CIRCLE PROJECTION

DISTANCE AND ANGLE CORRECT FROM CENTRE

TITLE NORTHERN EASTER ISLAND 17/06/67 EARTHQUAKE 11 STATIONS
CENTRE LATITUDE 4.5000°S
CENTRE LONGITUDE 104.7000°W
RADIAL DISTANCE 70.0000°

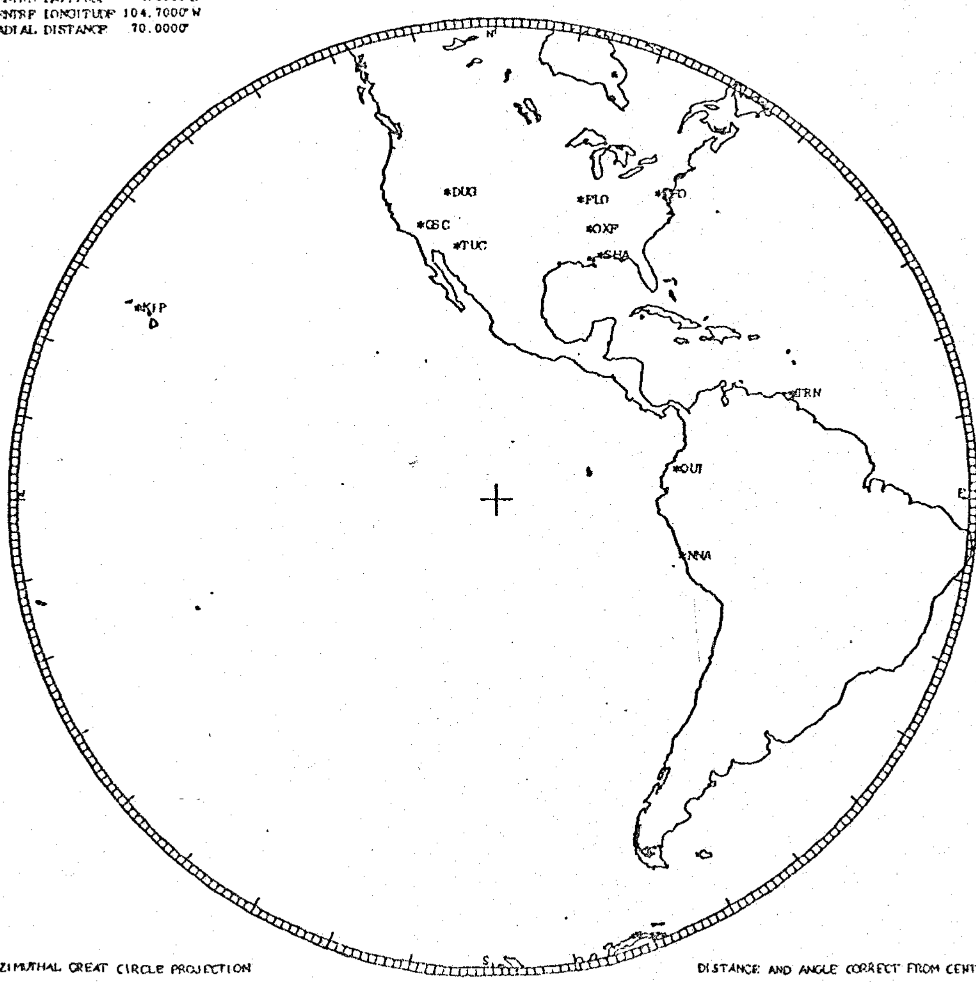

AZIMUTHAL GREAT CIRCLE PROJECTION

DISTANCE AND ANGLE CORRECT FROM CENTRE

World Wide Network of Standardized Seismograph Stations Used

In This Study

Station Number	Station Name	Station Abbr.
1	Addis Ababa, Ethiopia	AAE
2	Ann Arbor, Michigan	AAM
7	Albuquerque, New Mexico	ALQ
10	Aquila, Italy	AQU
11	Arequipa, Peru	ARE
12	Atlanta, Georgia	ATL
13	Athens, Greece	ATU
14	Baguio, Philippines	BAG
15	Bermuda, Colombia	BEC
17	Balboa Heights, Panama	BHP
18	Berkeley, (Strawberry) California	BKS
19	Blacksburg, Virginia	BLA
21	Bogota, Colombia	BOG
24	Caracus, Venezuela	CAR
26	Chiengmai, Thailand	CHG
27	Coppermine, Canada	CMC
28	College, (Fairbanks) Alaska	COL
29	Copenhagen, Denmark	COP
30	Corvallis, Oregon	COR
32	Dallas, Texas	DAL
33	Davao, Philippines	DAV
35	Junction, Texas	JCT
36	Dugway, Utah	DUG
38	Eskdalemuir, Scotland	ESK
39	Florissant, Missouri	FLO
40	Godhavn, Greenland	GDH
41	Georgetown, Washington, D.C.	GEO

Station Number	Station Name	Station Abbr.
43	Golden, Colorado	GOL
45	Hong Kong, China	HKC
48	Honiara, Guadalcanal, Solomon Is.	HNR
50	Istanbul, Turkey	IST
51	Jerusalem, Israel	JER
52	Kevo, Finland	KEV
53	Kipapa, Hawaii	KIP
55	Kongsberg, Norway	KON
56	Lahore, Pakistan	LAH
57	Kabul, Afghanistan	KBL
58	Longmire, Washington	LON
60	La Paz, Bolivia	LPB
61	La Palma, El Salvador	LPS
63	Lubbock, Texas	LUB
64	Matsushiro, Japan	MAT
65	Malaga, Spain	MAL
66	Manila, Philippines	MAN
67	Madison, Wisconsin	MDS
68	Songkla, Thailand	SNG
71	Meshed, Iran	MSH
74	Nairobi, Kenya	NAI
76	Nhatrang, South Vietnam	NHA
78	Nana, Peru	NNA
79	Nord, Greenland	NOR
81	Nurmijarvi, Finland	NUR
82	Ogdensburg, New Jersey	OGD
83	Oxford, Mississippi	OXF
85	Goldstone, California	GSC
86	Port Moresby, New Guinea	PMG

Station Number	Station Name	Station Abbr.
91	Porto, Portugal	PTO
92	Quetta, Pakistan	QUE
93	Quito, Ecuador	QUI
94	Rabaul, New Britain	RAB
100	Kap Tobin, Greenland	KTG
101	State College, Pennsylvania	SCP
102	Seoul, Korea	SEO
103	Spring Hill, Alabama	SHA
104	Shiraz, Iran	SHI
109	Stuttgart, Germany	STU
110	Tabriz, Iran	TAB
114	Shiraki, Japan	SHK
115	Toledo, Spain	TOL
117	Trieste, Italy	TRI
118	Trinidad, B.W.I.	TRN
119	Tucson, Arizona	TUC
121	Valentia, Ireland	VAL
123	Weston, Massachusetts	WES
124	Windhoek, South Africa	WIN
126	Lormes, France	LOR
222	Kirkenes, Norway	KRK

APPENDIX B

The Estimations of Q_{γ}^{-1} from Seismic Rayleigh Waves

The values of the specific attenuation factor determined at 79 frequencies are listed for eight events, the values from the earthquake merely demonstrate the unsuitability of such an event. Confidence limits at the 95% level are also quoted.

For the eight individual events the intercept of the regression line is also listed. So for each amplitude-distance plot the regression line is entirely determined.

Three sets of average Q_{γ}^{-1} values are also included. The events averaged are

1 The three atmospheric explosions at Novaya Zemlya

2 The two atmospheric explosions at S Sinkiang Prov., China.

3 All five atmospheric explosions.

Graphs of all these Q_{γ}^{-1} values, and confidence limits, have been described in Chapter 3.

NUVAYA ZEMLYA 27/9/62 ATMOSPHERIC 28 STATIONS

NSTAT = 28 NFA = 79 NFL = 40 T = 2.056

	FREQ.(HZ)	INVERSE Q & LIMITS		INTERCEPT & LIMITS	
1	0.01465	0.00715	0.00256	3.8820	0.1392
3	0.01709	0.00845	0.00303	3.9959	0.1607
5	0.01953	0.00689	0.00182	4.0693	0.1120
7	0.02197	0.00643	0.00257	4.1421	0.1624
9	0.02441	0.00491	0.00185	4.1722	0.1319
11	0.02686	0.00430	0.00170	4.1885	0.1352
13	0.02930	0.00526	0.00206	4.3056	0.1813
15	0.03174	0.00498	0.00164	4.3235	0.1589
17	0.03418	0.00425	0.00206	4.3023	0.2219
19	0.03662	0.00467	0.00244	4.3243	0.2863
21	0.03906	0.00554	0.00200	4.4016	0.2561
23	0.04150	0.00429	0.00248	4.2431	0.3478
25	0.04395	0.00360	0.00237	4.1827	0.3578
27	0.04639	0.00399	0.00178	4.2871	0.2886
29	0.04883	0.00414	0.00208	4.2692	0.3595
31	0.05127	0.00485	0.00174	4.3424	0.3183
33	0.05371	0.00505	0.00175	4.3165	0.3345
35	0.05615	0.00415	0.00178	4.1033	0.3577
37	0.05859	0.00527	0.00154	4.2431	0.3272
39	0.06104	0.00504	0.00141	4.2662	0.3151
41	0.06348	0.00471	0.00158	4.1362	0.3564
43	0.06592	0.00434	0.00185	4.0075	0.4328
45	0.06836	0.00454	0.00179	4.0387	0.4327
47	0.07080	0.00434	0.00163	3.9527	0.4067
49	0.07324	0.00353	0.00165	3.7526	0.4210
51	0.07568	0.00413	0.00156	3.9449	0.4087
53	0.07813	0.00368	0.00132	3.8768	0.3570
55	0.08057	0.00353	0.00137	3.7983	0.3735
57	0.08301	0.00371	0.00144	3.7956	0.4032
59	0.08545	0.00376	0.00142	3.8268	0.4133
61	0.08789	0.00337	0.00117	3.8030	0.3502
63	0.09033	0.00338	0.00111	3.7874	0.3414
65	0.09277	0.00306	0.00107	3.6735	0.3346
67	0.09521	0.00297	0.00101	3.6078	0.3240
69	0.09766	0.00240	0.00115	3.4662	0.3749
71	0.10010	0.00262	0.00107	3.4959	0.3652
73	0.10254	0.00246	0.00090	3.4902	0.3099
75	0.10498	0.00227	0.00097	3.4253	0.3417
77	0.10742	0.00199	0.00094	3.3913	0.3448
79	0.10986	0.00184	0.00096	3.3113	0.3600

	FREQ.(HZ)	INVERSE Q & LIMITS		INTERCEPT & LIMITS	
2	0.01587	0.01118	0.00293	4.0634	0.1455
4	0.01831	0.00891	0.00274	4.0722	0.1488
6	0.02075	0.00775	0.00251	4.1612	0.1525
8	0.02319	0.00581	0.00218	4.1818	0.1467
10	0.02563	0.00434	0.00177	4.1673	0.1335
12	0.02808	0.00489	0.00173	4.2508	0.1448
14	0.03052	0.00531	0.00188	4.3299	0.1740
16	0.03296	0.00440	0.00184	4.2982	0.1879
18	0.03540	0.00440	0.00235	4.3143	0.2642
20	0.03784	0.00515	0.00198	4.3694	0.2424
22	0.04028	0.00521	0.00225	4.3605	0.3009
24	0.04272	0.00358	0.00262	4.1418	0.3806
26	0.04517	0.00384	0.00207	4.2510	0.3236
28	0.04761	0.00409	0.00190	4.2940	0.3177
30	0.05005	0.00411	0.00204	4.2420	0.3613
32	0.05249	0.00547	0.00162	4.4149	0.3033
34	0.05493	0.00445	0.00191	4.1740	0.3747
36	0.05737	0.00464	0.00164	4.1570	0.3385
38	0.05981	0.00542	0.00147	4.2956	0.3193
40	0.06226	0.00486	0.00152	4.2208	0.3394
42	0.06470	0.00441	0.00163	4.0484	0.3737
44	0.06714	0.00453	0.00195	4.0280	0.4645
46	0.06958	0.00464	0.00167	4.0410	0.4106
48	0.07202	0.00383	0.00157	3.8108	0.3952
50	0.07446	0.00380	0.00159	3.8708	0.4111
52	0.07690	0.00421	0.00140	3.9504	0.3738
54	0.07935	0.00349	0.00133	3.8255	0.3599
56	0.08179	0.00345	0.00150	3.7462	0.4137
58	0.08423	0.00358	0.00137	3.9027	0.3890
60	0.08667	0.00339	0.00130	3.7630	0.3835
62	0.08911	0.00340	0.00119	3.7906	0.3602
64	0.09155	0.00341	0.00107	3.8050	0.3300
66	0.09399	0.00305	0.00098	3.6241	0.3092
68	0.09644	0.00253	0.00120	3.4778	0.3886
70	0.09888	0.00250	0.00110	3.5055	0.3677
72	0.10132	0.00269	0.00106	3.5383	0.3639
74	0.10376	0.00235	0.00087	3.4362	0.3038
76	0.10620	0.00211	0.00098	3.4097	0.3530
78	0.10864	0.00183	0.00094	3.3089	0.3501

NOVAYA ZEMLYA 22/10/62 ATMOSPHERIC 27 STATIONS

NSTAT = 27 NFA = 79 NFL = 40 T = 2.060

	FREQ.(HZ)	INVERSE Q & LIMITS		INTERCEPT & LIMITS	
1	0.01465	0.00705	0.00655	3.7054	0.2860
3	0.01709	0.00594	0.00646	3.8294	0.3231
5	0.01953	0.00595	0.00494	3.9102	0.2809
7	0.02197	0.00549	0.00441	3.7069	0.2832
9	0.02441	0.00450	0.00397	3.7537	0.2873
11	0.02686	0.00365	0.00334	3.8143	0.2691
13	0.02930	0.00467	0.00311	3.9292	0.2769
15	0.03174	0.00411	0.00255	3.9095	0.2541
17	0.03418	0.00328	0.00280	3.9139	0.3036
19	0.03662	0.00394	0.00305	3.9670	0.3656
21	0.03906	0.00574	0.00341	4.2105	0.4402
23	0.04150	0.00523	0.00314	4.2097	0.4414
25	0.04395	0.00414	0.00292	4.1233	0.4417
27	0.04639	0.00469	0.00247	4.2494	0.3999
29	0.04883	0.00446	0.00221	4.2225	0.3829
31	0.05127	0.00432	0.00252	4.1807	0.4618
33	0.05371	0.00340	0.00262	3.9934	0.5072
35	0.05615	0.00381	0.00267	4.0197	0.5448
37	0.05859	0.00460	0.00225	4.1828	0.4794
39	0.06104	0.00468	0.00241	4.1779	0.5309
41	0.06348	0.00501	0.00233	4.1623	0.5360
43	0.06592	0.00448	0.00212	4.0240	0.5024
45	0.06836	0.00420	0.00207	3.9897	0.5114
47	0.07080	0.00382	0.00204	3.8390	0.5141
49	0.07324	0.00340	0.00182	3.7560	0.4715
51	0.07568	0.00404	0.00173	3.8800	0.4663
53	0.07813	0.00401	0.00167	3.8753	0.4598
55	0.08057	0.00416	0.00149	3.8786	0.4205
57	0.08301	0.00298	0.00195	3.5201	0.5659
59	0.08545	0.00319	0.00164	3.6265	0.5560
61	0.08789	0.00266	0.00169	3.4655	0.5275
63	0.09033	0.00249	0.00139	3.4053	0.4394
65	0.09277	0.00279	0.00121	3.5703	0.3947
67	0.09521	0.00230	0.00130	3.4282	0.4345
69	0.09766	0.00250	0.00136	3.5195	0.4616
71	0.10010	0.00156	0.00128	3.2402	0.4408
73	0.10254	0.00209	0.00111	3.4000	0.3957
75	0.10498	0.00181	0.00100	3.2985	0.3637
77	0.10742	0.00197	0.00109	3.4280	0.4060
79	0.10986	0.00189	0.00117	3.4424	0.4477

	FREQ.(HZ)	INVERSE Q & LIMITS		INTERCEPT & LIMITS	
2	0.01587	0.01021	0.00649	3.8522	0.3034
4	0.01831	0.01035	0.00601	3.8632	0.3209
6	0.02075	0.00754	0.00461	3.8100	0.2786
8	0.02319	0.00484	0.00427	3.7070	0.2915
10	0.02563	0.00366	0.00342	3.7623	0.2612
12	0.02808	0.00412	0.00353	3.8753	0.2994
14	0.03052	0.00529	0.00267	3.9819	0.2503
16	0.03296	0.00324	0.00277	3.8742	0.2860
18	0.03540	0.00384	0.00322	3.9575	0.3646
20	0.03784	0.00423	0.00313	4.0196	0.3872
22	0.04028	0.00658	0.00334	4.3319	0.4496
24	0.04272	0.00408	0.00296	4.0865	0.4326
26	0.04517	0.00443	0.00281	4.1840	0.4391
28	0.04761	0.00485	0.00223	4.2874	0.3735
30	0.05005	0.00431	0.00243	4.1781	0.4319
32	0.05249	0.00397	0.00262	4.1230	0.4945
34	0.05493	0.00328	0.00267	3.9348	0.5308
36	0.05737	0.00434	0.00247	4.1171	0.5155
38	0.05981	0.00455	0.00223	4.1878	0.4838
40	0.06226	0.00512	0.00244	4.2228	0.5485
42	0.06470	0.00484	0.00221	4.1061	0.5166
44	0.06714	0.00416	0.00213	3.9695	0.5168
46	0.06958	0.00442	0.00204	4.0041	0.5095
48	0.07202	0.00341	0.00195	3.7517	0.5002
50	0.07446	0.00378	0.00179	3.8410	0.4733
52	0.07690	0.00404	0.00167	3.8698	0.4547
54	0.07935	0.00416	0.00164	3.9024	0.4558
56	0.08179	0.00372	0.00176	3.7425	0.5022
58	0.08423	0.00273	0.00199	3.4506	0.5895
60	0.08667	0.00304	0.00164	3.6171	0.5014
62	0.08911	0.00255	0.00156	3.4152	0.4895
64	0.09155	0.00269	0.00116	3.5189	0.3741
66	0.09399	0.00248	0.00130	3.4602	0.4275
68	0.09644	0.00237	0.00131	3.4738	0.4391
70	0.09888	0.00225	0.00131	3.4553	0.4479
72	0.10132	0.00148	0.00124	3.2015	0.4321
74	0.10376	0.00200	0.00102	3.3728	0.3661
76	0.10620	0.00186	0.00108	3.3302	0.3968
78	0.10864	0.00183	0.00107	3.4276	0.4020

NOVAYA ZEMLYA 24/12/62 ATMOSPHERIC 26 STATIONS

NSTAT = 26 NFA = 79 NFL = 40 T = 2.064

	FREQ.(HZ)	INVERSE Q & LIMITS		INTERCEPT & LIMITS	
1	0.01465	0.00880	0.00551	4.0931	0.2373
3	0.01709	0.00741	0.00451	4.0090	0.2269
5	0.01953	0.00676	0.00359	4.0325	0.2021
7	0.02197	0.00439	0.00300	4.0569	0.1895
9	0.02441	0.00398	0.00230	4.0904	0.1633
11	0.02686	0.00326	0.00204	4.1217	0.1622
13	0.02930	0.00478	0.00193	4.2688	0.1700
15	0.03174	0.00402	0.00181	4.2639	0.1771
17	0.03418	0.00319	0.00248	4.2109	0.2670
19	0.03662	0.00387	0.00296	4.2230	0.3479
21	0.03906	0.00473	0.00301	4.3315	0.3842
23	0.04150	0.00455	0.00263	4.3632	0.3675
25	0.04395	0.00459	0.00231	4.4359	0.3466
27	0.04639	0.00410	0.00246	4.3495	0.3994
29	0.04883	0.00408	0.00247	4.3477	0.4253
31	0.05127	0.00464	0.00240	4.4608	0.4408
33	0.05371	0.00476	0.00229	4.4782	0.4405
35	0.05615	0.00472	0.00215	4.4050	0.4323
37	0.05859	0.00491	0.00199	4.3853	0.4189
39	0.06104	0.00389	0.00205	4.1397	0.4495
41	0.06348	0.00346	0.00186	4.0101	0.4223
43	0.06592	0.00425	0.00183	4.1649	0.4254
45	0.06836	0.00487	0.00174	4.2986	0.4215
47	0.07080	0.00452	0.00169	4.2084	0.4245
49	0.07324	0.00463	0.00148	4.2273	0.3753
51	0.07568	0.00496	0.00139	4.3070	0.3663
53	0.07813	0.00481	0.00149	4.2758	0.4026
55	0.08057	0.00422	0.00182	4.0869	0.5065
57	0.08301	0.00369	0.00160	3.9694	0.4501
59	0.08545	0.00308	0.00166	3.7998	0.4784
61	0.08789	0.00305	0.00170	3.7888	0.4999
63	0.09033	0.00289	0.00157	3.7124	0.4746
65	0.09277	0.00266	0.00137	3.6651	0.4311
67	0.09521	0.00215	0.00108	3.5845	0.3521
69	0.09766	0.00295	0.00129	3.8156	0.4285
71	0.10010	0.00253	0.00123	3.6937	0.4199
73	0.10254	0.00166	0.00123	3.4308	0.4314
75	0.10498	0.00154	0.00139	3.3468	0.4995
77	0.10742	0.00197	0.00118	3.5079	0.4354
79	0.10986	0.00175	0.00109	3.4654	0.4113

	FREQ.(HZ)	INVERSE Q & LIMITS		INTERCEPT & LIMITS	
2	0.01587	0.00761	0.00568	4.0005	0.2654
4	0.01831	0.00748	0.00377	4.0498	0.2010
6	0.02075	0.00494	0.00336	4.0132	0.2003
8	0.02319	0.00422	0.00270	4.0744	0.1811
10	0.02563	0.00346	0.00216	4.0957	0.1624
12	0.02808	0.00408	0.00213	4.2078	0.1778
14	0.03052	0.00504	0.00175	4.3329	0.1625
16	0.03296	0.00303	0.00221	4.1949	0.2268
18	0.03540	0.00366	0.00290	4.2271	0.3263
20	0.03784	0.00440	0.00300	4.2733	0.3671
22	0.04028	0.00494	0.00298	4.3664	0.3980
24	0.04272	0.00431	0.00228	4.3949	0.3300
26	0.04517	0.00411	0.00223	4.3608	0.3470
28	0.04761	0.00435	0.00263	4.3901	0.4390
30	0.05005	0.00422	0.00243	4.3744	0.4312
32	0.05249	0.00476	0.00227	4.4925	0.4271
34	0.05493	0.00452	0.00219	4.4131	0.4308
36	0.05737	0.00509	0.00227	4.4248	0.4659
38	0.05981	0.00452	0.00188	4.3041	0.4035
40	0.06226	0.00338	0.00196	4.0173	0.4373
42	0.06470	0.00383	0.00186	4.0781	0.4285
44	0.06714	0.00463	0.00170	4.2479	0.4049
46	0.06958	0.00480	0.00180	4.2589	0.4439
48	0.07202	0.00468	0.00152	4.2441	0.3840
50	0.07446	0.00484	0.00135	4.2791	0.3485
52	0.07690	0.00508	0.00159	4.3166	0.4241
54	0.07935	0.00427	0.00157	4.1505	0.4308
56	0.08179	0.00421	0.00177	4.0785	0.4939
58	0.08423	0.00329	0.00158	3.8509	0.4507
60	0.08667	0.00317	0.00175	3.8301	0.5091
62	0.08911	0.00282	0.00163	3.7084	0.4860
64	0.09155	0.00309	0.00140	3.7726	0.4337
66	0.09399	0.00222	0.00135	3.5456	0.4332
68	0.09644	0.00249	0.00111	3.7068	0.3653
70	0.09888	0.00295	0.00137	3.8097	0.4617
72	0.10132	0.00185	0.00116	3.4885	0.4021
74	0.10376	0.00177	0.00130	3.4572	0.4631
76	0.10620	0.00144	0.00135	3.2959	0.4915
78	0.10864	0.00193	0.00117	3.5014	0.4362

NOVAYA ZEMLYA 7/11/68 UNDERGROUND 18 STATIONS

NSTAT = 18 NFA = 79 AFL = 40 T = 2.120

	FREQ.(HZ)	INVERSE Q & LIMITS		INTERCEPT & LIMITS	
1	0.01465	0.00498	0.00655	3.3055	0.3408
3	0.01709	0.00537	0.01187	3.1600	0.5186
5	0.01953	0.00790	0.00671	3.2702	0.3691
7	0.02197	0.00377	0.00593	2.9901	0.3727
9	0.02441	0.00522	0.00522	3.1169	0.3678
11	0.02686	0.00476	0.00566	3.0222	0.4320
13	0.02930	0.00387	0.00851	3.1344	0.6234
15	0.03174	0.00109	0.00719	2.9747	0.5813
17	0.03418	0.00507	0.00538	3.3760	0.5277
19	0.03662	0.00017	0.00586	3.0030	0.5515
21	0.03906	0.00311	0.00581	3.3163	0.5769
23	0.04150	0.00337	0.00550	3.4342	0.5839
25	0.04395	0.00278	0.00643	3.3357	0.7301
27	0.04639	0.00147	0.00527	3.1058	0.6345
29	0.04883	0.00255	0.00422	3.3400	0.5456
31	0.05127	0.00337	0.00335	3.5634	0.4576
33	0.05371	0.00504	0.00302	3.8016	0.4314
35	0.05615	0.00378	0.00329	3.7060	0.4918
37	0.05859	0.00356	0.00227	3.6613	0.3541
39	0.06104	0.00418	0.00239	3.7580	0.3926
41	0.06348	0.00310	0.00207	3.5901	0.3542
43	0.06592	0.00316	0.00206	3.5267	0.3637
45	0.06836	0.00431	0.00167	3.7262	0.3080
47	0.07080	0.00462	0.00211	3.8608	0.4056
49	0.07324	0.00444	0.00200	3.8707	0.3976
51	0.07568	0.00361	0.00248	3.6982	0.5103
53	0.07813	0.00311	0.00215	3.5281	0.4634
55	0.08057	0.00440	0.00212	3.8284	0.4705
57	0.08301	0.00358	0.00222	3.6627	0.5082
59	0.08545	0.00388	0.00192	3.7454	0.4558
61	0.08789	0.00404	0.00191	3.8283	0.4636
63	0.09033	0.00428	0.00245	3.8505	0.5998
65	0.09277	0.00451	0.00261	3.8795	0.6554
67	0.09521	0.00450	0.00228	3.8646	0.5885
69	0.09766	0.00452	0.00173	3.8441	0.4565
71	0.10010	0.00382	0.00221	3.6358	0.5899
73	0.10254	0.00371	0.00239	3.6139	0.6566
75	0.10498	0.00496	0.00220	4.0108	0.6283
77	0.10742	0.00467	0.00196	4.0083	0.5710
79	0.10986	0.00354	0.00152	3.6744	0.4539

	FREQ.(HZ)	INVERSE Q & LIMITS		INTERCEPT & LIMITS	
2	0.01587	0.00864	0.01101	3.3657	0.4764
4	0.01831	0.00473	0.01143	3.1307	0.5352
6	0.02075	0.01064	0.01032	3.3235	0.5512
8	0.02319	0.00302	0.00510	2.9872	0.3398
10	0.02563	0.00660	0.00564	3.1469	0.4135
12	0.02808	0.00605	0.00829	3.2002	0.5904
14	0.03052	0.00121	0.00809	2.9717	0.6233
16	0.03296	0.00402	0.00707	3.2267	0.6017
18	0.03540	0.00173	0.00754	3.1121	0.6914
20	0.03784	0.00183	0.00523	3.1602	0.5056
22	0.04028	0.00320	0.00576	3.3787	0.5921
24	0.04272	0.00328	0.00548	3.4283	0.6018
26	0.04517	0.00153	0.00547	3.1608	0.6403
28	0.04761	0.00216	0.00542	3.2042	0.6766
30	0.05005	0.00289	0.00391	3.4360	0.5203
32	0.05249	0.00420	0.00323	3.6883	0.4519
34	0.05493	0.00481	0.00285	3.8265	0.4162
36	0.05737	0.00306	0.00295	3.6007	0.4499
38	0.05981	0.00436	0.00218	3.7679	0.3488
40	0.06226	0.00339	0.00215	3.6529	0.3594
42	0.06470	0.00312	0.00221	3.5455	0.3838
44	0.06714	0.00394	0.00185	3.6709	0.3345
46	0.06958	0.00462	0.00212	3.7835	0.4004
48	0.07202	0.00439	0.00200	3.8548	0.3903
50	0.07446	0.00422	0.00227	3.8397	0.4590
52	0.07690	0.00311	0.00231	3.5576	0.4874
54	0.07935	0.00359	0.00195	3.6397	0.4256
56	0.08179	0.00393	0.00199	3.7636	0.4490
58	0.08423	0.00342	0.00203	3.6201	0.4740
60	0.08667	0.00419	0.00178	3.8542	0.4268
62	0.08911	0.00413	0.00218	3.8379	0.5318
64	0.09155	0.00439	0.00259	3.8508	0.6427
66	0.09399	0.00433	0.00229	3.8549	0.5825
68	0.09644	0.00454	0.00203	3.8730	0.5294
70	0.09888	0.00424	0.00186	3.7274	0.4943
72	0.10132	0.00399	0.00246	3.6567	0.6668
74	0.10376	0.00431	0.00246	3.7674	0.6883
76	0.10620	0.00490	0.00198	4.0515	0.5697
78	0.10864	0.00430	0.00171	3.9202	0.5060

CHINKY 17/6/67 24 STATIONS

NSTAT = 24 NFA = 79 NFL = 40 T = 2.070

	FREQ.(HZ)	INVERSE Q & LIMITS		INTERCEPT & LIMITS	
1	0.01465	0.00457	0.01150	3.5395	0.4400
3	0.01709	0.00084	0.00851	3.3745	0.3723
5	0.01953	0.00451	0.00977	3.5617	0.4615
7	0.02197	0.00512	0.00791	3.6531	0.4098
9	0.02441	0.01035	0.00777	3.9199	0.4520
11	0.02686	0.00832	0.00667	3.9056	0.4332
13	0.02930	0.00538	0.00597	3.8206	0.4341
15	0.03174	0.00472	0.00703	3.8146	0.5663
17	0.03418	0.00615	0.00568	4.0661	0.5101
19	0.03662	0.00335	0.00569	3.8345	0.5580
21	0.03906	0.00425	0.00657	3.9514	0.6956
23	0.04150	0.00532	0.00570	4.1486	0.6514
25	0.04395	0.00531	0.00459	4.2236	0.5635
27	0.04639	0.00303	0.00482	3.9929	0.6275
29	0.04883	0.00249	0.00524	3.8988	0.7223
31	0.05127	0.00433	0.00422	4.1287	0.6132
33	0.05371	0.00506	0.00408	4.2239	0.6270
35	0.05615	0.00508	0.00465	4.1903	0.7500
37	0.05859	0.00452	0.00453	4.1040	0.7634
39	0.06104	0.00489	0.00448	4.1361	0.7896
41	0.06348	0.00568	0.00419	4.2946	0.7703
43	0.06592	0.00602	0.00381	4.3625	0.7264
45	0.06836	0.00637	0.00334	4.4211	0.6635
47	0.07080	0.00483	0.00287	4.1017	0.5886
49	0.07324	0.00357	0.00283	3.8079	0.5983
51	0.07568	0.00273	0.00366	3.6151	0.8000
53	0.07813	0.00313	0.00357	3.7212	0.8061
55	0.08057	0.00316	0.00306	3.7972	0.7072
57	0.08301	0.00260	0.00363	3.6031	0.8688
59	0.08545	0.00215	0.00350	3.4722	0.8590
61	0.08789	0.00163	0.00324	3.3299	0.8128
63	0.09033	0.00232	0.00323	3.5061	0.8336
65	0.09277	0.00336	0.00296	3.8062	0.7873
67	0.09521	0.00258	0.00293	3.5622	0.7970
69	0.09766	0.00198	0.00272	3.4637	0.7579
71	0.10010	0.00289	0.00234	3.6192	0.6682
73	0.10254	0.00223	0.00222	3.4088	0.6511
75	0.10498	0.00209	0.00242	3.4258	0.7262
77	0.10742	0.00240	0.00248	3.5192	0.7619
79	0.10986	0.00067	0.00280	2.9519	0.8756

	FREQ.(HZ)	INVERSE Q & LIMITS		INTERCEPT & LIMITS	
2	0.01587	0.00262	0.00917	3.4666	0.3753
4	0.01831	0.00459	0.01021	3.5530	0.4630
6	0.02075	0.00354	0.00823	3.5367	0.4066
8	0.02319	0.00936	0.00743	3.8845	0.4083
10	0.02563	0.00789	0.00786	3.8080	0.4834
12	0.02808	0.00801	0.00625	3.9443	0.4297
14	0.03052	0.00289	0.00584	3.6687	0.4469
16	0.03296	0.00743	0.00628	4.0916	0.5344
18	0.03540	0.00418	0.00543	3.9194	0.5100
20	0.03784	0.00301	0.00708	3.7847	0.7213
22	0.04028	0.00458	0.00582	4.0418	0.6405
24	0.04272	0.00582	0.00531	4.2376	0.6296
26	0.04517	0.00409	0.00446	4.1088	0.5638
28	0.04761	0.00267	0.00501	3.9442	0.6711
30	0.05005	0.00289	0.00482	3.9476	0.6820
32	0.05249	0.00512	0.00405	4.2255	0.6043
34	0.05493	0.00523	0.00428	4.2405	0.6742
36	0.05737	0.00466	0.00448	4.1268	0.7379
38	0.05981	0.00479	0.00447	4.1324	0.7709
40	0.06226	0.00526	0.00412	4.1963	0.7416
42	0.06470	0.00601	0.00399	4.3413	0.7482
44	0.06714	0.00631	0.00355	4.4269	0.6915
46	0.06958	0.00628	0.00323	4.3744	0.6521
48	0.07202	0.00345	0.00270	3.8091	0.5630
50	0.07446	0.00353	0.00317	3.7902	0.6816
52	0.07690	0.00260	0.00368	3.6067	0.8182
54	0.07935	0.00337	0.00311	3.8206	0.7116
56	0.08179	0.00270	0.00360	3.6444	0.8482
58	0.08423	0.00251	0.00332	3.5969	0.8041
60	0.08667	0.00155	0.00347	3.3111	0.8617
62	0.08911	0.00176	0.00318	3.3578	0.8104
64	0.09155	0.00318	0.00323	3.7346	0.8459
66	0.09399	0.00278	0.00296	3.6473	0.7959
68	0.09644	0.00225	0.00292	3.4596	0.8046
70	0.09888	0.00234	0.00242	3.5363	0.6830
72	0.10132	0.00258	0.00241	3.4870	0.6984
74	0.10376	0.00186	0.00217	3.3223	0.6433
76	0.10620	0.00265	0.00256	3.6395	0.7766
78	0.10864	0.00151	0.00259	3.2600	0.8021

CHINKY 29/9/69 39 STATIONS

NSTAT = 39 NFA = 79 NFL = 40 T = 2.026

	FREQ.(HZ)	INVERSE Q & LIMITS		INTERCEPT & LIMITS	
1	0.01465	0.00612	0.00279	3.4906	0.1521
3	0.01709	0.00513	0.00217	3.3864	0.1369
5	0.01953	0.00702	0.00274	3.5440	0.1758
7	0.02197	0.00612	0.00202	3.6049	0.1536
9	0.02441	0.00495	0.00204	3.6135	0.1639
11	0.02686	0.00366	0.00182	3.6051	0.1641
13	0.02930	0.00325	0.00197	3.6599	0.1958
15	0.03174	0.00153	0.00191	3.5603	0.2103
17	0.03418	0.00116	0.00187	3.6056	0.2266
19	0.03662	0.00060	0.00196	3.5532	0.2587
21	0.03906	0.00037	0.00164	3.5110	0.2332
23	0.04150	0.00075	0.00137	3.5684	0.2103
25	0.04395	0.00171	0.00137	3.6425	0.2251
27	0.04639	0.00188	0.00130	3.6791	0.2281
29	0.04883	0.00203	0.00142	3.7075	0.2639
31	0.05127	0.00253	0.00141	3.7533	0.2766
33	0.05371	0.00297	0.00125	3.8197	0.2576
35	0.05615	0.00343	0.00139	3.8080	0.3010
37	0.05859	0.00314	0.00136	3.7018	0.3081
39	0.06104	0.00345	0.00121	3.7736	0.2855
41	0.06348	0.00310	0.00128	3.6394	0.3103
43	0.06592	0.00283	0.00119	3.5696	0.2976
45	0.06836	0.00238	0.00116	3.4461	0.3014
47	0.07080	0.00274	0.00101	3.4788	0.2698
49	0.07324	0.00229	0.00100	3.3498	0.2768
51	0.07568	0.00236	0.00096	3.3467	0.2692
53	0.07813	0.00250	0.00095	3.3209	0.2751
55	0.08057	0.00269	0.00082	3.4072	0.2425
57	0.08301	0.00261	0.00083	3.3466	0.2505
59	0.08545	0.00203	0.00082	3.2037	0.2555
61	0.08789	0.00199	0.00087	3.1418	0.2779
63	0.09033	0.00161	0.00081	3.0313	0.2670
65	0.09277	0.00149	0.00092	2.9834	0.3085
67	0.09521	0.00124	0.00087	2.9281	0.2980
69	0.09766	0.00155	0.00085	3.0534	0.3009
71	0.10010	0.00126	0.00077	3.0177	0.2783
73	0.10254	0.00110	0.00074	2.9183	0.2721
75	0.10498	0.00084	0.00069	2.8071	0.2644
77	0.10742	0.00091	0.00069	2.8225	0.2686
79	0.10986	0.00041	0.00062	2.6839	0.2415

	FREQ.(HZ)	INVERSE Q & LIMITS		INTERCEPT & LIMITS	
2	0.01587	0.00579	0.00262	3.4493	0.1498
4	0.01831	0.00705	0.00255	3.4798	0.1584
6	0.02075	0.00710	0.00260	3.6263	0.1792
8	0.02319	0.00558	0.00206	3.6088	0.1584
10	0.02563	0.00463	0.00201	3.6240	0.1715
12	0.02808	0.00334	0.00203	3.6252	0.1920
14	0.03052	0.00262	0.00187	3.6358	0.1954
16	0.03296	0.00101	0.00190	3.5477	0.2193
18	0.03540	0.00104	0.00190	3.6070	0.2404
20	0.03784	0.00033	0.00191	3.5080	0.2629
22	0.04028	0.00041	0.00144	3.5296	0.2141
24	0.04272	0.00118	0.00136	3.5963	0.2168
26	0.04517	0.00201	0.00137	3.6780	0.2326
28	0.04761	0.00198	0.00135	3.6965	0.2439
30	0.05005	0.00209	0.00149	3.7066	0.2853
32	0.05249	0.00256	0.00129	3.8176	0.2595
34	0.05493	0.00316	0.00129	3.8183	0.2723
36	0.05737	0.00311	0.00134	3.7180	0.2963
38	0.05981	0.00335	0.00129	3.7400	0.2976
40	0.06226	0.00339	0.00127	3.7452	0.3024
42	0.06470	0.00284	0.00123	3.5758	0.3031
44	0.06714	0.00254	0.00114	3.5009	0.2902
46	0.06958	0.00261	0.00110	3.4703	0.2895
48	0.07202	0.00252	0.00099	3.4259	0.2705
50	0.07446	0.00231	0.00099	3.3434	0.2771
52	0.07690	0.00242	0.00096	3.3187	0.2734
54	0.07935	0.00255	0.00083	3.3651	0.2431
56	0.08179	0.00280	0.00081	3.4179	0.2432
58	0.08423	0.00231	0.00084	3.2892	0.2577
60	0.08667	0.00200	0.00082	3.1578	0.2599
62	0.08911	0.00187	0.00082	3.1135	0.2658
64	0.09155	0.00149	0.00092	2.9737	0.3040
66	0.09399	0.00147	0.00081	2.9912	0.2741
68	0.09644	0.00130	0.00091	2.9530	0.3154
70	0.09888	0.00144	0.00079	3.0658	0.2832
72	0.10132	0.00117	0.00076	2.9765	0.2754
74	0.10376	0.00095	0.00072	2.8469	0.2710
76	0.10620	0.00088	0.00065	2.8226	0.2661
78	0.10864	0.00070	0.00062	2.7640	0.2412

ALEUTIAN ISLANDS 29/10/65 LONG SHOT 9 STATIONS

NSTAT = 9 NFA = 79 NFL = 40 T = 2.365

	FREQ.(HZ)	INVERSE Q & LIMITS		INTERCEPT & LIMITS	
1	0.01465	0.00092	0.02371	2.7879	0.9057
3	0.01709	0.01354	0.02123	3.0597	0.9154
5	0.01953	0.00627	0.01711	2.6845	0.7932
7	0.02197	0.00908	0.01547	2.9277	0.8339
9	0.02441	0.01267	0.01775	3.1447	1.0184
11	0.02686	0.00868	0.01172	2.9022	0.7251
13	0.02930	0.00367	0.00878	2.6537	0.5904
15	0.03174	0.00286	0.00531	2.7800	0.3850
17	0.03418	0.00105	0.00534	2.7739	0.4220
19	0.03662	-0.00013	0.00679	2.7794	0.5757
21	0.03906	0.00030	0.00730	2.8168	0.6733
23	0.04150	0.00024	0.00637	2.8083	0.6359
25	0.04395	-0.00004	0.00667	2.7984	0.7175
27	0.04639	0.00669	0.00761	3.4690	0.8725
29	0.04883	0.00485	0.00529	3.4349	0.6519
31	0.05127	0.00332	0.00405	3.2488	0.5317
33	0.05371	0.00161	0.00698	2.8908	0.9713
35	0.05615	0.00207	0.00774	2.8355	1.1350
37	0.05859	0.00220	0.01011	2.8561	1.5536
39	0.06104	0.00345	0.00649	3.0865	1.0519
41	0.06348	0.00545	0.00722	3.3576	1.2255
43	0.06592	0.00321	0.00969	3.1215	1.6812
45	0.06836	0.00279	0.00838	2.9995	1.5065
47	0.07080	0.00272	0.00655	2.8925	1.2211
49	0.07324	0.00461	0.00552	3.2606	1.0465
51	0.07568	0.00441	0.00507	3.1195	0.9936
53	0.07813	0.00301	0.00517	2.8153	1.0496
55	0.08057	0.00115	0.00561	2.3992	1.1743
57	0.08301	0.00270	0.00371	2.7222	0.8040
59	0.08545	0.00417	0.00312	3.0842	0.6815
61	0.08789	0.00098	0.00371	2.3520	0.8181
63	0.09033	-0.00066	0.00490	1.8728	1.1152
65	0.09277	0.00233	0.00371	2.5576	0.8608
67	0.09521	-0.00014	0.00458	2.1255	1.0965
69	0.09766	0.00149	0.00467	2.4893	1.1399
71	0.10010	0.00219	0.00419	2.4891	1.0476
73	0.10254	0.00177	0.00425	2.5161	1.0821
75	0.10498	0.00117	0.00455	2.4512	1.1794
77	0.10742	0.00001	0.00319	2.2150	0.8443
79	0.10986	0.00216	0.00278	2.7713	0.7439

	FREQ.(HZ)	INVERSE Q & LIMITS		INTERCEPT & LIMITS	
2	0.01587	0.00794	0.02206	2.9118	0.8958
4	0.01831	0.01273	0.01857	2.9536	0.8276
6	0.02075	0.00450	0.01692	2.6381	0.8400
8	0.02319	0.01216	0.01857	3.1301	1.0300
10	0.02563	0.01265	0.01290	3.1502	0.7699
12	0.02808	0.00331	0.00941	2.5698	0.6081
14	0.03052	0.00454	0.00658	2.8118	0.4596
16	0.03296	0.00160	0.00431	2.7713	0.3264
18	0.03540	-0.00053	0.00510	2.7079	0.4177
20	0.03784	0.00060	0.00738	2.8492	0.6540
22	0.04028	0.00072	0.00837	2.8158	0.8037
24	0.04272	-0.00100	0.00594	2.7178	0.6161
26	0.04517	0.00374	0.00600	3.1844	0.6660
28	0.04761	0.00657	0.00792	3.5208	0.9414
30	0.05005	0.00405	0.00394	3.3534	0.5013
32	0.05249	0.00251	0.00514	3.1142	0.6954
34	0.05493	0.00106	0.00759	2.7330	1.0842
36	0.05737	0.00288	0.00919	2.9152	1.3794
38	0.05981	0.00289	0.00862	3.0180	1.3603
40	0.06226	0.00472	0.00610	3.2200	1.0117
42	0.06470	0.00445	0.00887	3.2609	1.5209
44	0.06714	0.00298	0.00923	3.0794	1.6311
46	0.06958	0.00262	0.00707	2.9313	1.2949
48	0.07202	0.00371	0.00701	3.0595	1.3167
50	0.07446	0.00466	0.00430	3.2390	0.8279
52	0.07690	0.00404	0.00615	3.0237	1.2256
54	0.07935	0.00155	0.00440	2.4797	0.9066
56	0.08179	0.00139	0.00527	2.4664	1.1234
58	0.08423	0.00422	0.00264	3.0767	0.5753
60	0.08667	0.00194	0.00415	2.5713	0.9084
62	0.08911	0.00087	0.00381	2.3057	0.8535
64	0.09155	0.00103	0.00397	2.1857	0.9127
66	0.09399	0.00145	0.00415	2.4982	0.9781
68	0.09644	-0.00004	0.00459	2.1285	1.1074
70	0.09888	0.00173	0.00444	2.4514	1.0955
72	0.10132	0.00252	0.00414	2.6317	1.0456
74	0.10376	0.00105	0.00445	2.3973	1.1431
76	0.10620	0.00068	0.00418	2.3145	1.0906
78	0.10864	0.00108	0.00277	2.5320	0.7383

QUAKE 17/6/67 11 STATIONS

NSTAT = 11 NFA = 79 NFU = 40 T = 2.260

	FREQ.(HZ)	INVERSE Q & LIMITS		INTERCEPT & LIMITS	
1	0.01465	0.02483	0.03801	4.3679	0.9828
3	0.01709	0.01005	0.03998	3.9950	1.1631
5	0.01953	0.00650	0.02688	3.9759	0.8992
7	0.02197	0.00921	0.01931	4.0623	0.7255
9	0.02441	0.00156	0.01228	3.8465	0.5071
11	0.02686	0.00006	0.01159	3.7681	0.5310
13	0.02930	-0.00166	0.01225	3.7411	0.6172
15	0.03174	-0.00016	0.01876	3.7233	1.0349
17	0.03418	0.00194	0.01884	3.9393	1.1337
19	0.03662	0.00063	0.01508	3.8966	1.0213
21	0.03906	0.00197	0.01337	3.9714	0.9365
23	0.04150	0.00345	0.01468	4.0695	1.1263
25	0.04395	0.00598	0.01526	4.3824	1.2476
27	0.04639	0.00695	0.01243	4.4709	1.0796
29	0.04883	0.00905	0.01066	4.6856	0.9792
31	0.05127	0.00890	0.01106	4.6847	1.0720
33	0.05371	0.00551	0.01125	4.3435	1.1259
35	0.05615	0.00837	0.00742	4.6545	0.8086
37	0.05859	0.00579	0.00660	4.4288	0.7619
39	0.06104	0.00571	0.00808	4.3692	0.9783
41	0.06348	0.00538	0.00783	4.4539	1.0081
43	0.06592	0.00492	0.00588	4.3157	0.7902
45	0.06836	0.00526	0.00607	4.3521	0.8500
47	0.07080	0.00522	0.00720	4.4274	1.0547
49	0.07324	0.00897	0.00663	5.0194	1.0219
51	0.07568	0.00501	0.00479	4.3923	0.7795
53	0.07813	0.00645	0.00475	4.6208	0.8030
55	0.08057	0.00682	0.00381	4.7558	0.6729
57	0.08301	0.00571	0.00544	4.4966	1.0015
59	0.08545	0.00247	0.00486	3.7988	0.9469
61	0.08789	0.00119	0.00412	3.6124	0.8296
63	0.09033	0.00213	0.00493	3.7913	1.0249
65	0.09277	0.00278	0.00507	3.9214	1.0737
67	0.09521	0.00258	0.00480	3.8513	1.0519
69	0.09766	0.00128	0.00428	3.5448	0.9682
71	0.10010	0.00241	0.00364	3.7419	0.8235
73	0.10254	0.00203	0.00472	3.7840	1.0667
75	0.10498	0.00202	0.00588	3.6611	1.2440
77	0.10742	0.00063	0.00311	3.2874	0.7114
79	0.10986	0.00100	0.00492	3.4292	1.1377

	FREQ.(HZ)	INVERSE Q & LIMITS		INTERCEPT & LIMITS	
2	0.01587	0.02131	0.03824	4.2960	1.0485
4	0.01831	0.00492	0.03416	3.8931	1.0671
6	0.02075	0.01016	0.02119	4.1103	0.7524
8	0.02319	0.00329	0.01341	3.8638	0.5283
10	0.02563	0.00103	0.01217	3.8335	0.5297
12	0.02808	-0.00256	0.01124	3.6761	0.5402
14	0.03052	0.00015	0.01543	3.7746	0.8141
16	0.03296	0.00120	0.01607	3.8613	0.9264
18	0.03540	0.00068	0.01938	3.8736	1.2139
20	0.03784	0.00256	0.01391	4.0310	0.9400
22	0.04028	0.00179	0.01272	3.9585	0.9264
24	0.04272	0.00511	0.01777	4.2529	1.3976
26	0.04517	0.00634	0.01362	4.4159	1.1481
28	0.04761	0.00798	0.01131	4.5763	1.0102
30	0.05005	0.00861	0.00951	4.6585	0.8973
32	0.05249	0.00704	0.01165	4.5177	1.1425
34	0.05493	0.00840	0.00966	4.6065	1.0038
36	0.05737	0.00617	0.00694	4.4696	0.7782
38	0.05981	0.00619	0.00819	4.3902	0.9683
40	0.06226	0.00548	0.00776	4.4517	0.9685
42	0.06470	0.00526	0.00629	4.4155	0.8273
44	0.06714	0.00458	0.00620	4.2523	0.8509
46	0.06958	0.00516	0.00665	4.3803	0.9515
48	0.07202	0.00799	0.00731	4.8363	1.0980
50	0.07446	0.00681	0.00581	4.7022	0.9194
52	0.07690	0.00554	0.00432	4.4636	0.7165
54	0.07935	0.00707	0.00444	4.7576	0.7667
56	0.08179	0.00638	0.00464	4.6790	0.8362
58	0.08423	0.00440	0.00544	4.2006	1.0286
60	0.08667	0.00183	0.00519	3.6561	1.0270
62	0.08911	0.00165	0.00385	3.7343	0.7880
64	0.09155	0.00245	0.00552	3.8453	1.1563
66	0.09399	0.00316	0.00452	3.9839	0.9733
68	0.09644	0.00177	0.00467	3.6977	1.0398
70	0.09888	0.00117	0.00362	3.4663	0.8185
72	0.10132	0.00304	0.00421	3.9130	0.9496
74	0.10376	0.00165	0.00643	3.6527	1.3945
76	0.10620	0.00100	0.00414	3.4210	0.9062
78	0.10864	0.00087	0.00397	3.3479	0.9128

NOVAYA ZEMLYA 24/12/62 ATMOSPHERIC 26 STATIONS
NOVAYA ZEMLYA 27/9/62 ATMOSPHERIC 28 STATIONS
NOVAYA ZEMLYA 22/10/62 ATMOSPHERIC 27 STATIONS

	FREQ.(HZ)	INVERSE Q & LIMITS	
1	0.01465	0.007454	0.002240
3	0.01709	0.008463	0.002440
5	0.01953	0.007478	0.001752
7	0.02197	0.005510	0.001819
9	0.02441	0.004496	0.001498
11	0.02686	0.003797	0.001293
13	0.02930	0.004942	0.001296
15	0.03174	0.004426	0.001094
17	0.03540	0.003789	0.001407
19	0.03418	0.004070	0.001493
21	0.03906	0.005327	0.001513
23	0.04150	0.004638	0.001493
25	0.04395	0.004065	0.001385
27	0.04639	0.004200	0.001213
29	0.04883	0.004203	0.001239
31	0.05127	0.004645	0.001204
33	0.05371	0.004527	0.001199
35	0.05615	0.004251	0.001189
37	0.05859	0.004979	0.001040
39	0.06104	0.004575	0.001047
41	0.06348	0.004355	0.001039
43	0.06592	0.004344	0.001056
45	0.06836	0.004560	0.001021
47	0.07080	0.004263	0.000974
49	0.07324	0.003851	0.000907
51	0.07568	0.004378	0.000859
53	0.07813	0.004140	0.000811
55	0.08057	0.003929	0.000862
57	0.08301	0.003496	0.000907
59	0.08545	0.003376	0.000897
61	0.08789	0.003061	0.000829
63	0.09033	0.002966	0.000739
65	0.09277	0.002850	0.000668
67	0.09521	0.002512	0.000618
69	0.09766	0.002609	0.000691
71	0.10010	0.002313	0.000650
73	0.10254	0.002099	0.000590
75	0.10498	0.001907	0.000621
77	0.10742	0.001982	0.000585
79	0.10986	0.001819	0.000584

	FREQ.(HZ)	INVERSE Q & LIMITS	
2	0.01587	0.009868	0.002655
4	0.01831	0.008792	0.002256
6	0.02075	0.006789	0.001882
8	0.02319	0.005025	0.001676
10	0.02563	0.003868	0.001341
12	0.02808	0.004420	0.001350
14	0.03052	0.005215	0.001150
16	0.03296	0.003634	0.001231
18	0.03662	0.004028	0.001512
20	0.03784	0.004664	0.001463
22	0.04028	0.005466	0.001540
24	0.04272	0.003946	0.001442
26	0.04517	0.004082	0.001284
28	0.04761	0.004372	0.001234
30	0.05005	0.004197	0.001252
32	0.05249	0.004848	0.001174
34	0.05493	0.004174	0.001221
36	0.05737	0.004714	0.001148
38	0.05981	0.004911	0.000999
40	0.06226	0.004425	0.001060
42	0.06470	0.004326	0.001029
44	0.06714	0.004466	0.001064
46	0.06958	0.004638	0.001002
48	0.07202	0.003994	0.000919
50	0.07446	0.004132	0.000870
52	0.07690	0.004451	0.000847
54	0.07935	0.003930	0.000823
56	0.08179	0.003784	0.000916
58	0.08423	0.003397	0.000900
60	0.08667	0.003216	0.000853
62	0.08911	0.002968	0.000794
64	0.09155	0.003092	0.000665
66	0.09399	0.002616	0.000661
68	0.09644	0.002473	0.000663
70	0.09888	0.002579	0.000688
72	0.10132	0.002095	0.000629
74	0.10376	0.002064	0.000586
76	0.10620	0.001819	0.000626
78	0.10864	0.001866	0.000581

C/HINKY 17/6/67 24 STATICNS
CHINKY 29/9/69 39 STATIONS

	FREQ.(HZ)	INVERSE Q & LIMITS	
1	0.01465	0.005988	0.002847
3	0.01709	0.004783	0.002148
5	0.01953	0.006800	0.002630
7	0.02197	0.006068	0.001865
9	0.02441	0.005346	0.001957
11	0.02686	0.004008	0.001727
13	0.02930	0.003417	0.001759
15	0.03174	0.001791	0.001839
17	0.03418	0.001587	0.001695
19	0.03662	0.000845	0.001753
21	0.03906	0.000704	0.001657
23	0.04150	0.001147	0.001412
25	0.04395	0.002032	0.001288
27	0.04639	0.001980	0.001273
29	0.04883	0.002069	0.001393
31	0.05127	0.002694	0.001279
33	0.05371	0.003161	0.001177
35	0.05615	0.003585	0.001325
37	0.05859	0.003272	0.001294
39	0.06104	0.003592	0.001211
41	0.06348	0.003383	0.001219
43	0.06592	0.003148	0.001123
45	0.06836	0.002795	0.001063
47	0.07080	0.002952	0.000916
49	0.07324	0.002418	0.000900
51	0.07568	0.002401	0.000991
53	0.07813	0.002567	0.000978
55	0.08057	0.002743	0.000834
57	0.08301	0.002608	0.000935
59	0.08545	0.002043	0.000892
61	0.08789	0.001956	0.000884
63	0.09033	0.001684	0.000846
65	0.09277	0.001679	0.000870
67	0.09521	0.001384	0.000842
69	0.09766	0.001595	0.000812
71	0.10010	0.001431	0.000717
73	0.10254	0.001216	0.000687
75	0.10498	0.000962	0.000676
77	0.10742	0.001060	0.000682
79	0.10986	0.000439	0.000698

	FREQ.(HZ)	INVERSE Q & LIMITS	
2	0.01587	0.005496	0.002528
4	0.01831	0.006829	0.002605
6	0.02075	0.006846	0.002326
8	0.02319	0.005842	0.001916
10	0.02563	0.004870	0.001952
12	0.02808	0.003701	0.001817
14	0.03052	0.002639	0.001688
16	0.03296	0.001538	0.001763
18	0.03540	0.001309	0.001690
20	0.03784	0.000568	0.001871
22	0.04028	0.000772	0.001467
24	0.04272	0.001584	0.001364
26	0.04517	0.002191	0.001273
28	0.04761	0.002039	0.001325
30	0.05005	0.002161	0.001389
32	0.05249	0.003154	0.001192
34	0.05493	0.003355	0.001223
36	0.05737	0.003258	0.001275
38	0.05981	0.003486	0.001248
40	0.06226	0.003576	0.001201
42	0.06470	0.003158	0.001168
44	0.06714	0.002929	0.001069
46	0.06958	0.002993	0.001012
48	0.07202	0.002613	0.000887
50	0.07446	0.002436	0.000941
52	0.07690	0.002438	0.000997
54	0.07935	0.002639	0.000850
56	0.08179	0.002784	0.000919
58	0.08423	0.002336	0.000887
60	0.08667	0.001955	0.000891
62	0.08911	0.001857	0.000847
64	0.09155	0.001656	0.000900
66	0.09399	0.001604	0.000809
68	0.09644	0.001404	0.000864
70	0.09888	0.001538	0.000742
72	0.10132	0.001320	0.000718
74	0.10376	0.001043	0.000668
76	0.10620	0.001074	0.000692
78	0.10864	0.000784	0.000663

NOVAYA ZEMLYA 24/12/62 ATMOSPHERIC 26 STATIONS
CHINKY 17/6/67 24 STATIONS
NOVAYA ZEMLYA 27/9/62 ATMOSPHERIC 28 STATIONS
NOVAYA ZEMLYA 22/10/62 ATMOSPHERIC 27 STATIONS
CHINKY 29/9/69 39 STATIONS

	FREQ.(HZ)	INVERSE Q & LIMITS			FREQ.(HZ)	INVERSE Q & LIMITS	
1	0.01465	0.006772	0.001755	2	0.01587	0.007490	0.001802
3	0.01709	0.006378	0.001591	4	0.01831	0.007803	0.001686
5	0.01953	0.007186	0.001492	6	0.02075	0.006817	0.001457
7	0.02197	0.005820	0.001277	8	0.02319	0.005433	0.001246
9	0.02441	0.004912	0.001195	10	0.02563	0.004363	0.001141
11	0.02686	0.003902	0.001045	12	0.02808	0.004063	0.001096
13	0.02930	0.004187	0.001058	14	0.03052	0.003941	0.000983
15	0.03174	0.003125	0.001021	16	0.03296	0.002606	0.001036
17	0.03418	0.002642	0.001045	18	0.03540	0.002677	0.001119
19	0.03662	0.002532	0.001142	20	0.03784	0.002614	0.001155
21	0.03906	0.003010	0.001102	22	0.04028	0.003154	0.001055
23	0.04150	0.002953	0.001022	24	0.04272	0.002803	0.000987
25	0.04395	0.003079	0.000941	26	0.04517	0.003163	0.000895
27	0.04639	0.003119	0.000867	28	0.04761	0.003236	0.000891
29	0.04883	0.003165	0.000914	30	0.05005	0.003208	0.000918
31	0.05127	0.003699	0.000865	32	0.05249	0.004027	0.000827
33	0.05371	0.003866	0.000833	34	0.05493	0.003775	0.000855
35	0.05615	0.003925	0.000873	36	0.05737	0.004005	0.000842
37	0.05859	0.004150	0.000808	38	0.05981	0.004218	0.000777
39	0.06104	0.004096	0.000783	40	0.06226	0.004009	0.000785
41	0.06348	0.003875	0.000783	42	0.06470	0.003746	0.000763
43	0.06592	0.003750	0.000758	44	0.06714	0.003704	0.000745
45	0.06836	0.003689	0.000726	46	0.06958	0.003819	0.000703
47	0.07080	0.003612	0.000663	48	0.07202	0.003298	0.000632
49	0.07324	0.003123	0.000631	50	0.07446	0.003285	0.000630
51	0.07568	0.003410	0.000642	52	0.07690	0.003461	0.000639
53	0.07813	0.003362	0.000620	54	0.07935	0.003282	0.000583
55	0.08057	0.003329	0.000593	56	0.08179	0.003286	0.000641
57	0.08301	0.003063	0.000643	58	0.08423	0.002879	0.000626
59	0.08545	0.002726	0.000626	60	0.08667	0.002602	0.000608
61	0.08789	0.002526	0.000596	62	0.08911	0.002426	0.000572
63	0.09033	0.002337	0.000550	64	0.09155	0.002385	0.000541
65	0.09277	0.002273	0.000532	66	0.09399	0.002116	0.000509
67	0.09521	0.001954	0.000505	68	0.09644	0.001945	0.000529
69	0.09766	0.002109	0.000521	70	0.09888	0.002070	0.000498
71	0.10010	0.001888	0.000475	72	0.10132	0.001718	0.000467
73	0.10254	0.001666	0.000442	74	0.10376	0.001556	0.000435
75	0.10498	0.001430	0.000451	76	0.10620	0.001445	0.000458
77	0.10742	0.001524	0.000440	78	0.10864	0.001332	0.000432
79	0.10986	0.001144	0.000444				

APPENDIX C

The Instrument Response

Each Rayleigh wave train used in this work was recorded by a long period, vertical component instrument of the World-Wide Standard Seismograph Network (WWSSN). It is necessary to correct these seismograms for instrumental effects which influence both amplitude and phase. The corrections applied to the seismogram in the time domain for instrumental magnification and group delay time - which must necessarily be introduced - have been described by Brune, Nafe and Oliver (1960). The group delay time, t_u, at angular frequency ω is

$$t_u = \frac{d\emptyset(\omega)}{d\omega}$$

where $\emptyset(\omega)$ is the phase shift caused by the instrument. This usually amounts to several seconds and may significantly affect the measured group velocities.

In the frequency domain the complex seismogram spectrum $A(\omega)$ is corrected for instrumental effects by using the complex instrumental transfer function $I(\omega)$ and dividing at each frequency to form

$$A'(\omega) = \frac{A(\omega)}{I(\omega)}$$

$I(\omega)$ contains both amplitude and phase information and may be obtained by several methods, but not all are possible or convenient in the present case. If the seismograph system constants are known then $I(\omega)$ may be calculated algebraically. Each seismogram contains a calibration pulse - the system response to a step of acceleration - this may be Fourier analysed and $I(\omega)$ obtained directly. This latter process is difficult because it is difficult to digitise sharp calibration pulses to sufficient accuracy. Further, the calibration pulse is introduced while the seismometer is operational and recording ground motion, and therefore must contain noise superimposed onto the calibrating pulse. Alternatively the blanket response quoted by the WWSSN for all seismographs may be assumed. But examination of calibration pulses on several film chips from different stations shows great differences in amplitude and phase response for different instruments. An individual correction for each seismogram is required. Mitchell and Landisman (1969) advocate a "least-squares inversion" technique to determine seismograph constants and hence $I(\omega)$, but this is too time consuming when 200 seismograms are involved. An alternative technique proposed by Espinosa, Sutton and Miller (1962, 1965) was eventually chosen.

Espinosa et al. (1965) have determined a set of analog standard transient responses to a step of acceleration which would be shown by a variety of instrument systems, each with specified characteristic parameters. Appendix VI of Espinosa et al. contains a computing program written by Brune which obtains $I(\omega)$ by choosing the standard transient response, from a library of 78, which best matches the transient observed on the seismogram. A least squares deviation is calculated between six points measured from the observed transient and the analogous points on the standard library transients, the seismograph parameters corresponding to the best fitting transient are then used to calculate $I(\omega)$.

The six necessary measurements are shown in Figure C.1 which is taken from Espinosa et al. (1965). The time points P_1 to P_6 are measured from the initial break time of the calibration pulse. All the measurements are made from a baseline which takes into account the lateral motion of the recording pen on the drum. It is also necessary to know the mass of the seismometer (kg), the motor constant of the seismometer in newton/mA and the calibration current in mA. All the instruments have a seismometer mass of 11.2 kg and the motor constant and calibration current are marked on each film chip in the appropriate units.

Brune's program was adapted and incorporated into the subroutine WWSSN and is listed with the program TSAP (Burton and Blamey 1972). The measurements P_1 to P_6 were taken when the Rayleigh wave train was digitised

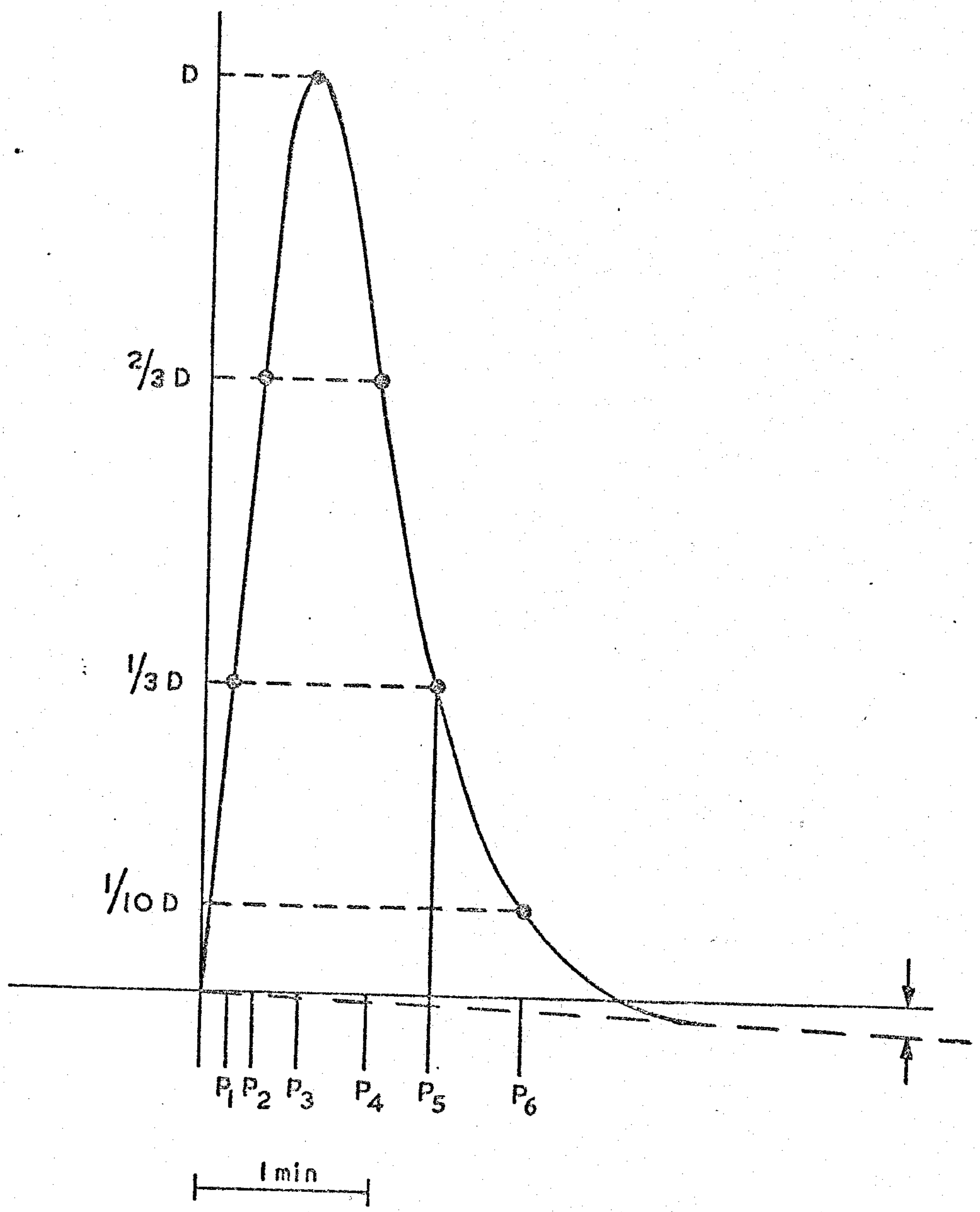

FIGURE C.1 TRANSIENT RESPONSE AS USED FOR COMPUTER COMPARISON WITH STANDARD TRANSIENT RESPONSE CASES and the same digitising units of measure were used. These measurements are scaled to the appropriate absolute values within the subroutine WWSSN.

Four typical instrumental magnification curves calculated by this method are shown in Figure C.2. These correspond to the stations AAE, COP, MDS and QUE when they recorded the event NZA 24/12/62. According to the film chips the nominal magnification at 20s period for these stations is 750, 750, 1500 and 3000 respectively. These absolute values of magnification have been ignored in Figure C.2 to illustrate the discrepancy between instruments of the position of the peak period response. This shows a surprising variation between systems which are supposedly standard. A blanket WWSSN instrumental response would have hidden this source of error and have been inappropriate in work requiring amplitude determinations for a wide range of recording stations.

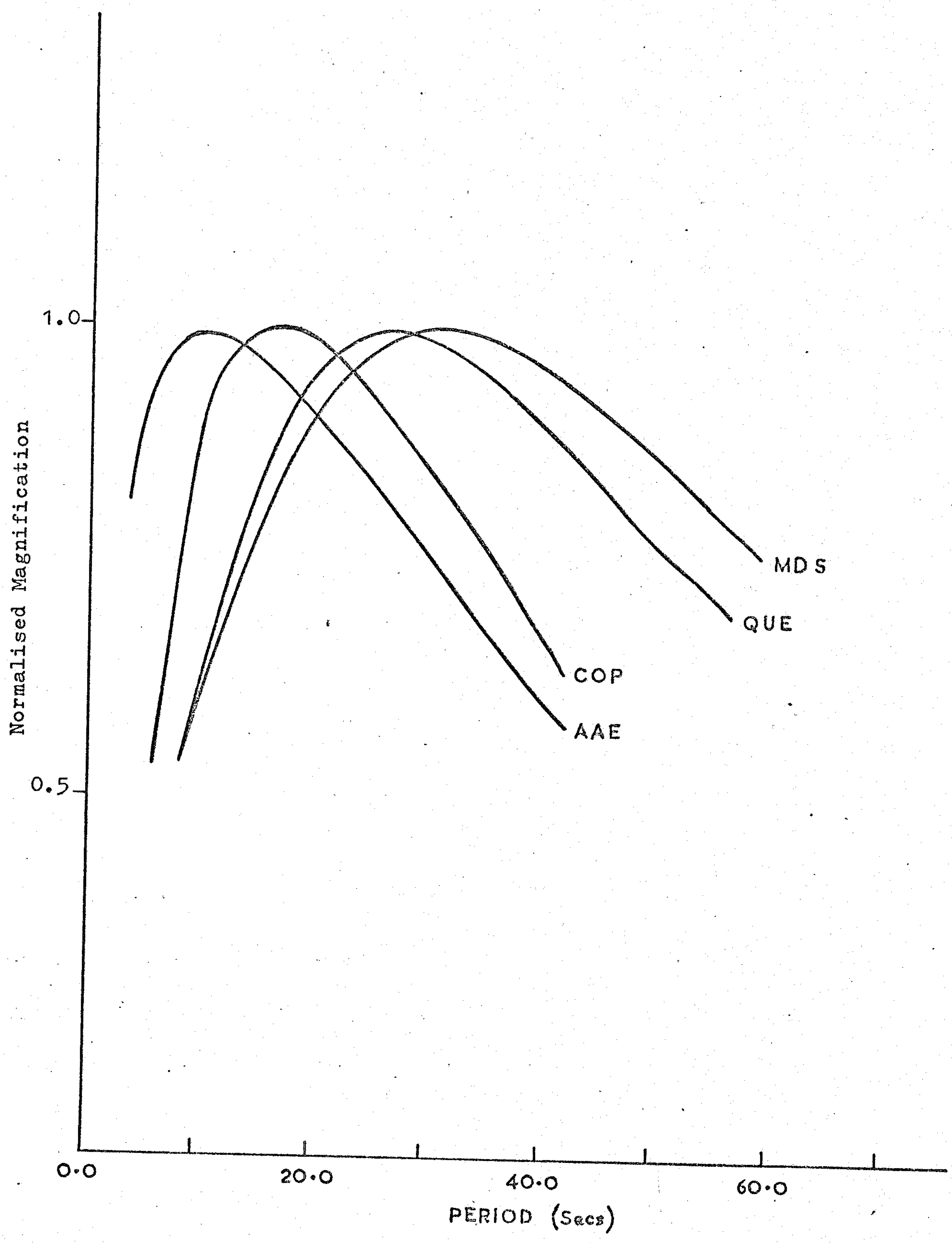

FIGURE C.2 WWSSN INSTRUMENT MAGNIFICATIONS

APPENDIX D

Least Squares fitting of "the best" straight line

The "best line" appropriate to the experimental data

The variation of amplitude with distance for Rayleigh waves has already been expressed in a linear form. An amplitude term ($\log_{10}(A\sqrt{E \sin \Delta})$) plotted as the ordinate variable Y_i against a distance term $\frac{\pi E \Delta f}{U} \log_{10} e$ or abscissa variable X_i yields values of the specific attenuation factor Q_γ^{-1}. The gradient of the plot is the negative value of Q_γ^{-1}. For each of the j events analysed there are n_j stations or n_j pairs of points (X_i, Y_i). If a and b are the best estimates of the gradient and intercept formed from these points then

$$Y_i = aX_i + b \qquad i=1 \text{-----} n_j \qquad \text{D.1}$$

The method used to determine a and b depends on what is known about the errors in X_i and Y_i. Adcock (1880) determined a and b by minimising "the sum of the squares of the normals from the n points to the required line". However, this is a special case and has tacitly assumed that the weights $\omega(X_i)$, $\omega(Y_i)$ assigned to X_i, Y_i are equal.

Other methods are particularly applicable to certain types of data. The papers by McIntyre et al. (1966) and Brooks et al. (1968) assume knowledge of errors or standard deviation at each point, that is for each point (X_i, Y_i) the values $(\sigma_{X_i}, \sigma_{Y_i})$ are also known. For their application, determination of the best isochron for Rb^{87}/Sr^{86} isotope ratios, each ratio is itself the subject of an experiment and so the errors $(\sigma_{X_i}, \sigma_{Y_i})$ are well determined at each point. Adjustments to obtain the best line are then made along the diagonal to the rectangle of sides $\sigma_{X_i}, \sigma_{Y_i}$ at each point.

There are many possible simplifying assumptions, like the above, which can be made. The paper by D York (1967) depicts the geometrical implications of many of these assumptions. For example the often used assumptions that the X_i are exactly known ($\omega(X_i) = \infty$) implies that all adjustments made to obtain the required line are necessarily parallel to the y axis.

York (1966) has obtained a "least squares cubic" equation for the gradient a when both X_i and Y_i are subject to errors.

$$a^3 \sum_i \frac{W_i^2 U_i^2}{\omega(X_i)} - 2a^2 \sum_i \frac{W_i^2 U_i V_i}{\omega(X_i)} - a\left[\sum_i W_i U_i^2 - \sum_i \frac{W_i^2 V_i^2}{\omega(X_i)}\right] + \sum W_i U_i V_i = 0 \qquad \text{D2}$$

and

$$W_i = \frac{\omega(X_i)\,\omega(Y_i)}{a^2\omega(Y_i) + \omega(X_i)} \qquad \text{D3}$$

$$\overline{X} = \frac{\sum_i W_i X_i}{\sum_i W_i} \qquad \text{D4}$$

$$\overline{Y} = \frac{\sum_i W_i Y_i}{\sum_i W_i} \qquad \text{D5}$$

$$U_i = X_i - \overline{X} \qquad \text{D6}$$

$$V_i = Y_i - \overline{Y} \qquad \text{D7}$$

Obviously equation D.2 is not really a cubic, but an estimate of a in equation D.3 reduces it to one. Equation D.2 may then be solved for the gradient.

It is useful to rewrite equation D.3 as

$$W_i = \frac{\omega(Y_i)}{a^2\left(\frac{\omega(Y_i)}{\omega(X_i)}\right) + 1} \qquad \text{D8}$$

We expect values no greater than .01 for the specific attenuation factor, Q_γ^{-1}, of Rayleigh waves; this is of course equal to the gradient for the experimental data. Further, it has already been shown that errors in the amplitude term are far greater than in the distance term for the data used. Equation D.8 becomes

$$W_i = \frac{\omega(Y_i)}{10^{-4}\left(\frac{\omega(Y_i)}{\omega(X_i)}\right) + 1} \qquad \text{D9}$$

with $$\omega(Y_i) << \omega(X_i) \qquad D.10$$

therefore

$$W_i \sim \omega(Y_i)$$

The errors caused by this approximation are obviously negligible for the present case.

Returning to equation D.2 we note that the first two terms are of order 10^{-6} and 10^{-4} respectively and contain the term $1/\omega(X_i)$, these may be safely neglected with respect to the third term which is of order 10^{-2}. Equation D.2 therefore becomes

$$a\left[\sum_i \omega(Y_i)U_i^2 - \sum_i \frac{(\omega(Y_i))^2 V_i^2}{\omega(X_i)}\right] = \sum_i \omega(Y_i)U_i V_i \qquad D.12$$

and using condition D.10 the second term may again be neglected giving

$$a = \frac{\sum_i \omega(Y_i)U_i V_i}{\sum_i \omega(Y_i)U_i^2} \qquad D.13$$

This result is the one which would be obtained from the simple regression of "y" on "x". The weights $\omega(Y_i)$ were all set to unity because for the experimentally determined values of amplitude there was no reason to do otherwise.

Regression Formulae

The derivation of formulae relevant to regression calculations are to be found in many books on statistics, for example J T Ractliff's "Elements of Mathematical Statistics" (1967). The formulae used in this work are listed below.

The points on the regression line corresponding to (X_i, Y_i) are (x_{ir}, y_{ir}) with $x_{ir} = X_i$, the line is

$$y_{ir} = a\,x_{ir} + b \qquad D.14$$

In addition to the previous notation the regression formulae are written in terms of variances (var) and covariances (cov) whenever possible, because the abbreviations VAR and COV are used during calculations in the computer subroutine LSTSQR.

Formulae are listed in the order in which it is reasonable to calculate them for computing purposes.

$$\mathrm{var}(X_i) = \frac{\sum_i U_i^2}{n_j} \qquad \text{D.15}$$

$$\mathrm{var}(Y_i) = \frac{\sum_i V_i^2}{n_j} \qquad \text{D.16}$$

$$\mathrm{cov}(X_i, Y_i) = \frac{\sum_i U_i V_i}{n_j} \qquad \text{D.17}$$

$$a = \frac{\mathrm{cov}(X_i, Y_i)}{\mathrm{var}(X_i)} \qquad \text{D.18}$$

$$b = \overline{Y}_i - a\,\overline{X}_i \qquad \text{D.19}$$

the product-moment correlation coefficient, r

$$r = \frac{\mathrm{cov}(X_i, Y_i)}{\sqrt{\mathrm{var}(X_i)\mathrm{var}(Y_i)}} \qquad \text{D.20}$$

the residual sum of squares about the regression line, RSS

$$\mathrm{RSS} = \sum_i (Y_i - y_{ir})^2 = (1-r^2)n \; \mathrm{var}\;(Y_i) \qquad \text{D.21}$$

$$\mathrm{var}\; a = \frac{(1-r^2)\mathrm{var}(Y_i)}{(n-2)\mathrm{var}(X_i)} \qquad \text{D.22}$$

$$\mathrm{var}\; b = \mathrm{var}\; a \frac{\sum_i X_i^2}{n_j} \qquad \text{D.23}$$

confidence limits on a and b require Student's "t" with n_j-2 degrees of freedom at the appropriate confidence level and are

$$a \pm t\sqrt{\mathrm{var}\; a} \qquad \text{D.24}$$

and

$$b \pm t \sqrt{\mathrm{var}\ b} \qquad \text{D.25}$$

the scatter about the calculated regression line is

$$y_{ir} = a\,x_{ir} + b \pm t \sqrt{\frac{RSS}{n_j - 2}} \qquad \text{D.26}$$

The subroutine LSTSQR is incorporated into the program AVD to determine values of the specific attenuation factor and confidence limits. Values of the correlation coefficient, r, indicate how reasonable a fit a line gives to the data. For zero correlation between the X_i and Y_i

$$r \sqrt{\frac{(n_j - 2)}{(1 - r^2)}} \qquad \text{D.27}$$

is distributed as Student's "t" with (n_j-2) degrees of freedom. (Miller and Kahn, 1962, p112.) The significance of r for each line is calculated in this way.

The values of Q_γ^{-1} and confidence limits are listed in Appendix B for each event.

APPENDIX E

The Comparison of Two Regression Lines

For the two regression lines (j=1 or 2)

$$y_{1ir} = a_1 x_{1ir} + b_1 \qquad \text{E.1}$$

$$y_{2ir} = a_2 x_{2ir} + b_2$$

with n_1, n_2 points each it is often necessary to compare them to determine if the observables (X_{ji}, Y_{ji}) come from the same population, have the same gradient a_j and the same intercept b_j. If all three comparisons show equality then the two lines are statistically the same line.

For amplitude-distance plots these comparisons will have geophysical significance. The first comparison will demonstrate if the energy from an event, at two frequencies or over two paths, has sampled similar environments. The further tests indicate if the attenuation differs and if the event size (or energy between frequencies) differs.

Statistics for making these comparisonsare described by K A Brownlee (1965) and the relevant tests and formulae are listed below.

For each regression the residual sums of squares may be estimated as

$$\sum_{i}^{n_j} (y_{jir} - Y_{ji})^2 \qquad \text{E.3}$$

$$= n_j \operatorname{var}(Y_j) - \frac{\operatorname{cov}(X_j, Y_j)}{\operatorname{var}(X_j)} \qquad \text{E.4}$$

and the mean squares estimated as

$$s_j^2 = \frac{\sum_i (y_{jir} - Y_{ji})^2}{n_j - 2} \qquad \text{E.5}$$

If the two sets of data are samples from the same population then the two values s_j^2 are estimates of the same variance σ^2 and Fisher's variance ratio "F" test may be performed to test this hypothesis.

$$F = \frac{s_1^2}{s_2^2} \qquad \text{NFTEST} \qquad \text{E.6}$$

If this test is passed σ^2 is estimated by

$$s^2 = \frac{(n_1-2)s_1^2+(n_2-2)s_2^2}{n_1-2 + n_2-2} \qquad \text{E.7}$$

If the gradients are equal then a_1-a_2 is normally distributed about zero with variance

$$\text{var}(a_1-a_2) = \frac{\sigma^2}{n_1\text{var}(X_1)} + \frac{\sigma^2}{n_2\text{var}(X_2)} \qquad \text{E.8}$$

and the variable

$$\frac{a_1 - a_2}{s\left[\left(\frac{1}{n_1\text{var}(X_1)}\right)+\left(\frac{1}{n_2\text{var}(X_2)}\right)\right]^{1/2}} \qquad \text{NATEST} \qquad \text{E.9}$$

is distributed as t with (n_1+n_2-4) degrees of freedom. This variable gives the second test.

If a_1 and a_2 are the same then a joint estimate may be obtained.

$$a = \frac{n_1\text{cov}(X_1,Y_1) + n_2\text{cov}(X_2,Y_2)}{n_1\text{var}(X_1) + n_2\text{var}(X_2)} \qquad \text{E.10}$$

As might be expected this equation is similar to the analogous equation (D.18) for the gradient of a single regression line, for the comparison of two such lines the analogy must occur throughout.

The variance of the joint gradient is

$$\text{var}(a) = \frac{\sigma^2}{n_1\text{var}(X_1) + n_2\text{var}(X_2)} \qquad \text{E.11}$$

and σ^2 is estimated from the new residual sum of squares

$$\text{RSS} = n_1\text{var}(Y_1) - \frac{n_1(\text{cov}(X_1,Y_1))^2}{\text{var}(X_1)} + \left[\begin{array}{l}\text{similar term}\\ \text{in } X_2,\ Y_2\end{array}\right] \qquad \text{E.12}$$

which has n_1+n_2-3 degrees of freedom, the analogy with the equations D.20 to D.22 is again obvious.

If the gradients are equal it is possible to test for complete equality of the lines, which depends on equality of the intercepts. The statistic to be tested is

$$\frac{(b_1-b_2) - a(\overline{X}_1-\overline{X}_2)}{S\left[\frac{1}{n_1} + \frac{1}{n_2} + (\overline{X}_1-\overline{X}_2)^2/(n_1\text{var}(X_1)+n_2\text{var}(X_2))\right]^{1/2}} \quad \text{NBTEST} \qquad \text{E.13}$$

which is distributed as t with n_1+n_2-3 degrees of freedom. The new S is determined from the new RSS of equation E.12.

These statistics are used in the computer programs C2L and CNL. The terms NFTEST, NATEST and NBTEST are used in these programs to both indicate the result of a particular test and as a switch for subsequent tests. The values 0, 1 or 2 are assigned to NFTEST indicating that the test was failed, passed or not performed. Obviously, if the values 0 or 2 are obtained then subsequent tests may be switched off.

The Average Gradient for Several Regression Lines

The average Q_Y^{-1} values subsequently determined for several events (n_E events) required estimation of the average gradient for several regression lines. Such averages were determined irrespective of the individual population variances (the results of NFTEST) although any discrepancies were noted.

The formulae of Brownlee were generalised to give

$$a = \frac{\sum_j^{n_E} n_j \text{ cov}(X_j,Y_j)}{\sum_j^{n_E} n_j \text{ var}(X_j)} \qquad \text{E.14}$$

with variance

$$\text{var}(a) = \frac{\sigma^2}{\sum_j^{n_E} n_j \text{ var}(X_j)} \qquad \text{E.15}$$

and σ^2 is now estimated from the total of the residual sums of squares

$$\text{RSS} = \sum_j^{n_E} n_j \text{ var}(Y_j) - \sum_j^{n_E} \frac{n_j(\text{cov}(X_j,Y_j))^2}{\text{var}(X_j)} \qquad \text{E.16}$$

which has $\sum_{j}^{n_E} (n_j-1)-1$ degrees of freedom.

These formulae are used in the program QBAR which is listed in Appendix G along with the programs C2L and CNL.

APPENDIX F

F1 Proof 1

To obtain the relation between the imaginary part of a bodily wave velocity and the specific attenuation factor:

For a body wave we have the wave propagation term

$$\exp\left[i(\omega t - kx) \right] \tag{F1.1}$$

where ω is angular frequency, t is time, k the wave number and x is the distance travelled. The phase velocity $\alpha = \omega / k$ and so we have

$$\exp\left[i(\omega t - \frac{\omega x}{\alpha}) \right] \tag{F1.2}$$

and ignoring time dependence

$$\exp\left[-i(\frac{\omega x}{\alpha}) \right] \tag{F1.3}$$

If the velocity α is complex of the form

$$\alpha = \alpha_o + I(\delta \alpha) \tag{F1.4}$$

then we have

$$\exp\left[- i\left(\frac{\omega x(\alpha_o - I(\delta \alpha))}{\alpha_o^2} \right) \right]$$

$$= \exp\left[\frac{-i\omega x}{\alpha_o} \right] \exp\left[\frac{-\omega x I(\delta \alpha)}{\alpha_o^2} \right] \tag{F1.5}$$

and the attenuation coefficient, γ, is therefore

$$\gamma = \frac{-\omega I(\delta \alpha)}{\alpha_o^2} \tag{F1.6}$$

But the attenuation coefficient, in terms of the specific attenuation factor Q_α^{-1} is

$$\gamma = \frac{-\pi f Q_\alpha^{-1}}{\alpha_o} \tag{F1.7}$$

where f is frequency, and so

$$I(\delta\alpha) = \frac{Q_\alpha^{-1} \alpha_o}{2} \tag{F1.8}$$

F2 Proof 2

Dispersion and dissipation are causally linked. To obtain the relation between the real part of a body wave velocity and the specific attenuation factor:

Futterman's (1962) equations relating the real and imaginary parts of the refractive index $n(\omega)$ are (Futterman's equations A-13[1] and A-14[1])

$$R(n(\omega_1) - n(\infty)) = \frac{2}{\pi} P \int_0^\infty \frac{I(n(\omega))\,\omega}{\omega^2 - \omega_1^2}\, d\omega \qquad \text{F2.1}$$

$$R(n(o) - n(\infty)) = \frac{2}{\pi} P \int_0^\infty \frac{I(n(\omega))}{\omega}\, d\omega \qquad \text{F2.2}$$

For a body wave velocity α (compressional wave) with R and I parts we may write

$$\alpha = \alpha_o + \delta\alpha \qquad \text{F2.3}$$

where

$$\delta\alpha = R(\delta\alpha) + I(\delta\alpha) \qquad \text{F2.4}$$

and using Futterman's formulation

$$R(\alpha(\omega_1) - \alpha(\infty)) = \frac{2}{\pi} P \int_0^\infty \frac{I(\alpha(\omega))\,\omega}{\omega^2 - \omega_1^2}\, d\omega \qquad \text{F2.5}$$

$$R(\alpha(o) - \alpha(\infty)) = \frac{2}{\pi} P \int_0^\infty \frac{I(\delta\alpha(\omega))}{\omega}\, d\omega \qquad \text{F2.6}$$

Futterman makes the assumption that there is no attenuation for infinite frequencies, that is

$$\alpha(\infty) = \alpha_o \qquad \text{F2.7}$$

and so

$$R(\alpha(\omega_1) - \alpha(\infty)) = R(\delta\alpha(\omega_1)) \qquad \text{F2.8}$$

$$R(\alpha(o) - \alpha(\infty)) = R(\delta\alpha(o)) \qquad \text{F2.9}$$

If we make the assumption that the dispersive effect of dissipation is very small then

$$\alpha(\omega_1) \sim \alpha(o) \qquad \text{F2.10}$$

and equation F2.6 is adequate to estimate $R(\delta\alpha(\omega))$ which gives

$$R(\delta\alpha(\omega)) = \frac{2}{\pi} P\int_{o}^{\infty} \frac{I(\delta\alpha(\omega))}{\omega} d\omega \qquad \text{F2.11}$$

but

$$I(\delta\alpha(\omega)) = \frac{-Q_{\alpha}^{-1}\alpha_{o}}{2} \qquad \text{F2.12}$$

therefore

$$R(\delta\alpha(\omega)) = \frac{P}{\pi}\int_{o}^{\infty} \frac{Q_{\alpha}^{-1}\alpha_{o}}{\omega} d\omega \qquad \text{F2.13}$$

$$R(\delta\alpha(\omega)) = \frac{\alpha_{o}Q_{\alpha}^{-1}}{\pi} \ln {}^{\omega}/_{\omega_{o}} \qquad \text{F2.14}$$

The lower bound frequency ω_o is inserted to eliminate the singularity. Similarly, for shear waves of velocity β

$$R(\delta\beta(\omega)) = \frac{\beta_{o}Q_{\beta}^{-1}}{\pi} \ln {}^{\omega}/_{\omega_{o}} \qquad \text{F2.15}$$

APPENDIX G

Computer Program Listings

This appendix contains the listings of six programs used in this study. The large program TSAP, which determines spectral amplitudes and group velocities, is listed by Burton and Blamey (1972). The major subroutine HH of the Hedgehog inversion program was developed by Mr B L N Kennett and Dr V P Valus. Many of these programs produce graphs using a Stromberg-Carlson 4060 plotter; several of the routines used to produce graphs are taken or adapted from Young and Douglas (1968). All of the programs are written in Fortran IV for the AWRE IBM 360/75 computer.

The listing of each program starts with a comprehensive block of comment cards. These cards detail the purpose, method of use and the output of the program so only a brief description of each program is given here.

The six programs are:

1 AVD

This program takes the theoretical equation for the variation of Rayleigh wave amplitude with distance from an event and fits a simple regression line to the observed data. The variation of Rayleigh wave amplitude with distance is such that

$$\text{AMPLITUDE TERM} = Q_\gamma^{-1} \times \text{DISTANCE TERM} + \text{CONSTANT}$$

therefore the gradient of the regression line estimates Q_γ^{-1}. Confidence limits on Q_γ^{-1} are calculated. So that the various regression lines may be compared the program calculates the regression line parameters for future use, these are: the mean and variance of the abscissa and ordinate, and the covariance.

2 CNL

3 C2L

4 QBAR

These three programs use the theory and formulae of Appendix E. The data are the regression line parameters provided by the program AVD.

The program CNL uses the regression line data at each frequency from a single explosion. The regression line at one frequency is compared to the lines at every other frequency; this process cycles through all the frequencies in turn.

C2L compares the regression line data at one frequency from one explosion with the corresponding data at the same frequency from a second explosion. The data for two distinct explosions are therefore compared at all the available matching frequencies.

The last program of this set, QBAR, determines the average gradient for several regression lines. Average Q_γ^{-1} and confidence limits are therefore obtained for each frequency using several explosions instead of one, this is irrespective of the yield of the individual explosions.

5 QRALEY

Theoretical calculations of the specific attenuation function $Q_\gamma^{-1}(f)$ of Rayleigh waves are carried out by this program for a chosen layered model. The model must comprise values of the body wave velocities and specific attenuation factors for each of the NOL layers, that is α_i, β_i, $Q_{\alpha i}^{-1}$, $Q_{\beta i}^{-1}$ for i=1...NOL.

Three frequency dependent terms must also be known. The group velocity U(f) must be known for the layered model at each frequency of interest. Derivatives of the wavenumber, $\frac{\partial k_o}{\partial \alpha_{ol}}$ and $\frac{\partial k_o}{\partial \beta_{ol}}$, must be known at each frequency and for each layer. Finally, a condition may be writte into the program uniquely relating Q_α^{-1} and Q_β^{-1}. The theory from which $Q_\gamma^{-1}(f)$ is calculated is given in Chapter 4.

6 HEDGEHOG

The Hedgehog procedure inverts the observed Rayleigh wave specific attenuation factor $Q_{\gamma o}^{-1}(f)$, which is frequency dependent, into a depth dependent attenuation model for Q_{α}^{-1} and Q_{β}^{-1}. A velocity-depth model and values of U(f), $\frac{\partial k_o}{\partial \alpha_{o1}}$, $\frac{\partial k_o}{\partial \beta_{o1}}$, similar to those used in the modelling for QRALEY must also be assumed.

The Hedgehog process described by Burton and Kennett (1972) differs from usual Monte-Carlo techniques in that after obtaining an acceptable model by a random process the next model is not selected at random but is chosen by an organised process - the aim being to delineate a region of connected solutions rather than an assortment of haphazard and unconnected solutions.

AVD

```
C
C
C
C
C     Q AMPLITUDE/DISTANCE PLOTS AT SEVERAL FREQUENCIES.
C     ************************************************
C
C
C     CALCULATES THE SPECIFIC ATTENUATION FACTOR FOR RAYLEIGH WAVES.
C     *************************************************************
C
C
C     THIS PROGRAM TAKES THE EQUATION
C
C      LOG(A*SQRT(E*SIN(DELTA)))=(QM1)*(-PI*E*DELTA*F/U)+CONSTANT
C
C     AND FITS
C
C                          ' Y = QM1*X + CONSTANT '
C
C     WHICH IS A SIMPLE REGRESSION LINE
C
C
C       A       SPECTRAL AMPLITUDE IN MICRON*SECONDS
C       E       RADIUS OF EARTH = 6371KM
C       DELTA   ANGULAR SEPERATION OF EVENT-RECORDING SITE
C       QM1     THE SPECIFIC ATTENUATION FACTOR FOR RAYLEIGH WAVES
C       F       FREQUENCY HZ
C       U       GROUP VELOCITY KM/S
C
C
C     THE TERM SQRT(E*SIN(DELTA)) CORRECTS A FOR GEOMETRICAL SPREADING
C
C
C     ******************************************************************
C
C     INPUT
C     *****
C
C
C     THE FOLLOWING CARDS ARE READ IN
C
C       1 AN SC4060 CARD REQUIRED FOR GRAPHICAL OUTPUT
C
C       2 TITLE(I)  TITLE FOR THE EVENT BEING PROCESSED
C
C       3 NSTAT,NFA,NFU,T
C
C         NSTAT  NUMBER OF STATIONS FOR THE EVENT
C         NFA    NUMBER OF AMPLITUDE VALUES,A,AT SPECTRAL FREQUENCIES FA
C         NFU    NUMBER OF GROUP VELOCITIES,U,AT SPECTRAL FREQUENCIES FU
C                THE GROUP VELOCITY FREQUENCIES MUST CORRESPOND TO THE
C                FIRST,THIRD,FIFTH AMPLITUDE FREQUENCY ETC.
C         T      STUDENT'S 'T' ON NSTAT-2 DEGREES OF FREEDOM TO DETERMINE
C                CONFIDENCE LIMITS
C
C       4 STATN(I),DELTA(I),TMTLEA(I)
C
C         STATN  RECORDING STATION NAME
C         DELTA  DISTANCE (DEGREES) BETWEEN EVENT-RECORDING STATION
C
C       5 A BLOCK OF NFA CARDS,EACH CARD CONTAINING
C
C         FA(I),AMTRX(I,J)
C
C         FA     FREQUENCY FOR THE SPECTRAL AMPLITUDES
C         AMTRX  THE SPECTRAL AMPLITUDES
C
C       6 A BLOCK OF NFU CARDS,EACH CARD CONTAINING
C
C         FU(I),UMTRX(I,J)
C
C         FU      FREQUENCY FOR THE GROUP VELOCITIES
C         UMTRX  THE GROUP VELOCITY
C
C
C     THE BLOCK OF CARDS 4,5,6 IS REPEATED FOR EACH STATION,NSTAT BLOCKS
C
C
C     ******************************************************************
C
C     OUTPUT
C     ******
C
C     PRINTOUT
C     ********
C
C
C       1 A SUMMARY OF STATION NAMES,EPICENTRE-STATION SEPERATION
C         AND GEOMETRICAL SPREADING TERM
C       2 THE AMPLITUDE SPECTRUM AND GROUP VELOCITY FOR EACH STATION
C       3 THE AMPLITUDE/DISTANCE TERMS FOR EACH FREQUENCY AND THE
C         BEST LINE FIT
C       4 A SUMMARY OF INVERSE Q,INTERCEPTS OF THE BEST LINE AND 95P.C.
C         CONFIDENCE LIMITS FOR EACH FREQUENCY
C
C
C     PUNCHOUT
C     ********
C
C
C       1 AMPLITUDE/DISTANCE TERMS FOR EACH FREQUENCY (IF REQUIRED)
C       2 INVERSE Q VALUES,INTERCEPTS AND 95P.C. CONFIDENCE LIMITS AT
```

```
C           EACH FREQUENCY
C         3 REGRESSION PARAMETERS FOR EACH A/D LINE E.G. MEAN OF 'X' AND 'Y'
C           VARIANCES AND COVARIANCE.CARDS USED IN PROGRAMS C2L AND CNL
C
C        GRAPHS
C        ******
C
C         1 AMPLITUDE/DISTANCE FOR EACH FREQUENCY (IF REQUIRED)
C         2 INVERSE Q VALUES AND 95P.C. CONFIDENCE LIMITS
C
C
C        ***************************************************************
C        ***************************************************************
C
C
C
      COMMON /GRFF/ TITLE(20), XMAX, XMIN,YMAX, YMIN, INDX, INDY, IND,
     1IDOT, ANSTR1, IF, XLIMIT, YLIMIT, SCALX, SCALY
      DIMENSION AMTRX(40,99),UMTRX(40,99),FA(99),FU(99),TITLEA(40),
     1          DELTA(40),DELTAR(40),GEOMSP(40),DIST(40),STATN(40),
     2          X2(40,99),Y2(40,99),X1(40),Y1(40),
     3          TEMPU(99),CM1(99),QLIM(99),INT(99),INTLIM(99),
     4          XBAR(99),YBAR(99),VARX(99),VARY(99),COVXY(99)
      REAL INT,INTLIM
      REAL*8 TITLE,STATN,TITLEA
      REAL*8 DUMMY,BLANK
      DATA BLANK/8H        /
C
      CALL SCLIBR
C
      PI=4.0*ATAN(1.0)
      DTOR=PI/180.0
      E=6371.0
      DO 990 I=6,20
      TITLE(I)=BLANK
  990 CONTINUE
      CALL DATIM(TITLE(16),DUMMY)
C     -------------------------------------------------------------------
C
C     INPUT DATA
C     ----------
C
  998 READ (5,1,END=999)(TITLE(I),I=6,15)
    1 FORMAT(10A8)
      PRINT 2,(TITLE(I),I=6,16)
    2 FORMAT(1H1,//,10X,10A8,20X,A8,//)
      READ 10,NSTAT,NFA,NFU,T
   10 FORMAT(3I10,F10.5)
      PRINT 15,NSTAT,NFA,NFU,T
   15 FORMAT(10X,'NSTAT =',I5,5X,'NFA =',I5,5X,'NFU =',I5,5X,'T =',F6.3)
C
      READ 20,STATN(1),DELTA(1),TITLEA(1)
   20 FORMAT(A8,F12.5,2X,A8)
      READ 25,(FA(I),AMTRX(1,I),I=1,NFA)
   25 FORMAT(2E15.7)
      READ 25,(FU(I),UMTRX(1,I),I=1,NFU)
C
      DO 30 J=2,NSTAT
      READ 20,STATN(J),DELTA(J),TITLEA(J)
      READ 45,(AMTRX(J,I),I=1,NFA)
      READ 45,(UMTRX(J,I),I=1,NFU)
   45 FORMAT(15X,E15.7)
   30 CONTINUE
C     -------------------------------------------------------------------
C
C     GEOMETRICAL SPREADING CORRECTION (GEOMSP).
C     ------------------------------------------
C
      DO 110 J=1,NSTAT
      DELTAR(J)=DTOR*DELTA(J)
      DIST(J)=DELTAR(J)*E
      GEOMSP(J)=SQRT(E*SIN(DELTAR(J)))
  110 CONTINUE
      PRINT 46
   46 FORMAT(//,10X,'STATION',11X,'DATA NO.',11X,'DELTAD',12X,'DELTAR',
     111X,'DISTANCE(KMS)',10X,'SQRT(E*SIN(DELTAR))',//)
      PRINT 47,(STATN(J),TITLEA(J),DELTA(J),DELTAR(J),DIST(J),GEOMSP(J),
     1J=1,NSTAT)
   47 FORMAT(10X,A8,12X,A8, 9X,F6.2,12X,F6.4,12X,F8.1,12X,F12.2)
C     -------------------------------------------------------------------
C
C     GROUP VELOCITY SET UP IN MATRIX UMTRX S.T. FREQUENCIES
C     ------------------------------------------------------
C     ARE SAME AS FOR AMPLITUDES.
C     ---------------------------
C
      DO 60 J=1,NSTAT
      DO 70 I=1,NFU
      TEMPU(I)=UMTRX(J,I)
   70 CONTINUE
      DO 80 I=2,NFU
      UMTRX(J,2*I-2)=(TEMPU(I)+TEMPU(I-1))/2.0
      UMTRX(J,2*I-1)=TEMPU(I)
   80 CONTINUE
   60 CONTINUE
      DO 65 J=1,NSTAT
      PRINT 66,STATN(J)
   66 FORMAT(1H1,//,10X,A8,/,10X,'--------'/,10X,'1.INDEX 2.FREQUENCY 3.
     1AMPLITUDE 4.GROUP VELOCITY',//)
      PRINT 67,(I,FA(I),AMTRX(J,I),UMTRX(J,I),I=1,NFA)
```

```
   67   FORMAT(3(I6,F8.5,2E13.5))
   65   CONTINUE
C       ------------------------------------------------------------------
C
C       CALCULATE AMPLITUDE/DISTANCE TERMS FOR EACH FREQUENCY
C       --------------------------------------------------------
C
        ELG10=0.43429
        FAC1=PI*ELG10
        DO 90 I=1,NFA
        FAC2=FAC1*FA(I)
        DO 100 J=1,NSTAT
        X2(J,I)=FAC2*DIST(J)/QMTRX(J,I)
  100   CONTINUE
   90   CONTINUE
        DO 120 I=1,NFA
        DO 130 J=1,NSTAT
        Y2(J,I)=ALOG10(AMTRX(J,I))+ALOG10(GEOMSP(J))
        X1(J)=X2(J,I)
        Y1(J)=Y2(J,I)
  130   CONTINUE
        PRINT 125,FA(I)
  125   FORMAT(1H1,/,10X,'AMPLITUDE/DISTANCE PLOT AT FREQUENCY =',F8.5,' (
       1HZ)',//)
        PRINT 126,(J,X1(J),Y1(J),J=1,NSTAT)
  126   FORMAT(3(I5,2E15.7))
        PUNCH 127,FA(I)
  127   FORMAT(F10.7,'HZ    AMPLITUDE/DISTANCE FACTORS')
C       PUNCH 128,(X1(J),Y1(J),J,I,STATN(J),TITLEA(J),J=1,NSTAT)
  128   FORMAT(2E15.7,15X,I5,'A/C',2X,I3,2X,A8,4X,A8)
C       ------------------------------------------------------------------
C
C       INVERSE Q LEAST SQUARES VALUES.
C       --------------------------------
C       'BEST LINE FIT'
C       ---------------
C
        CALL LSTSQR(X1,Y1,NSTAT,QM1(I),INT(I),R,XBAR(I),YBAR(I),QLIM(I),
       1INTLIM(I),SDY1PC,T,VARX(I),VARY(I),COVXY(I))
        QM1(I)=-QM1(I)
        ANSTR1=1.0
        YMAX=6.0
        YMIN=1.0
C       CALL CARGRF(X1,Y1,NSTAT)
C
        CALL TSP(130,48,42)
        CALL C4020H
        PRINT 700
  700   FORMAT('FREQUENCY(HZ) =')
        CALL C4020F(FA(I),7,4)
        CALL ENDFME
  120   CONTINUE
C
C       AMPLITUDE/DISTANCE PLOTS SUMMATION OVER ALL FREQUENCIES.
        DO 140 J=1,NSTAT
        X1(J)=0.0
        Y1(J)=0.0
        DO 150 I=1,NFA
        X1(J)=X1(J)+X2(J,I)
        Y1(J)=Y1(J)+AMTRX(J,I)*AMTRX(J,I)
  150   CONTINUE
        X1(J)=X1(J)/NFA
        ANFA=NFA
        Y1(J)=0.5*ALOG10(Y1(J))+ALOG10(GEOMSP(J)/SQRT(ANFA))
  140   CONTINUE
        PRINT 135
  135   FORMAT(1H1,//,10X,'AMPLITUDE/DISTANCE PLOTS SUMMATION',//)
        PRINT 126,(J,X1(J),Y1(J),J=1,NSTAT)
        PUNCH 136
  136   FORMAT(15X,'AMPLITUDE/DISTANCE PLOTS SUMMATION')
        K=NFA+1
        PUNCH 128,(X1(J),Y1(J),J,K,STATN(J),TITLEA(J),J=1,NSTAT)
        CALL LSTSQR(X1,Y1,NSTAT,QM1(K),INT(K),R,XBAR(K),YBAR(K),QLIM(K),
       1INTLIM(K),SDY1PC,T,VARX(K),VARY(K),COVXY(K))
        QM1(K)=-QM1(K)
        ANSTR1=1.0
        YMAX=6.0
        YMIN=1.0
        CALL CARGRF(X1,Y1,NSTAT)
C
        CALL TSP(130,48,42)
        CALL C4020H
        PRINT 701
  701   FORMAT('AMPLITUDE/DISTANCE PLOTS SUMMATION')
        CALL ENDFME
C       ------------------------------------------------------------------
C
C       SUMMARY OF INVERSE Q VALUES AND CONFIDENCE LIMITS.
C       ------------------------------------------------
C
        PRINT 2,(TITLE(I),I=6,16)
        PRINT 15,NSTAT,NFA,NFL,T
        PRINT 160
  160   FORMAT(/,2('           FREQ.(HZ)     INVERSE Q & LIMITS   INTERCEPT & LI
       1MITS         '),/)
        PRINT 170,(I,FA(I),QM1(I),QLIM(I),INT(I),INTLIM(I),I=1,NFA)
  170   FORMAT(2(I6,F9.5,F13.5,F9.5,F11.4,F8.4,10X))
C       ------------------------------------------------------------------
C
C       PUNCHOUT
C       --------
C
```

```
      PUNCH 1,(TITLE(I),I=6,15)
      PUNCH 10,NFA
      PUNCH 180,(FA(I),CMI(I),CLIM(I),INT(I),INTLIM(I),I,I=1,NFA)
  180 FORMAT(F10.7,5X,4E15.7,15)
      CALL OGRAPH(FA,CMI,CLIM,NFA)
      PUNCH 1,(TITLE(I),I=6,15)
      PUNCH 10,NFA
      PUNCH 190,(FA(I),NSTAT,XBAR(I),YBAR(I),VARX(I),VARY(I),COVXY(I),
     1I,I=1,NFA)
  190 FORMAT(F7.5,I3,5E13.5,I5)
      GO TO 998
  999 CALL FINISH
      RETURN
      END
C
C
C
C
      SUBROUTINE LSTSCR(X,Y,N,A,B,R,XBAR,YBAR,SDATPC,SDBTPC,SDYTPC,T,
     1VARX,VARY,COVXY)
C
C     DETERMINES THE SIMPLE LINEAR REGRESSION LINE - 'THE BEST LINE'
C
C     *****************************************************************
C     *****************************************************************
C     *****************************************************************
C
      DIMENSION X(N),Y(N)
C
      SUMX=0.0
      SUMY=0.0
      SUMXX=0.0
      SUMYY=0.0
      SUMXY=0.0
C
      DO 10 I=1,N
      SUMX=SUMX+X(I)
      SUMY=SUMY+Y(I)
      SUMXX=SUMXX+X(I)*X(I)
      SUMYY=SUMYY+Y(I)*Y(I)
      SUMXY=SUMXY+X(I)*Y(I)
   10 CONTINUE
C
      EN=N
      EN2=EN-2.0
      XBAR=SUMX/EN
      YBAR=SUMY/EN
      VARX=SUMXX/EN-XBAR*XBAR
      VARY=SUMYY/EN-YBAR*YBAR
      COVXY=SUMXY/EN-XBAR*YBAR
      SDX=SQRT(VARX)
      SDY=SQRT(VARY)
C
      A=COVXY/VARX
      B=YBAR-A*XBAR
      R=A*SQRT(VARX/VARY)
C
      RR=R*R
      RSS=EN*VARY*(1.0-RR)
      PARAM=RSS/(EN2*EN*VARX)
C
      SDYTPC=T*SQRT(RSS/EN2)
      SDATPC=T*SQRT(PARAM)
      SDBTPC=T*SQRT((PARAM*SUMXX)/EN)
C
      STUDT=SQRT((RR*EN2)/(1.0-RR))
C     ----------------------------------------------------------------
C
C     PRINTOUT
C     --------
C
      PRINT 20,XBAR,VARX,SDX,YBAR,VARY,SDY,A,SDATPC,B,SDBTPC,
     1R,STUDT,SDYTPC
   20 FORMAT(//8X,'MEAN OF X =',F10.5,16X,'VARIANCE OF X =',F11.5,15X,
     1'STANDARD DEVIATION OF X =',F10.5,//,8X,'MEAN OF Y =',F10.5,16X,
     2'VARIANCE OF Y =',F10.5,16X,'STANDARD DEVIATION OF Y =',F10.5,
     3///,51X,'GRADIENT A =',F13.6,' +OR-',F13.6,///,50X,'INTERCEPT B =',
     4F13.6,' +OR-',F13.6,///,8X,'PRODUCT MOMENT CORRELATION COEFFICIENT
     5 =',F6.2,5X,'STUDENTS T =',F5.2,
     65X,'SCATTER IN CALCULATED Y VALUES =',F10.5)
C
C     ----------------------------------------------------------------
      RETURN
      END
C
C
C
C
      SUBROUTINE OGRAPH(X,Y,Z,N)
C
C     GRAPHS VALUES OF Q,Y(I),CONFIDENCE LIMITS,Z(I),AT FREQUENCIES X(I).
C
C     REQUIRES THE PROGRAM CARGRF TO PRODUCE GRAPHS.
C      SEE AWRE REPORT NO. O-41/68 (J.B.YOUNG & A.DOUGLAS)
C
C
C     *****************************************************************
C     *****************************************************************
C
      COMMON /GRFF/ TITLE(20), XMAX, XMIN,YMAX, YMIN, INDX, INDY, IND,
```

```
     1IDOT, ANSTR1, IF, XLIMIT, YLIMIT, SCALX, SCALY
      DIMENSION X(N),Y(N),Z(N),YLIM(2),XATLIM(2)
      REAL*8 TITLE
      IND=1
      IDOT=0
      ANSTR1=1.0
      IF=3
      XMAX=0.0
      XMIN=0.0
      YMAX=0.0175
      YMIN=0.0
      CALL CARGRF(X,Y,N)
C     NOW OVERGRAPH THE 5P.C. LIMITS.
C     NEW CARGRF PARAMETERS.
      IND=2
      IDOT=32
      ANSTR1=2.0
      DO 190 I=1,N
      YLIM(2)=Y(I)+Z(I)
      YLIM(1)=Y(I)-Z(I)
      XATLIM(2)=X(I)
      XATLIM(1)=X(I)
      CALL CARGRF(XATLIM,YLIM,2)
190   CONTINUE
      RETURN
      END
C
C
C
C
C     NEW CARGRF
C
C
C
C         FROM THE  CALL CARGRF(X,Y,N)  THIS PACKAGE PLOTS N POINTS
C     THE CARTESIAN CO-ORDINATES OF THE ITH POINT BEING SPECIFIED AS
C     X(I),Y(I)
C
C         THE OPTIONS ARE SET BY USING THE COMMON -
C
C     COMMON /GRFF/ TITLE(20), XMAX, XMIN, YMAX, YMIN, INDX, INDY, IND,
C    1IDOT, ANSTR1, IF, XLIMIT, YLIMIT, SCALX, SCALY
C
C         THE TITLE ARRAY CARRIES INFORMATION FOR ANNOTATING THE OUTPUT
C     GRAPH.  THIS ARRAY MUST BE SET UP AS FOLLOWS -
C
C         TITLE(1)  -)
C             .      )CONTAINS 24 HOLLERITH CHARACTERS GIVING THE UNITS
C         TITLE(3)  -)OF THE ABSCISSAE
C
C         TITLE(4)   )CONTAINS 16 HOLLERITH CHARACTERS GIVING THE UNITS
C         TITLE(5)   )OF THE ORDINATE
C
C         TITLE(6)  -)
C             .      )CONTAINS 80 HOLLERITH CHARACTERS GIVING A TITLE TO
C             .      )THE GRAPH
C         TITLE(15) -)
C
C         TITLE(16) -CONTAINS 8 HOLLERITH CHARACTERS GIVING DATE OF
C                    PROCESSING
C         TITLE(17) -CONTAINS 8 HOLLERITH CHARACTERS GIVING TIME OF
C                    PROCESSING
C         TITLE(18) -)
C             .      )UNUSED
C         TITLE(20) -)
C
C         XMAX )SET BOTH EQUAL IF PROGRAM TO CHOOSE THE ABSCISSAE
C         XMIN )SCALE. OTHERWISE SET TO CHOSEN LIMITS OF ABSCISSAE SCALE
C
C         YMAX )SET BOTH EQUAL IF PROGRAM TO CHOOSE THE ORDINATE SCALE
C         YMIN )OTHERWISE SET TO CHOSEN VALUES OF ORDINATE SCALE
C
C     INDX IS AN INDICATOR FOR PLOTTING THE ABSCISSAE ON A LOG SCALE
C       INDX=1 ABSCISSAE ON LINEAR SCALE
C       INDX=2 ABSCISSAE ON LOG SCALE
C
C     INDY IS A SIMILAR INDICATOR FOR THE ORDINATE SCALE
C
C     N.B. CONTENTS OF ARRAYS ARE MODIFIED USING LOG SCALE
C
C     IND IS AN INDICATOR FOR CONTROLLING FRAME CALLS -
C       IND=1 CARGRF CALLS ADVFLM AND PLOTS ON A NEW FRAME
C          =2 CARGRF PLOTS ON THE CURRENT FRAME
C
C     IDOT IS THE SC4020 CODE OF THE REQUIRED PLOTTING SYMBOL
C
C     ANSTR1 INDICATES WHETHER THE PLOTTED POINTS HAVE TO BE JOINED UP
C       ANSTR1=1. POINTS NOT JOINED
C             =2. POINTS JOINED
C
C     IF SPECIFIES TYPE OF OUTPUT
C       IF=1 OUTPUT ON MICROFILM
C         =2 OUTPUT ON HARD COPY
C         =3 OUTPUT ON BOTH MICROFILM AND HARD COPY
C
C     REWRITTEN BY J.B.YOUNG FOR THE IBM 360/75 ON 03/04/72
C
C
      SUBROUTINE CARGRF(X,Y,N)
C
      DIMENSION X(N), Y(N)
C
```

```
      COMMON /GRFF/ TITLE(20), XMAX, XMIN, YMAX, YMIN, INDX, INDY, IND,
     1IDOT, ANSTR1, IF, XLIMIT, YLIMIT, SCALX, SCALY
C
      REAL*8 TITLE,DATE
C
      REAL*4 INSTR1,JOIN/4HJOIN/,BLANK/4H    /
C
      INTEGER*4 PLACEX,PLACEY,XPLOT1,XPLOT2,YPLOT1,YPLOT2,XPOS,YPOS
C
C
      CALL DATIM(DATE,TITLE(17))
      IF(IF)2,2,1
    1 IF(IF-4)3,3,2
    2 IF=3
    3 IF(IND.NE.2)IND=1
      IF(INDX.NE.2)INDX=1
      IF(INDY.NE.2)INDY=1
      IF(IDOT.GT.63)IDOT=48
      INSTR1=JOIN
      IF(ANSTR1.EQ.1.)INSTR1=BLANK
C
      GO TO (30,10),INDX
   10 POSXT=POSMIN(X,N)
      DO 20 I=1,N
      IF(X(I).LT.POSXT)X(I)=POSXT
      X(I)=ALOG10(X(I))
   20 CONTINUE
   30 GO TO (60,40),INDY
   40 POSYT=POSMIN(Y,N)
      DO 50 I=1,N
      IF(Y(I).LT.POSYT)Y(I)=POSYT
      Y(I)=ALOG10(Y(I))
   50 CONTINUE
C
   60 GO TO (100,200),IND
C
C
  100 IF(XMAX-XMIN)110,120,110
  110 XMX=XMAX
      XMN=XMIN
      GO TO 130
  120 CALL AMAX(X,N,XMX)
      CALL AMIN(X,N,XMN)
  130 IF(YMAX-YMIN)140,150,140
  140 YMX=YMAX
      YMN=YMIN
      GO TO 160
  150 CALL AMAX(Y,N,YMX)
      CALL AMIN(Y,N,YMN)
  160 CALL ADVFLM(IF)
C
C
  200 CALL SCALEN(X,XLIMIT,SCALX,PLACEX,XFACTR,N,XMX,XMN)
      CALL SCALEN(Y,YLIMIT,SCALY,PLACEY,YFACTR,N,YMX,YMN)
      XPLOT1=(X(1)-XLIMIT)*SCALX+123.
      YPLOT1=923.-(Y(1)-YLIMIT)*SCALY
      IF(N.NE.2) IDOT=1
      IF(N.GT.63) IDOT=0                                                ***
      CALL PLOT(XPLOT1,IDOT,YPLOT1)                                     ***
      DO 230 I=2,N
      IF(N.NE.2) IDOT=I
      IF(N.GT.63) IDOT=0                                                ***
      XPLOT2=(X(I)-XLIMIT)*SCALX+123.                                   ***
      YPLOT2=923.-(Y(I)-YLIMIT)*SCALY
      CALL PLOT(XPLOT2,IDOT,YPLOT2)
      IF(INSTR1-JOIN)220,210,220
  210 CALL VECTOR(XPLOT1,YPLOT1,XPLOT2,YPLOT2)
  220 YPLOT1=YPLOT2
      XPLOT1=XPLOT2
  230 CONTINUE
C
      GO TO (300,400),IND
C
C
  300 CALL VECTOR(115,923,1003,923)
      CALL VECTOR(123,931,123,43)
      DO 310 I=1,11
      XPOS=203+(I-1)*80
      YPOS=43+(I-1)*80
      CALL VECTOR(XPOS,923,XPOS,931)
      CALL VECTOR(115,YPOS,123,YPOS)
  310 CONTINUE
      DO 370 I=1,3
      XLIM=XLIMIT+FLOAT(I-1)*XFACTR*4.
      GO TO (330,320),INDX
  320 XPOS=92+(I-1)*320
      CALL TSP(XPOS,48,942)
      CALL C4020E(10.**XLIM,11,4)
      GO TO 340
  330 XPOS=20+PLACEX*8+(I-1)*320
      CALL TSP(XPOS,48,942)
      CALL C4020F(XLIM,13,PLACEX)
  340 YPOS=915-(I-1)*320
      YLIM=YLIMIT+FLOAT(I-1)*YFACTR*4.
      GO TO (360,350),INDY
  350 CALL TSP(28,48,YPOS)
      CALL C4020E(10.**YLIM,11,4)
      GO TO 370
  360 CALL TSP(12,48,YPOS)
      CALL C4020F(YLIM,13,PLACEY)
  370 CONTINUE
C
```

```
      IF(TITLE(16).NE.DATE)GO TO 400
      CALL TSP(760,48,958)
      CALL HORAM(TITLE(1),24)
      CALL TSP(48,48,291)
      CALL VERAM(TITLE(4),16)
      CALL TSP(130,48,23)
      CALL HORAM(TITLE(6),80)
C
C
  400 RETURN
      END
      SUBROUTINE SCALEN(X,XLIMIT,SCALX,IPLACE,FACTOR,N,XMAX,XMIN)
C
C     COMPUTES SCALING VALUES FOR CARGRF
C
C
      DIMENSION X(N)
      DOUBLE PRECISION XRG,R,FACT,S
C
      XRG=XMAX-XMIN
      IF(XRG.LT..00000000C1)XRG=1.0D0
C
      R=0.0D0
    1 IF(XRG.LT.(10.0D0**R*.000000001)) GO TO 2
      R=R+1.0D0
      GO TO 1
    2 FACT=(10.0D0**(R-1.0D0)*.000000000125)
      S=0.0D0
    3 IF(XRG.LE.FACT*(2.0D0**S)) GO TO 4
      S=S+1.0D0
      GO TO 3
    4 FACTOR=(FACT*(2.0D0**S))*10.0D-2
C
      XLIMIT=FLOAT(IFIX(XMIN/FACTOR))*FACTOR
      IF(XMIN.LT.XLIMIT)XLIMIT=XLIMIT-FACTOR
      SCALX=80./FACTOR
      IPLACE=12.-R
      IF(IPLACE.LT.1)IPLACE=1
      RETURN
      END
      FUNCTION POSMIN (X,N)
C
C     FINDS MINIMUM POSITIVE VALUE OF ARRAY X
C
C
      DIMENSION X(N)
C
      DO 1 KQ=1,N
      IF(X(KQ).LE.0.0)GO TO 1
      GO TO 5
    1 CONTINUE
      PRINT 6
    6 FORMAT(132H1AN ARRAY FROM WHICH THE SMALLEST POSITIVE VALUE WAS RE
     1QUESTED FOR GRAPHING WAS ALL NEGATIVE  YOUR JOB HAS THEREFORE BEEN
     2 TERMINATED)
      CALL FINISH
      CALL EXIT
    5 KP=KQ
    2 IF(KQ-N)3,4,4
    3 KQ=KQ+1
      IF(X(KQ).LE.0.0)GO TO 2
      IF(X(KP)-X(KQ))2,5,5
    4 POSMIN=X(KP)
      RETURN
      END
      SUBROUTINE AMAX (X,N,XMAX)
C
C     FINDS MAXIMUM VALUE OF ARRAY X
C
C
      DIMENSION X(N)
C
      KQ = 1
    2 KP = KQ
    5 IF(KQ -N)3,4,4
    3 KQ = KQ + 1
      IF(X(KP) - X(KQ))2,5,5
    4 XMAX = X(KP)
      RETURN
      END
      SUBROUTINE AMIN (X,N,XMIN)
C
C     FINDS MINIMUM VALUE OF ARRAY X
C
C
      DIMENSION X(N)
C
      KQ = 1
    5 KP = KQ
    2 IF(KQ-N)3,4,4
    3 KQ = KQ + 1
      IF(X(KP) - X(KQ))2,5,5
    4 XMIN = X(KP)
      RETURN
      END
```

```
C
C
C
C
C     MAIN MULTIPLE COMPARISON OF REGRESSION LINES.
C     ********************************************
C
C
C
C
C     COMPARES RESIDUAL VARIANCES,GRADIENTS & INTERCEPTS FOR REGRESSION LINES
C
C     REFERENCE
C     *********
C
C      K.A.BROWNLEE  'STATISTICAL THEORY & METHODOLOGY' P349-- (WILEY 65)
C
C
C     A TYPICAL REGRESSION LINE IS OF THE FORM
C
C              ' Y = AX + B '
C
C                Y  VARIABLE WITH ERRORS
C                X  INDEPENDENT VARIABLE,NO ERRORS
C                A  GRADIENT
C                B  INTERCEPT
C
C
C     TWO SUCH LINES ARE TO BE COMPARED,EACH LINE HAS N POINTS
C
C
C     PRINTS OUT MATRICES OF COMPARISON WHICH CONTAIN THE NUMBERS 0 , 1 OR 2
C
C       COMPARISON=0   TEST FAILED           BAD COMPARISON
C       COMPARISON=1   TEST PASSED           GOOD COMPARISON
C       COMPARISON=2   TEST NOT CONDUCTED    NO COMPARISON
C
C
C       NFTEST  TEST FOR EQUALITY OF RESIDUAL VARIANCES OF LINES
C       NATEST  TEST FOR EQUALITY OF GRADIENTS OF LINES
C       NBTEST  TEST FOR EQUALITY OF INTERCEPTS OF LINES
C
C
C     ***************************************************************
C
C     INPUT
C     *****
C
C       1 TITLE(I)
C
C         A TITLE FOR THE DATA BEING PROCESSED
C
C       2 FTABL1,FTABL2,TA,TB
C
C         FTABL1 = FTABL2 = F(N-2,N-2)          FISHER'S 'F'
C         TA     = T(2N-4)                      STUDENT'S 'T'
C         TB     = T(2N-3)                      STUDENT'S 'T'
C
C       3 NFA
C
C         THE NUMBER OF REGRESSION LINES (THE NUMBER OF FREQUENCIES)
C
C       4 A BLOCK OF NFA CARDS,EACH CARD CONTAINING
C
C         FREQ(I),N,XBAR(I),YBAR(I),VARX(I),VARY(I),COVXY(I)
C
C         FREQ    FREQUENCY  HZ
C         N       NUMBER OF POINTS FOR LINE,HENCE DEGREES OF FREEDOM
C         XBAR    MEAN OF 'X'
C         YBAR    MEAN OF 'Y'
C         VARX    VARIANCE OF 'X'
C         VARY    VARIANCE OF 'Y'
C         COVXY   COVARIANCE OF 'X' & 'Y'
C
C
C     ***************************************************************
C
C     OUTPUT
C     ******
C
C     PRINTOUT
C     ********
C
C       1 THE INPUT DATA
C       2 THE NFTEST MATRIX-----COMPARISON OF VARIANCE
C       3 THE NATEST MATRIX-----COMPARISON OF GRADIENTS
C       4 THE NBTEST MATRIX-----COMPARISON OF INTERCEPTS
C
C
C     ***************************************************************
C     ***************************************************************
C
C
C
      DIMENSION FREQ(79),XBAR(79),YBAR(79),VARX(79),VARY(79),COVXY(79),
     1          A(79),B(79),VRSS(79),
     2          NFTEST(79,79),NATEST(79,79),NBTEST(79,79),
     3          TITLE(20)
      REAL*8 TITLE,DUMMY
```

```
      CALL DATIM(TITLE(16),DUMMY)
C     ------------------------------------------------------------------
C
C     INPUT DATA
C     ----------
C
  998 READ(5,10,END=999)(TITLE(I),I=6,15)
      PRINT 85,(TITLE(I),I=6,16)
      READ 5,FTABL1,FTABL2,TA,TB
      PRINT5,FTABL1,FTABL2,TA,TB
    5 FORMAT(4F10.5)
   10 FORMAT(10A8)
      READ 20,NFA
      PRINT 20,NFA
   20 FORMAT(1X,I9)
      READ 30,(FREQ(I),N,XBAR(I),YBAR(I),VARX(I),VARY(I),COVXY(I),
     1       I=1,NFA)
      PRINT31,(FREQ(I),N,XBAR(I),YBAR(I),VARX(I),VARY(I),COVXY(I),
     1       I=1,NFA)
   30 FORMAT(F7.5,I3,5E13.5)
   31 FORMAT(1X,F7.5,I3,5E13.5)
C     ------------------------------------------------------------------
C
      DO 50 I=1,NFA
      DO 40 J=1,NFA
      NFTEST(I,J)=2
      NATEST(I,J)=2
      NBTEST(I,J)=2
   40 CONTINUE
   50 CONTINUE
      DO 60 I=1,NFA
      CALL REGR(N,XBAR(I),YBAR(I),VARX(I),VARY(I),COVXY(I),A(I),B(I),
     1     VRSS(I))
   60 CONTINUE
C
      DO 80 I=2,NFA
      K=I-1
      DO 70 J=1,K
      CALL FTEST(VRSS(I),VRSS(J),FTABL1,FTABL2,NFTEST(I,J),NSIZE,F)
      IF(NFTEST(I,J).EQ.1) CALL CLINES(
     1 TA,TB,N,N,XBAR(I),XBAR(J),YBAR(I),YBAR(J),VARX(I),VARX(J),
     2 VARY(I),VARY(J),
     3 COVXY(I),COVXY(J),VRSS(I),VRSS(J),ANEW,VARA,
     4 NATEST(I,J),NBTEST(I,J))
   70 CONTINUE
   80 CONTINUE
      PRINT 85,(TITLE(I),I=6,16)
   85 FORMAT(1H1,/,10X,10A8,20X,A8,/)
      PRINT 90
   90 FORMAT(40X,'FTEST MATRIX',/)
      DO 100 I=1,NFA
      PRINT 110,(NFTEST(I,J),J=1,I)
  100 CONTINUE
  110 FORMAT(10X,79I1)
      PRINT 85,(TITLE(I),I=6,16)
      PRINT 120
  120 FORMAT(40X,'ATEST (GRADIENTS) MATRIX',/)
      DO 130 I=1,NFA
      PRINT 110,(NATEST(I,J),J=1,I)
  130 CONTINUE
      PRINT 85,(TITLE(I),I=6,16)
      PRINT 140
  140 FORMAT(40X,'BTEST (INTERCEPTS) MATRIX',/)
      DO 150 I=1,NFA
      PRINT 110,(NBTEST(I,J),J=1,I)
  150 CONTINUE
C
      GO TO 998
  999 RETURN
      END
C
C
C
C
      SUBROUTINE REGR(N,XBAR,YBAR,VARX,VARY,COVXY,A,B,VRSS)
C
C     FOR THE REGRESSION LINE 'Y = AX + B' THIS CALCULATES
C
C                A        THE GRADIENT
C                B        THE INTERCEPT
C                VRSS     THE VARIANCE OF THE RESIDUAL SUM OF SQUARES
C
C     GIVEN----
C
C                N        THE NUMBER OF LINE POINTS
C                XBAR     MEAN OF 'X'
C                YBAR     MEAN OF 'Y'
C                VARX     VARIANCE OF 'X'
C                VARY     VARIANCE OF 'Y'
C                COVXY    COVARIANCE OF 'X' & 'Y'
C
C
C     ******************************************************************
C     ******************************************************************
C
C
      A=COVXY/VARX
      B=YBAR-A*XBAR
      EN=N
      EN2=EN-2.0
      RSS=EN*VARY-EN*A*COVXY
      VRSS=RSS/EN2
```

```
      RETURN
      END
C
C
C
C
      SUBROUTINE FTEST(V1,V2,FTABL1,FTABL2,NFTEST,NSIZE,F)
C
C     EQUALITY OF VARIANCES
C     *********************
C
C     THIS SUBROUTINE PERFORMS FISHER'S 'F' TEST ON THE VARIANCES V1 & V2
C     SETS NFTEST TO 0 IF TEST FAILED,TO 1 IF TEST PASSED
C
C
C     ****************************************************************
C     ****************************************************************
C
C
      IF(V1.GT.V2) GO TO 1
      F=V2/V1
      NSIZE=2
      FTABL1=FTABL2
      GO TO 2
    1 F=V1/V2
      NSIZE=1
    2 IF(F.LT.FTABL1) GO TO 3
      NFTEST=0
      GO TO 4
    3 NFTEST=1
    4 RETURN
      END
C
C
C
C
      SUBROUTINE CLINES(TA,TB,N1,N2,XBAR1,XBAR2,YBAR1,YBAR2,VARX1,VARX2,
     1VARY1,VARY2,COVXY1,COVXY2,VRSS1,VRSS2,A,VARA,NATEST,NBTEST)
C
C
C
C     COMPARES TWO REGRESSION LINES
C     *****************************
C
C     FIRST THE PROGRAM COMPARES THE GRADIENTS OF TWO LINES.IF THESE
C     ARE STATISTICALLY THE SAME IT THEN COMPARES THE INTERCEPTS
C
C     IT ASSIGNS THE VALUES 0 , 1 OR 2 TO NATEST(COMPARE GRADIENTS) AND
C     TO NBTEST(COMPARE INTERCEPTS)
C        COMPARISON=0   TEST FAILED          BAD COMPARISON
C        COMPARISON=1   TEST PASSED          GOOD COMPARISON
C        COMPARISON=2   TEST NOT CONDUCTED   NO COMPARISON
C
C
C     ****************************************************************
C     ****************************************************************
C
C
      NATEST=0
      NBTEST=2
      EN1=N1
      EN12=EN1-2.0
      EN2=N2
      EN22=EN2-2.0
      SQXX1=EN1*VARX1
      SQXX2=EN2*VARX2
      SQYY1=EN1*VARY1
      SQYY2=EN2*VARY2
      SQXY1=EN1*COVXY1
      SQXY2=EN2*COVXY2
C
      VRSS=(EN12*VRSS1+EN22*VRSS2)/(EN12+EN22)
      S=SQRT(VRSS)
      ATEST=(A1-A2)/(S*((1.0/SQXX1)+(1.0/SQXX2)))
      ATEST=ABS(ATEST)
      IF(ATEST.LT.TA) NATEST=1
      IF(NATEST.EQ.0) RETURN
      NBTEST=0
      SQXY=SQXY1+SQXY2
      SQXX=SQXX1+SQXX2
      A=SQXY/SQXX
      RSS=(EN12+EN22)*VRSS
      VARA=RSS/((EN1+EN2-3.0)*SQXX)
C
      S=SQRT(VARA*SQXX)
      DIF=XBAR1-XBAR2
      BTEST=(YBAR1-YBAR2-A*DIF)/(S*SQRT((1.0/EN1)+(1.0/EN2)+((DIF*DIF)
     1      /SQXX)))
      BTEST=ABS(BTEST)
      IF(BTEST.LT.TB) NBTEST=1
      RETURN
      END
```

C2L

```
C
C
C
C
C     MAIN COMPARISON OF PAIRED REGRESSION VALUES FOR NFA PAIRED LINES.
C     ******************************************************************
C
C
C
C
C     COMPARES RESIDUAL VARIANCES,GRADIENTS & INTERCEPTS FOR REGRESSION LINES
C
C     REFERENCE
C     *********
C
C      K.A.BROWNLEE  'STATISTICAL THEORY & METHODOLOGY' P349-- (WILEY 65)
C
C
C     A TYPICAL REGRESSION LINE IS OF THE FORM
C
C              ' Y = AX + B '
C
C                Y  VARIABLE WITH ERRORS
C                X  INDEPENDENT VARIABLE,NO ERRORS
C                A  GRADIENT
C                B  INTERCEPT
C
C
C     TWO SUCH LINES ARE TO BE COMPARED,THE LINES HAVE N1 AND N2 POINTS
C
C
C     PRINTS OUT RESULTS OF COMPARISON WHICH ARE THE NUMBERS 0 , 1 OR 2
C
C       COMPARISON=0   TEST FAILED          BAD COMPARISON
C       COMPAPISON=1   TEST PASSED          GOOD COMPARISON
C       COMPARISON=2   TEST NOT CONDUCTED   NO COMPARISON
C
C
C       NFTEST  TEST FOR EQUALITY OF RESIDUAL VARIANCES OF LINES
C       NATEST  TEST FOR EQUALITY OF GRADIENTS OF LINES
C       NBTEST  TEST FOR EQUALITY OF INTERCEPTS OF LINES
C
C
C     ******************************************************************
C
C     INPUT
C     *****
C
C       1 TITLE(I)
C
C         A TITLE FOR THE REGRESSION DATA
C
C       2 NFA
C
C         THE NUMBER OF PAIRS OF LINES TO BE COMPARED
C
C       3 A BLOCK OF NFA CARDS,EACH CARD CONTAINING
C
C         FREQ(J),N(I),XBAR(I,J),YBAR(I,J),VARX(I,J),VARY(I,J),COVXY(I,J)
C
C         FREQ    FREQUENCY  HZ
C         N       NUMBER OF POINTS FOR LINE,HENCE DEGREES OF FREEDOM
C         XBAR    MEAN OF 'X'
C         YBAR    MEAN OF 'Y'
C         VARX    VARIANCE OF 'X'
C         VARY    VARIANCE OF 'Y'
C         COVXY   COVARIANCE OF 'X' & 'Y'
C
C
C     THE CARDS 1--3 ARE REPEATED FOR THE SECOND BLOCK OF DATA TO FORM
C     NFA PAIRS OF LINES
C
C
C       4 FTABL1,FTABL2,TA,TB
C
C         FTABL1 = F(N1-2,N2-2)            FISHER'S 'F'
C         FTABL2 = F(N2-2,N1-2)            FISHER'S 'F'
C         TA     = T(N1+N2-4)              STUDENT'S 'T'
C         TB     = T(N1+N2-3)              STUDENT'S 'T'
C
C
C     ******************************************************************
C
C     OUTPUT
C     ******
C
C     PRINTOUT
C     ********
C
C       1 THE INPUT DATA
C       2 A TABLE OF FREQUENCY VALUES,GRADIENT LINE 1,GRADIENT LINE 2,
C         RESULTS OF FTEST,ATEST AND BTEST AND THE NEW RESULTANT GRADIENT
C         (IF FORMED) AND CONFIDENCE LIMITS ON IT
C
C
C
C     ******************************************************************
C     ******************************************************************
C
```

```
C
C
      DIMENSION FREQ(79),
     1          N(2),XBAR(2,79),YBAR(2,79),VARX(2,79),VARY(2,79),
     2          COVXY(2,79),A(2,79),B(2,79),VRSS(2,79),
     3          ANEW(79),VANEW(79),CONLIM(79),
     4          NFTEST(79),NATEST(79),NBTEST(79),
     5          TITLE(2,20)
      REAL*8 TITLE,DUMMY
  998 DO 40 I=1,2
      CALL DATIM(TITLE(I,16),DUMMY)
C     ------------------------------------------------------------------
C
C     INPUT DATA
C     ----------
C
      READ (5,10,END=999)(TITLE(I,J),J=6,15)
      PRINT 65,(TITLE(I,J),J=6,16)
   10 FORMAT(10A8)
      READ 20,NFA
      PRINT 20,NFA
   20 FORMAT(1X,I9)
      READ 30,(FREQ(J),N(I),XBAR(I,J),YBAR(I,J),VARX(I,J),VARY(I,J),
     1COVXY(I,J),J=1,NFA)
      PRINT31,(FREQ(J),N(I),XBAR(I,J),YBAR(I,J),VARX(I,J),VARY(I,J),
     1COVXY(I,J),J=1,NFA)
   30 FORMAT(F7.5,I3,5E13.5)
   31 FORMAT(1X,F7.5,I3,5E13.5)
   40 CONTINUE
      READ 50,FTABL1,FTABL2,TA,TB
      PRINT 50,FTABL1,FTABL2,TA,TB
   50 FORMAT(4F10.5)
C     ------------------------------------------------------------------
C
      DO 60 J=1,NFA
      NFTEST(J)=2
      NATEST(J)=2
      NBTEST(J)=2
      ANEW(J)=0.0
      VANEW(J)=0.0
      CONLIM(J)=0.0
   60 CONTINUE
      PRINT 65,(TITLE(1,I),I=6,16)
      PRINT 66,(TITLE(2,I),I=6,16)
   65 FORMAT(1H1,/,10X,10A8,20X,A8)
   66 FORMAT(10X,10A8,20X,A8,//)
      PRINT 67
   67 FORMAT(25X,'FREQUENCY        A1           A2        NFTEST    NATEST     NB
     1TEST  NEW GRADIENT & LIMITS',/)
      DO 90 J=1,NFA
      DO 70 I=1,2
      CALL REGR(N(I),XBAR(I,J),YBAR(I,J),VARX(I,J),VARY(I,J),COVXY(I,J),
     1A(I,J),B(I,J),VRSS(I,J))
   70 CONTINUE
      CALL FTEST(VRSS(1,J),VRSS(2,J),FTABL1,FTABL2,NFTEST(J),NSIZE,F)
      IF(NFTEST(J).EQ.1) CALL CLINES
     1(TA,TB,N(1),N(2),XBAR(1,J),XBAR(2,J),YBAR(1,J),YBAR(2,J),
     2VARX(1,J),VARX(2,J),VARY(1,J),VARY(2,J),COVXY(1,J),COVXY(2,J),
     3VRSS(1,J),VRSS(2,J),ANEW(J),VANEW(J),
     4NATEST(J),NBTEST(J))
      IF(NFTEST(J).EQ.1) CONLIM(J)=TB*SQRT(VANEW(J))
      PRINT 80,J,FREQ(J),A(1,J),A(2,J),NFTEST(J),NATEST(J),NBTEST(J),
     1ANEW(J),CONLIM(J)
   80 FORMAT(10X,I10,3X,3F10.6,I7,2I10,5X,2F10.6)
   90 CONTINUE
      GO TO 998
  999 RETURN
      END
C
C
C
C
      SUBROUTINE REGR(N,XBAR,YBAR,VARX,VARY,COVXY,A,B,VRSS)
C
C     FOR THE REGRESSION LINE 'Y = AX + B' THIS CALCULATES
C
C               A       THE GRADIENT
C               B       THE INTERCEPT
C               VRSS    THE VARIANCE OF THE RESIDUAL SUM OF SQUARES
C
C     GIVEN----
C
C               N       THE NUMBER OF LINE POINTS
C               XBAR    MEAN OF 'X'
C               YBAR    MEAN OF 'Y'
C               VARX    VARIANCE OF 'X'
C               VARY    VARIANCE OF 'Y'
C               COVXY   COVARIANCE OF 'X' & 'Y'
C
C
C     ******************************************************************
C     ******************************************************************
C
C
      A=COVXY/VARX
      B=YBAR-A*XBAR
      EN=N
      EN2=EN-2.0
      RSS=EN*VARY-EN*A*COVXY
      VRSS=RSS/EN2
      RETURN
      END
```

```
C
C
C
C
      SUBROUTINE FTEST(V1,V2,FTABL1,FTABL2,NFTEST,NSIZE,F)
C
C     EQUALITY OF VARIANCES
C     *********************
C
C     THIS SUBROUTINE PERFORMS FISHER'S 'F' TEST ON THE VARIANCES V1 & V2
C     SETS NFTEST TO 0 IF TEST FAILED,TO 1 IF TEST PASSED
C
C
C     *****************************************************************
C     *****************************************************************
C
C
      IF(V1.GT.V2) GO TO 1
      F=V2/V1
      NSIZE=2
      FTABL1=FTABL2
      GO TO 2
    1 F=V1/V2
      NSIZE=1
    2 IF(F.LT.FTABL1) GO TO 3
      NFTEST=0
      GO TO 4
    3 NFTEST=1
    4 RETURN
      END
C
C
C
C
      SUBROUTINE CLINES(TA,TB,N1,N2,XBAR1,XBAR2,YBAR1,YBAR2,VARX1,VARX2,
     1VARY1,VARY2,COVXY1,COVXY2,VRSS1,VRSS2,A,VARA,NATEST,NBTEST)
C
C
C     COMPARES TWO REGRESSION LINES
C     *****************************
C
C     FIRST THE PROGRAM COMPARES THE GRADIENTS OF TWO LINES.IF THESE
C     ARE STATISTICALLY THE SAME IT THEN COMPARES THE INTERCEPTS
C
C     IT ASSIGNS THE VALUES 0 , 1 OR 2 TO NATEST(COMPARE GRADIENTS) AND
C     TO NBTEST(COMPARE INTERCEPTS)
C         COMPARISON=0   TEST FAILED          BAD COMPARISON
C         COMPARISON=1   TEST PASSED          GOOD COMPARISON
C         COMPARISON=2   TEST NOT CONDUCTED   NO COMPARISON
C
C
C     *****************************************************************
C     *****************************************************************
C
C
      NATEST=0
      NBTEST=2
      EN1=N1
      EN12=EN1-2.0
      EN2=N2
      EN22=EN2-2.0
      SQXX1=EN1*VARX1
      SQXX2=EN2*VARX2
      SQYY1=EN1*VARY1
      SQYY2=EN2*VARY2
      SQXY1=EN1*COVXY1
      SQXY2=EN2*COVXY2
C
      VRSS=(EN12*VRSS1+EN22*VRSS2)/(EN12+EN22)
      S=SQRT(VRSS)
      ATEST=(A1-A2)/(S*((1.0/SQXX1)+(1.0/SQXX2)))
      ATEST=ABS(ATEST)
      IF(ATEST.LT.TA) NATEST=1
      IF(NATEST.EQ.0) RETURN
      NBTEST=0
      SQXY=SQXY1+SQXY2
      SQXX=SQXX1+SQXX2
      A=SQXY/SQXX
      RSS=(EN12+EN22)*VRSS
      VARA=RSS/((EN1+EN2-3.0)*SQXX)
C
      S=SQRT(VARA*SQXX)
      DIF=XBAR1-XBAR2
      BTEST=(YBAR1-YBAR2-A*DIF)/(S*SQRT((1.0/EN1)+(1.0/EN2)+((DIF*DIF)
     1       /SQXX)))
      BTEST=ABS(BTEST)
      IF(BTEST.LT.TB) NBTEST=1
      RETURN
      END
```

QBAR

```
C
C
C
C
C     AVERAGE GRADIENTS FOR A SET OF REGRESSION LINES------AVERAGE QI
C     ***************************************************************
C
C
C
C
C     QI IS THE SPECIFIC ATTENUATION FACTOR FOR RAYLEIGH WAVES
C
C
C     THIS PROGRAM CALCULATES THE AVERAGE GRADIENT FOR SEVERAL SETS OF
C     REGRESSION LINES
C
C
C     FOR NDATA BLOCKS OF DATA (EVENTS),EACH BLOCK CONTAINING NFA
C     REGRESSION LINE PARAMETERS (FROM AMPLITUDE-DISTANCE PLOTS AT NFA
C     FREQUENCIES) THE PROGRAM CALCULATES NFA AVERAGE GRADIENTS (AVERAGE
C     INVERSE Q VALUES,QI,AT NFA FREQUENCIES) CONFIDENCE LIMITS ON THE
C     AVERAGES ARE ALSO OBTAINED.
C
C
C     NOTE
C     ****
C
C     THIS PROGRAM REQUIRES THE SUBROUTINE-----
C
C     SUBROUTINE REGR(N,XBAR,YBAR,VARX,VARY,COVXY,A,B,VRSS)
C
C
C     ******************************************************************
C
C     INPUT
C     *****
C
C       1 NDATA
C         THE NUMBER OF BLOCKS OF DATA(EVENTS)TO BE AVERAGED
C
C       2 TA
C
C         STUDENT'S 'T' TO DETERMINE CONFIDENCE LIMITS ON THE AVERAGE QI
C         THE DEGREES OF FREEDOM ARE-----THE SUM OF THE NUMBER OF POINTS
C         FOR EACH LINE,MINUS THE NUMBER OF EVENTS,MINUS ONE
C
C       3 TITLE(I,J)
C
C         A TITLE FOR ONE BLOCK OF REGRESSION DATA (FOR ONE EVENT)
C
C       4 NFA
C
C         THE NUMBER OF REGRESSION LINES PER EVENT (FOR FREQUENCIES F)
C         NFA MUST BE THE SAME FOR EACH EVENT
C
C       5 A BLOCK OF NFA CARDS,EACH CARD CONTAINING
C
C         F(J),N(I),XBAR(I,J),YBAR(I,J),VARX(I,J),VARY(I,J),COVXY(I,J)
C
C         F       FREQUENCY  HZ
C         N       NUMBER OF POINTS FOR LINE,HENCE DEGREES OF FREEDOM
C         XBAR    MEAN OF 'X'
C         YBAR    MEAN OF 'Y'
C         VARX    VARIANCE OF 'X'
C         VARY    VARIANCE OF 'Y'
C         COVXY   COVARIANCE OF 'X' & 'Y'
C
C
C     THE CARDS 3--5 ARE REPEATED FOR EACH OF THE NDATA BLOCKS (EVENTS)
C     TO FORM NFA AVERAGES
C
C
C     ******************************************************************
C
C     OUTPUT
C     ******
C
C     PRINTOUT
C     ********
C
C       1 THE INPUT DATA
C       2 A TABLE OF FREQUENCY,AVERAGE QI AND CONFIDENCE LIMITS
C
C
C     PUNCHOUT
C     ********
C
C       1 THE AVERAGE VALUES OF QI AND CONFIDENCE LIMITS AT FREQUENCIES
C         F ARE PUNCHED OUT
C
C
C
C     ******************************************************************
C     ******************************************************************
C
C
C
      DIMENSION F(80),
     1N(9),XBAR(9,80),YBAR(9,80),VARX(9,80),VARY(9,80),
```

```
     2COVXY(9,80),A(9,80),VRSS(9,80),
     3ANEW(80),VANEW(80),CONLIM(80),
     4TITLE(9,20),QRM1(80),
     5EN(9),ENM2(9),SQXX(9),SQYY(9),SCXY(9)
      REAL*8 TITLE,DUMMY
C     ------------------------------------------------------------------
C
C     INPUT DATA
C     ----------
C
998   READ (5,10,END=999) NDATA
10    FORMAT(1X,I9)
      PRINT11,NDATA
11    FORMAT(1H1,1X,I9)
      READ 30,TA
      PRINT31,TA
      DO 40 I=1,NDATA
      CALL DATIM(TITLE(I,16),DUMMY)
      READ 20,(TITLE(I,J),J=6,15)
      PRINT 25,(TITLE(I,J),J=6,16)
20    FORMAT(10A8)
25    FORMAT(1H1,10X,10A8,20X,A8)
      READ 10,NFA
      PRINT10,NFA
      READ 30,(F(J),N(I),XBAR(I,J),YBAR(I,J),VARX(I,J),VARY(I,J),
     1COVXY(I,J),J=1,NFA)
      PRINT31,(F(J),N(I),XBAR(I,J),YBAR(I,J),VARX(I,J),VARY(I,J),
     1COVXY(I,J),J=1,NFA)
30    FORMAT(    F7.5,I3,5E13.5)
31    FORMAT(1X,F7.5,I3,5E13.5)
40    CONTINUE
C     ------------------------------------------------------------------
C
C
      DO 70 J=1,NFA
      SQXXNU=0.0
      SQYYNU=0.0
      SQXYNU=0.0
      DENOM =0.0
      RSS   =0.0
      DO 60 I=1,NDATA
      CALL REGR(N(I),XBAR(I,J),YBAR(I,J),VARX(I,J),VARY(I,J),CCVXY(I,J),
     1        A(I,J),B,VRSS(I,J))
      EN(I)=N(I)
      ENM2(I)=EN(I)-2.0
      SQXXNU=EN(I)*VARX(I,J)+SQXXNU
      SQXYNU=EN(I)*COVXY(I,J)+SQXYNU
      RSS=ENM2(I)*VRSS(I,J)+RSS
      DENOM=ENM2(I)+DENOM
60    CONTINUE
      ANEW(J)=SQXYNU/SQXXNU
      QRM1(J)=-ANEW(J)
      VANEW(J)=RSS/((DENOM+NDATA-1.0)*SQXXNU)
      CONLIM(J)=TA*SQRT(VANEW(J))
70    CONTINUE
C
C
C     ------------------------------------------------------------------
C     OUTPUT
C     ------
C
C     PRINTOUT
C     --------
C
      DO 80 I=1,NCATA
      IF(I    .EQ.1) PRINT 25,(TITLE(1,J),J=6,16)
      IF(I    .NE.1) PRINT 26,(TITLE(I,J),J=6,16)
26    FORMAT(1X,10X,10A8,20X,A8)
80    CONTINUE
      PRINT 85
85    FORMAT(/,2(26X,'FREQ.(HZ)   INVERSE Q & LIMITS',10X),/)
      PRINT 90,(I,F(I),QRM1(I),CONLIM(I),I=1,NFA)
90    FORMAT(2(20X,I5,F9.5,F11.6,F10.6,10X))
C
C     PUNCHOUT
C     --------
C
      DO 92 I=1,NDATA
92    PUNCH 20,(TITLE(I,J),J=6,15)
      PUNCH 95,(F(I),QRM1(I),CONLIM(I),I,I=1,NFA)
95    FORMAT(F10.7,5X,2E15.7,30X,I5)
C     ------------------------------------------------------------------
C
      GO TO 998
999   RETURN
      END
```

```
C
C
C
C
C     QRALEY MAIN
C     ***********
C
C
C      THIS PROGRAM MAKES THEORETICAL CALCULATIONS OF THE ATTENUATION
C     COEFFICIENT,GAMMA,AND THE SPECIFIC ATTENUATION FACTOR,QI,FOR
C     RAYLEIGH WAVES AT NPERPT FREQUENCIES.AN ATTENUATION MODEL WITH NOL
C     LAYERS IS REQUIRED.
C
C
C     THE PROGRAM USES THE EQUATIONS
C
C         GAMMA =      SUM      (0.5*DKBYDA*A*QAI + 0.5*DKBYDB*B*QBI)
C                  OVER LAYERS
C
C             QI  =  (-U*GAMMA)/(PI*FREQ)
C
C
C      GAMMA   THE ATTENUATION COEFFICIENT
C      A       THE VELOCITY OF COMPRESSIONAL BODILY WAVES
C      QAI     THE SPECIFIC ATTENUATION FACTOR FOR COMPRESSIONAL WAVES
C      DKBYDA  THE PARTIAL DERIVATIVES OF THE WAVENUMBER,K, W.R.T. THE
C              COMPRESSIONAL VELOCITY,A
C      B       THE VELOCITY OF SHEAR BODILY WAVES
C      QBI     THE SPECIFIC ATTENUATION FACTOR FOR SHEAR WAVES
C      DKBYDB  THE PARTIAL DERIVATIVES OF THE WAVENUMBER,K, W.R.T. THE
C              SHEAR VELOCITY,B
C
C      QI      THE SPECIFIC ATTENUATION FACTOR FOR RAYLEIGH WAVES
C      U       THE GROUP VELOCITY
C      FREQ    FREQUENCY  HZ
C
C
C     ****************************************************************
C
C     INPUT
C     *****
C
C     THE FOLLOWING CARDS ARE READ IN
C
C       1 AN SC4060 CARD TO PRODUCE GRAPHS
C
C       2 TITLE(I)
C
C         A TITLE FOR THE MODEL UNDER CONSIDERATION
C
C       3 GRAPH1(I)
C
C         A TITLE FOR THE GRAPH OF GAMMA AS A FUNCTION OF FREQUENCY
C
C       4 GRAPH2(I)
C
C         A TITLE FOR THE GRAPH OF QI AS A FUNCTION OF FREQUENCY
C
C       5 NOL,NPERPT
C
C         NOL     THE NUMBER OF LAYERS IN THE MODEL
C         NPERPT  THE NUMBER OF FREQUENCIES TO BE USED
C
C       6 A BLOCK OF NOL CARDS,EACH CARD CONTAINING
C
C         QAI(I),QBI(I)
C
C         QAI      THE SPECIFIC ATTENUATION FACTOR FOR COMPRESSIONAL
C                  WAVES IN EACH LAYER
C         QBI      THE SPECIFIC ATTENUATION FACTOR FOR SHEAR WAVES IN
C                  EACH LAYER
C
C       7 A BLOCK OF NOL CARDS,EACH CARD CONTAINING
C
C         A(I),B(I)
C
C         A        COMPRESSIONAL BODILY WAVE VELOCITY FOR EACH LAYER
C         B        SHEAR BODILY WAVE VELOCITY FOR EACH LAYER
C
C       8 A BLOCK OF NPERPT CARDS,EACH CARD CONTAINING
C
C         FREQ(I),U(I)
C
C         FREQ     FREQUENCY  HZ
C         U        GROUP VELOCITY
C
C       9 A BLOCK OF NPERPT CARDS,EACH CARD CONTAINING NOL VALUES
C
C         DKBYDA(I,J)
C
C         DKBYDA PARTIAL DERIVATIVES OF THE WAVENUMBER,K, W.R.T. A FOR
C                EACH LAYER AND AT EACH FREQUENCY
C
C      10 A BLOCK OF NPERPT CARDS,EACH CARD CONTAINING NOL VALUES
C
C         DKBYDB(I,J)
C
C         DKBYDB PARTIAL DERIVATIVES OF THE WAVENUMBER,K, W.R.T. B FOR
C                EACH LAYER AND AT EACH FREQUENCY
C
```

```
C
C
C      NOTE THAT THE ABOVE CARDS 2 TO 10 MAY BE REPEATED FOR ANY
C      NUMBER OF MODELS
C
C
C      ****************************************************************
C
C      OUTPUT
C      ******
C
C      PRINTOUT
C      ********
C
C        1 THE ORIGINAL MODEL OF A,B,QAI,QBI
C        2 THE GROUP VELOCITY CURVE
C        3 A TABLE OF THE PARTIAL DERIVATIVES W.R.T. A
C        4 A TABLE OF THE PARTIAL DERIVATIVES W.R.T. B
C        5 A SUMMARY TABLE OF GAMMA AS A FUNCTION OF FREQUENCY
C        6 A SUMMARY TABLE OF QI AS A FUNCTION OF FREQUENCY
C
C
C      PUNCHOUT
C      ********
C
C        1 THE VALUES OF QI AND FREQUENCY ARE PUNCHED OUT
C
C
C      GRAPHS
C      ******
C
C        1 THE GROUP VELOCITY CURVE
C        2 THE ATTENUATION COEFFICIENT AS A FUNCTION OF FREQUENCY
C        3 THE SPECIFIC ATTENUATION FACTOR AS A FUNCTION OF FREQUENCY
C        4 THE DERIVATIVES FOR EACH LAYER AS A FUNCTION OF FREQUENCY
C          (IF REQUIRED)
C
C
C
C
C
C      ****************************************************************
C      ****************************************************************
C
C
      DIMENSION U(90),PERIOD(90),GAMMA(90),QI(90),FREQ(90)
      DIMENSION TITLE(20),GRAPH1(20),GRAPH2(20)
      DIMENSION DERIVA(90),DERIVB(90)
      COMMON /LAYER/A(20),B(20),QAI(20),QBI(20),DKBYDA(90,10),
     1              DKBYDB(90,10),NOL
      REAL*8 TITLE,GRAPH1,GRAPH2,DUMMY
      CALL SCLIBR
      NGRAPH=2
  100 READ(5,1,END=999)(TITLE(I),I=6,15)
      READ 1,(GRAPH1(I),I=6,15)
      READ 1,(GRAPH2(I),I=6,15)
    1 FORMAT(10A8)
      CALL DATIM(TITLE(16),DUMMY)
      CALL DATIM(GRAPH1(16),DUMMY)
      CALL DATIM(GRAPH2(16),DUMMY)
      PRINT 2,(TITLE(I),I=6,16)
    2 FORMAT(1H1,///,20X,10A8,20X,A8)
C     ----------------------------------------------------------------
C
C     INPUT DATA
C     ----------
C
      READ 3,NOL,NPERPT
    3 FORMAT(2I10)
      PRINT 4,NOL,NPERPT
    4 FORMAT(///30X,'NLAYERS = ',I5,10X,'NPERPT = ',I5)
      READ 5,(QAI(I),QBI(I),I=1,NOL)
      READ 5,(A(I),B(I),I=1,NOL)
    5 FORMAT(2F10.5)
      READ 6,(FREQ(I),U(I),I=1,NPERPT)
    6 FORMAT(2F10.6)
      DO 7 I=1,NPERPT
      READ 9,(DKBYDA(I,J),J=1,NOL)
    7 CONTINUE
      DO 8 I=1,NPERPT
      READ 9,(DKBYDB(I,J),J=1,NOL)
    8 CONTINUE
    9 FORMAT(6F12.9)
C     ----------------------------------------------------------------
C
C     CONDITION
C     ---------
C
      QBI(1)=2.29*QAI(1)
      QBI(2)=2.29*QAI(2)
      QBI(3)=2.51*QAI(3)
      QBI(4)=2.51*QAI(4)
      QBI(5)=2.51*QAI(5)
      QBI(6)=2.19*QAI(6)
C     ----------------------------------------------------------------
C
C     CALCULATION OF GAMMA FOR A PARTICULAR PERIOD.
C     ---------------------------------------------
C
      DO 10 I=1,NPERPT
      GAMMAT=0.0
      CALL ATTEN(GAMMAT,I)
      GAMMA(I)=GAMMAT
```

```
   10   CONTINUE
C       ----------------------------------------------------------------------
C
C       PRINT OUT ORIGINAL MODEL.
C       ------------------------
C
        PRINT 2,(TITLE(I),I=6,16)
        PRINT 4,NOL,NFERPT
        PRINT 148
        PRINT 149,(J,A(J),B(J),QAI(J),QBI(J),J=1,NOL)
  148   FORMAT(//,10X,'NLAYER',8X,'A',14X,'B',13X,'QAI',12X,'QBI',/)
  149   FORMAT(8X,I5,4F15.5)
C
        PRINT 11
   11   FORMAT(1H1,//,10X,'FREQUENCY & GROUP VELOCITY',/,
     1                10X,'--------------------------',//)
        PRINT 12,(I,FREQ(I),U(I),I=1,NPERPT)
   12   FORMAT(10X,I2,2X,F8.6,2X,F9.6)
        PRINT 145
  145   FORMAT(1H1,//,10X,'DERIVATIVES W.R.T. ALPHA (DK/DALPHA)',/,
     1                10X,'------------------------------------',//)
        DO 13 I=1,NPERPT
   13   PRINT 147,(I,(DKBYDA(I,J),J=1,NOL))
        PRINT 146
  146   FORMAT(1H1,//,10X,'DERIVATIVES W.R.T. BETA (DK/DBETA)',/,
     1                10X,'----------------------------------',//)
        DO 14 I=1,NPERPT
   14   PRINT 147,(I,(DKBYDB(I,J),J=1,NOL))
  147   FORMAT(10X,I2,3X,6F14.9)
        CALL GRAPH(FREQ,U,NPERPT,TITLE,0)
C       ----------------------------------------------------------------------
C
C       GRAPH GAMMA(I) V FREQ(I)
C       ------------------------
C
        PRINT 15
   15   FORMAT(1H1,//,30X,'SUMMARY TABLE OF GAMMA(I)/FREQ(I)',/
     1                30X,'---------------------------------',//
     2                28X,'CALC.NO.     FREQ          GAMMA',/)
        PRINT 16,(I,FREQ(I),GAMMA(I),I=1,NPERPT)
   16   FORMAT(28X,I5,5X,F10.5,2X,F10.5)
C
        CALL GRAPH(FREQ,GAMMA,NPERPT,GRAPH1,1)
C       ----------------------------------------------------------------------
C
C       CALCULATION OF QI FOR RAYLEIGH WAVES OF A PARTICULAR FREQUENCY.
C       ---------------------------------------------------------------
C       GRAPH RAYLEIGH QI(I) V FREQ(I)
C       ------------------------------
C
        PRINT 17
   17   FORMAT(1H1,//,30X,'TABLE OF RAYLEIGH QI(I)/FREQ(I)',/
     1                30X,'-------------------------------',//
     2                28X,'CALC.NO.     FREQ          RAYLEIGH QI(I)',/)
        PI=4.0*ATAN(1.0)
        DO 18 I=1,NPERPT
        QI(I)=(-1.0*U(I)*GAMMA(I))/(PI*FREQ(I))
   18   CONTINUE
        PRINT 19,(I,FREQ(I),QI(I),I=1,NPERPT)
C       ----------------------------------------------------------------------
C
C       PUNCHOUT
C       --------
C
        PUNCH 1,(TITLE(I),I=6,15)
        PUNCH 3,NPERPT
        PUNCH 19,(I,FREQ(I),QI(I),I=1,NPERPT)
   19   FORMAT(28X,I5,5X,F10.5,6X,F10.5)
C
        CALL GRAPH(FREQ,QI,NPERPT,GRAPH2,1)
C       ----------------------------------------------------------------------
C
C       GRAPH DERIVATIVES (IF REQUIRED)
C       -------------------------------
C
        IF(NGRAPH.NE.1) GO TO 191
        NGRAPH=NGRAPH+1
        DO 191 J=1,NOL
        DO 192 I=1,NPERPT
        DERIVA(I)=DKBYDA(I,J)
        DERIVB(I)=DKBYDB(I,J)
  192   CONTINUE
        CALL GRAPH(FREQ,DERIVA,NPERPT,TITLE,0)
        CALL GRAPH(FREQ,DERIVB,NPERPT,TITLE,0)
  191   CONTINUE
        CALL ADVFLM(3)
        CALL ENDFME
C
        GO TO 100
  999   CALL FINISH
        RETURN
        END
C
C
C
C
        SUBROUTINE ATTEN(GAMMAT,NPER)
C
C
C       CALCULATES ATTENUATION COEFF. AT NPER POINT OF FREQ OR PERIOD.
C       VALUE RETURNED IS -----GAMMAT.
C
```

```
C
C      ******************************************************************
C      ******************************************************************
C
C
       COMMON /LAYER/A(20),B(20),QAI(20),QBI(20),DKBYDA(90,10),
      1            DKBYDB(90,10),NOL
C      CALCULATE GAMMAT
       GAMMAT=0.0
       DO 1 I=1,NOL
       GAMMAT=GAMMAT+DKBYDA(NPER,I)*A(I)*0.5*QAI(I)
      1        +DKBYDB(NPER,I)*B(I)*0.5*QBI(I)
     1 CONTINUE
C
       RETURN
       END
C
C
C
C
       SUBROUTINE GRAPH(X,Y,N,TITLE,NAME)
C
C
C      1 SUBROUTINE GRAPHS N VALUES OF X AGAINST Y.
C      2 IF NAME=0 THE GRAPH IS UNTITLED.
C        IF NAME=1THEN TITLE MUST BE READ IN AND SDATE CALLED
C       BEFORE THIS SUBROUTINE IS CALLED.
C      3 CALL SCLIBR ESSENTIAL IN MAIN PROGRAM.
C      4 REQUIRES THE PROGRAM CARGRF TO PRODUCE GRAPHS.
C       SEE AWRE REPORT NO. C-41/68 (J.B.YOUNG & A.DOUGLAS)
C
C      ******************************************************************
C      ******************************************************************
C
C
       COMMON /GRFF/ ATITLE(20),XMAX,XMIN,YMAX,YMIN,INDX,INDY,IND,IDOT,
      1ANSTR1,IF,XLIMIT,YLIMIT,SCALX,SCALY
C
       DIMENSION X(N),Y(N)
       DIMENSION TITLE(20),BTITLE(20)
       REAL*8 TITLE,ATITLE,BTITLE,DUMMY,BLANK
C
       DATA BLANK/8H        /
       DATA BTITLE/4CHFREQUENCY (HZ)            AMPLITUDE          /
C
       DO 1 I=17,20
       TITLE(I)=BLANK
     1 CONTINUE
       DO 5 I=1,5
       TITLE(I)=BTITLE(I)
     5 CONTINUE
C
       IF (NAME.EQ.1) GO TO 2
       DO 3 I=6,15
       TITLE(I)=BLANK
     3 CONTINUE
       CALL DATIM(TITLE(16),DUMMY)
     2 CONTINUE
       DO 4 I=1,20
       ATITLE(I)=TITLE(I)
     4 CONTINUE
C
C      SET CARGRF PARAMETERS
C
       INDX=1
       INDY=1
       IND=0
       IDOT=42
       ANSTR1=2.0
       IF=3
C
       XMAX=0.0
       XMIN=0.0
       YMAX=0.0
       YMIN=0.0
C
       CALL CARGRF(X,Y,N)
C
C
       RETURN
       END
```

```
C
C
C
C
C      'HEDGEHOG' MAIN
C      ***************
C
C
C      THIS PROGRAM INVERTS THE OBSERVED SPECIFIC ATTENUATION FACTOR AS
C      AFUNCTION OF FREQUENCY FOR RAYLEIGH WAVES INTO AN ATTENUATION
C      MODEL AS A FUNCTION OF DEPTH
C
C
C      REFERENCE
C      *********
C
C      P.W.BURTON & B.L.N.KENNETT 'UPPER MANTLE ZONE OF LOW Q'
C                                  (NATURE PHYS. SCI.  238  PP87-90)
C
C
C      ACKNOWLEDGEMENTS
C      ****************
C
C      FOR THE SUBROUTINE HH---'HEHGEHOG'---THANKS TO B.L.N.KENNETT
C                                           AND TO V.P.VALLUS
C
C      ******************************************************************
C
C
C      INPUT
C      *****
C
C      THE FOLLOWING CARDS ARE READ IN
C
C        1 TITLE(I)
C
C          A TITLE FOR THE DATA CURRENTLY BEING INVERTED
C
C        2 K
C
C          FOR K READ IN THE NUMBER OF LAYERS,NOL,IN THE MODEL
C
C        3 A BLOCK OF NOL CARDS,EACH CARD CONTAINING
C
C          LIMIT1(I),LIMIT2(I),STEP(I)
C
C          LIMIT1 THE LOWER LIMIT ON THE SPECIFIC ATTENUATION FACTOR
C                 FOR A LAYER (COMPRESSIONAL WAVES)
C          LIMIT2 THE UPPER LIMIT ON THE SPECIFIC ATTENUATION FACTOR
C                 FOR A LAYER (COMPRESSIONAL WAVES)
C          STEP   THE INCREMENT USED TO STEP ALONG FROM LIMIT1 TO LIMIT2
C
C        4 STAPE,RANK,INT1,INT2,N,NMAX,ALG
C
C          SEE SUBROUTINE HH FOR EXPLANATION
C          NMAX-N IS THE NUMBER OF MODELS TO BE TESTED
C
C        5 NOL,NPERPT
C
C          NOL    THE NUMBER OF LAYERS IN THE MODEL
C          NPERPT THE NUMBER OF FREQUENCIES TO BE USED
C
C        6 A BLOCK OF NOL CARDS,EACH CARD CONTAINING
C
C          A(I),B(I)
C
C          A      COMPRESSIONAL BODILY WAVE VELOCITY FOR EACH LAYER
C          B      SHEAR BODILY WAVE VELOCITY FOR EACH LAYER
C
C        7 A BLOCK OF NPERPT CARDS,EACH CARD CONTAINING
C
C          FREQ(I),U(I)
C
C          FREQ   FREQUENCY  HZ
C          U      GROUP VELOCITY
C
C        8 A BLOCK OF NPERPT CARDS,EACH CARD CONTAINING NOL VALUES
C
C          DKBYDA(I,J)
C
C          DKBYDA PARTIAL DERIVATIVES OF THE WAVENUMBER,K, W.R.T. A FOR
C                 EACH LAYER AND AT EACH FREQUENCY
C
C        9 A BLOCK OF NPERPT CARDS,EACH CARD CONTAINING NOL VALUES
C
C          DKBYDB(I,J)
C
C          DKBYDB PARTIAL DERIVATIVES OF THE WAVENUMBER,K, W.R.T. B FOR
C                 EACH LAYER AND AT EACH FREQUENCY
C
C       10 A BLOCK OF NPERPT CARDS,EACH CARD CONTAINING
C
C          QMI(I),PRES(I)
C
C          QMI    THE OBSERVED VALUES FOR THE SPECIFIC ATTENUATION
C                 FACTORS OF RAYLEIGH WAVES
C          PRES   CONFIDENCE LIMITS ON THE QMI
C
C       11 AMAX,ASUM
C
```

```
C          PRECISION MEASURES ON THE FIT OF ANY MODEL TESTED
C          SEE REFERENCE BURTON & KENNETT
C
C
C      ******************************************************************
C
C      OUTPUT
C      ******
C
C      PRINTOUT
C      ********
C
C      THE PRINTOUT LISTS GOOD CONNECTED REGIONS FOUND BY 'HEDGEHOG' AND
C      GOOD POINTS OUTSIDE THE CONNECTED REGIONS (FOUND BY MONTE-CARLO)
C
C
C
C      ******************************************************************
C      ******************************************************************
C
C
C
      INTEGER STAPE,RANK,ALG
      REAL LIMIT1(20),LIMIT2(20),STEP(20)
      COMMON /HHG/ K,LIMIT1,LIMIT2,STEP,STAPE,RANK,
     1INT1,INT2,N,NMAX,ALG
      COMMON /LARA/A(20),B(20),DKBYDA(80,10),DKBYDB(80,10),NOL
      COMMON /PERO/FREQ(80),U(80),NPERPT
      COMMON /TEMP/ TA(80,10),TG(80),OMI(80),PRES(80),ASUM,AMAX
      REAL*8 TITLE(12)
      CALL DATIM(TITLE(11),TITLE(12))
C     ------------------------------------------------------------------
C
C     INPUT DATA
C     ----------
C
      READ 1,(TITLE(I),I=1,10)
    1 FORMAT(10A8)
      PRINT 2,(TITLE(I),I=1,11)
    2 FORMAT(1H1,//,10X,10A8,20X,A8,//)
      READ(5,51) K
   51 FORMAT(I3)
      READ(5,52) ((LIMIT1(I),LIMIT2(I),STEP(I)),I=1,K)
   52 FORMAT(3F10.5)
      READ(5,53) STAPE,RANK,INT1,INT2,N,NMAX,ALG
   53 FORMAT(7I6)
C
      READ(5,103) NOL,NPERPT
  103 FORMAT(2I10)
      READ(5,105) (A(I),B(I),I=1,NOL)
  105 FORMAT(2F10.5)
      READ(5,106)(FREQ(I),U(I),I=1,NPERPT)
  106 FORMAT(2F10.6)
      DO 7 I=1,NPERPT
      READ(5,109) (DKBYDA(I,J),J=1,NOL)
    7 CONTINUE
      DO 8 I=1,NPERPT
      READ(5,109) (DKBYDB(I,J),J=1,NOL)
    8 CONTINUE
  109 FORMAT(6F12.9)
      READ(5,110) (OMI(I),PRES(I),I=1,NPERPT)
      READ(5,106) AMAX,ASUM
  110 FORMAT(15X,2E15.7)
C     ------------------------------------------------------------------
C
      PI = 4.0*ATAN(1.0)
      DO 20 I=1,NPERPT
      TG(I)=-U(I)/(PI*FREQ(I))
      DO 21 J=1,NOL
      TB = 0.5*A(J)*DKBYDA(I,J)
      TA(I,J) = TB+0.375*A(J)*A(J)*DKBYDB(I,J)/B(J)
   21 CONTINUE
   20 CONTINUE
C
      CALL HH
      RETURN
      END
C
C
C
C
C     SUBROUTINE EST(K,POINT,RESULT) -
C
C     SUBROUTINE OF COMPARISON FOR A POINT
C
C     RESULT=0 IF POINT IS GOOD ONE
C     RESULT=1 IF POINT IS BAD ONE
C
C
C     ******************************************************************
C     ******************************************************************
C
C
      SUBROUTINE EST(K,OAI,RESULT)
      INTEGER RESULT
      COMMON /LARA/A(20),B(20),DKBYDA(80,10),DKBYDB(80,10),NOL
      COMMON /PERO/FREQ(80),U(80),NPERPT
      COMMON /TEMP/ TA(80,10),TG(80),OMI(80),PRES(80),ASUM,AMAX
      DIMENSION OAI(K),OBI(6),CRI(80)
      RESULT=1
      DO 30 I = 1,NOL
```

```
      QBI(I)=QAI(I)*3.0*A(I)*A(I)/(4.0*B(I)*B(I))
30    CONTINUE
      BSUM = 0.0
      BMAX = 0.0
      DO 31 I=1,NPERPT
      GAM = 0.0
      DO 32 J=1,NOL
      GAM=GAM+TA(I,J)*QAI(J)
32    CONTINUE
      QRI(I) = TG(I)*GAM
      QS = (QRI(I)-CMI(I))/FRES(I)
      BSUM = BSUM+QS*QS
      IF(BMAX-ABS(QS))34,34,31
34    BMAX = ABS(QS)
      NMAX = I
31    CONTINUE
      PNP = FLOAT(NPERPT)
      BSUM = SQRT(BSUM/PNP)
      IF(AMAX-BMAX) 37,35,35
35    IF(ASUM-BSUM) 37,36,36
36    RESULT = 0
37    IF(RESULT-C) 39,38,39
38    WRITE(6,49)
      WRITE(6,50) RESULT,BSUM,NMAX,BMAX
      WRITE(6,51) QAI,QBI
49    FORMAT(1X,'RESULT    SUMDEV    NMAX    MAXDEV')
50    FORMAT(1X,I6,F10.6,I6,F10.6)
51    FORMAT(6F14.5)
39    RETURN
      END
C
C
C
C
C     SUBROUTINE HH
C
C     PURPOSE
C
C     TESTING POINTS AND KNOTS IN VARIABLE SPACE
C     BY A COMBINATION OF MONTE-CARLO AND
C     HEDGEHOG METHODS
C
C     PARAMETERS
C
C     K        -NUMBER OF VARIABLES
C     LIMIT1   -LOWER LIMITS ON VARIABLES
C     LIMIT2   -UPPER LIMITS ON VARIABLES
C     STEP     -STEPS ALONG VARIABLES
C     STAPE    -STATE OF A TAPE
C               STAPE = 0 - TAPE IS EMPTY
C               STAPE = 1 - TAPE IS BUSY
C     RANK     -RANK OF NEIGHBOUR KNOTS
C     INT1     -INTERVAL BETWEEN REWRITING ON A TAPE. AFTER
C               ESTIMATION OF INT1 KNOTS BY HEDGEHOG METHOD TAPE
C               WILL BE REWRITTEN
C     INT2     -INTERVAL BETWEEN PRINTING I1, I2, I3
C     N        -INITIAL NUMBER OF A RANDOM POINT
C     NMAX     -LAST NUMBER OF A RANDOM POINT
C     ALG      -ALGORITHM OF WORK
C              ALG=1 - MONTE-CARLO METHOD ONLY FOR CHOICE OF NEW POINTS
C              ALG=2 - MONTE-CARLO METHOD ONLY FOR CHOICE OF NEW KNOTS
C              ALG=3 - SEARCH BY MONTE - CARLO METHOD FOR GOOD POINT.
C                      THEN GO TO HEDGEHOG METHOD
C              ALG=4 - SEARCH BY MONTE-CARLO METHOD FOR GOOD POINT.
C                      THEN NEAREST KNOT IS ESTIMATED. IF KNOT IS GOOD
C                      GO TO HEDGEHOG METHOD
C              ALG=5 - SEARCH BY MONTE-CARLO METHOD FOR GOOD KNOTS.
C                      THEN GO TO HEDGEHOG METHOD
C
C     SUBROUTINES USED
C
C     EST (K, POINT, RESULT ) - SUBROUTINE OF COMPARISON
C                                FOR A POINT
C              RESULT=0 IF POINT IS GOOD ONE
C              RESULT=1 IF POINT IS BAD ONE
C
C     FUNCTIONS USED
C
C     FA01AS(I) - PSEUDO-RANDOM-NUMBER GENERATOR FROM LIBRARY
C
C     VARIABLES AND ARRAYS
C
C     POINT    -POINT FROM VARIABLE SPACE
C     KNOT     -KNOT OF COORDINATE NET IN VARIABLE SPACE
C     LIST     -LIST OF GOOD KNOTS
C     I1       -NUMBER OF KNOTS IN A LIST
C     I2       -NUMBER OF KNOTS IN A LIST FOR WHICH ALL
C               NEIGHBOURS ARE TRIED
C     BKNOT    -BASIC KNOTS FOR WHICH NEIGHBOURING KNOTS ARE
C               TRIED
C     I3       -NUMBER OF NEIGHBOURING KNOTS WHICH WERE
C               TRIED BEFORE LAST LISTING ON TAPE
C     I4       -CURRENT NUMBER OF NEIGHBOURING KNOT
C     I5       -VARIABLE FOR SWITCHING OFF WRITING OF A
C               LIST ON A TAPE
C               I5=1 - WRITING IS SWITCHED ON
C               I5=2 - WRITING IS SWITCHED OFF
C     I6       -MARK FOR EXISTENCE OF A BASIC KNOT
C     CRANK    -CURRENT RANK OF NEIGHBOURS
C     SI       -VECTOR OF SIGNS OF VARIABLE INCREMENT
C     II       -INDICES OF INCREMENTED VARIABLES
C     LII      -LAST VALUES OF II
```

```
C      ISUM     -NUMBER OF VARIABLES OF A KNOT WHICH ARE
C               DIFFERENT ON TAKING ONE STEP FROM A KNOT
C               IN A LIST
C      CINT1    -CURRENT VALUE OF INTERVAL BETWEEN
C               WRITING ON A TAPE
C      CINT2    -CURRENT VALUE OF INTERVAL BETWEEN
C               PRINTING I1, I2, I4
C      I7       -SWITCHING VARIABLE ON COMPARISON OF
C               A KNOT AND ITS NEIGHBOUR IN LIST
C      N1       -CURRENT NUMBER OF POINT IN MONTE-CARLO
C               METHOD
C
C
C      ****************************************************************
C      ****************************************************************
C
C
       SUBROUTINE HH
C
       INTEGER RESULT, CRANK, CINT1, CINT2
       REAL POINT(20),KNOT(20),LIST(1000)
       DIMENSION BKNOT(20),SI(20),II(20),LII(20)
C
C      THESE OPERATORS INTEGER, REAL, COMMON MUST BE REPEATED
C      IN MAIN PROGRAM
       INTEGER STAPE,RANK,ALG
       REAL LIMIT1(20),LIMIT2(20),STEP(20)
       COMMON /HHG/ K,LIMIT1,LIMIT2,STEP,STAPE,RANK,INT1,INT2,
      1N,NMAX,ALG
C
       DATA I1/0/,I2/0/,I3/0/,I4/0/,I5/1/,I6/2/,N1/0/,
      1CINT1/0/,CINT2/0/
       N1=N1-1
       IF (STAPE.EQ.0) GO TO 100
       REWIND 2
       READ(2)I1,I2,I3
       KI1=K*I1
       READ (2) (LIST(I),I=1,KI1)
       WRITE(6,304) I1,I2,I3
  304  FORMAT('TAPE WAS READ. I1=',I5,'. I2=',I5,'. I3=',I5)
       IF(I1.EQ.I2)GO TO 100
     1 IF(I1.NE.I2)GO TO 4
       GO TO (2,3),I5
     2 KI1=K*I1
       I4=0
       REWIND 2
       WRITE(2)I1,I2,I4
       WRITE(2) (LIST(I),I=1,KI1)
       STAPE=1
       WRITE(6,305) I1
  305  FORMAT(' REGION ENDED. TAPE IS REWRITTEN.I1=',I5)
     3 GO TO 100
C
C      CHOICE OF A NEW BASIC KNOT, PUTTING CONSTRUCTION OF
C      NEIGHBOUR KNOTS ON A STARTING LINE
     4 KI2=K*I2
       DO 5 I=1,K
       J1=KI2+I
       BKNOT(I)=LIST(J1)
     5 SI(I)=-1.
  205  CRANK=0
       I4=0
       I6=1
C
C      CHOICE OF A NEW NEIGHBOUR KNOT
     6 IF(I6.NE.1)GO TO 1
     7 IF(CRANK.NE.0)GO TO 15
     8 CRANK=CRANK+1
       IF(CRANK.LE.RANK)GO TO 9
C
C      RETURN TO CHOICE OF A NEW BASIC KNOT
       IF(I5.NE.1)GO TO 208
       IF(I2.LE.I1)I2=I2+1
  208  I3=0
       I6=2
       GO TO 1
     9 DO 10 I=1,CRANK
       II(I)=I
    10 LII(I)=K-CRANK+I
    11 DO 12 I=1,K
    12 KNOT(I)=BKNOT(I)
    14 DO 214 I=1,CRANK
       J=II(I)
       KNOT(J)=BKNOT(J)+SI(I)*STEP(J)
       IF((KNOT(J).LT.LIMIT1(J)).OR.(KNOT(J).GT.LIMIT2(J)))GO TO 15
  214  CONTINUE
       GO TO 19
C
C      PASSAGE TO A NEW NEIGHBOUR
    15 I=CRANK
    16 SI(I)=SI(I)+2
       IF(SI(I).LT.2.)GO TO 14
       SI(I)=-1.
       I=I-1
       IF(I.NE.0)GO TO 16
C
       I=CRANK
       II(I)=II(I)+1
       IF(II(I).LE.LII(I))GO TO 11
    17 I=I-1
       IF(I.EQ.0)GO TO 8
       II(I)=II(I)+1
```

```
      IF(II(I).GT.LII(I))GC TC 17
      JI=CRANK-1
      DO 18 J=1,JI
   18 II(J+1)=II(J)+1
      GO TO 11
C
C     CHECK IF KNCT HAS OCCURED BRFURE
   19 I7=1
   20 IF(I2.EQ.0)GO TC 23
      DO 22 I=1,I2
      ISUM=0
      J1=K*(I-1)
      DO 21 J=1,K
      J2=J1+J
      R=(LIST(J2)-KNOT(J))/STEP(J)
      IF(R.LT.0.)R=-R
      IF(R.LT.0.1)GC TO 21
      IF(R.GT.1.9)GC TC 22
      ISUM=ISUM+1
   21 CONTINUE
      IF(ISUM.LE.RANK)GC TC 24
   22 CONTINUE
   23 GO TO (25,41), I7
   24 GO TO (15,37), I7
C
C     ESTIMATION OF KNCT
   25 IF(I4.GE.I3)GC TC 26
      I4=I4+1
      GO TO 15
   26 CALL EST(K,KNCT,RESULT)
      I4=I4+1
      IF(RESULT.EC.1)GO TC 28
      WRITE(6,315) RESULT,(KNCT(L),L=1,K)
  315 FORMAT(/,' KNCT WAS ESTIMATED BY HEDGEHOG. RESULT=',I1/
     1' KNOT=',1PE14.5,/(6X,1PE14.5))
      IF(RESULT.EC.1)GO TC 28
C
C     PLACE GOOD KNCT IN A LIST
  226 J=K*I1
      IF(J+K.GT.10CC)GO TO 34
      DO 27 I=1,K
      J1=J+I
   27 LIST(J1)=KNCT(I)
      I1=I1+1
      IF(I5.NE.1)I6=2
      I5=1
C
C     WRITING I1,I2,I4,LIST CN A TAPE
   28 GO TO(228,30),I5
  228 CINT1=CINT1+1
      IF(CINT1.LT.INT1)GO TC 3C
   29 KI1=K*I1
      REWIND 2
      WRITE(2)I1,I2,I4
      WRITE(2)(LIST(I),I=1,KI1)
      STAPE=1
      WRITE(6,318) I1,I2,I4
  318 FORMAT(' TAPE WAS REWRITTEN. I1=',I5,'. I2=',I5,'. I3=',I5)
      CINT1=0
C
C     PRINTING I1,I2,I4
   30 CINT2=CINT2+1
      IF(CINT2.LT.INT2)GO TC 33
   31 WRITE(6,32)  I1,I2,I4
   32 FORMAT(' I1=',I5,5X,'I2=',I5,5X,'I3=',I5)
      CINT2=0
   33 GO TO 6
C
C     LIST OVERFLOW
   34 WRITE(6,35)
   35 FORMAT(' TOO MANY KNCTS FOR A LIST. EXECUTION TERMINATED.')
      RETURN
C
C     HEDGEHOG OPERATICN CN A KNOT FROM MUNTE-CARLO TECHNIQUE
C     CHECK IF KNOT HAS OCCURED BEFORE
   36 I7=2
      GO TO 20
   37 WRITE(6,38) I,RESULT
   38 FORMAT(' RANDCM KNCT IS NEIGHBOUR OF ',I5,' KNUT ',
     1'IN A LIST. RESULT=',I1)
      GO TO 100
   41 IF(RESULT.EC.C)GC TC 226
      DO 42 I=1,K
      BKNOT    (I)=KNCT(I)
   42 SI(I)=-1
      WRITE(6,320) (BKNCT(L),L=1,K)
  320 FORMAT(' BAD RANDCM KNCT WILL BE USED AS BKNOT'
     1/' BKNOT=',1PE14.5,/(7X,1PE14.5))
      I3=0
      I5=2
      GO TO 205
C
C     CHOICE OF NEW PCINT BY MCNTE-CARLO METHOD
  100 N1=N1+1
      IF(N1.LE.NMAX)GC TO 1C2
      WRITE(6,1C1) NMAX
  101 FORMAT(' NUMBER CF RANDCM POINTS MORE THAN NMAX=',
     1I5,'. EXECUTICN TERMINATED.')
      RETURN
  102 DO 103 I=1,K
  103 POINT(I)=LIMIT1(I)+(LIMIT2(I)-LIMIT1(I))*FA01AS(1)
      IF(N1.LT.N)GO TC 10C
```

```
      GO TO (104,1C6,104,1C4,1C6), ALG
 104  CALL EST(K,POINT,RESULT)
      IF(RESULT.EC.1)GC TC 1CO
      WRITE(6,1C5) N1,(PCINT(I),I=1,K)
 105  FORMAT(/' GOCD PCINT ',I5/(1PE14.5))
      IF(ALG.EQ.1)GC TO 1CC
C
 106  DO 107 I=1,K
      J=(POINT(I)-LIMIT1(I))/STEP(I)+0.5
      R=J
 107  KNOT(I)=LIMIT1(I)+STEF(I)*R
      CALL EST(K,KNCT,RESULT)
      IF(RESULT.EC.1)GC TC 110
      WRITE(6,1C8) N1,(KNCT(I),I=1,K)
 108  FORMAT(/' GOOD KNCT ',I5,/(1PE14.5))
 109  GO TO (100,10C,36,36,36), ALG
 110  GO TO (100,10C,36,1CC,100), ALG
      RETURN
      END
```

REFERENCES

Adcock, R. J. (1880). A Problem in Least Squares. Analyst 1880, 5, p53-54.

Anderson, D. L., and Archambeau, C. B. (1964). The Anelasticity of the Earth. J.G.R. 69, 10, p2071-2084.

Anderson, D. L., Ben-Menahem, A., and Archambeau, C. B. (1965). Attenuation of Seismic Energy in the Upper Mantle. J.G.R. 70, No 6, p1441-1448.

Anderson, D. L., and Sammis, C. (1970). "Partial Melting in the Upper Mantle". Phys.Earth Planet.Int. 3, p41-50.

Backus, G., and Gilbert, F. (1968). The Resolving Power of Gross Earth Data. Geophys.J.Roy.Astr.Soc. 16, p169-205.

Barazangi, M., Isacks, B., and Oliver, J. (1972). Propagation of Seismic Waves through and Beneath the Lithosphere that Descends under the Tonga Island Arc. J.G.R. 77, 5, p952-958.

Båth, M. (1968). Mathematical Aspects of Seismology. Developments in Solid Earth Geophysics 4. Elsevier Publishing Company.

Bogert, R. P., Healy, M. J., and Tukey, J. W. (1962). The Quefrency Alanysis of Time Series for Echoes: Cepstrum, Pseudo-Autocovariance, Cross-Cepstrum and Saphe Cracking. In 'Time Series Analysis' (Wiley), Ed. Rosenblatt, M. Ch. 15, p209-243, Appendix 1 (p240-242).

Born, W. T. (1941). The Attenuation Constant of Earth Materials. Geophysics, 6, p132-148.

Brooks, C., Wendt, I., and Harre, J. (1968). A Two-Error Regression Treatment and its Application to Rb-Sr and Initial Sr^{87}/Sr^{86} Ratios of Younger Variscan Granitic Rocks from the Schwarzwald Massif, Southwest Germany. J.G.R. 73, 18, p6071-6084.

Brownlee, K. A. (1965). Statistical Theory and Methodology in Science and Engineering. Ch. 11, 2nd Edition, John Wiley and Sons.

Brune, J. N. (1962). Attenuation of Dispersed Wave Trains. BSSA 52, 1, p109-112.

Brune, J. N., Nafe, J. E., and Alsop, L. E. (1961). The Polar Phase Shift of Surface Waves on a Sphere. B.S.S.A. 51, 2, p247-257.

Brune, J. N., Nafe, J. E., and Oliver, J. E. (1960). A Simplified Method for the Analysis and Synthesis of Dispersed Wave Trains. J.G.R. 65, 1, p287-304.

Brune, J. N., and Oliver, J. E. (1959). The Seismic Noise of the Earth's Surface. B.S.S.A. 49, 4, p349-353.

Buchbinder, G. G. R. (1972). Comments on Paper by Mansour Niazi, "Seismic Dissipation in Deep Seismic Zones from the Spectral Ratio of pP/P". J.G.R. Letters 77, 8, p1586-1587.

Bullen, K. E. (1965). An Introduction to the Theory of Seismology. 3rd Edition. C.U.P.

Burton, P. W., and Blamey, C. (1972). A Computer Program to Determine the Spectrum and a Dispersion Characteristic of a Transient Signal. HMSO, AWRE Report No 0-48/72.

Burton, P. W., and Kennett, B. L. N. (1972). Upper Mantle Zone of Low Q. Nature Phys.Sci. 238, 84, p87-90.

Carpenter, E. W., and Davies, D. (1966). Frequency Dependent Seismic Phase Velocities; an Attempted Reconciliation between the Jeffreys/Bullen and the Gutenberg Models of the Upper Mantle. Nature 212, 5058, p134-135.

Carpenter, E. W., and Marshall, P. D. (1970). Surface Waves Generated by Atmospheric Nuclear Explosions, United Kingdom Atomic Energy Authority. HMSO, AWRE Report No 0-88/70.

Carpenter, E. W., and Thirlaway, H. I. S. (1966). Proceedings of the Vesiac Special Study Conference on Seismic Signal Anomalies, Travel Times, Amplitudes and Pulse Shapes. Inst.Sci. and Technol., Univ. of Michigan. pp119-140.

Der, Z., Masse, R., and Landisman, M. (1970). Effects of Observational Errors on the Resolution of Surface Waves at Intermediate Distances. J.G.R. 75, 17, p3399-3409.

Douglas, A., Corbishley, D. J., Blamey, C., and Marshall, P. D. (1972). Estimating the Firing Depth of Underground Explosions. Nature, Phys.Sci. 237, 5349, p26-28.

Douglas, A., Hudson, J. A., and Kembhavi, V. K. (1971). The Analysis of Surface Wave Spectra using a Reciprocity Theorem for Surface Waves. Geophys.J.Roy.Astr.Soc. 23, p207-223.

Dziewonski, A., Bloch, S., and Landisman, M. (1969). A Technique for the Analysis of Transient Seismic Signals. BSSA 59, 1, p427-444.

Enochson, L. D. and Otnes, R. K. (1968). Programming and Analysis for Digital Time Series Data. The Shock and Vibration Centre, Naval Research Laboratory, Washington DC.

Espinosa, A. F., Sutton, G. H., and Miller, H. J. (1962). A Transient Technique for Seismograph Calibration. BSSA 52, 4, p767-779.

Espinosa, A. F., Sutton, G. H., and Miller, H. J. (1965). A Transient Technique for Seismograph Calibration - Manual and Standard Set of Theoretical Transient Responses. Geophysics Laboratory, Inst, of Sci. and Tech., University of Michigan.

Ewing, W. M., Jardetzky, W. S., and Press, F. (1957). Elastic Waves in Layered Media. McGraw-Hill.

Frasier, C. W., and Filson, J. (1972). A Direct Measurement of the Earth's Short Period Attenuation Along a Teleseismic Ray Path. J.G.R. 77, 20, p3782-3787.

Futterman, W. I. (1962). Dispersive Body Waves. J.G.R. 67, 13, p5279-5291.

Goodman, N. R. (1960). Measuring Amplitude and Phase. Journal of the Franklin Institute. 270, p437-450.

Green, D. H. and Ringwood, A. E. (1970). Mineralogy of peridotitic Composition under Upper Mantle Conditions. Phys.Earth Planet.Int. 3, p359-371.

Haskell, N. A. (1953). The Dispersion of Surface Waves on Multilayered Media. B.S.S.A. 43, p17-34.

Haskell, N. A. (1964). Radiation Pattern of Surface Waves from Point Sources in a Multi-Layered Medium. B.S.S.A. 54, 1, p377-393.

Ibrahim, A. K. (1971). The Amplitude Ratio PcP/P and the Core-Mantle Boundary. Pure and Applied Geophysics (PAGEOPH) 91, 8, p114-133.

Jackson, D. D., and Anderson, D. L. (1970). Physical Mechanisms of Seismic-Wave Attenuation. Revs. of Geophysics and Space Physics. 8, No 1, p1-64.

Jeffreys, Sir Harold. (1961). Small Corrections in the Theory of Surface Waves. Geo.J.Roy.Astr.Soc. 6, No 1, p115-117.

Kanamori, H. (1970). Velocity and Q of Mantle Waves. Phys.Earth Planet. Interiors. 2, p259-275.

Kanamori, H. and Press, F. (1970). How Thick is the Lithosphere. Nature 226, p330-331.

Keilis-Borok, V. I. and Yanovskaya, T. B. (1967). Inverse Problems of Seismology (Structural Review). Geophys.J.Roy.Astr.Soc. 13, p223-234.

Knopoff, L. (1964). 'Q'. Revs of Geophysics, 2, No 4, p625-660.

Knopoff, L. (1969). Attenuation of Seismic Waves in the Mantle. In 'The Earth's Crust and Upper Mantle'. American Geophysical Union. Geophysical Monograph 13, p273-275.

Knopoff, L., Aki, K., Archambeau, C. B., Ben-Menahem, A., and Hudson, J. A. (1964). Attenuation of Dispersed Waves. J.G.R. Letters 69, 8, p1655-1657.

Kolsky, H. (1953). Stress Waves in Solids. O.U.P.

Kolsky, H. (1956). The Propagation of Stress Pulses in Viscoelastic Solids. Phil.Mag.Ser. 8, Vol 1, No 8, p693-710.

Kovach, R. L., and Anderson, D. L. (1964). Attenuation of Shear Waves in the Upper and Lower Mantle. B.S.S.A. 54, p1855-1864.

Lambert, I. B., and Wyllie, P. J. (1970a). Melting in the Deep Crust and Upper Mantle and the Nature of the Low-Velocity Layer. Phys.Earth Planet.Int. 3, p316-322.

Lambert, I. B., and Wyllie, P. J. (1970b). Low Velocity Zone of the Earth's Mantle: Incipient Melting Cuased by Water. Science 169, p764-766.

Lomnitz, C. (1962). Application of the Logarithmic Creep Law to Stress Wave Attenuation in the Solid Earth. J.G.R. 67, p365-368.

Marshall, P. D. (1970). Aspects of the Spectral Differences between Earthquakes and Underground Explosions. Geophys.J.Roy.Astr.Soc. 20, p397-416.

Marshall, P. D., and Basham, P. W. (1972). Discrimination between Earthquakes and Underground Explosions Employing an Improved M_s Scale. Geophy. J.Roy.Astr.Soc. 28, p431-458.

Marshall, P. D., and Burton, P. W. (1971). The Source-Layering Function of Underground Explosions and Earthquakes - An Application of a 'Common Path' Method. Geophys.J.Roy.Astr.Soc. 24, p533-537.

Marshall, P. D., and Carpenter, E. W. (1966). Estimates of Q for Rayleigh Waves. Geophys.J.Roy.Astr.Soc. 10, p549-550.

Marshall, P. D., Carpenter, E. W., Douglas, A., and Young, J. B. (1966). Some Seismic Results of the LONGSHOT Explosion. HMSO, AWRE Report No O-67/66.

Marshall, P. D., Corbishley, D. J., and Gibbs, P. G. (1970). Some Seismic Results of the MILROW Underground Nuclear Explosion. HMSO, AWRE Report No O-47/70.

Mason, W., and Kuo, J. T. (1971). Internal Friction of Pennsylvania Slate. J.G.R. 76, 8, p2084-2089.

McIntyre, G. A., Brooks, C., Compston, W., and Turek, A. (1966). The Statistical Assessment of Rb-Sr Isochrons. J.G.R. 71, 22, p5459-5468.

Miller, R. L., and Kahn, J. S. (1962). Statistical Analysis in the Geological Sciences. John Wiley and Sons.

DURHAM UNIVERSITY SCIENCE 31 MAY 1973 SECTION LIBRARY

Mitchell, B. J. and Landisman, M. (1969). Electromagnetic Seismograph Constants by Least Squares Inversion. B.S.S.A. 59, 3, p1335-1348.

Niazi, M. (1971). Seismic Dissipation in Deep Seismic Zones from the Spectral Ratio of pP/P. J.G.R. 76, 14, p3337-3343.

Oliver, J. (1962). A Summary of Observed Seismic Surface Wave Dispersion. B.S.S.A. 52, 1, 81-86.

Pekeris, C. L. (1948). The Theory of Propagation of Explosive Sound in Shallow Water. Geol.Soc.Am.Mem., 27.

Peselnick, L., and Zietz, I. (1959). Internal Friction of Fine Grained Limestones at Ultrasonic Frequencies. Geophys. 24, p285-296.

Pinkerton, J. M. M. (1947). A Pulse Method for the Measurement of Ultrasonic Absorption in Liquids: Results for Water. Nature 160, p128-129.

Press, F. (1970a). Regionalized Earth Models. J.G.R. 75, No 32, p6575-6581.

Press, F. (1970b). Earth Models Consistent with Geophysical Data. Phys.Earth and Planet.Int. 3, p3-22.

Press, F., and Healy, J. (1957). Absorption of Rayleigh Waves in Low-Loss Media. Journal of Applied Physics. 28, 11, p1323-1325.

Ractliffe, J. F. (1967). Elements of Mathematical Statistics. 2nd Edition. O.U.P.

Ringwood, A. E. (1969). Composition and Evolution of the Upper Mantle. In "The Earth's Crust and Upper Mantle". American Geophysical Union. Geophysical Monograph 13, p1-17.

Robinson, E. A. (1966). Collection of Fortran II Programs for Filtering and Spectral Analysis of Single Channel Time Series. Geophysical Prospecting 14, Appendix 1 p42.

Scheffe, H. (1964). The Analysis of Variance. John Wiley and Sons.

Spetzler, H., and Anderson, D. L. (1968). The Effect of Temperature and Partial Melting on Velocity and Attenuation in a Simple Binary System. J.G.R. 73, No 18, p6051-6060.

Strick, E. (1967). The Determination of Q, Dynamic Viscosity and Transient Creep Curves from Wave Propagation Measurements. Geophys.J.Roy.Astr. Soc. 13, p197-218.

Takeuchi, H., Dorman, J., and Saito, M. (1964). Partial Derivatives of Surface Wave Phase Velocity with Respect to Physical Parameter Changes within the Earth. J.G.R. 69, 16, p3429-3441.

Teng, T. L. (1968). Attenuation of Body Waves and the Q Structure of the Mantle. J.G.R. 73, p2195-2208.

Teng, T. L. (1969). Attenuation of Body Waves and the Q Structure of the Mantle. J.G.R. 74, p6720-6722.

Thomson, W. T. (1950). Transmission of Elastic Waves Through a Stratified Solid Medium. Journal of Applied Physics. 21, p89-93.

Toksoz, M. N., Ben-Menahem, A., and Harkrider, D. G. (1964). Determination of Source Parameters of Explosions and Earthquakes by Amplitude Equalisation of Seismic Surface Waves. I Underground Nuclear Explosions. J.G.R. 69, p4355-4366.

Handbook (1965). World Wide Standard Seismograph Network. Geophysics Laboratory. University of Michigan.

Yamakawa, N., and Sato, Y. (1964). Q of Surface Waves. Journal of Physics of the Earth. 12, 1, p5-18.

York, D., (1966). Least Squares Fitting of a Straight Line. Canadian Journal of Physics 44, p1079-1086.

York, D. (1967). The Best Isochron. Earth and Planet.Sci. Letters 2, p479-482.

Young, J. B., and Douglas, A. (1968). Map, Time Series and Other Plotting Routines for Use with the Stromberg-Carlson 4020 Plotter. HMSO, AWRE Report No O-41/68.

Young, J. B., and Gibbs, P. G. (1968). GEDESS: A Series of Computer Programs for Deriving Information at Selected Seismic Recording Sites, for Signals from Known Hypocentres. HMSO, AWRE Report No O-54/68.

Zener, C. (1948). Elasticity and Anelasticity of Metals. Univer. of
Chicago Press, Chicago, Illinois.

DURHAM UNIVERSITY
SCIENCE
31 MAY 1973
SECTION
LIBRARY

United Kingdom Atomic Energy Authority

AWRE, Aldermaston

AWRE REPORT NO. 048/72

A Computer Program to Determine the Spectrum and a Dispersion Characteristic of a Transient Signal

P W Burton
C Blamey

C16

550.34:681.3.06
681.3.06:550.34

SBN 85518030 7

TABLE OF CONTENTS

SUMMARY

The program described determines the Fourier amplitude and phase spectra, and the group velocity of a dispersed seismic surface wave signal (sampled at equal time intervals) as a function of frequency. Group velocity, a dispersion characteristic, is produced by a multiple filtering technique.

The program contains an option to generate and remove instrumental effects for World-Wide Standard Seismograph Network (WWSSN) types of instruments.

1. INTRODUCTION

The seismic surface waves generated by earthquakes and explosions are usually strongly dispersed (see for example figure 1), that is, the velocity at which the energy in the signal travels (the group velocity) is a function of frequency. This dispersion has two causes; the major contribution is a geometrical dispersion effect. The amplitudes of the longer period surface waves decay more slowly with depth than do the amplitudes of the shorter period components, but the group velocity of a surface wave component depends directly on the velocity of propagation of shear and compressional waves; these usually increase with depth in the earth. So the group velocity for the longer periods is usually greater than for shorter periods. If the wave propagation is not perfectly elastic a further minor degree of dispersion must exist as can be shown from arguments of causality.

In analysing surface waves one of the most important determinations is the relationship between group velocity and frequency. For example, from such a relationship it is possible to estimate the wave velocity, and therefore density, as a function of depth for the path followed by the surface waves between earthquake source and receiver. Various visual methods are available for determining the group velocity curve but in recent years computer techniques have refined these measurements and this report describes a program based on the method of Dziewonski et al. [1] which is an improvement on Dziewonski's original method.

The program was written as part of a study of the non-elastic attenuation effects on Rayleigh surface waves. This requires the evaluation of the absolute amplitude spectrum, as well as the group velocities, for a signal. A procedure to obtain the spectrum is thus included in the program. Further, because the recorded signals are usually distorted by recording instruments the program includes an option to remove these effects when they are known.

2. OUTLINE OF THE METHOD

To make the analyses the signal is passed through a series of narrow band-pass filters centred on different frequencies. The time when the amplitude of the filtered signal is maximum for each of the filtered records is then taken as the group arrival time of the group of frequencies in the signal centred on the centre frequency of the filter. Knowing the distance the signal has travelled from its source and the origin time of the earthquake (or explosion) the group velocity of each frequency can be computed. Group velocity, rather than the natural group arrival time, is used as the dispersion characteristic because it is independent of the distance between event and recording site. The group velocity curve obtained from the signal of figure 1 is shown in figure 5. An interesting feature of this curve is the extensive minimum section which implies that many frequencies arrive at the same time; this means that there will be a large amplitude spike in the time domain and this is easily identified in the time series of figure 1 (to the seismologist this is an Airy phase).

To analyse dispersion we are asking the question when does energy of frequency f (Hz) arrive? To answer this we need a narrow band-pass filter of mean frequency f and good joint frequency-time resolution to filter the time series. In choosing a narrow band filter a compromise must be made between a filter that is so narrow that the filtered signal is smeared out and the maximum amplitude is thus difficult to estimate in time, and a filter that is so wide that strong frequency components that lie well away from the filter centre frequency are nevertheless passed by the filter and possibly dominate the filtered signal (thus producing a spurious arrival time). In this program we follow Dziewonski et al. and use the Gaussian function as a filter because it optimises these conditions. A set of such filters is generated at different central frequencies; these are of constant Q (the ratio of peak frequency to bandwidth) to ensure uniform resolution for all f. For further discussion of optimum filter design see Inston et al. [2].

It is difficult to determine the maximum in each filtered signal even when the best filter is used because the filtered signal oscillates about zero. However, it is possible to determine the envelope to this oscillating signal by using the modulus of the analytic signal function (see appendix C). In practice it is usual to contour the envelope amplitudes as a function of group velocity and frequency. Such contouring creates a 2-D matrix which tabulates instantaneous envelope amplitudes as this function of group velocity and frequency.

Figures 6, 7 and 8 illustrate the procedure. Figure 6(a) is the signal generated by an atmospheric nuclear explosion at Novaya Zemlya, USSR, and recorded by a long period, vertical component seismometer at a WWSSN station at Kongsberg, Norway (a surface propagation distance of 2522 km). The signal-to-noise ratio is good for this record and it is assumed that this will be so for any record to be analysed. The dispersion in the signal is obvious visually and three frequencies, f_L, f_I and f_H, are indicated. Scales of arrival time measured from the onset time of the event and the equivalent group velocity are shown below the seismogram and it is clear from this that the group velocity of f_L is about 3.2 km/s and for f_H about 2.5 km/s.

Figure 6(e) shows the record after filtering with a Gaussian filter centred on 0.033 Hz, the frequency of f_L, 6(f) is the Hilbert transform of 6(e) and 6(d) is the envelope of 6(e) obtained by forming the modulus of the analytic function from the filtered trace and its Hilbert transform. Similarly figure 7 shows the results of filtering the record with a filter centred on f_I and the corresponding envelope while figure 8 is the result for f_H. Picking the peaks of the three envelopes gives a three point group velocity/frequency relationship of:-

f_L	0.033 Hz	3.17 km/s
f_I	0.051 Hz	2.64 km/s
f_H	0.088 Hz	2.55 km/s

Figure 4 shows envelope heights in db (normalised to 99 db) as the matrix function of group velocity and frequency. The group velocity/frequency curve stands out as a ridge on this plot.

To obtain the amplitude spectrum the original seismogram is Fourier transformed using a procedure based on the Cooley-Tukey algorithm (see appendices A and B). The amplitude and phase spectra of the Kongsberg record are shown in figures 2 and 3. At this stage the amplitude and phase response are uncorrected for the effects of the recording instrument. Given the instrument response its effects can be removed simply by dividing the observed complex spectrum by the instrument spectrum. As the signals we have analysed were recorded principally at WWSSN stations the program contains an option to generate and remove the effects of WWSSN long period recording systems. Details of the instrument calibration pulse and instrument parameters are read into the computer for each signal and this information is compared to a reference library of WWSSN instrument calibration pulses and parameters; the best match obtained is then used to generate the instrument response. The subroutine for obtaining these WWSSN instrument calibrations is based on a similar program written by J N Brune (see appendix E).

This program can be applied to other types of signal recorded by different instruments by inserting the relevant instrument transfer function. The program has been written to facilitate this exchange and the present instrument package may easily be replaced by another, or just omitted.

3. PROGRAM SPECIFICATION

The program is written in Fortran IV for the AWRE IBM 360/75. When all the available options are included the required storage is 200k. Output is in the form of a paper printout and additional options are available for punched cards for the amplitude spectrum and group velocities, SC4060 graphical output and film. The maximum number of digits in the time series signal is 1024. The maximum size which may be requested for the group velocity/frequency matrix is 120/120.

4. DATA

The time series has to be in digital form, with a constant sampling interval. The time between the event origin time and the first digit in the time series must be known, as must the distance between the event and recording site. (In this version this distance is expressed in degrees, measured round the great circle of propagation on the Earth's surface, and converted to kilometres within the program.)

5. PROGRAM PROCEDURE

5.1 Spectral analysis

5.1.1 Preparation for Fourier analysis

The parameter cards (section 5) which specify the operations to be carried out and the digital time series, sampled at intervals of DELA seconds, are read in. The time series is stored in the array SEIS(I), cosine tapered at both ends and fitted to a mean baseline to reduce the Gibbs' phenomenon, and eliminate "square wave" effects caused by a time series superimposed onto a non-zero baseline. If required the seismogram may be inverted and/or samples removed from the front.

The NSEIS data points of the digital time series are now set to N points by adding zeros, where $N = 2^{L+1}$ and L is the first integer which makes N ⩾ NSEIS. This condition is an intrinsic requirement of the Cooley-Tukey algorithm used in the Fast Fourier Transform routine COOL; the Fourier analysis procedure is then very rapid (4000 points in one second).

5.1.2 The Fourier analysis

Cosine and sine transforms are obtained using COOL and these easily relate to the Fourier transform.

Harmonic frequencies are determined by the values of N and sampling interval DELA.

The Nyquist frequency is defined as

$$f_{NYQ} = \frac{1}{2.0 \times DELA} \text{ Hz},$$

the fundamental frequency is

$$Df = \frac{f_{NYQ}}{NBY2} \text{ Hz } (NBY2 = \frac{N}{2})$$

and the harmonic frequencies are

$$f_{i+1} = i \times Df \quad (0 \leqslant i \leqslant NBY2).$$

These frequencies are stored in array FREQ(I). The transform of SEIS(I) is stored in the complex array Z(I) (appendix B).

Expressions for the amplitude and phase at these frequencies are given in appendix A. No information is obtained for frequencies greater than f_{NYQ}. The amplitude and phase spectra obtained from the Kongsberg record are shown in figures 2 and 3.

5.1.3 Absolute values

If absolute values are required the instrument transfer function is formed by subroutine WWSSN and is stored in the complex array P(I) (appendix E). The instrument effect is removed by division at each frequency creating

$$Z'(I) = \frac{Z(I)}{P(I)} .$$

Spectral amplitudes and phases are recalculated and the spectrum may be smoothed if required. This completes spectral analysis of the time series.

5.2 Dispersion

5.2.1 Preparation for filtering

The velocity of travel to the first, VSF, and last, VSL, seismogram samples are computed and then the velocity to each digit in the time series is stored in the two-dimensional array TABLE (1,I) $(0 \leq I \leq N)$. The velocity array covering the range of interest is created and stored in VSTEP(I) by subtracting a chosen VSTEP from VSF, storing the result, and continuing until VSL is reached. There must not be more than 120 velocities.

5.2.2 The filter

Filter centre frequencies are chosen and stored in FREQC(I). These are chosen to correspond to a set of the harmonics selected at regular intervals from FREQ(I). The two arrays, FREQ(I) and VSTEP(I), specify the frequencies and group velocities for which instantaneous envelope amplitudes will subsequently be stored in the 2-D dispersion matrix.

The filter parameters BAND and DWF are used to shape the Gaussian filter function. BAND is dimensionless and gives the relative bandwidth for all the filters used (to preserve constant Q), that is

$$\text{BAND} = \frac{\text{FREQC(I) - Filter Low Frequency}}{\text{FREQC(I)}}$$

and a typical value is BAND = 0.20. The value of DWF specifies the decay rate, or roll-off, of the Gaussian filter. It is the ratio of the filter maximum amplitude at its central frequency to its amplitude at its lowest frequency, specified above by BAND.

This filter is created by subroutine GAUSSA at the harmonic frequencies FREQ(I), and is stored symmetrically in P(I) about FREQC(I).

5.2.3 Response to the filter

The analytic signal at a particular frequency (ie, the envelope components of the filter response to the seismogram, at a particular frequency) is formed by multiplication of Z'(I) and P(I), storing the result in P'(I) and transforming to the time domain. The instantaneous amplitude of the analytic signal is obtained by forming the modulus of P'(I) and storing the values in TABLE (2,I) (appendix C).

We now have the situation of figure 6 where for a particular filter centre frequency (which is the same as an harmonic of the Fourier transform of the time series) we have two arrays - containing instantaneous amplitudes of the analytic signal and the corresponding velocity (obtained from arrival time). We are only interested in the selected velocities VSTEP(I) and therefore interpolate between the values of TABLE to obtain instantaneous amplitudes at the velocities of interest. Results are stored in one column of the 2-D matrix E(I,J).

The sequence of operations, starting at creation of the filter, is repeated for each frequency of interest and the results stored in subsequent columns of E, which has a maximum size of 120 × 120 (appendix D).

5.2.4 Group velocities

The maximum value of E is determined and set to 99 db, all other values of E being scaled relatively to give the matrix of figure 4. For each frequency of filter analysis, ie, FREQC(I), the maximum value of the relevant column of E is obtained and the corresponding velocity is the group velocity (velocity of the maximum energy content at each frequency).

5.3 Output

There is a comprehensive printout consisting of:-

(1) The input seismogram and parameters.

(2) Spectral amplitudes and phases.

(3) Instrumental magnification and phase.

(4) Spectral amplitudes and phases after instrument removal.

(5) The seismogram after instrument removal.

(6) Filter information.

(7) Group velocity against frequency.

(8) The 2-D matrix E of instantaneous analytic signal amplitudes (in relative db) as a function of frequency and velocity (figure 4).

Also graphs [3] where relevant, on paper and film may be obtained and the smoothed spectral amplitudes and the group velocities punched out. The graphs used for figures 2, 3 and 5 are examples of this output.

6. PARAMETER CARDS

The data cards should be made up as follows with formats as specified in the listing of the program. The value +1 performs an option, 0 omits it, where appropriate.

(1) An SC4060 card for graphics.

(2) A block of 78 cards which are a reference library of WWSSN calibration pulses (appendix E).

The remaining block of cards should be repeated as many times as there are signals to be analysed.

(1) TITLEA(I) A title card with columns 73 - 80 containing an identification label, eg, DATA 001.

(2)	STANAM(I)	Name of recording station.
	DELTAD	Distance in degrees between event and recording station. Program uses 1° ≡ 111.1 km.
	MHOUR) MIN) SEC)	GMT origin time of event in hours, minutes and seconds.
	MHRGMT) MINGMT) SECGMT)	GMT of first sample.
	NSEIS	Number of samples in time series.
(3)	DELA	Sample interval in seconds.
	IVSEIS	Invert the seismogram.
	NUMCUT	Remove NUMCUT samples from the front of the seismogram and correct the first sample time by NUMCUT × DELA.
	NBASE	Correct the seismogram to a mean baseline.
	NCOSTP	Cosine taper NCOSTP points at both ends of seismogram.
	NCOMB	Number of points in the comb used to smooth the Fourier amplitude spectrum. Set to an even number.

NAFLO	Index number of the frequency array FREQ(I) referring to the lowest frequency of interest in the amplitude spectrum. All frequencies lower than NAFLO × Df are removed.
NINSTR	If this is set to 1 then remove the instrument effect.
NUGRUP	Calculate group velocities.
NFLO	Index number for FREQ(I) referring to the lowest frequency of interest, NFLO × Df, for group velocity determination. Also NFLO must be greater than NAFLO.
NFHI	Index number of the highest frequency of interest for group velocity determination.
NFSTEP	The interval between adjacent frequencies of interest for group velocity determination is NFSTEP × Df. Note filter central frequencies FREQC(I) are such that FREQC(I) = FREQ(NFLO-1) = NFLO × Df etc.
BAND	Dimensionless, relative bandwidth of Gaussian filter.
DWF	Decay rate of Gaussian window function.
DV	Velocity step along the seismogram. The velocities to the first and last seismogram samples, VSF and VSL, are known. This group velocity range is divided into 120, or less, values of group velocity by suitable choice of DV.
(4) NG1 ⋮ NG9 ⋮ NG15	Several graphs of the seismogram, amplitude, phase, instrument response and group velocity are available. These are described in detail in the program listing.
NP1	Punch out the smoothed amplitude/frequency spectrum of the seismogram.
NP2	Punch out the group velocity/frequency curve.
(5) FMT	Read in the variable format used to input the seismogram.
	Cards 6 and 7 if, and only if, NINSTR = 1.
(6) TITLEB	A title card for the instrumentation data.

(7) This card contains measurements from the WWSSN calibration pulse and WWSSN seismometer constants. If required, a full description of these parameters is in the program listing.

(8) SEIS(I) The digital time series in format FMT containing NSEIS points and sampled every DELA seconds.

7. ACKNOWLEDGMENTS

We would like to thank Messrs J B Young and A Douglas for their help during the preparation of this program. We would also like to thank Messrs A Douglas and P D Marshall, and Dr H I S Thirlaway for useful criticism of this text.

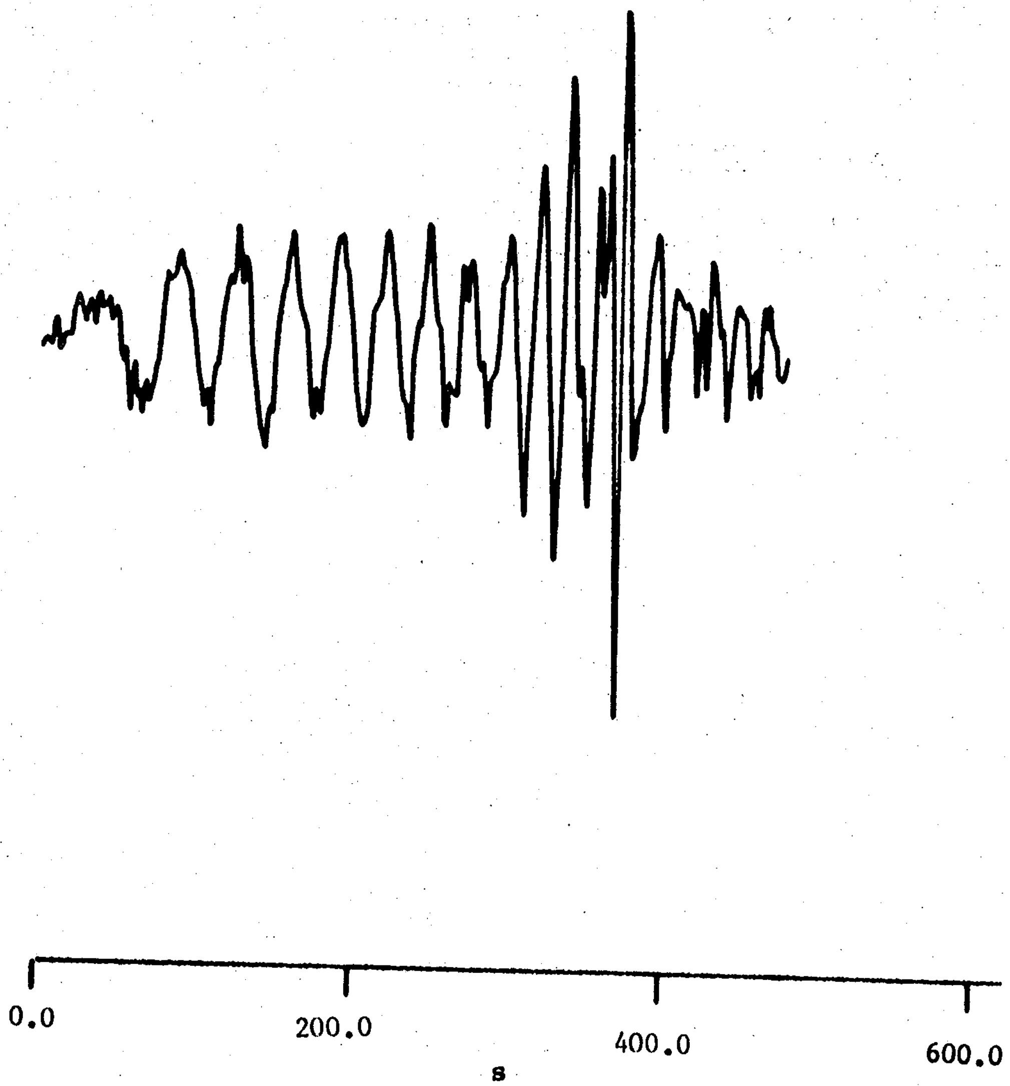

FIGURE 1. A SEISMIC RAYLEIGH WAVE FROM NOVAYA ZEMLYA WHICH WAS RECORDED AT KONGSBERG, NORWAY (DISTANCE IS 2522 km)

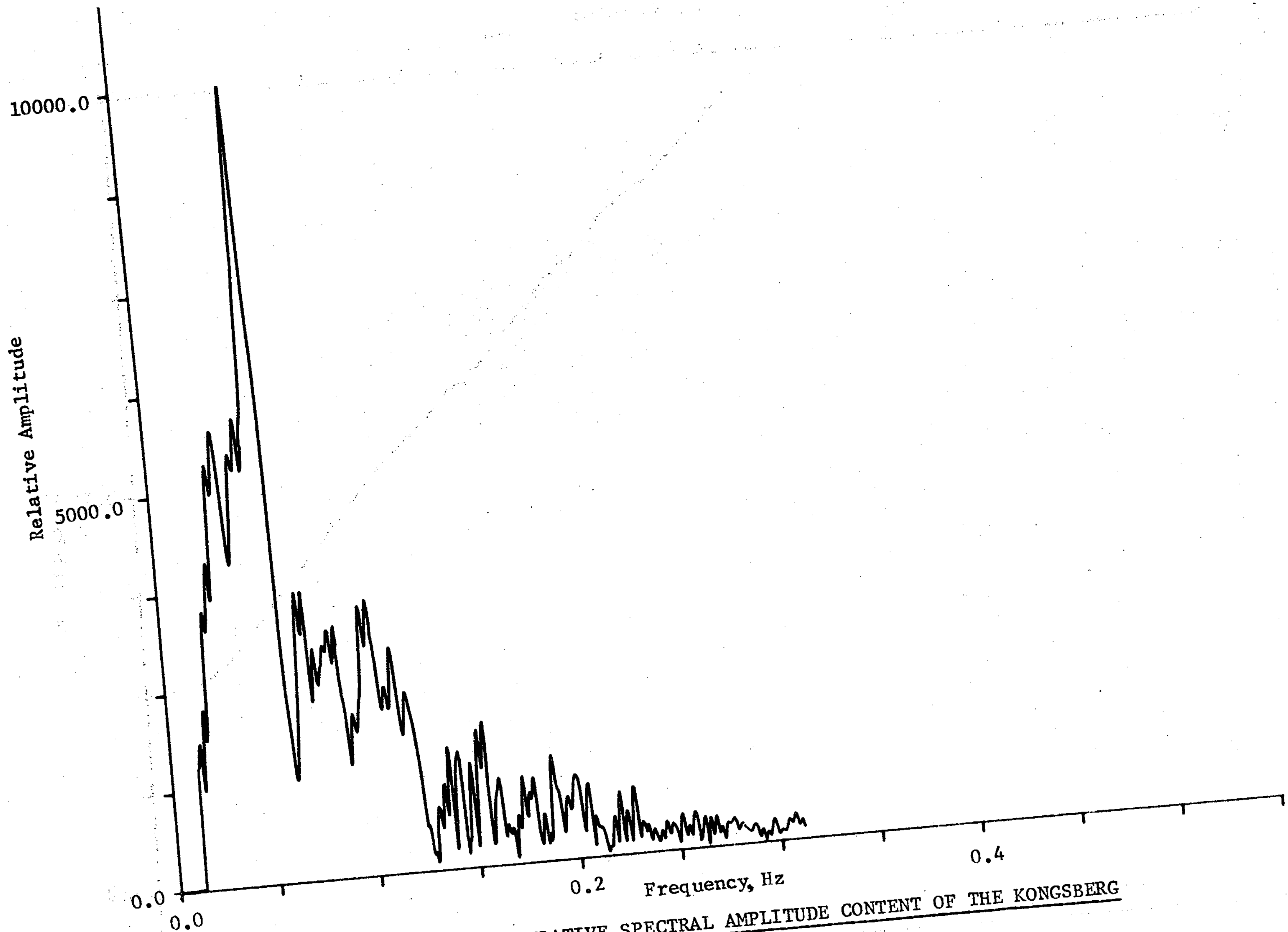

FIGURE 2. THE RELATIVE SPECTRAL AMPLITUDE CONTENT OF THE KONGSBERG RECORD

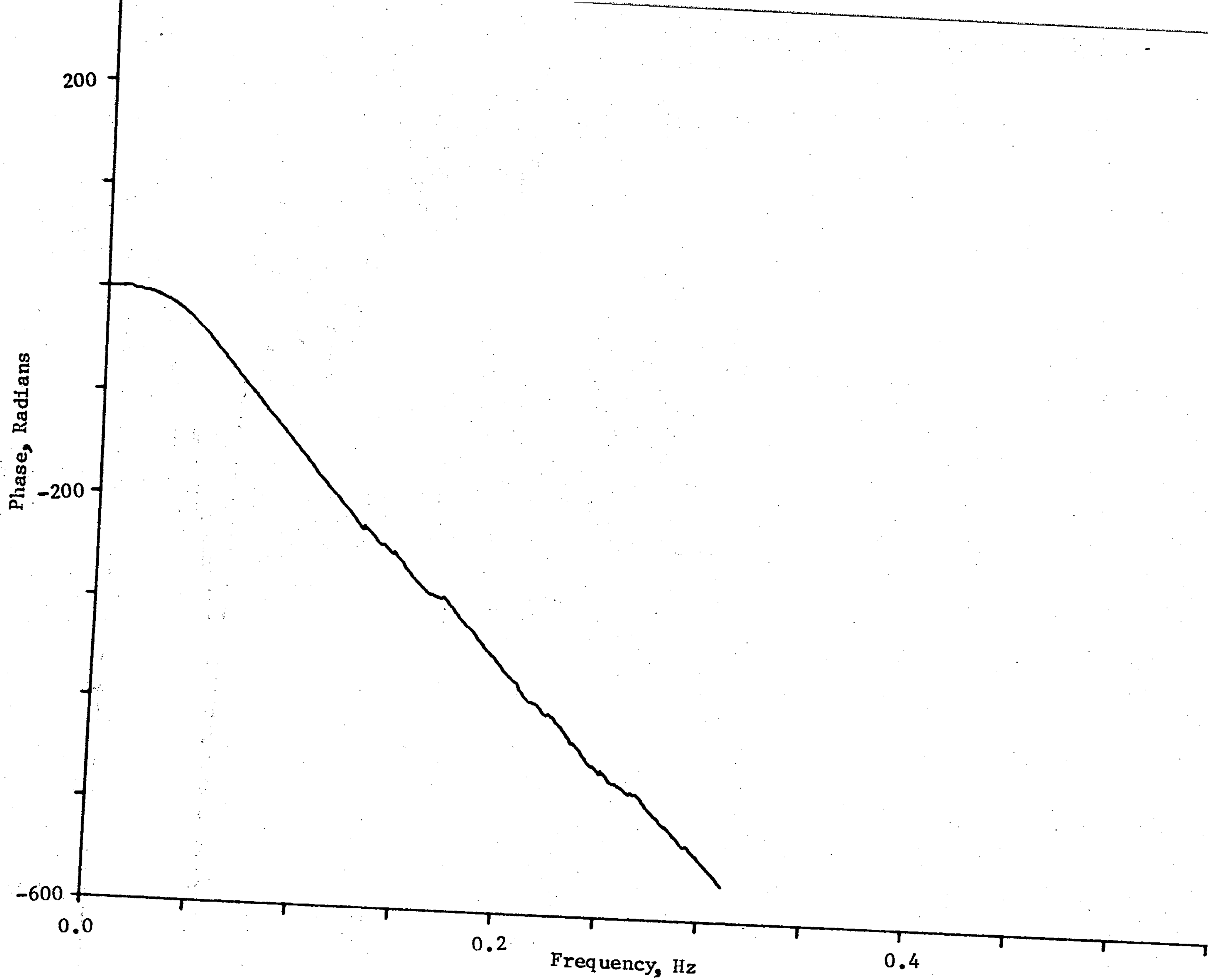

FIGURE 3. THE SPECTRAL PHASE CONTENT OF THE KONGSBERG RECORD

```
      0.015                          0.076
4.04 82.86.81.66.61.70.70.68.64.65.67.65.64.58.58.49.58.63.
4.00 82.87.83.68.59.69.70.69.65.64.68.67.65.58.58.37.59.65.
3.96 82.87.84.70.57.69.71.69.64.64.68.68.65.58.58.52.59.66.
3.92 82.87.85.72.56.68.71.70.63.65.69.69.65.57.55.57.59.66.
3.88 82.88.86.73.57.66.71.71.62.67.68.69.66.55.47.60.60.64.
3.84 82.88.87.75.60.64.70.71.64.69.68.68.66.55.55.62.60.60.
3.80 82.88.88.77.63.61.70.72.67.70.67.66.67.62.63.64.61.57.
3.76 82.88.89.79.65.58.69.73.70.70.67.60.67.67.67.66.65.65.
3.72 82.88.89.80.68.57.69.73.72.71.67.57.68.71.70.68.68.68.
3.68 82.88.90.82.69.58.69.74.73.71.68.63.69.72.71.70.68.68.
3.64 82.88.91.83.71.61.68.74.73.71.70.67.70.72.71.71.68.61.
3.60 82.88.91.85.72.64.68.74.72.72.71.69.70.70.71.70.66.60.
3.56 82.88.92.86.73.67.68.74.70.73.72.69.69.67.69.68.65.65.
3.52 82.88.92.87.74.69.68.73.66.73.72.69.66.64.66.64.65.63.
3.48 81.87.92.89.75.69.69.72.57.72.72.69.59.62.61.58.64.59.
3.44 81.87.92.90.76.69.70.71.56.71.71.67.56.62.59.57.63.63.
3.40 81.86.92.91.78.68.72.69.63.69.69.64.60.62.60.63.65.67.
3.36 81.86.92.92.80.65.73.69.65.67.67.61.59.63.64.67.69.68.
3.32 80.85.91.93.82.65.74.68.66.68.66.60.53.63.68.71.72.69.
3.28 80.84.91.93.83.68.74.68.67.69.66.56.51.62.70.73.74.73.
3.24 80.84.90.94.85.71.73.68.67.69.67.58.53.58.70.73.74.74.
3.20 79.83.89.94.87.74.72.66.65.69.67.65.60.64.70.72.73.73.
3.16 79.81.88.94.88.76.69.65.61.66.65.68.68.69.71.69.69.66.
3.12 79.80.86.94.90.78.64.67.56.58.61.68.71.72.70.63.62.62.
3.08 78.79.85.94.91.80.64.71.56.61.58.67.71.73.72.65.63.68.
3.04 78.78.83.93.92.82.70.72.61.65.61.65.71.72.73.73.71.71.
3.00 77.77.80.92.93.84.73.72.64.59.62.60.70.70.70.74.75.74.
2.96 76.76.78.90.94.86.72.71.60.59.63.56.68.67.63.71.75.76.
2.92 76.75.76.89.94.88.66.73.61.68.63.64.67.69.64.73.74.75.
2.88 75.74.74.87.94.91.75.78.73.71.62.66.69.69.70.74.74.72.
2.84 74.73.74.85.93.93.84.83.79.75.61.64.71.64.70.71.74.72.
2.80 74.73.73.82.92.95.90.88.83.76.63.70.71.63.60.70.70.73.
2.76 73.72.73.80.90.96.94.91.86.76.65.76.75.72.72.70.62.59.
2.72 72.72.73.78.89.96.97.93.87.80.75.80.81.79.75.61.71.75.
2.68 71.72.73.76.87.96.98.95.85.83.84.85.84.84.83.82.82.82.
2.64 70.72.73.75.86.95.99.97.83.86.90.89.84.80.87.89.90.89.
2.60 69.72.72.74.85.92.99.98.90.90.93.93.90.88.92.94.94.92.
2.56 68.72.72.74.82.89.97.98.94.93.94.94.94.95.95.96.95.93.
2.52 66.72.71.74.78.85.95.97.95.93.92.92.93.94.94.92.89.88.
2.48 65.71.71.73.73.79.93.94.91.90.85.84.88.88.88.84.73.76.
2.44 62.70.70.72.68.69.90.91.81.85.77.78.77.75.80.81.81.81.
2.40 59.69.68.69.68.60.87.88.78.81.79.75.72.69.77.76.73.74.
2.36 54.67.66.63.70.71.84.85.83.81.75.67.71.73.72.71.60.67.
```

Velocity, km/s

Frequency, Hz

FIGURE 4. THE MATRIX E AND THE SELECTED GROUP VELOCITY CURVE (KONGSBERG RECORD)

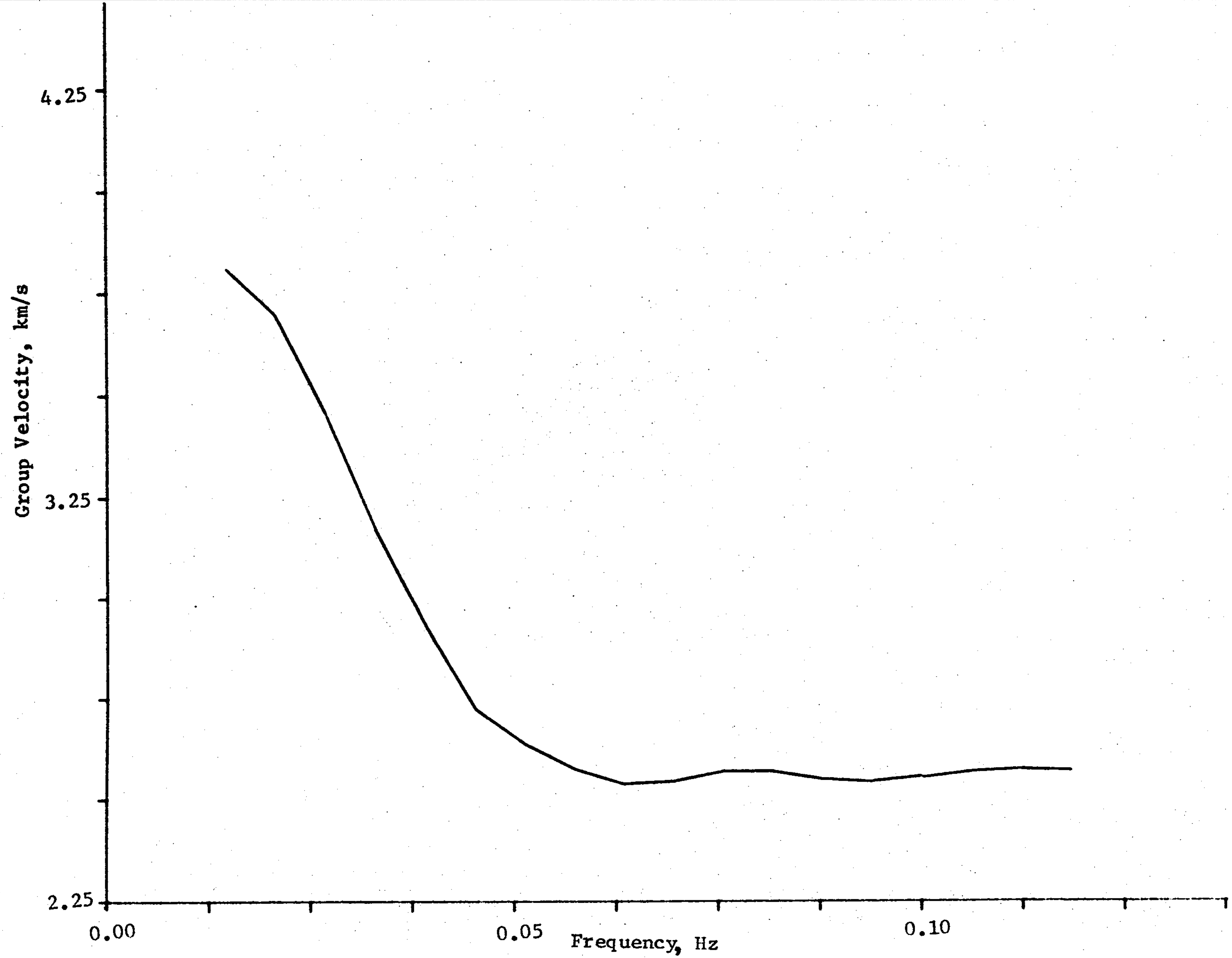

FIGURE 5. THE GROUP VELOCITY CURVE (KONGSBERG RECORD)

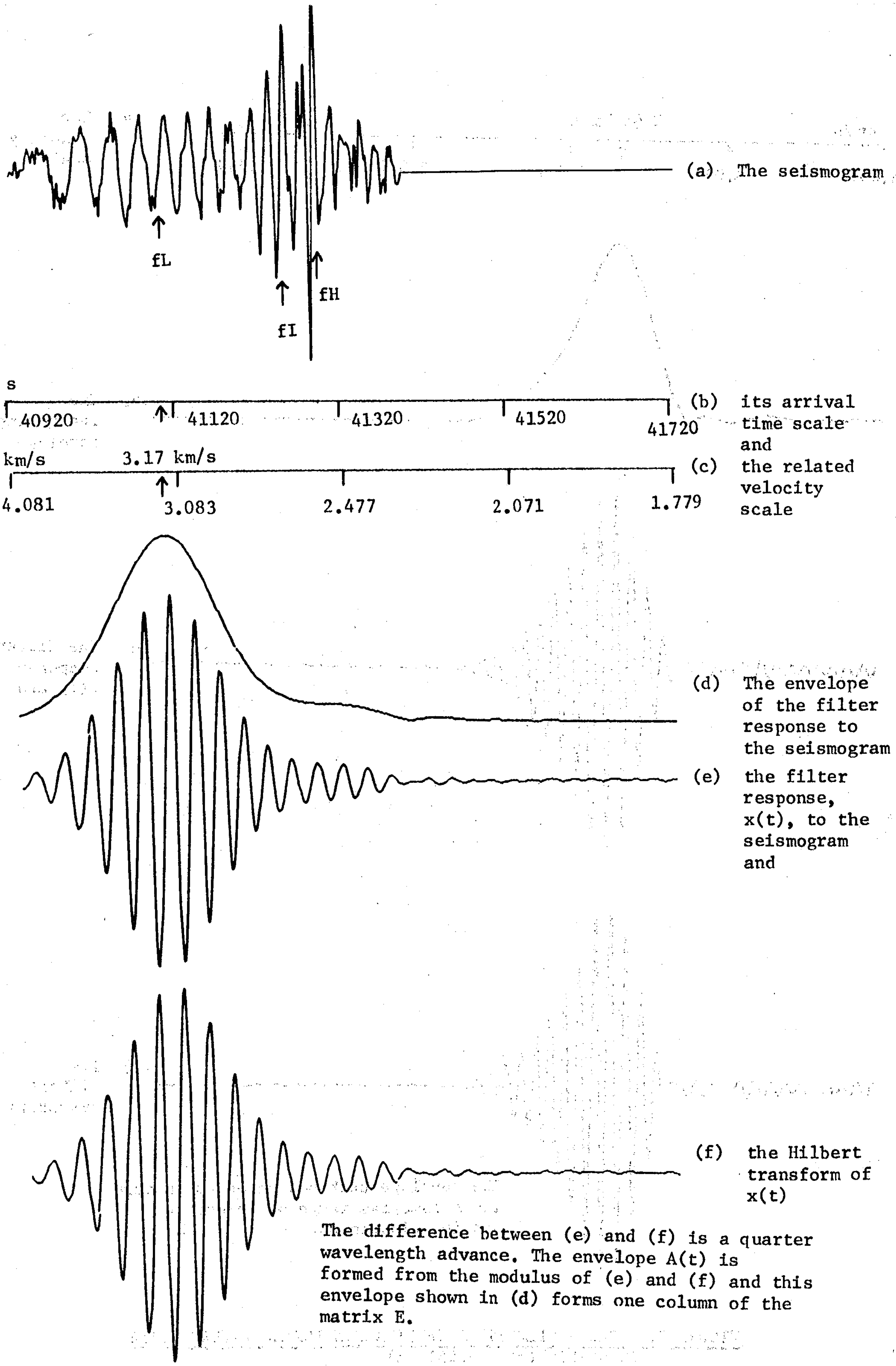

The difference between (e) and (f) is a quarter wavelength advance. The envelope A(t) is formed from the modulus of (e) and (f) and this envelope shown in (d) forms one column of the matrix E.

FIGURE 6. A GROUP VELOCITY DETERMINATION FOR A LOWER FREQUENCY (fL = 0.033 Hz)

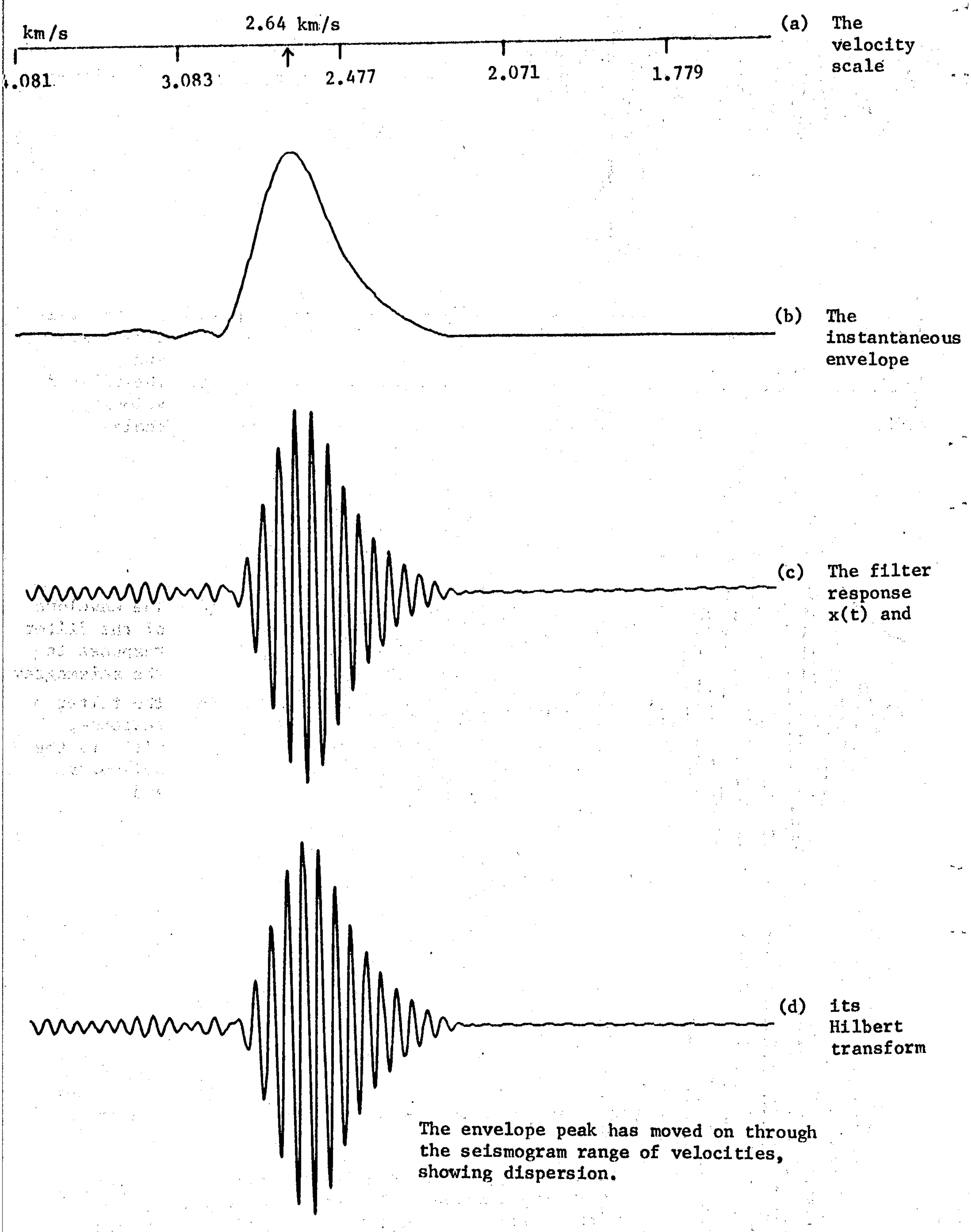

FIGURE 7. A GROUP VELOCITY DETERMINATION FOR AN INTERMEDIATE FREQUENCY (fI = 0.051 Hz)

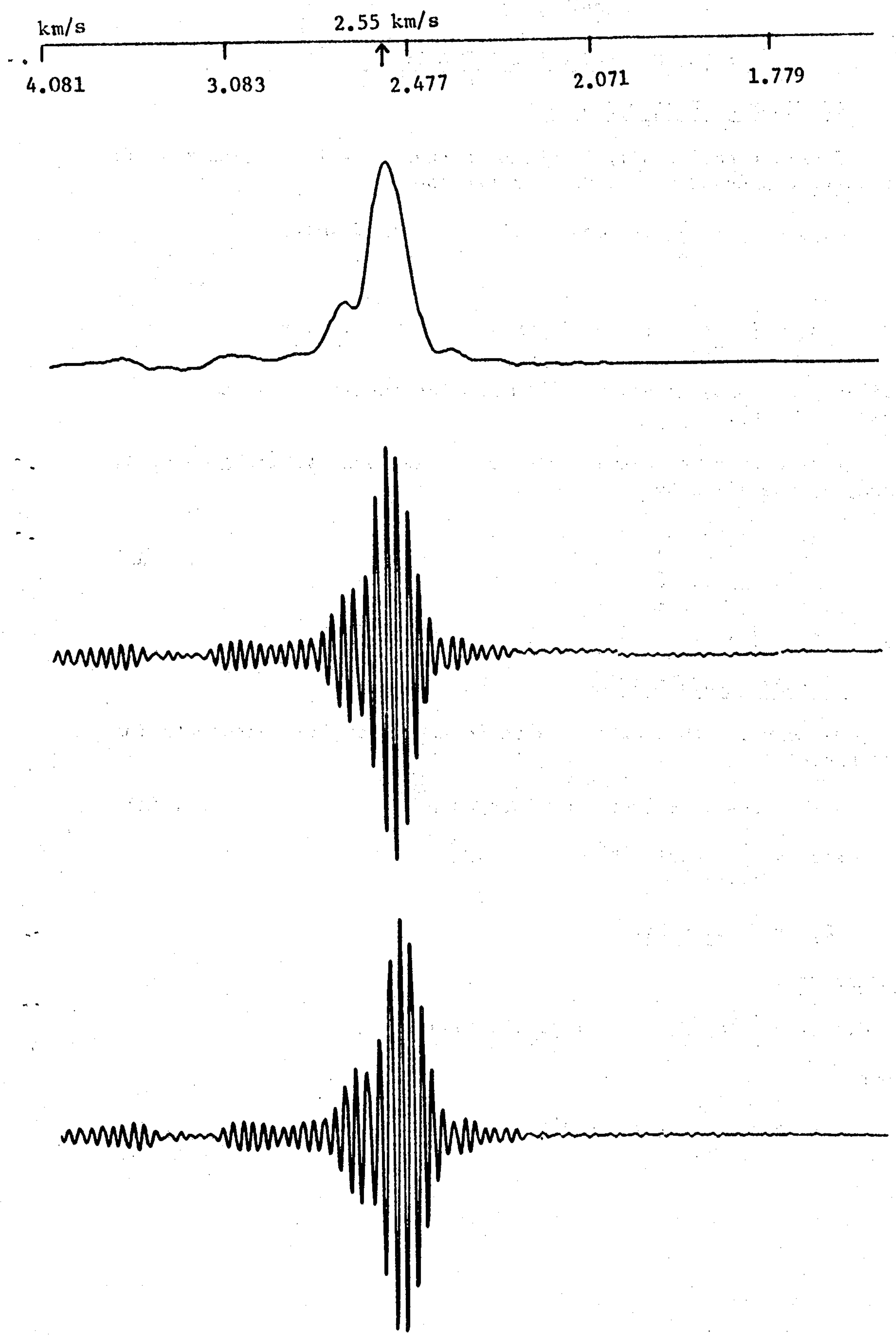

FIGURE 8. A GROUP VELOCITY DETERMINATION FOR A HIGHER FREQUENCY (fH = 0.088 Hz). FIGURES 7 AND 8 GIVE SIMILAR GROUP VELOCITIES BECAUSE THERE IS A MINIMUM TURNING POINT IN THE DISPERSION CURVE, FIGURE 5 (AN AIRY PHASE IN THE TIME DOMAI

APPENDIX A

COSINUSOIDAL AND COMPLEX TRANSFORMS

A1. CONTINUOUS, PERIODIC DATA

If the function x(t) is periodic (period = T, frequency = Df) then it maybe expressed as the Fourier series

$$x(t) = \frac{a_o}{2} + \sum_{j=1}^{\infty} (a_j \cos 2\pi jDft + b_j \sin 2\pi jDft)$$

$$a_j = \frac{2}{T} \int_{-T/2}^{T/2} x(t) \cos 2\pi jDftdt \quad j = 1 \ldots\ldots \infty \qquad \ldots\ldots(A1)$$

and similarly b_j. Orthogonality of cosinusoids easily gives the coefficients a_j, b_j.

In the frequency domain discrete line spectral amplitudes, A, and phase, ϕ, are given by

$$\left.\begin{aligned} A_j &= (a_j{}^2 + b_j{}^2)^{\frac{1}{2}} \\ \phi_j &= \tan^{-1} \left(\frac{b_j}{a_j}\right) \end{aligned}\right\} \qquad \ldots\ldots(A2)$$

at $f_j = j \times Df$.

A2. COMPLEX REPRESENTATION

De Moivre's theorem allows us to use a complex representation for (A1) since

$$e^{ip\theta} = \cos p\theta + i \sin p\theta \text{ (integer p)} \qquad \ldots\ldots(A3)$$

$$x(t) = \sum_{j=-\infty}^{\infty} C_j e^{i2\pi jDft},$$

where $C_{\pm j} = \frac{1}{2} (a_j \mp b_j)$,

or alternatively

$$C_j(f_j) = \frac{1}{2} (a_j(f_j) - \text{sign } (f_j)b_j(f_j))$$

therefore

$$C_j(f_j) = \frac{1}{T} \int_{-T/2}^{T/2} x(t)e^{-i2\pi jDft}dt. \qquad \ldots\ldots(A4)$$

A3. CONTINUOUS, NON-PERIODIC, TRANSIENT DATA

The traditional step is to allow the fundamental period to tend to infinity and produce a Fourier transform pair. The coefficients $C_j(f_j)$ become the continuous functional $X(f)$ and $f_{j+1} - f_j \rightarrow 0$. The Fourier transform pair to be used here may be obtained as

$$X(f) = \int_{-\infty}^{\infty} x(t)e^{-i2\pi ft}dt \qquad \text{.....(A5a)}$$

$$x(t) = \int_{-\infty}^{\infty} X(f)e^{+i2\pi ft}df. \qquad \text{.....(A5b)}$$

An important consequence of equation (A3) is that

$$(e^{ip\theta})^* = e^{-ip\theta}$$

and if $x(t)$ is wholly real in equations (A4) and (A5a) it follows that

$$X^*(f) = X(-f)$$

and therefore values of the functional $X(f)$ are dependently related about $f = 0$, and concern over calculations for negative frequencies is reduced.

A4. DISCRETE DATA OF FINITE LENGTH

We have the time series $x(t)$ sampled at N points giving the values x_n ($n = 0$ ..... $N - 1$). There is a constant time interval Dt between adjacent values of x_n and adapting equation (A5a) gives

$$X(f_j) = Dt \sum_{n=0}^{N-1} x_n e^{-i2\pi f_j nDt}. \qquad \text{.....(A6)}$$

It is apparent that $X(f)$ now assumes discrete values at the frequencies $f_j (|f_j| < \infty)$.

Expanding (A6)

$$X(f_j) = Dt \sum_{n=0}^{N-1} x_n(\cos 2\pi f_j nDt - i \sin 2\pi f_j nDt)$$

and therefore

$$Csp(f_j) = |sign(f_j)| \, Dt \sum_{n=0}^{N-1} x_n \cos 2\pi f_j nDt$$

$$Ssp(f_j) = sign(f_j) \, Dt \sum_{n=0}^{N-1} x_n \sin 2\pi f_j nDt$$

and again if x_n is real then $X^*(f_j) = X(-f_j)$.

The values of $Csp(f_j)$ and $Ssp(f_j)$ must be evaluated at discrete frequencies f_j. For maximum information from the data, of length T, use

$$f_j = j \times Df = \frac{j}{T} = \frac{j}{N \times Dt} \qquad |j| \leq \frac{N}{2}$$

and

$$f_{NYQ} = \frac{1}{2 \times Dt}$$

is the highest frequency, the Nyquist, which can be discriminated in the data. If no frequencies greater than f_{NYQ} are present in the continuous series $x(t)$ then the above procedure exactly represents $x(t)$ for all t, even though it was only sampled at times nDt.

The new expressions for amplitude and phase, which should be compared to equations (A2), are

$$\left.\begin{aligned} A_j &= (Csp^2 + Ssp^2)^{\frac{1}{2}} \\ \phi_j &= \tan^{-1} \left(- \text{sign } (f) \frac{Ssp}{Csp}\right) \\ \text{at} \quad f_j &= j \times Df. \end{aligned}\right) \quad .....(A7)$$

It is worth noting that the dimensions of spectral amplitudes A are length × time, eg, micron seconds.

APPENDIX B

SCALING THE COOLEY-TUKEY CALCULATIONS AND THE SUBROUTINE COOL

B1. SCALING

Recursion formulae have been obtained which reduce computation time for Fourier transforms considerably. For discrete data of finite length we have equation (A6)

$$X(f_j) = Dt \sum_{n=0}^{N-1} x_n e^{-i2\pi f_j nDt}$$

and since $f_j = \frac{j}{N \times Dt}$ we obtain

$$X(f_j) = Dt \sum_{n=0}^{N-1} x_n e^{-\frac{i2\pi jn}{N}} \qquad |j| \leq \frac{N}{2}$$

Computational algorithms of the Cooley-Tukey type are derived from series of the type

$$Z_j = \sum_{n=0}^{N-1} Y_n e^{-\frac{i2\pi jn}{N}}, \qquad \text{.....(B2)}$$

where Z_j and Y_n are complex [4].

For machine computation equation (B2) gives results which are not unit dependent because the scale factor Dt has been omitted. Similarly on the reverse transform the factor Df is omitted. To obtain absolute values after applying COOL to the complex array Z(I):-

(1) Time to frequency, scale factor is Dt(Dt = DELA)

$$Z'(I) = Z(I) \times DELA.$$

(2) Frequency to time, scale factor is Df = 1/NDt

$$Z'(I) = \frac{Z(I)}{N \times DELA}.$$

B2. SUBROUTINE COOL

The digital time series x_n must have N points where N is some power of 2, that is, $N = 2^L$. An extra power of 2, as in this program, ensures that convolution formed by multiplication of two transforms in the frequency domain gives accurate values over the time domain range of interest [5]. Also x_n is stored in the real part of a complex array Z. The Fortran statement CALL COOL (L, Z, +1) performs the direct transform. On return from this call the storage in Z is:-

(1) ReZ contains the cosine spectrum, $Csp(f_j)$.

(2) ImZ contains the sine spectrum $Ssp(f_j)$.

Also Z(1) contains the dc component to be set to zero. The components are folded about the array index number (N/2) + 1, NBY2P1, so that

$$Z(NBY2P1 + I) = Z^{*}(NBY2P1-I)$$

for I = 0 ... (N/2) - 1. Therefore the cosine spectrum is reflected symmetrically and the sine spectrum antisymmetrically. This creates negative frequency components in stores NBY2P1 + 1 to N of Z(I). Amplitude and phase are given by equation (A7).

Reverse transforms would be formed by storing components as they are obtained above, but calling COOL with -1.0 replacing +1.0. The time series is then returned in ReZ(I) [5].

APPENDIX C

THE ANALYTIC SIGNAL FOR "ENVELOPE" DETERMINATION

C1. ENVELOPE DEFINITION

It is difficult to define the envelope to an oscillating signal because the envelope only occasionally touches the signal and may be poorly defined between contacts.

For the real function $x(t)$ consider the complex function $\hat{x}(t)$

$$\hat{x}(t) = x(t) - iHx(t),$$

where H is an operator representing the Hilbert transform. If these functions have a mean frequency $\bar{f}$ then

$$x(t) = A(t)\,e^{i2\pi\bar{f}t},$$

where $A(t)$ is complex. We may now define the instantaneous amplitude of our exactly defined envelope as $|A(t)|$ [6].

C2. FREQUENCY COMPONENTS OF THE ENVELOPE

Consider the Fourier transforms of $x(t)$ and $Hx(t)$; F is the Fourier operator:-

$$Fx(t) = A(w) + i \text{ sign } (w)B(w) \qquad (w = 2\pi f)$$

$$\begin{aligned} FHx(t) &= i \text{ sign } (w)Fx(t) \\ &= i \text{ sign } (w)(A(w) + i \text{ sign } (w)B(w)) \\ &= -B(w) + i \text{ sign } (w)A(w). \end{aligned}$$

The Fourier transform of the analytic signal has components:-

$$\begin{aligned} F\hat{x}(t) &= Fx(t) - iFHx(t) \\ &= A(w) + i \text{ sign } (w)B(w) + iB(w) + \text{sign } (w)A(w) \\ &= \left.\begin{matrix} 2(A(w) + iB(w)) \\ \\ 0 \end{matrix}\right) \begin{matrix} w > 0 \\ \\ w < 0. \end{matrix} \end{aligned}$$

The components of the analytic signal are zero at all negative frequencies and twice the value of the Fourier components of the time signal for positive frequencies.

C3. COMPUTATION

Instantaneous amplitudes of the analytic signal are now easily calculated:-

(1) Calculate the Fourier transform of x(t), obtaining the complex array Z(w).

(2) Set the negative frequency components of Z to zero (ie, those with array indices greater than NBY2P1 up to N).

(3) Calculate the inverse Fourier transform of Z and hence revert to the time domain obtaining $\hat{x}(t)$, which is complex.

(4) Calculate instantaneous amplitudes of the envelope, $|A(t)|$, where

$$|A(t)| = (x(t)^2 + (Hx(t))^2)^{\frac{1}{2}}.$$

Note: The maximum value of $|A(t)|$ is used to determine the group velocity at frequency f for which A(t) has been obtained. The values of $|A(t)|$ for a particular filter frequency are stored in one column of the matrix E. Figures 6, 7 and 8 each show the use of this envelope for group velocity determination and how the envelope relates to its two components.

APPENDIX D

MULTIPLE WINDOW FILTERING IN THE FREQUENCY DOMAIN TO DETERMINE DISPERSION

D1. MULTIPLE FILTERING

A set of r passband filters of constant Q, that is, the ratio peak frequency to bandwidth is constant, and different centre peak frequencies $f_j (1 \leqslant j \leqslant r)$, is chosen. Therefore each filter "windows" a certain passband of the frequency spectrum [1].

Windowing the frequency spectrum of the time series around chosen frequencies allows us to measure signal amplitude as a function of both frequency and time of arrival of energy at that frequency. Time of arrival is easily related to a secondary quantity - group velocity - which is independent of the event to recording station separation. There are p values of group velocity, $u_i (1 \leqslant i \leqslant p)$. We have a two-dimensional, $p \times r$, matrix $E(u,f)$ and chose the group velocity at frequency f_j, out of the p possible values u_i, to be such that $E(u_i, f_j)$ is the maximum value of the column $E(u, f_j)$. This is done for all frequencies f_j to obtain the group velocity curve $u(f_j) (1 \leqslant j \leqslant r)$. This process is illustrated in the sequence of figures 6, 7 and 8 and the results are summarised by the matrix E in figure 4.

D2. THE FILTER

The filter chosen must have good resolution in both domains; we cannot sacrifice resolving power in one domain for improvement in the other. The Gaussian is chosen because for practical purposes the product of its resolution in the two domains is maximum [2,7].

The multiple filters are constant Q of relative bandwidth BAND. For the jth filter the upper and lower frequencies are:-

$$f_j{}^u = (1 + \text{BAND}) f_j$$

$$f_j{}^l = (1 \not\pm \text{BAND}) f_j .$$

The passband Gaussian filter for central frequency f_j is

$$W_j(f) = \begin{cases} 0 & f < f_j{}^l \\ e^{-\alpha \left(\frac{f - f_j}{f_j}\right)^2} & f_j{}^l \leqslant f \leqslant f_j{}^u \\ 0 & f > f_j{}^u \end{cases}$$

where ALPHA determines the resolution or filter roll-off. The filter roll-off is also specified by β where

$$\beta = \ln\left(\frac{W(f_j)}{W(f_j^1)}\right)$$

and therefore

$$\alpha = \frac{\beta}{BAND^2}.$$

(The ratio $W(f_j)/W(f_j^1)$ is read into the computer as the parameter DWF, for example, DWF = 10.0.) Each filter $W_j(f)$ is chosen so that $W(f_j) = 1$ at the central frequency.

The array of central frequencies f_j chosen for the filters is chosen to exactly correspond to harmonic frequencies obtained from the Fourier analysis of the time series. This eliminates errors in previous work which did not match these frequencies [1].

D3. COMPUTATION

The Fourier transform of x(t) is contained in the complex array Z(I), including the non-independent values for negative frequency components. A particular windowing filter is fed into the complex array P(I); this could be done for positive and negative frequency components. For the filter centred at f_j multiplication at each harmonic frequency achieves the required window filtering of the signal

$$Z'(I) = Z(I) \times P(I)$$

and inverse Fourier transform of Z'(I) would give the filtered seismogram at frequency f_j. This would be an oscillating signal of approximately mean frequency f_j, because for $W_j(f)$ we have $\bar{f} = f_j$ because the filter is symmetric about f_j.

Preferably we require the envelope, in the time domain, to Z'(I); this is obtained by setting the negative frequency components to zero (appendix C). This is simply accomplished by just storing the filter in the positive frequency range of P(I) before multiplication and transformation (appendix B, section B2).

APPENDIX E

INSTRUMENTATION PACKAGE

This is an adapted version of a program written by Brune. Full details will be found in the Vesiac report [8]. It is only applicable to long period WWSSN instruments.

If the user wishes to consider an alternative instrument response he should do the following:-

(1) Remove the 78 card library of calibration pulses and the subroutine SSLIBR which reads in this library.

(2) Rewrite subroutine WWSSN (TMCRNS) so that on return from this subroutine the complex array P(I) contains the new instrument transfer function. Also TMCRNS is the conversion factor from one arbitrary unit of displacement for the time series to microns.

(3) The parameter cards 7 and 8 must be altered or removed, as appropriate for the new instrument.

APPENDIX F

PROGRAM LISTING

```
C     TIME  SERIES ANALYSIS PROGRAM
C     ----------------------------
C
C       THE PROGRAM READS IN A DIGITAL SIGNAL SAMPLED AT EQUAL INTERVALS
C     OF TIME. THE SIGNAL IS FOURIER ANALYSED PRODUCING SPECTRAL PHASE
C     AND AMPLITUDE CONTENT AT THE HARMONIC FREQUENCIES. ABSOLUTE VALUES
C     MAY BE OBTAINED BY REMOVING THE INSTRUMENT RESPONSE. A MULTIPLE
C     FILTERING TECHNIQUE IS APPLIED TO PRODUCE A CHARACTERISTIC OF THE
C     DISPERSION -- THE GROUP VELOCITY.
C
C
C
C       GENERAL REFERENCE -- DZIEWONSKI,BLOCH AND LANDISMAN  1969
C     'A TECHNIQUE FOR THE ANALYSIS OF TRANSIENT SEISMIC SIGNALS'
C     BULLETIN OF THE SEISMOLOGICAL SOCIETY OF AMERICA.  59,1, P427-444.
C
C       THE ORIGINAL PURPOSE OF THE PROGRAM WAS TO ANALYSE RAYLEIGH
C     WAVES FROM SEISMIC EVENTS.
C
C-----------------------------------------------------------------------
C
C     OUTPUT
C     ------
C
C     PRINTOUT.
C        1. INPUT OPTION PARAMETERS AND INPUT SIGNAL DATA.
C        2. SPECTRAL AMPLITUDE AND PHASE AT THE HARMONIC FREQUENCIES.
C        3. INSTRUMENTAL MAGNIFICATION AND PHASE AT HARMONIC FREQUENCIES.
C        4. SPECTRAL AMPLITUDE AND PHASE AFTER INSTRUMENT REMOVAL.
C        5. THE SIGNAL AFTER INSTRUMENT REMOVAL.
C        6. INFORMATION ABOUT THE FILTERS.
C        7. GROUP VELOCITY V. FREQUENCY  (KMS/SEC V. HZ)
C        8. THE 2-D MATRIX E -- INSTANTANEOUS ANALYTIC SIGNAL AMPLITUDES
C                               AS A FUNCTION OF FREQUENCY AND VELOCITY.
C
C
C
C     GRAPHS.
C        GRAPHS AT MOST OF THE ABOVE STAGES MAY BE REQUESTED FROM SC4060.
C
C
C     PUNCHOUT.
C        1. THE SMOOTHED FOURIER AMPLITUDE SPECTRUM V. FREQUENCY.
C        2. THE GROUP VELOCITY CURVE V. SELECTED HARMONIC FREQUENCIES.
C
C     MUCH OF THIS OUTPUT IS OPTIONAL.
C
C-----------------------------------------------------------------------
```

```
C
C     HARMONIC FREQUENCIES.
C     ---------------------
C
C
C       SIGNAL OF NSEIS SAMPLES AT INTERVALS DELA SECONDS. NSEIS SET TO
C     N WHERE N/2 GREATER THAN OR EQUAL TO NSEIS AND IS A POWER OF 2.
C
C       1. FUNDAMENTAL FREQUENCY IS     DF = 1/(N*DELA)
C
C       2. FREQUENCY  HARMONICS ARE     FREQ(I) = (I-1)*DF
C
C       3. THE NYQUIST FREQUENCY IS     FNYQ = 1/(2*DELA)
C
C------------------------------------------------------------------------------
C
C     TO USE THIS PROGRAM.
C     --------------------
C
C
C     THE PARAMETER CARDS AND DATA SHOULD BE PUNCHED AS FOLLOWS
C
C     CARD 1. THE RELEVANT SC4060 CARD.
C
C     CARD 2. A 78 CARD LIBRARY OF WWSSN SEISMOMETER CALIBRATION PULSES.
C
C     CARD 3. FORMAT(10A8)
C
C             TITLEA  TITLE FOR THE DATA. IN COLUMNS 73-80 PUNCH AN
C                     IDENTIFICATION LABEL E.G. DATA 001
C
C     CARD 4. FORMAT(8A1,F12.5,I2,I2,F3.1,3X,I2,I2,F3.1,3X,I10)
C
C             STANAM  NAME OF THE RECORDING STATION.
C
C             DELTAD  DISTANCE IN DEGREES BETWEEN EVENT AND RECORDING
C                     STATION. PROGRAM USES 1DEGREE = 111.1 KMS.
C
C             MHOUR   HOURS.
C             MIN     MINUTES.        GMT ORIGIN TIME OF EVENT.
C             SEC     SECONDS.
C
C             MHRGMT  HOURS.
C             MINGMT  MINUTES.        GMT TIME OF FIRST SAMPLE.
C             SECGMT  SECONDS.
C
C             NSEIS   NUMBER OF SAMPLES IN THE DIGITAL TIME SERIES.
C                     NOT MORE THAN 2048.
C
C     CARD 5. FORMAT(F5.1,11I5,3F5.2)
C
C             DELA    INTERVAL BETWEEN SAMPLES (SECONDS).
C
C             IVSEIS  INVERT THE SIGNAL.  (IFF IVSEIS = 1)
C
C             NUMCUT  REMOVE NUMCUT SAMPLES FROM THE FRONT OF THE SIGNAL
C                     AND CORRECT THE FIRST SAMPLE TIME BY NUMCUT*DELA.
```

```
NBASE    CORRECT THE SIGNAL TO A MEAN BASELINE.
         (IF NBASE = 1)

NCOSTP   COSINE TAPER NCOSTP POINTS AT BOTH ENDS OF SIGNAL.

NCOMB    NUMBER OF POINTS IN THE COMB USED TO SMOOTH THE
         FOURIER AMPLITUDE SPECTRUM. MUST BE EVEN. THE COMB
         IS ADVANCED NCOMB/2 POINTS THROUGH THE SPECTRUM
         FOR EACH SMOOTHING OPERATION.

NAFLO    INDEX NO. FOR THE FREQUENCY ARRAY FREQ(I) WHICH
         REFERS TO THE LOWEST FREQUENCY OF INTEREST IN THE
         AMPLITUDE SPECTRUM. ALL FREQUENCIES LOWER THAN
         FREQ(NAFLO+1) = NAFLO*DF ARE REMOVED.

NINSTR   REMOVE THE INSTRUMENT RESPONSE.  (IFF NINSTR = 1)

NUGRUP   CALCULATE GROUP VELOCITIES.  (IFF NUGRUP = 1)

NFLO     INDEX NO. FOR FREQ(I) REFERRING TO THE LOWEST
         FREQUENCY OF INTEREST,NFLO*DF,FOR GROUP VELOCITY
         DETERMINATION. IGNORE FREQUENCY FREQ(NFLO) AND
         BELOW. NFLO MUST BE GREATER THAN NAFLO.

NFHI     INDEX NO. FOR FREQ(I) REFERRING TO THE HIGHEST
         FREQUENCY OF INTEREST,NFHI*DF,FOR GROUP VELOCITY
         DETERMINATION. IGNORE FREQ(NFHI) AND ABOVE.

NFSTEP   INTERVAL BETWEEN ADJACENT FREQUENCIES FOR GROUP
         VELOCITY DETERMINATION IS NFSTEP*DF.
         N.B. THESE ARE THE FILTER CENTRE FREQUENCIES FREQC
         SUCH THAT FREQC(1) = FREQ(NFLO+1) = NFLO*DF ETC.

BAND     DIMENSIONLESS,RELATIVE BANDWIDTH OF GAUSS FILTER.

DWF      DECAY RATE GAUSSIAN FILTER WINDOWING FUNCTION.

DV       VELOCITY STEP ALONG THE SIGNAL. VELOCITY TO FIRST
         SAMPLE = VSF,TO LAST SAMPLE = VSL. CHOOSE DV TO
         DIVIDE VSF-VSL INTO AT MOST 120 VALUES OF VELOCITY

CARD 6. FORMAT(15I1,5X,2I1)  SELECTION OF GRAPHS AS OUTPUT.

NG1      INPUT SIGNAL.

NG2      ADJUSTED SIGNAL PRIOR TO FOURIER ANALYSIS.

NG3      SPECTRAL AMPLITUDE / FREQUENCY (HZ).

NG4      SPECTRAL PHASE (RADIANS) / FREQUENCY (HZ).

NG5      SEISMOMETER CALIBRATION PULSE (WWSSN INSTRUMENT
         RESPONSE TO A STEP OF ACCELERATION).

NG6      INSTRUMENT RESPONSE AMPLITUDE / FREQUENCY (HZ).

NG7      INSTRUMENT RESPONSE PHASE (RADS.) / FREQUENCY (HZ)
```

```
      NG8      SIGNAL WITH INSTRUMENT EFFECT REMOVED.

      NG9      SPECTRAL AMPLITUDE (MICRONS*SECS) / FREQUENCY (HZ)
               INSTRUMENT RESPONSE REMOVED.

      NG10     SPECTRAL PHASE (RADIANS) / FREQUENCY (HZ).
               INSTRUMENT RESPONSE REMOVED.

      NG11     SMOOTHED SPECTRAL AMPLITUDE / FREQUENCY (HZ).

      NG12     GROUP VELOCITY (KMS/SEC) / FREQUENCY (HZ).

      NG13     GROUP VELOCITY (KMS/SEC) / PERIOD (SECONDS).

      NG14     CONTOUR PLOT (AMPLITUDE CONTOURS AT 5DB. INTERVALS
               FOR THE GROUP VELOCITY / FREQUENCY MATRIX).

      NG15     NOT USED.

                        SELECTION OF PUNCHED CARDS AS OUTPUT.

      NP1      PUNCH OUT FREQUENCY / SMOOTHED AMPLITUDE (2E15.7)
               PLUS IDENTIFICATION LABELS AND A CARD COUNT.

      NP2      PUNCH OUT FREQUENCY / GROUP VELOCITY IN (2E15.7)
               PLUS IDENTIFICATION LABELS AND A CARD COUNT.

      N.B. --  THESE OPTIONS ONLY CARRIED OUT WHEN THE OPTION
               PARAMETER IS SET TO 1 E.G. NG5 = 1.

 CARD 7. FORMAT(10A8)

      FMT      VARIABLE FORMAT USED TO INPUT THE SIGNAL.

 ------- CARDS 8 AND 9 OMITTED UNLESS NINSTR = 1.

 CARD 8. FORMAT(10A8)

      TITLEB   TITLE CARD FOR THE INSTRUMENT DATA.

 CARD 9. FORMAT(10F5.1,22X,2I4) WWSSN INSTRUMENT CALIBRATION DATA.

      Q11      TIME WHEN RISING PULSE IS 1/3 OF MAXIMUM HEIGHT.
      Q22      TIME WHEN RISING PULSE IS 2/3 OF MAXIMUM HEIGHT.
      Q33      TIME WHEN RISING PULSE IS AT  MAXIMUM HEIGHT.
      Q44      TIME WHEN FALLING PULSE IS 2/3 ETC.
      Q55      TIME WHEN FALLING PULSE IS 1/3 ETC.
      Q66      TIME WHEN FALLING PULSE IS 1/10 ETC.

      FMASS    SEISMOMETER MASS IN KGMS.
      G        SEISMOMETER MOTOR CONSTANT(NEWTONS/MAMP).
      CLR      CALIBRATION CURRENT(MAMP).
      DEFL     MAXIMUM HEIGHT OF DEFLECTION(MM).

      LABEL    LABEL OF PARTICULAR SEISMOGRAPH CONCERNED.
      NSCALE   CHOICE OF TWO POSSIBLE SCALES WHICH CONVERT THE
               MEASURED VALUES OF Q11 ETC. AND DEFL FROM
               ARBITRARY UNITS INTO SECONDS AND MMS.
```

```
C
C             N.B. -- REMOVAL OF THIS PARTICULAR INSTRUMENT PROBABLY
C                     ONLY RELEVANT TO MY WORK. REFERENCE IS VESIAC
C                     SPECIAL REPORT NO. 4410-106-X 'A TRANSIENT
C                     TECHNIQUE FOR SEISMOGRAPH CALIBRATION-MANUAL AND
C                     STANDARD SET OF THEORETICAL TRANSIENT RESPONSES.'
C                     BY ESPINOSA,SUTTON AND MILLER. (OCTOBER 1965).
C
C             N.B. -- THIS PARTICULAR INSTRUMENT IS EASILY REPLACED.
C                     SEE 'C' REPORT.
C
C     ------- CARDS 8 AND 9 OMITTED UNLESS NINSTR = 1.
C
C
C     CARD1C. FORMAT IS FMT.
C
C             SEIS    DIGITAL SIGNAL DATA. NOT MORE THAN 1024 POINTS.
C
C     CARDS 3 TO 10 REPEATED FOR ANY NUMBER OF SIGNALS.
C
C
C      ---------------------------------------------------------------
C-----------------------------------------------------------------------
C-----------------------------------------------------------------------
C
C     MAIN
C
C
      COMMON/CC1/Z(2048),CZERO,P(2048)
      COMMON/CC2/SEIS(2048),FREQ(1024),AMP(1024),PHASE(1024)
      COMMON/CC3/STANAM(8),DELTAD,DELTA,ORIGTM,GMTSEC
      COMMON/CC4/NSEIS,DELA,IVSEIS,NUMCUT,NBASE,NCOSTP,NCOMB,NAFLO,
     1           NINSTR,NGRUP,NFLO,NFHI,NFSTEP,BAND,CWF,DV,NAFLO1
      COMMON/CC5/NG1,NG2,NG3,NG4,NG5,NG6,NG7,NG8,NG9,NG10,NG11,NG12,NG13
     1           ,NG14,NG15,NP1,NP2
      COMMON/C06/TITLEA(20),DATE,BLANK,TITLEB(20)
      COMMON/CC9/Q1(78),Q2(78),Q3(78),Q4(78),Q5(78),Q6(78),HH1(78),HH2(7
     18),SSIGMA(78),TT1(78),TT2(78),FAC(78),BA,CA,DA,TFAC(78)
      COMMON/C1C/G11,G22,G33,G44,G55,G66,FMASS,G,CUR,DEFL,LABEL,NSCALE
      COMPLEX Z,CZERO,P
      REAL*8 TITLEA,TITLEB,DATE,DUMMY,BLANK
      DATA DUMMY/'        '/
      BLANK=DUMMY
      CALL SCLIBR
      CALL TIMER
      CALL SSLIBR
      CZERO=CMPLX(0.0,0.0)
C
      CALL DATIM(DATE,DUMMY)
  100 READ(5,10,END=999)(TITLEA(I),I=6,15)
   10 FORMAT(10A8)
      PRINT 20,DATE
   20 FORMAT(1H1,///,5X,'SURFACE WAVE ANALYSIS',90X,A8)
      PRINT 30
   30 FORMAT(5X,'---------------------',90X,'--------'/)
      PRINT 40,(TITLEA(I),I=6,15)
   40 FORMAT(20X,10A8//)
```

```
C
      CALL INPUT
      CALL TRACE1
      IF(NINSTR.NE.1.AND.NG11.NE.1.AND.NP1.NE.1) GO TO 50
      CALL TRACE2
 50   IF(NUGRUP.NE.1) GO TO 60
      CALL UGRUP
C
 60   CALL ADVFLM(3)
      CALL ENDFME
      CALL TIMER
      GO TO 100
 999  CALL FINISH
      END
      SUBROUTINE  SSLIBR
C
C     READS IN LIBRARY OF WWSSN CALIBRATION PULSE PARAMETERS.
C     SEE VESIAC REPORT.
C
      COMMON/CC9/Q1(78),Q2(78),Q3(78),Q4(78),Q5(78),Q6(78),HH1(78),HH2(7
     18),SSIGMA(78),TT1(78),TT2(78),FAC(78),BA,CA,DA,TFAC(78)
      DO 1 I=1,78
      READ 2,Q1(I),Q2(I),Q3(I),Q4(I),Q5(I),Q6(I),HH1(I),HH2(I),SSIGMA(I)
     1,TT1(I),TT2(I),FAC(I),BA,CA,DA,TFAC(I)
 2    FORMAT(16F5.1)
      FAC(I)=(FAC(I)*DA)/(BA*CA)/2.0
 1    CONTINUE
      RETURN
      END
      SUBROUTINE INPUT
C
C     READS IN INPUT PARAMETER OPTIONS AND THE INPUT SIGNAL.
C
      COMMON/CC2/SEIS(2048)
      COMMON/CC3/STANAM(8),DELTAD,DELTA,ORIGTM,GMTSEC
      COMMON/CC4/NSEIS,DELA,IVSEIS,NUMCUT,NBASE,NCOSTP,NCOMB,NAFLO,
     1           NINSTR,NUGRUP,NFLO,NFHI,NFSTEP,BAND,DWF,DV,NAFLO1
      COMMON/CC5/NG1,NG2,NG3,NG4,NG5,NG6,NG7,NG8,NG9,NG10,NG11,NG12,NG13
     1           ,NG14,NG15,NP1,NP2
      COMMON/CC6/TITLEA(20),DATE,BLANK,TITLEB(20)
      COMMON/C10/Q11,Q22,Q33,Q44,Q55,Q66,FMASS,G,CUR,DEFL,LABEL,NSCALE
      DIMENSION FMT(10)
      REAL*8 TITLEA,TITLEB,FMT,BLANK,DATE
      READ 10,STANAM,DELTAD,MHOUR,MIN,SEC,MHRGMT,MINGMT,SECGMT,NSEIS
 10   FORMAT(8A1,F12.5,I2,I2,F3.1,3X,I2,I2,F3.1,3X,I10)
C
      READ 20,      DELA,IVSEIS,NUMCUT,NBASE,NCOSTP,NCOMB,NAFLO,NINSTR,
     1NUGRUP,NFLO,NFHI,NFSTEP,BAND,DWF,DV
 20   FORMAT(F5.1,11I5,3F5.2)
      ORIGTM=3600.0*FLOAT(MHOUR)+60.0*FLOAT(MIN)+SEC
      GMTSEC=3600.0*FLOAT(MHRGMT)+60.0*FLOAT(MINGMT)+SECGMT
      GMTLO=0.2*60.0*DELTAD+ORIGTM
      GMTHI=1.0*60.0*DELTAD+ORIGTM
      IF(GMTSEC.GE.GMTLO.AND.GMTSEC.LE.GMTHI) GO TO 30
      PRINT 25
 25   FORMAT(10X,'FAILED TIME TEST')
 30   DELTA=DELTAD*111.1
      PRINT 40,STANAM,DELTAD,DELTA,MHOUR ,MIN   ,SEC   ,ORIGTM,
     1                               MHRGMT,MINGMT,SECGMT,GMTSEC
```

```
40   FORMAT(///10X,'STATION NAME IS ',8A1,
    1      //10X,'DISTANCE OF RECORDING STATION FROM EPICENTRE ',F10.
    2      5,2X,'DEGREES',3X,'OR',3X,F10.4,1X,'KILOMETRES',
    3      ///10X,'ORIGIN TIME OF EVENT ',6X,I2,1X,'HOURS',3X,I2,1X,
    4      'MINS',3X,F4.1,1X,'SECS',10X,'(IN SECONDS) = ',F11.3,
    5      //10X,'GMT TIME OF FIRST SAMPLE ',2X,I2,1X,'HOURS',3X,I2,
    6      1X,'MINS',3X,F4.1,1X,'SECS',10X,'(IN SECONDS) = ',F11.3)
     PRINT50,NSEIS,DELA,IVSEIS,NUMCUT,NBASE,NCOSTP,NCOMB,NAFLO,NINSTR,
    1NUGRUP,NFLO,NFHI,NFSTEP,BAND,DWF,DV
50   FORMAT(///10X,'NSEIS  = ',I5,10X,'DELA    = ',F6.2, 9X,'IVSEIS = ',
    1                           I5,10X,'NUMCUT = ',I5   ,
    2      //10X,'NBASE  = ',I5,10X,'NCOSTP = ',I5   ,10X,'NCOMB   = ',
    3                           I5,10X,'NAFLO  = ',I5   ,
    4      //10X,'NINSTR = ',I5,10X,'NUGRUP = ',I5   ,10X,'NFLO    = ',
    5                           I5,10X,'NFHI   = ',I5   ,
    6      //10X,'NFSTEP = ',I5,10X,'BAND   = ',F6.2, 9X,'DWF     = ',
    7                         F6.2, 9X,'DV     = ',F6.2)
     READ 60,NG1,NG2,NG3,NG4,NG5,NG6,NG7,NG8,NG9,NG10,NG11,NG12,NG13,
    1        NG14,NG15,NP1,NP2
60   FORMAT(15I1,5X,2I1)
     PRINT70,NG1,NG2,NG3,NG4,NG5,NG6,NG7,NG8,NG9,NG10,NG11,NG12,NG13,
    1        NG14,NG15,NP1,NP2
70   FORMAT(///10X,'GRAPH AND PUNCH SELECTION',
    1      //10X,5I1,1X,5I1,1X,5I1,2X,2I1)
     READ 80,FMT
     PRINT90,FMT
80   FORMAT(10A8)
90   FORMAT(//10X,'INPUT FORMAT IS ',10A8)
     IF(NINSTR.EQ.0) GO TO 110
     READ 80,(TITLEB(I),I=6,15)
     READ 100,Q11,Q22,Q33,Q44,Q55,Q66,FMASS,G,CUR,DEFL,LABEL,NSCALE
100  FORMAT(10F5.1,22X,2I4)
110  READ FMT,(SEIS(I),I=1,NSEIS)
     PRINT 120,(SEIS(I),I=1,NSEIS)
120  FORMAT(1H1///10X,'SEISMOGRAM ORIGINAL DATA',
    1      //,(1X,12F10.0))
C
     RETURN
     END
     SUBROUTINE TRACE1
C
C    PREPARES THE SIGNAL FOR FOURIER ANALYSIS AND FOURIER ANALYSES IT.
C
     COMMON/GRFF/TITLE(20),XMAX,XMIN,YMAX,YMIN,INCX,INCY,IND,IDOT,
    1            ANSTR1,IF,XLIMIT,YLIMIT,SCALX,SCALY
     COMMON/C01/Z(2048),CZERO
     COMMON/C02/SEIS(2048),FREQ(1024),AMP(1024),PHASE(1024)
     COMMON/C03/STANAM(8),DELTAD,DELTA,ORIGTM,GMTSEC
     COMMON/C04/NSEIS,DELA,IVSEIS,NUMCUT,NBASE,NCOSTP,NCOMB,NAFLO,
    1           NINSTR,NUGRUP,NFLO,NFHI,NFSTEP,BAND,DWF,DV,NAFLO1
     COMMON/C05/NG1,NG2,NG3,NG4,NG5,NG6,NG7,NG8,NG9,NG10,NG11,NG12,NG13
    1           ,NG14,NG15,NP1,NP2
     COMMON/C06/TITLEA(20),DATE,BLANK
     COMMON/C07/N,NBY2,NBY2P1,NPOW2,FNYQ,DF
     DIMENSION ATITLE(20),BTITLE(20),CTITLE(20)
     REAL*8 TITLE,ATITLE,BTITLE,CTITLE,TITLEA,TYPEMN,TYPE,BLANK,DATE
     COMPLEX Z,CZERO
     DATA ATITLE/'                        SECONDS                SEISMOGRAM AF
```

```
     1TER ANY ADJUSTMENTS IMMEDIATELY PRIOR TO TRANSFORMING BY FOURIER.
     2 '/
      DATA BTITLE/'FREQUENCY (HZ)              AMPLITUDE          AMPLITUDE / F-
     1REQUENCY (HZ) FOR ADJUSTED SEISMOGRAM.
     2 '/
      DATA CTITLE/'FREQUENCY (HZ)              PHASE (RADIANS) PHASE (RADIAN-
     1) / FREQUENCY (HZ) FOR ADJUSTED SEISMOGRAM.
     2 '/
      DATA TYPEMN/'MEAN     '/
      ATITLE(16)=DATE
      BTITLE(16)=DATE
      CTITLE(16)=DATE
C     SET UP N
      NTEST=NSEIS-NUMCUT
      IF(NTEST.GT.2048) CALL EXIT
      N=2
 10   IF(NTEST.LE.N) GO TO 20
      N=2*N
      GO TO 10
 20   N=2*N
      IF(N.GT.2048) CALL EXIT
      CALL POW(N,NBY2,NBY2P1,NPOW2)
      FNYQ=1.0/(2.0*DELA)
      DF=FNYQ/FLOAT(NBY2)
      PRINT 30,N,NBY2,NBY2P1,NPOW2,FNYQ,DF
 30   FORMAT(///10X,'N = ',I5,5X,'NBY2 = ',I5,5X,'NBY2P1 = ',I5,5X,
     1       'NPOW2 = ',I5,5X,'FNYQ = ',F9.5,5X,'DF = ',F9.6,/)
C
      FREQ(1)=0.0
      DO 40 I=2,NBY2
      FREQ(I)=FREQ(I-1)+DF
 40   CONTINUE
      IF(NG1.NE.1) GO TO 70
      DO 50 I=1,5
      TITLEA(I)=BLANK
 50   CONTINUE
      TITLEA(3)=ATITLE(3)
      DO 60 I=17,20
      TITLEA(I)=BLANK
 60   CONTINUE
      TITLEA(16)=DATE
      CALL TIMSER(TITLEA,SEIS,NSEIS,DELA,3)
C
 70   IF(IVSEIS.NE.1) GO TO 85
      DO 80 I=1,NSEIS
      SEIS(I)=-1.0*SEIS(I)
 80   CONTINUE
C
 85   IF(NUMCUT.EQ.0) GO TO 95
      NSEIS=NSEIS-NUMCUT
      GMTSEC=GMTSEC+FLOAT(NUMCUT)*DELA
      DO 90 I=1,NSEIS
      J=I+NUMCUT
      SEIS(I)=SEIS(J)
 90   CONTINUE
C
 95   IF(NBASE.EQ.0) GO TO 100
      IF(NBASE.EQ.1)TYPE=TYPEMN
      IP1=0
      CALL BASE(SEIS,NSEIS,TYPE,IP1)
```

```
C
 10C  IF(NCOSTP.EQ.0) GC TC 110
      PI=4.0*ATAN(1.0)
      CALL NPCSTP(SEIS,NSEIS,NCCSTP,1,PI)
C
 11C  NSESP1=NSEIS+1
      DO 12C I=NSESP1,N
      SEIS(I)=C.C
 12C  CONTINUE
C
      IF(NG2.NE.1) GC TC 130
      CALL TIMSER(ATITLE,SEIS,N,DELA,3)
C     FOURIER TRANSFCRM CF SIGNAL.
 13C  CALL ZRLOAD(N,SEIS,Z)
      CALL COCL(NPCW2,Z,+1.0)
C     FILTER OUT LOW FREQUENIES UP TC NAFLO*DF.
      IF(NAFLC.EQ.0) NAFLC=1
      DO 140 I=1,NAFLC
      Z(I)=CZERO
      AMP(I)=C.C
      PHASE(I)=C.C
 14C  CONTINUE
C
      NAFLO1=NAFLC+1
      DO 150 I=NAFLC1,NBY2
      Z(I)=DELA*Z(I)
      AMP(I)=CABS(Z(I))
      XA=-1.C*AIMAG(Z(I))
      XB=REAL(Z(I))
      IF(XA.EQ.C.C.CR.XB.EC.0.0) GC TC 145
      PHASE(I)=ATAN2(XA,XB)
      GO TO 15C
 145  PHASE(I)=C.C
 15C  CONTINUE
      CALL FILLUP(NBY2P1,Z)
C
      IF(NG3.NE. 1) GC TC 170
      DO 160 I=1,20
      TITLE(I)=BTITLE(I)
 16C  CONTINUE
      CALL CARGRF(FREC,AMP,NBY2)
C
 17C  IF(NG4.NE.1) GC TC 190
      DO 18C I=1,20
      TITLE(I)=CTITLE(I)
 18C  CONTINUE
      CALL DRUM(NBY2,PHASE)
      CALL CARGRF(FREQ,PHASE,NBY2)
 19C  IF(NG3.NE.1.AND.NG4.NE.1) GC TC 210
      PRINT 2C0,(I,FREQ(I),AMP(I),PHASE(I),I=NAFLO1,NBY2,10)
 2CC  FORMAT(1H1///8X,'SEISMCGRAM SPECTRUM',
     1        //,2(8X,'FRECUENCY',6X,'AMPLITUDE',8X,'PHASE',5X),
     2        //,2(I5,3E15.7))
C
 21C  RETURN
      END
      SUBROUTINE TRACE2
```

```
C
C     REMOVES THE INSTRUMENT EFFECT CALCULATED BY SUBROUTINE WWSSN AND
C     SMOOTHS THE SPECTRAL AMPLITUDE / FREQUENCY GRAPH.
C
      COMMON/GRFF/TITLE(20),XMAX,XMIN,YMAX,YMIN,INDX,INCY,IND,ICOT,
     1            ANSTRI,IF,XLIMIT,YLIMIT,SCALX,SCALY
      COMMON/CC1/Z(2048),CZERC,P(2048)
      COMMON/CO2/SEIS(2048),FREQ(1024),AMP(1024),PHASE(1024)
      COMMON/CC3/STANAM(8),DELTAD
      COMMON/CC4/NSEIS,DELA,IVSEIS,NUMCUT,NBASE,NCOSTP,NCOMB,NAFLO,
     1          NINSTR,NLGRUP,NFLO,NFHI,NFSTEP,BAND,CWF,DV,NAFLO1
      COMMON/CC5/NG1,NG2,NG3,NG4,NG5,NG6,NG7,NG8,NG9,NG10,NG11,NG12,NG13
     1          ,NG14,NG15,NP1,NP2
      CCMMON/CC6/TITLEA(20),DATE,BLANK,TITLEB(20)
      COMMON/CC7/N,NBY2,NBY2P1,NPOW2,FNYQ,DF
      DIMENSICN ATITLE(20),TIT1(5),TIT2(5)
      REAL*8 DATE,BLANK,TITLEA,TITLEB,ATITLE,TIT1,TIT2,TITLE
      COMPLEX Z,CZERO,P
      DATA ATITLE/'                               SECCNDS                          SEISMOGRAM WI
     1TH EFFECT CF SEISMCMETER REMCVEC.
     2 '/
      DATA TIT1/'FREQUENCY (HZ)           AMP(MICRON*SECS)'/
      DATA TIT2/'PHASE (RADIANS) AMPLITCEAMP-MAGNIFCATION'/
      TITLE(16)=DATE
      DO 1C I=1,N
      P(I)=CZERC
      SEIS(I)=C.0
 1C   CONTINUE
      DO 20 I=6,15
      TITLE(I)=TITLEA(I)
 2C   CONTINUE
      IF(NINSTR.NE.1) GC TC 175
      CALL WWSSN(TMCRNS)
      DO 30 I=6,15
      TITLE(I)=TITLEA(I)
 3C   CONTINUE
      DO 8C I=NAFLO1,NBY2
      IF(REAL(P(I)).EQ.0.0.AND.AIMAG(P(I)).EQ.0.0) GO TO 40
      Z(I)=Z(I)/P(I)
      GO TO 5C
 4C   Z(I)=CZERC
 5C   AMP(I)=TMCRNS*CABS(Z(I))
      XA=-1.0*AIMAG(Z(I))
      XB=REAL(Z(I))
      IF(XA.EQ.C.C.CR.XB.EC.0.0) GC TC 60
      PHASE(I)=ATAN2(XA,XB)
      GO TO 8C
 6C   PHASE(I)=C.C
      PRINT 7C,I,XA,XB
 7C   FORMAT(//1CX,I5,2F10.5)
 8C   CONTINUE
      CALL FILLLP(NBY2P1,Z)
C
      IF(NG8.NE.1) GC TC 130
      DO 90 I=1,NBY2
      P(I)=TMCRNS*Z(I)
 9C   CONTINUE
      CALL FILLLP(NBY2P1,P)
      CALL COOL(NPOW2,P,-1.0)
      DO 100 I=1,N
      P(I)=P(I)/(DELA*FLCAT(N))
      SEIS(I)=REAL(P(I))
```

```
100   CONTINUE
      PRINT 110,(SEIS(I),I=1,NSEIS)
110   FORMAT(1H1///10X,'SEISMOGRAM WITHOUT INSTRUMENT (MICRONS)',//,
     1       (1X,12F10.3))
      ATITLE(16)=DATE
      DO 120 I=17,20
      ATITLE(I)=BLANK
120   CONTINUE
      IF=3
      CALL TIMSER(ATITLE,SEIS,N,DELA,IF)
C
130   DO 140 I=1,5
      TITLE(I)=TIT1(I)
140   CONTINUE
      IF(NG9.NE.1) GO TO 160
      NM=NBY2-NAFLO1
      CALL CARGRF(FREQ(NAFLO1),AMP(NAFLO1),NM)
160   IF(NG10.NE.1) GO TO 165
      TITLE(4)=TIT2(1)
      TITLE(5)=TIT2(2)
      CALL DRUM(NBY2,PHASE)
      CALL CARGRF(FREQ(NAFLO1),PHASE(NAFLO1),NM)
165   PRINT 170,(I,FREQ(I),AMP(I),PHASE(I),I=NAFLO1,NBY2,10)
170   FORMAT(1H1///8X,'SEISMOGRAM SPECTRUM WITHOUT INSTRUMENT',
     1       //,2(8X,'FREQUENCY',6X,'AMPLITUDE',8X,'PHASE',5X),
     2       //,2(I5,3E15.7))
175   IF(NG11.NE.1.AND.NP1.NE.1) GO TO 280
      NSHIFT=NCOMB/2
      INDF=1
      CALL SMOOTH(AMP,FREQ,NBY2,NCOMB,NSHIFT,KNFL,INDF)
      PRINT 180,(I,FREQ(I),AMP(I),I=1,KNFL)
180   FORMAT(1H1/8X,'SMOOTHED AMPLITUDE SPECTRUM',
     1       //,3(8X,'FREQUENCY',6X,'AMPLITUDE',3X),
     2       //,3(I5,2E15.7))
      IF(NG11.NE.1) GO TO 190
      TITLE(4)=TIT1(4)
      TITLE(5)=TIT1(5)
      IF(NINSTR.EQ.1) GO TO 185
      TITLE(4)=TIT2(3)
      TITLE(5)=BLANK
185   CALL CARGRF(FREQ,AMP,KNFL)
190   IF(NP1.NE.1) GO TO 280
C     PUNCH SMOOTHED AMP./FREQ. SPECTRUM IN (2E15.7).
      PUNCH 220,STANAM,DELTAD,TITLEA(15)
220   FORMAT(8A1,F12.5,2X,A8)
      NL=1
      NH=KNFL
      FLO=NFLO*DF
      FHI=NFHI*DF
230   IF(FREQ(NL).GE.FLO) GO TO 240
      NL=NL+1
      GO TO 230
240   IF(FREQ(NH).LE.FHI) GO TO 250
      NH=NH-1
      GO TO 240
250   PUNCH 260,(FREQ(I),AMP(I),I,STANAM,TITLEA(15),I=NL,NH)
260   FORMAT(2E15.7,15X,I5,'A',9X,8A1,4X,A8)
      PRINT 270,NL,NH
270   FORMAT(/10X,'FREQUENCY RANGE OF PUNCHED OUT SPECTRUM',
     1       //10X,'NL =',I4,5X,'NH =',I4)
280   RETURN
      END
```

```
      SUBROUTINE  WWSSN(INCRNS)
C
C     CALCULATES THE THEORETICAL INSTRUMENT RESPONSE MATCHING NEAREST
C     TO THE OBSERVED DATA. SEE VESIAC REPORT.
C
      COMMON/GRFF/TITLE(20),XMAX,XMIN,YMAX,YMIN,INDX, INDY, IND, IDOT,
     1           ANSTR1,IF,XLIMIT,YLIMIT,SCALX,SCALY
      COMMON/CC1/Z(2048),CZERC,P(2048)
      COMMON/CO2/SEIS(2048),FREQ(1024),AMP(1024),PHASE(1024)
      COMMON/C04/NSEIS,DELA,IVSEIS,NUMCUT,NBASE,NCOSTP,NCOMB,NAFLO,
     1           NINSTR,NUGRUP,NFLC,NFHI,NFSTEP,BAND,CWF,DV,NAFLO1
      COMMON/CC5/NG1,NG2,NG3,NG4,NG5,NG6,NG7,NG8,NG9,NG10,NG11,NG12,NG13
     1,NG14,NG15,NP1,NP2
      COMMON/CC6/TITLEA(20),DATE,BLANK,TITLEB(20)
      COMMON/C07/N,NBY2,NBY2P1,NPCW2,FNYQ,DF
      COMMON/CC9/Q1(78),Q2(78),Q3(78),Q4(78),Q5(78),Q6(78),HH1(78),HH2(7
     18),SSIGMA(78),TT1(78),TT2(78),FAC(78),BA,CA,DA,TFAC(78)
      COMMON/C1C/Q11,Q22,Q33,Q44,Q55,Q66,FMASS,G,CUR,DEFL,LABEL,NSCALE
      COMPLEX Z,CZERC,P,AYEM,PCW
      DIMENSION ATITLE(7),RMS(78)
      REAL*8 TITLEA,DATE,BLANK,TITLEB,ATITLE,TITLE
      AYEM=CMPLX(0.0,-1.0)
      DATA ATITLE/'FREQUENCY (HZ)  SECCNDS AMP-MAGNIFCATIONPHASE (RADIAN
     1S) '/
      PRINT 1C,(TITLEB(I),I=6,15)
   10 FORMAT(1H1///10X,'SEISMCMETER CALIBRATION PULSE  (RESPONSE TO A ST
     1EP OF ACCELERATICN).'///,
     2       1CX,10A8/)
      PI=4.0*ATAN(1.0)
      TITLE(16)=DATE
      AMP(1)=C.C
      PHASE(1)=C.C
      P(1)=CZERO
C     NSCALE    FOR MY OWN USE ONLY WITH A.G.I. DATA
C     THERE ARE TWO DIFFERENT WWSSN FILM CHIP SCALES
C     TWO SCALE FACTORS FOR A.G.I. DATA ARE
C          1. 1 A.G.I. UNIT = 0.32258 SECS. (SCALE1)
C          2. 1 A.G.I. UNIT = 0.16313 SECS. (SCALE2)
      SCALE=0.32258
      IF(NSCALE.EQ.2) SCALE=0.16313
      Q11=SCALE*Q11
      Q22=SCALE*Q22
      Q33=SCALE*Q33
      Q44=SCALE*Q44
      Q55=SCALE*Q55
      Q66=SCALE*Q66
C     FOR MY A.G.I. DATA 1 UNIT DISPLACEMENT IN Y = 0.08 MM.
      DEFL=0.C8*DEFL
      PRINT 20,LABEL,NSCALE,Q11,Q22,Q33,Q44,Q55,Q66,FMASS,G,CUR,DEFL
   2C FORMAT(1CX'CALIBRATICN PULSE DATA LABEL NUMBER =', I5/
     1       1CX'NSCALE =',I4,//
     2   12X,'Q11         Q22         Q33         Q44         Q55         Q66
     3 FMASS       G           CUR         DEFL',//
     4     9X,1C(F8.4,2X),/)
      IF(Q33.NE.C.C) GC TC 40
      PRINT 3C
   3C FORMAT(/1CX,'Q33 = 0.0')
      CALL EXIT
C     NLIBR=78
      PRINT 50,NLIBR
```

```
50    FORMAT(10X,'NUMBER OF LIBRARY SEISMOGRAPHS =',I5,/)
C
      DO 90 I=1,NLIBR
      A=((Q1(I)-Q11)/Q11)**2
      B=((Q2(I)-Q22)/Q22)**2
      C=((Q3(I)-Q33)/Q33)**2
      D=((Q4(I)-Q44)/Q44)**2
      E=((Q5(I)-Q55)/Q55)**2
C
      IF(Q66) 70,60,70
60    F=0.0
      GO TO 80
70    F=((Q6(I)-Q66)/Q66)**2
80    RMS(I)=SQRT(A+B+C+D+E+F)
90    CONTINUE
C
      CALL AMINN(RMS,NLIBR,RMSMIN,NMIN)
C     BEST FITTING LIBRARY SEISMOGRAPH CHARACTERISTICS.
      K=NMIN
      H1=HH1(K)
      H2=HH2(K)
      SIGMA=SSIGMA(K)
      T1=TT1(K)
      T2=TT2(K)
      TTFAC=TFAC(K)
      FFAC=FAC(K)
      PRINT 100,K,RMSMIN
100   FORMAT(10X,'BEST FITTING LIBRARY SEISMOGRAPH IS NUMBER',I5,//
     1          10X,'WITH R.M.S. DEVIATION =',F10.6/)
C
      B2=4.0*H1*H2*(1.0-SIGMA**2)
      C1=T1/T2
C
      U=TTFAC/T1
      D1=C1*C1*(U**4)-(1.0+(C1+B2)*C1)*(U**2)+1.0
      D2=2.0*U*((C1*H1+H2)*C1*U*U-(H1+C1*H2))
      F1=U/SQRT(D1*D1+D2*D2)
      FMFAC=(FMASS*DEFL*FFAC)/(G*CUR*F1)
C     CALCULATE AMPLITUDE RESPONSE(MAGNIFCATION) AND PHASE.
      DO 110 I=2,NBY2
      U=1.0/(FREQ(I)*T1)
      D1=C1*C1*(U**4)-(1.0+(C1+B2)*C1)*(U**2)+1.0
      D2=2.0*U*((C1*H1+H2)*C1*U*U-(H1+C1*H2))
      F1=U/SQRT(D1*D1+D2*D2)
      AMP(I)=F1*FMFAC
      PHASE(I)=ATAN(D1/D2)
      IF(D2.GE.0.0) PHASE(I)=PHASE(I)+PI
      PHASE(I)=PHASE(I)+PI
      P(I)=CMPLX(AMP(I)*COS(PHASE(I)),-1.0*AMP(I)*SIN(PHASE(I)))
110   CONTINUE
C
      IF(NG5.NE.1.AND.NG6.NE.1.AND.NG7.NE.1) GO TO 180
      DO 120 I=5,15
      TITLE(I)=TITLEB(I)
120   CONTINUE
      IF(NG5.NE.1) GO TO 160
      DO 130 I=2,NBY2
      POW=(2.0*PI*FREQ(I))**(-3.0)
      P(I)=-1.0*AYEM*P(I)*POW
```

```
 130  CONTINUE
      CALL FILLUP(NBY2P1,P)
C     FREQ TO TIME.
      CALL COOL(NPOW2,P,-1.0)
      DO 140 I=1,N
      P(I)=P(I)/(DELA*FLOAT(N))
      SEIS(I)=REAL(P(I))
 140  CONTINUE
      TITLE(3)=ATITLE(3)
      IF=3
      CALL TIMSER(TITLE,SEIS,N,DELA,IF)
C
      DO 150 I=2,NBY2
      P(I)=CMPLX(AMP(I)*COS(PHASE(I)),-1.0*AMP(I)*SIN(PHASE(I)))
 150  CONTINUE
      P(1)=CZERO
C
 160  IF(NG6.NE.1.AND.NG7.NE.1) GO TO 200
      NM=NBY2-NAFLO1
      TITLE(1)=ATITLE(1)
      TITLE(2)=ATITLE(2)
      TITLE(3)=BLANK
      IF(NG6.NE.1) GO TO 170
      TITLE(4)=ATITLE(4)
      TITLE(5)=ATITLE(5)
      CALL CARGRF(FREQ(NAFLO1),AMP(NAFLO1),NM)
C
 170  IF(NG7.NE.1) GO TO 180
      TITLE(4)=ATITLE(6)
      TITLE(5)=ATITLE(7)
      CALL DRUM(NBY2,PHASE)
      CALL CARGRF(FREQ(NAFLO1),PHASE(NAFLO1),NM)
 180  PRINT 190,(I,FREQ(I),AMP(I),PHASE(I),I=NAFLO1,NBY2,10)
 190  FORMAT(1H1///8X,'INSTRUMENT RESPONSE',
     1       //,2(8X,'FREQUENCY',6X,'AMPLITUDE',8X,'PHASE',5X),
     2       //,2(I5,3E15.7))
C
 200  TMCRNS=80.0
      DO 210 I=1,NBY2
      J=NBY2+I
      SEIS(I)=0.0
      SEIS(J)=0.0
      AMP(I)=0.0
      PHASE(I)=0.0
 210  CONTINUE
      RETURN
      END
      SUBROUTINE UGRUP

      PERFORMS THE MULTIPLE FILTERING ANALYSIS TO PRODUCE THE DISPERSION
      CHARACTERISTIC AS A FUNCTION OF FREQUENCY AND VELOCITY OF ARRIVAL
      I.E. THE 2-D MATRIX E.

      COMMON/CC1/Z(2048),CZERO,P(2048)
      COMMON/CC8/E(120,120)
      COMMON/CC4/NSEIS,DELA,IVSEIS,NUMCUT,NBASE,NCOSTP,NCOMB,NAFLO,
     1           NINSTR,NUGRUP,NFLO,NFHI,NFSTEP,BAND,CWF,DV,NAFLO1
```

```
      COMMON/CC7/N,NBY2,NBY2P1,NPOW2,FNYQ,CF
      COMMON/C03/STANAM(8),DELTAD,DELTA,CRIGTM,GMTSEC
      COMMON/C02/SEIS(2048),FREQ(1024),AMP(1024),PHASE(1024)
      DIMENSION VSTEP(120),FREQC(120),TABLE(2,2048)
      COMPLEX Z,CZERO,P
      EQUIVALENCE (VSTEP(1),SEIS(1)),
     1            (FREQC(1),SEIS(121)),
     2            (TABLE(1,1),SEIS(1025))
      DO 5 I=1,1024
      J=1024+I
      SEIS(I)=C.0
      SEIS(J)=C.C
      FREQ(I)=C.C
      AMP(I)=C.C
      PHASE(I)=C.C
    5 CONTINUE
C     VELOCITY TC FIRST & LAST SAMPLES.
      TF=GMTSEC
      VSF=DELTA/(TF-CRIGTM)
      TL=GMTSEC+FLOAT(N-1)*DELA
      VSL=DELTA/(TL-ORIGTM)
      PRINT 1C,CRIGTM,GMTSEC,TL,VSF,VSL
   10 FORMAT(1H1//10X,'GRCUP VELOCITY CALCULATION',
     1            /10X,'--------------------------',
     2            //10X,'CRIGIN TIME OF EVENT IS ',F10.2,2X,'SECONDS',
     3            //10X,'TIME OF FIRST SAMPLE IS ',F10.2,2X,'SECONDS',
     4            //10X,'TIME OF LAST  SAMPLE IS ',F10.2,2X,'SECONDS',
     5            //10X,'VELCCITY TC FIRST SAMPLE IS ',F7.3,1X,'KMS/SEC',
     6            //10X,'VELCCITY TC LAST  SAMPLE IS ',F7.3,1X,'KMS/SEC')
C     VELOCITY TO EACH E(I).(EACH DIGIT IN TIME SERIES)
      DO 20 I=1,N
      K=N-I+1
      TABLE(1,I)=DELTA/(GMTSEC+FLOAT(K-1)*DELA-ORIGTM)
   2C CONTINUE
C     MAKE SURE NC. CF VELCCITIES IS LE TC 120.
      IF(VSF.GT.5.0) VSF=5.0
   3C NLIM=(VSF-VSL)/DV
      IF(NLIM.LE.12C) GC TC 40
      DV=2.0*DV
      GO TO 3C
C
   4C K=1
      VSTEP(1)=VSF-DV
   5C IF(VSTEP(K).LE.VSL) GC TC 60
      K=K+1
      VSTEP(K)=VSTEP(K-1)-DV
      GO TO 5C
   6C NROW=K-1
      PRINT 7C,NROW
   7C FORMAT(/10X,'NO. CF VELOCITY STEPS = NROW =',I5)
C     SET UP FILTER VALUES.
      BETA=ALOG(DWF)
      ALPHA=BETA/BAND**2
      PRINT 8C,BETA,ALPHA,DF
   8C FORMAT(/10X,'BETA = ',F8.3,5X,' ALPHA = ',F8.3,5X,'FUNDAMENTAL DF =
     1 ',F8.6)
C
      CALL ZERO2D(E,120,120)
```

```
C
C     CHOOSE CENTRE FRECUENCIES.
      NCOL=1
      IF(NFLO.LT.NAFLO1) CALL EXIT
      FREQC(1)=NFLO*DF
      NFCTWO=NFLO+NFSTEP
      DO 90 I=NFCTWO,NFHI,NFSTEP
      NCOL=NCOL+1
      FREQC(NCOL)=FREQC(NCOL-1)+NFSTEP*DF
   90 CONTINUE
      PRINT 100,NCOL
  100 FORMAT(/10X,'NUMBER OF FREQUENCY STEPS = NCOL =', I5)
C
      IF(NCOL.GT.120) CALL EXIT
      DO 140 J=1,NCOL
      JCOL=J
      CALL GAUSSA(FREQC(J),ALPHA,JCOL)
      DO 110 I=1,N
      P(I)=P(I)*Z(I)
  110 CONTINUE
      CALL COOL(NPOW2,P,-1.0)
      DO 120 I=1,N
      K=N-I+1
      TABLE(2,I)=CABS(P(K))/(FLOAT(NBY2)*DELA)
  120 CONTINUE
C
      DO 130 I=1,NROW
      CALL LOOK(I,2,N,TABLE,VSTEP(I),E(J,I))
  130 CONTINUE
  140 CONTINUE
C
      CALL UEMTRX(NROW,NCOL)
      RETURN
      END
      SUBROUTINE GAUSSA(FC,ALPHA,JCOL)
C
C     CREATES IN THE FREQUENCY DOMAIN A BANDPASS GAUSSIAN FILTER OF
C     SPECIFIED 'Q'.
C
      COMMON/CC1/Z(2048),CZERO,P(2048)
      COMMON/CC7/N,NBY2,NBY2P1,NPOW2,FNYQ,DF
      COMMON/CC4/NSEIS,DELA,IVSEIS,NUMCUT,NBASE,NCOSTP,NCOMB,NAFLO,
     1           NINSTR,NUGRUP,NFLO,NFHI,NFSTEP,BAND,DWF,DV,NAFLO1
      COMPLEX Z,CZERO,P,CPXONE
      CPXONE=(1.0,0.0)
      DO 10 I=1,N
      P(I)=CZERO
   10 CONTINUE
      LM1=FC/DF+0.5
      L=LM1+1
C
      FLO=(1.0-BAND)*FC
      FHI=(1.0+BAND)*FC
      LL=(FC-FLO)/DF+0.5
      CHECK FILTER IS WITHIN TIME SERIES.
      IF((FC-FLOAT(LL)*DF).GT.0.0.AND.(FC+FLOAT(LL)*DF).LT.FNYQ)GO TO 30
      PRINT 20,FC,LL
   20 FORMAT(//10X,'FC =',F10.5,5X,'LL =',I5)
      CALL EXIT
```

```
30    P(L)=CPXONE
C     CHECK FILTER WIDTH.
      IF(LL.GE.1) GO TO 50
      PRINT 40,LL
40    FORMAT(//10X,'CHECK PARAMETER BAND.     LL =', I5)
      CALL EXIT
50    FF=FC
      DO 60 I=1,LL
      J=L-I
      K=L+I
      FF=FF-DF
      PONENT=-ALPHA*((FF-FC)/FC)**2
      P(J)=CMPLX(EXP(PONENT),0.0)
      P(K)=P(J)
60    CONTINUE
      NFILT=2*LL+1
C
      IF(JCOL.EQ.1) PRINT 70
70    FORMAT(/10X,'FC=FILTER CENTRE FREQUENCY (HZ)    FC=(L-1)*DF',
     1      /10X,'L=FREQUENCY ARRAY INDEX NO. CORRESPONDING TO FC',
     2      /10X,'FLO & FHI ARE FILTER BAND LIMITS   FLO=(1-BAND)*FC',
     3      /10X,'NFILT=NO. OF FILTER POINTS',
     4      //6X,'NCOL',9X,'L',10X,'FC',13X,'FLO',10X,'FHI',12X,'NFILT'
     5      )
      PRINT 80,JCOL,L,FC,FLO,FHI,NFILT
80    FORMAT(2(5X,I5),3(5X,F10.5),5X,I5)
C
      RETURN
      END
      SUBROUTINE LEMTRX(NROW,NCOL)
C
C     PRODUCES THE GROUP VELOCITY / FREQUENCY CURVE FROM E BY OBTAINING
C     THE VELOCITY OF THE MAXIMUM ENERGY ARRIVAL AT EACH FREQUENCY.
C     SCALES THE MATRIX E RELATIVE TO A MAXIMUM VALUE OF 99DB.
C
      COMMON/GRFF/TITLE(20),XMAX,XMIN,YMAX,YMIN,INDX,INDY,IND,IDOT,
     1            ANSTR1,IF,XLIMIT,YLIMIT,SCALX,SCALY
      COMMON/C02/SEIS(1024)
      COMMON/C03/STANAM(8)
      COMMON/C04/NSEIS,DELA,IVSEIS,NUMCUT,NBASE,NCOSTP,NCOMB,NAFLO,
     1            NINSTR,NUGRUP,NFLO,NFHI,NFSTEP,BAND,DWF,DV,NAFLO1
      COMMON/C05/NG1,NG2,NG3,NG4,NG5,NG6,NG7,NG8,NG9,NG10,NG11,NG12,NG13
     1            ,NG14,NG15,NP1,NP2
      COMMON/C06/TITLEA(20),DATE,BLANK
      COMMON/C08/E(120,120)
      DIMENSION VSTEP(120),FREQC(120),X(120),Y(120),U(120),PERIOD(120),
     1            ATITLE(6)
      REAL*8 ATITLE,TITLE,TITLEA,DATE,BLANK
      EQUIVALENCE (VSTEP(1),SEIS(1)),
     1            (FREQC(1),SEIS(121)),
     2            (X(1),SEIS(241)),
     3            (Y(1),SEIS(361)),
     4            (U(1),SEIS(481)),
     5            (PERIOD(1),SEIS(601))
      DATA ATITLE/'FREQUENCY (HZ)  PERIOD (SECONDS)GRP.VEL. KMS/SEC'/
      DO 10 I=1,NROW
      X(I)=VSTEP(I)
```

```
 10   CONTINUE
      EMAX=0.0
      DO 40 J=1,NCOL
      DO 20 I=1,NROW
      Y(I)=E(J,I)
 20   CONTINUE
      CALL AMAXN(Y,NROW,U(J),IR)
      YMAX=ABS(U(J))
      IF(EMAX.GE.YMAX) GO TO 30
      IRM=IR
      JCM=J
      EMAX=YMAX
C     QUADRATIC FIT ABOUT MAXIMUM VALUE.
 30   X0=X(IR)
      A=0.5*(Y(IR-1)+Y(IR+1)-2.0*Y(IR))
      B=0.5*(-Y(IR-1)+Y(IR+1))
      C=Y(IR)
      PERIOD(J)=1.0/FREQC(J)
      U(J)=X0+0.5*B/A*DV
 40   CONTINUE
      PRINT 50,(J,FREQC(J),PERIOD(J),U(J),J=1,NCOL)
 50   FORMAT(1H1/20X,'FREQUENCY (HZ) & PERIOD (SECS)/GROUP VELOCITY (KMS
     1/SECS)',
     2       //,3(7X,'FREQUENCY',5X,'PERIOD',5X,'U VELOCITY '),
     3       //,3(I4,3E13.5))
      PRINT 60,EMAX,IRM,JCM
 60   FORMAT(//10X,'EMAX =',E15.7,5X,'IRM =',I5,5X,'ICM =',I5)
      DO 70 I=6,16
      TITLE(I)=TITLEA(I)
 70   CONTINUE
      TITLE(3)=BLANK
      TITLE(4)=ATITLE(5)
      TITLE(5)=ATITLE(6)
      IF(NG12.NE.1) GO TO 80
      TITLE(1)=ATITLE(1)
      TITLE(2)=ATITLE(2)
      CALL CARGRF(FREQC,U,NCOL)
 80   IF(NG13.NE.1) GO TO 90
      TITLE(1)=ATITLE(3)
      TITLE(2)=ATITLE(4)
      CALL CARGRF(PERIOD,U,NCOL)
 90   IF(NP2.NE.1) GO TO 130
C     PUNCH FREQUENCY (HZ) AND GROUP VELOCITY (KMS/SEC) IN (2E15.7).
      PUNCH 120,(FREQC(I),U(I),I,STANAM,TITLEA(15),I=1,NCOL)
 120  FORMAT(2E15.7,15X,I5,'U',9X,8A1,4X,A8)
C
 130  DO 150 J=1,NCOL
      DO 140 I=1,NROW
      E(J,I)=20.0*ALOG10(E(J,I)/EMAX)+99.0
 140  CONTINUE
 150  CONTINUE
C     PRINT OUT E MATRIX.
      N42=(NCOL-1)/42+1
      DO 200 IZ=1,N42
      NLOW=(IZ-1)*42+1
      NHY=NLOW+41
      IF(NHY.GT.NCOL) NHY=NCOL
      PRINT 160
 160  FORMAT(1H1//50X,'MATRIX OF E(I)',///)
      IF(IZ.EQ.1) PRINT 170,(FREQC(I),I=1,NHY,10)
```

```
170   FORMAT(7X,F5.3,4(25X,F5.3))
      DO 180 I=1,NRCW
      PRINT 190,VSTEP(I),(E(J,I),J=NLCW,NHY)
180   CONTINUE
190   FORMAT(1X,F4.2,1X,42F3.0)
200   CONTINUE
C
      IF(NG14.NE.1) GO TO 210
      CALL CONTUR(E,NCOL,NRCW,120,5.0,5.0,100.0,3)
210   RETURN
      END
      SUBROUTINE COOL(N,XX,SIGNI)
C
C     THIS SUBROUTINE WAS PROGRAMMED BY I.MACLEOD, DEPT. OF
C     ENGINEERING PHYSICS,A.N.U. AND HAS BORROWED FROM D. MCCOWAN'S
C     COOL AND IBM'S HARM.
C
C     SINGLE PRECISION VERSION MODIFIED BY J.B.YOUNG FOR THE 360/75.
C
C
C
C
      DIMENSION W(14),XX(1),NBIT(20),JNT(20)
C
C
      INTEGER OFFSET
C
C
      DATA NX/0/
C
C
      IF(NX.GT.0)GO TO 100
      ROOT2=SQRT(2.0)
      PI2=8.0*ATAN(1.0)
C
100   NX=2**N
      NX2=NX+NX
      NX2LS1=NX2-1
      NX2LS2=NX2-2
      NXON8=NX/8
      NXON4=NXON8+NXON8
      NXON2=NXON4+NXON4
      CON1=PI2/FLOAT(NX)
      IF(SIGNI.GT.0.0)GO TO 120
C
      DO 110 K=1,NX2LS1,2
      XX(K+1)=-XX(K+1)
110   CONTINUE
C
120   DO 130 K=1,N
      JNT(K)=2**(N-K)
130   CONTINUE
C
      LSTART=N-N/3*3+1
      IF(LSTART.EQ.1)GO TO 200
      IF(LSTART.EQ.2)GO TO 150
      LBLOK2=NXON2
      L2BLOK=LBLOK2-1
C
      DO 140 K0=1,L2BLOK,2
      K1=K0+LBLOK2
      K2=K1+LBLOK2
      K3=K2+LBLOK2
      A0R=XX(K0)+XX(K2)
```

```
      ACI =XX(K0+1)+XX(K2+1)
      A1R =XX(K0)-XX(K2)
      A1I =XX(K0+1)-XX(K2+1)
      A2R =XX(K1)+XX(K3)
      A2I =XX(K1+1)+XX(K3+1)
      A3R =XX(K1)-XX(K3)
      A3I =XX(K1+1)-XX(K3+1)
      XX(K0)=A0R+A2R
      XX(K0+1)=A0I+A2I
      XX(K1)=A0R-A2R
      XX(K1+1)=A0I-A2I
      XX(K2)=A1R-A3I
      XX(K2+1)=A1I+A3R
      XX(K3)=A1R+A3I
      XX(K3+1)=A1I-A3R
  140 CONTINUE
      GO TO 200
C
  150 LBLOK2=NX
      L2BLOK=LBLOK2-1
      DO 160 K0=1,L2BLOK,2
      K1=K0+LBLOK2
      A1R=XX(K1)
      A1I=XX(K1+1)
      XX(K1)=XX(K0)-A1R
      XX(K1+1)=XX(K0+1)-A1I
      XX(K0)=XX(K0)+A1R
      XX(K0+1)=XX(K0+1)+A1I
  160 CONTINUE
C
C
  200 DO 300 M=LSTART,N,3
      LBLOK2=NX/2**(M+1)
      L2BLOK=LBLOK2-1
      LBLOK1=L2BLOK-1
      LBLOK8=LBLOK2*8
      LBLAST=NX2-LBLOK8+1
C
      DO 210 K=4,N
      NBIT(K)=0
  210 CONTINUE
C
      NW=0
C
      DO 290 OFFSET=1,LBLAST,LBLOK8
      IF(OFFSET.EQ.1)GO TO 220
      ARG=CON1*FLOAT(NW)
      W(1)=COS(ARG)
      W(2)=SIN(ARG)
      CSSQA=W(1)*W(1)
      W(3)=CSSQA+CSSQA-1.0
      W(4)=W(1)*W(2)
      W(4)=W(4)+W(4)
      W(5)=W(3)*W(1)-W(4)*W(2)
      W(6)=W(4)*W(1)+W(3)*W(2)
      CSSQ2A=W(3)*W(3)
      W(7)=CSSQ2A+CSSQ2A-1.0
      W(8)=W(4)*W(3)
      W(8)=W(8)+W(8)
```

```
      W(9)=W(7)*W(1)-W(8)*W(2)
      W(10)=W(8)*W(1)+W(7)*W(2)
      CSSQ3A=W(5)*W(5)
      W(11)=CSSQ3A+CSSQ3A-1.0
      W(12)=W(6)*W(5)
      W(12)=W(12)+W(12)
      W(13)=W(7)*W(5)-W(8)*W(6)
      W(14)=W(8)*W(5)+W(7)*W(6)
  220 LBLOKO=OFFSET+LBLCK1
C
      DO 260 K0=OFFSET,LBLCKO,2
      K1=K0+LBLCK2
      K2=K1+LBLCK2
      K3=K2+LBLCK2
      K4=K3+LBLCK2
      K5=K4+LBLCK2
      K6=K5+LBLCK2
      K7=K6+LBLCK2
      XK0WR=XX(K0)
      XK0WI=XX(K0+1)
      IF(OFFSET.NE.1) GO TO 240
      XK1WR=XX(K1)
      XK1WI=XX(K1+1)
      XK2WR=XX(K2)
      XK2WI=XX(K2+1)
      XK3WR=XX(K3)
      XK3WI=XX(K3+1)
      XK4WR=XX(K4)
      XK4WI=XX(K4+1)
      XK5WR=XX(K5)
      XK5WI=XX(K5+1)
      XK6WR=XX(K6)
      XK6WI=XX(K6+1)
      XK7WR=XX(K7)
      XK7WI=XX(K7+1)
      GO TO 250
  240 XK1WR=XX(K1)*W(1)-XX(K1+1)*W(2)
      XK1WI=XX(K1)*W(2)+XX(K1+1)*W(1)
      XK2WR=XX(K2)*W(3)-XX(K2+1)*W(4)
      XK2WI=XX(K2)*W(4)+XX(K2+1)*W(3)
      XK3WR=XX(K3)*W(5)-XX(K3+1)*W(6)
      XK3WI=XX(K3)*W(6)+XX(K3+1)*W(5)
      XK4WR=XX(K4)*W(7)-XX(K4+1)*W(8)
      XK4WI=XX(K4)*W(8)+XX(K4+1)*W(7)
      XK5WR=XX(K5)*W(9)-XX(K5+1)*W(10)
      XK5WI=XX(K5)*W(10)+XX(K5+1)*W(9)
      XK6WR=XX(K6)*W(11)-XX(K6+1)*W(12)
      XK6WI=XX(K6)*W(12)+XX(K6+1)*W(11)
      XK7WR=XX(K7)*W(13)-XX(K7+1)*W(14)
      XK7WI=XX(K7)*W(14)+XX(K7+1)*W(13)
  250 A0R=XK0WR+XK4WR
      A0I=XK0WI+XK4WI
      A1R=XK1WR+XK5WR
      A1I=XK1WI+XK5WI
      A2R=XK2WR+XK6WR
      A2I=XK2WI+XK6WI
      A3R=XK3WR+XK7WR
      A3I=XK3WI+XK7WI
      A4R=A0R+A2R
      A4I=A0I+A2I
```

```
      A5R =A0R-A2R
      A5I =A0I-A2I
      A6R =A1R+A3R
      A6I =A1I+A3I
      A7R =A3I-A1I
      A7I =A1R-A3R
      XX(K0)=A4R+A6R
      XX(K0+1)=A4I+A6I
      XX(K1)=A4R-A6R
      XX(K1+1)=A4I-A6I
      XX(K2)=A5R+A7R
      XX(K2+1)=A5I+A7I
      XX(K3)=A5R-A7R
      XX(K3+1)=A5I-A7I
      A0R=XK0WR-XK4WR
      A0I=XK0WI-XK4WI
      A8R=XK1WR-XK5WR
      A8I=XK1WI-XK5WI
      A1R=A8R-A8I
      A1I=A8R+A8I
      A2R=XK6WI-XK2WI
      A2I=XK2WR-XK6WR
      A8R=XK3WR-XK7WR
      A8I=XK3WI-XK7WI
      A3R=A8R-A8I
      A3I=A8R+A8I
      A4R=A0R+A2R
      A4I=A0I+A2I
      A5R=A0R-A2R
      A5I=A0I-A2I
      A6R=(A1R-A3I)/ROOT2
      A6I=(A1I+A3R)/ROOT2
      A7R=(A3R-A1I)/ROOT2
      A7I=(A3I+A1R)/ROOT2
      XX(K4)=A4R+A6R
      XX(K4+1)=A4I+A6I
      XX(K5)=A4R-A6R
      XX(K5+1)=A4I-A6I
      XX(K6)=A5R+A7R
      XX(K6+1)=A5I+A7I
      XX(K7)=A5R-A7R
      XX(K7+1)=A5I-A7I
  260 CONTINUE
C
      DO 280 K=4,N
      IF(NBIT(K).NE.0)GO TO 270
      NBIT(K)=1
      NW=NW+JNT(K)
      GO TO 290
  270 NBIT(K)=0
      NW=NW-JNT(K)
  280 CONTINUE
C
  290 CONTINUE
  300 CONTINUE
C
C
      NW=0
C
      DO 310 K=1,N
      JNT(K)=JNT(K)+JNT(K)
      NBIT(K)=0
```

```
  310   CONTINUE
C
        K=0
        IF(NW.LE.K)GO TO 320
        HOLDR=XX(NW+1)
        HOLDI=XX(NW+2)
        XX(NW+1)=XX(1)
        XX(NW+2)=XX(2)
        XX(1)=HOLDR
        XX(2)=HOLDI
C
  320   DO 340 M=1,N
        IF(NBIT(M).NE.0)GO TO 330
        NBIT(M)=1
        NW=NW+JNT(M)
        GO TO 350
  330   NBIT(M)=0
        NW=NW-JNT(M)
  340   CONTINUE
C
  350   DO 390 K=2,NX2LS2,2
        IF(NW.LE.K)GO TO 360
        HOLDR=XX(NW+1)
        HOLDI=XX(NW+2)
        XX(NW+1)=XX(K+1)
        XX(NW+2)=XX(K+2)
        XX(K+1)=HOLDR
        XX(K+2)=HOLDI
C
  360   DO 380 M=1,N
        IF(NBIT(M).NE.0)GO TO 370
        NBIT(M)=1
        NW=NW+JNT(M)
        GO TO 390
  370   NBIT(M)=0
        NW=NW-JNT(M)
  380   CONTINUE
C
  390   CONTINUE
C
        IF(SIGNI.GT.0.0)GO TO 420
C
        DO 410 K=1,NX2LS1,2
        XX(K+1)=-XX(K+1)
  410   CONTINUE
C
C
  420   RETURN
        END
        SUBROUTINE POW(N,NBY2,NBY2P1,NPOW2)
C
C
        NBY2=N/2
        NBY2P1=NBY2+1
        A=(N-1)/2
        NPOW2=ALOG10(A)/ALOG10(2.0)+2.0
        RETURN
        END
        SUBROUTINE ZRLOAD(N,X,Z)
```

```
C
C
      DIMENSICN X(N),Z(N)
      COMPLEX Z
      DO 1 I=1,N
      Z(I)=CMPLX(X(I),C.0)
 1    CONTINUE
      RETURN
      END
      SUBROUTINE FILLUF(NCPTS,Z)
C
C
      DIMENSION Z(1)
      COMPLEX Z,CZERC
      CZERO=CMPLX(C.C,0.0)
      AN=NOPTS-2
      N=ALOG1C(AN)/ALCG1C(2.0)+1.0
      N1=(2**N)+1
      N2=2**(N+1)
      N1M1=N1-1
      DO 1 I=2,N1M1
      NN=N2-I+2
      Z(NN)=CCNJG(Z(I))
 1    CONTINUE
      Z(N1)=CZERC
      RETURN
      END
C                   GENERAL USER SUBROUTINE TIMER
C                   ------- ---- ---------- -----
C
C    FROM THE CALL - CALL TIMER
C     THE TIME FROM THE LAST CALL TIMER IS PRINTEC OUT
C     THE FIRST CALL SETS UP TIMER
C
      SUBROUTINE TIMER
      DATA DIFF/0./
      IF(DIFF) 2,1,2
C
 1    CALL CLOCK(DIFF)
      DIFF=DIFF*6C.
      RETURN
C
 2    CALL CLOCK(TIME)
      TIME=TIME*6C.
      DIFF=TIME-DIFF
      PRINT 3, DIFF
 3    FORMAT(8CX,29HTIME ELAPSED FRCM LAST CALL =,F10.4,8H SECONDS)
      DIFF=TIME
      RETURN
C
      END
      SUBROUTINE BASE (X,N,TYPE, IP1)
C
C
      DIMENSION X(N)
      REAL*8 MEAN,TYPE                                                  ***
      DATA MEAN/8HMEAN    /
```

```
C      IND=3---------COSINE TAPER COSINE TAPER BACK END OF CURVE
C
C      ----------------------------------------------------------------
C
C      X------IS THE ARRAY.
C
C      N-----IS THE NUMBER OF POINTS IN THE ARRAY.
C
C      NO ------IS THE STARTING NUMBER.
C
C      ----------------------------------------------------------------
C
C
       DIMENSION X(N)
C
       AND = NO-1
       PHI = PI/AND
       CPHI = COS(PHI)
       SPHI = SIN(PHI)
       CTHET1 = 1.
       STHET1 = 0.
       CTHET2 = 1.
       STHET2 = 0.
C
       DO 1  I = 1,NO
       GO TO (2,3,4),IND
     2 IA = N-I+1
     3 IN=I
       GO TO 5
     4 IN = N-I+1
     5 X(IN) = 0.5*X(IN)*(1. - CTHET2)
       GO TO (6,9,9),IND
     6 X(IA) = 0.5*X(IA)*(1. - CTHET2)
     9 CALL SINCOS(CPHI,SPHI,CTHET1,STHET1,CTHET2,STHET2)
     1 CONTINUE
C
       RETURN
       END
       SUBROUTINE SINCOS (CPHI,SPHI,CTHET1,STHET1,CTHET2,STHET2)
C
C
       CTHET2 = CTHET1*CPHI - STHET1*SPHI
       STHET2 = STHET1*CPHI + CTHET1*SPHI
       CTHET1 = CTHET2
       STHET1 = STHET2
       RETURN
       END
       SUBROUTINE DRUM(LPHZ,PHZ)
C
C      DRUM MAKES PHASE CURVE CONTINUOUS
C
       DIMENSION PHZ(LPHZ)
       PI=4.0*ATAN(1.0)
       PI2=2.0*PI
       PJ=0.
       DO 40 I=2,LPHZ
       IF(ABS(PHZ(I)+PJ-PHZ(I-1))-PI)40,40,10
    10 IF(PHZ(I)+PJ-PHZ(I-1))20,40,30
    20 PJ=PJ+PI2
       GO TO 40
```

```
C
      SUMX = C
      SUMIX = C
      AN = N
      IF(TYPE - MEAN)1,2,1
    1 IND = 1
      GO TO 3
    2 IND = 2
    3 DO 4  I = 1,N
      AI = I
      SUMX = SUMX + X(I)
      GO TO (5,4),IND
    5 SUMIX = SUMIX + AI*X(I)
    4 CONTINUE
      XBAR = SUMX/AN
      GO TO (6,7),IND
    6 XINTO = (((4.*AN)+2.)*SUMX-6.*SUMIX)/(AN*(AN-1.))
      PHI = ((12.*SUMIX)-6.*(AN+1.)*SUMX)/(AN*(AN+1.)*(AN-1.))
      DO 20 I = 1,N
      AI = I
      X(I) = X(I) - AI*PHI - XINTC
   20 CONTINUE
      PRINT 10, PHI , XBAR
   10 FORMAT(//4X,49HDATA HAS BEEN CORRECTED TO LEAST SQUARES BASELINE/
     14X,32HGRADIENT OF LEAST SQUARES LINE =,F10.5,8X,14HMEAN OF DATA =
     2F10.5)
      GO TO 8
C
    7 DO 30  I = 1,N
      X(I) = X(I) - XBAR
   30 CONTINUE
      PRINT 11, XBAR
   11 FORMAT(//4X,40HDATA HAS BEEN CORRECTED TO MEAN BASELINE//4X,
     114HMEAN OF DATA =,F10.4)
    8 SUMX2 = C
      SUMX3 = C
      DO 9  I = 1,N
      X2 = X(I)*X(I)
      SUMX2 = SUMX2 + X2
      SUMX3 = SUMX3 + X2*X(I)
    9 CONTINUE
      VARX = SUMX2/AN
      A3MNT = SUMX3/AN
      SKEW = (A3MNT*A3MNT)/(VARX**3.)
      PRINT 12, VARX, SKEW
   12 FORMAT(/4X,18HVARIANCE OF DATA =,E10.4,8X,10HSKEWNESS =,F10.4)
      IP1 = IP1 + 1
      GO TO (14,15),IP1
   15 PRINT 16,(I, X(I),  I = 1,N)
   16 FORMAT(//4X,24HTHE BASELINED DATA IS --//5(4X,6HSAMPLE,4X,4HX(I),
     13X)/(5(4X,I5,2X,F10.5)))
C
   14 RETURN
      END
      SUBROUTINE NPCSTP(X,N,NC,IND,PI)
C
C     ------------------------------------------------------------------
C
C     IND=1---------COSINE TAPER BOTH ENDS OF CURVE.
C     IND=2---------COSINE TAPER FRONT END OF CURVE.
```

```
 3C    PJ=PJ-PI2
   4C PHZ(I)=PHZ(I)+PJ
      RETURN
      END
      SUBROUTINE  SMOOTH (X,F,N,NB,NS,KN,IND)
C
C
C     ***********************************************************************
C
C     INPUT PARAMETERS AND RETURNED DATA.
C
C     ***********************************************************************
C
C     X=ARRAY TO BE SMOOTHED (SAY) AMPLITUDES.
C
C     F=ARRAY OF CORRESPONDING (SAY) FREQUENCIES.
C
C     N=NUMBER OF POINTS IN ARRAY X.
C
C     NB=NUMBER OF FREQUENCY BANDS TO BE INCLUDED IN EACH SMOOTHED VALUE
C        -----SET TO AN EVEN NUMBER.
C
C     NS=NUMBER OF FREQUENCY BANDS BETWEEN STEPS (E.G. NB=16 , NS=8 ).
C
C     KN=NUMBER OF SMOOTHED POINTS FED BACK.
C
C     IND=1  SMOOTH X AND F .
C        =2  SMOOTH X ONLY.
C
C     ***********************************************************************
C     ***********************************************************************
C
C
      DIMENSION  X(N),  F(N)
C
      NN=N/NB
      NN=NB*(NN-1)+1
C
      DO 1 K=1,NN,NS
      KN=(K-1)/NS+1
      SUM=0.
      DO 2 I=1,NB
      II=I+K-1
      IF(II.GE.N) II=N-1
      SUM=(X(II)+X(II+1))*0.5+SUM
    2 CONTINUE
      KB=K+NB
      IF(KB.GT.N) KB=N
      X(KN)=SUM/FLOAT(NB)
      GO TO (3,1),IND
    3 F(KN)=(F(K)+F(KB))*0.5
    1 CONTINUE
C
      RETURN
      END
      SUBROUTINE ZERO2D(X,IFIRST,J2ND)
C
C     SETS DOUBLE ARRAY TO ZERO
C
      DIMENSION X(IFIRST,J2ND)
      DO 1 J=1,J2ND
      DO 2 I=1,IFIRST
      X(I,J)=0.0
```

```
  2     CONTINUE
  1     CONTINUE
        RETURN
        END
        SUBROUTINE LOOK(IARGUM,M,N,TABLE,VALIN,VALOT)
C
C       **************
C       IMPORTANT NOTE
C       **************
C          TABLE(1,I) VALUES MUST BE IN INCREASING ORDER OF MAGNITUDE.
C
C
C       IARGUM IS THE INDEX OF THE CURRENT VALUE BEING LOOKED UP IN THE
C       TABLE.
C       VALIN IS A VALUE OF THE VARIABLE STORED IN THE FIRST
C       COLUMN OF TABLE,AND VALOT IS THE CORRESPONDING VALUE OF THE
C       VARIABLE STORED IN THE SECOND COLUMN OF TABLE.
C
C
        DIMENSION TABLE(M,N)
C
C
        NM1=N-1
        DO 1 IT=1,NM1
        IF(TABLE(1,IT)-VALIN)1,2,3
  1     CONTINUE
C
        PRINT 600,VALIN,IARGUM
 600    FORMAT(1H0,20X,13HLOOK ARGUMENTF10.3,13H NOT IN TABLE,'IARGUM=',
       1 I7)
C
        CALL EXIT
C
  2     VALOT=TABLE(2,IT)
        RETURN
  3     DIFF1=TABLE(1,IT-1)-VALIN
        DIFF2=TABLE(1,IT-2)-VALIN
        DIFF3=TABLE(1,IT)-VALIN
        DIFF4=TABLE(1,IT+1)-VALIN
  4     TERM4=(TABLE(2,IT-1)*DIFF3-TABLE(2,IT)*DIFF1)/(DIFF3-DIFF1)
        TERM1=(DIFF3*(TABLE(2,IT-2)*DIFF1-TABLE(2,IT-1)*DIFF2))/(DIFF1-DIF
       1F2)
        TERM3=(DIFF4*(TERM1-(DIFF2*TERM4)))/(DIFF3-DIFF2)
  5     TERM1=DIFF4*TERM4
        TERM2=(DIFF1*(TABLE(2,IT)*DIFF4-TABLE(2,IT+1)*DIFF3))/(DIFF4-DIFF3
       1)
        TERM4=(DIFF2*(TERM1-TERM2))/(DIFF4-DIFF1)
        VALOT=(TERM3-TERM4)/(DIFF4-DIFF2)
C
  6     RETURN
        END
        SUBROUTINE AMAXN(X,N,XMAX,KP)
C
C
        DIMENSION X(N)
        KQ=1
  2     KP=KQ
  5     IF(KQ-N)3,4,4
  3     KQ=KQ+1
        IF(X(KP)-X(KQ))2,5,5
  4     XMAX=X(KP)
        RETURN
        END
        SUBROUTINE AMINN(X,N,XMIN,KP)
```

```
C
C
      DIMENSION X(N)
      KQ=1
    2 KP=KQ
    5 IF (KQ-N) 3,4,4
    3 KQ=KQ+1
      IF (X(KP)-X(KQ)) 5,5,2
    4 XMIN=X(KP)
      RETURN
      END
C     SUBROUTINE TIMSER(TITLE,X,N,DELA,IF)
C
C        THIS ROUTINE PLOTS N VALUES OF THE ARRAY X. DELA IS THE
C     SAMPLING INTERVAL AND IF IS AN INDICATOR WHICH SPECIFIES THE TYPE
C     OF SC4020 OUTPUT REQUIRED.
C          IF IF=1 OUTPUT IS ON MICROFILM
C             IF=2 OUTPUT IS ON HARD COPY
C             IF=3 OUTPUT IS ON BOTH MICROFILM AND HARD COPY.
C
C        TITLE IS A 20 ELEMENT ARRAY CARRYING DATA FOR ANNOTATING THE
C     OUTPUT GRAPHS. THE TITLE ARRAY IS SET UP AS FOLLOWS
C
C          TITLE(1)  - UNUSED
C          TITLE(2)  - UNUSED
C          TITLE(3)  - CONTAINS 8 HOLLERITH CHARACTERS GIVING THE UNITS
C                      OF THE TIME SERIES E.G. SECONDS
C          TITLE(4)  - UNUSED
C          TITLE(5)  - UNUSED
C
C          TITLE(6)  -)
C             .       )CONTAINS 80 HOLLERITH CHARACTERS GIVING A TITLE TO
C             .       )THE GRAPH
C          TITLE(15) -)
C          TITLE(16)   CONTAINS 8 HOLLERITH CHARACTERS GIVING DATE
C          TITLE(17) -)
C             .       )CONTAINS 24 HOLLERITH CHARACTERS GIVING A SUBTITLE
C          TITLE(19) -)TO THE GRAPH
C          TITLE(20) - UNUSED
C
C
      SUBROUTINE TIMSER(TITLE,X,N,DELA,IF)
C
      DIMENSION X(N), TITLE(20)
      REAL*8 TITLE,SECS                                              **
      DATA  SECS/8HSECS    /
C
      CALL AMAX(X,N,XMAX)
      CALL AMIN(X,N,XMIN)
      XRG=XMAX-XMIN
      RANGE=300./XRG
      IF(DELA.EQ..04444.AND.TITLE(3).EQ.SECS)GO TO 20
      S=6.
      IF(N.LE.100)S=7.
      R=0.
    3 IF(DELA.LT.(10.**R*.0000001))GO TO 2
      R=R+1.
      GO TO 3
    2 IF(R.LT.1.)GO TO 99
      INTER = 10.**(8.-R)*DELA + 0.5
      AINTER = FLOAT(INTER)/(10.**(S-R))
      ANXL=(6.*AINTER)/DELA
      GO TO 4
```

```
C
   20 AINTER=5.
      ANXL=675.
C
    4 NXL=ANXL
      NXS=3*NXL
      CONST=800./ANXL
      NT=N/NXS
      NT=NT+1
C
      DO 10 I=1,NT
      CALL ADVFLM(IF)
      IBEGIN=(I-1)*NXS+1
      IEND=NXS
      IF(I*NXS.GT.N)IEND=N-((I-1)*NXS)
      CALL RECORF(X(IBEGIN),1,IEND,XMIN,RANGE,CONST,AINTER,TITLE,NXL)
 10   CONTINUE
C
      CALL ENDFME
   99 RETURN
      END
      SUBROUTINE RECORF(X,IBEGIN,IEND,XMIN,RANGE,CONST,AINTER,TITLE,NXL)
C
C
      INTEGER BASE,POS,BASEL,BASEY,AMARK,XPLOT1,XPLOT2,TPLOT1,TPLOT2
      DIMENSION X(IEND), TITLE(20)
      REAL*8 TITLE                                                    ***
C
      CALL TSP(120,48,8)
C
      DO 1 I=6,15
      CALL HORAM(TITLE(I),8)
 1    CONTINUE
      CALL TSP(120,48,24)
      DO 30 I=17,19
      CALL HORAM(TITLE(I),8)
   30 CONTINUE
C
      DO 5 I=1,3
      BASE=340*I-170
      CALL VECTOR(111,BASE,911,BASE)
      POS=BASE+40
      CALL TSP(801,48,POS)
      CALL HORAM(TITLE(3),8)
      BASEL=BASE+12
      BASEY=BASEL+20
C
      DO 10 J=1,7
      ANMBR=FLOAT(J-1)*AINTER
      AMARK=(FLOAT((J-1)*5)*80.)/3. + 111.
      CALL VECTOR(AMARK,BASE,AMARK,BASEL)
      AMARK=AMARK-40
      CALL TSP(AMARK,48,BASEY)
      CALL C4C2CF(ANMBR,6,1)
 10   CONTINUE
 5    CONTINUE
```

```
C
C
      IBEGI1=IBEGIN+1
      XPLOT1=32C.-(X(IBEGIN)-XMIN)*RANGE
      TPLOT1=111.
      DO 15 I=IBEGI1,IEND
      ILINE=(I-1)/NXL+1
      XPLOT2=34C.*FLCAT(ILINE)-(X(I)-XMIN)*RANGE-20.
      TPLOT2=FLOAT(I-IBEGIN-((ILINE-1)*NXL))*CONST+111.
      IF(I.EQ.(NXL+1).CR.I.EQ.(2*NXL+1))GC TO 20
      CALL VECTOR(TPLCT1,XPLCT1,TPLCT2,XPLOT2)
 2C   XPLOT1=XPLCT2
      TPLOT1=TPLCT2
 15   CONTINUE
C
      CALL TSP(939,48,23)
      CALL HORAM(TITLE(16),8)
C
      RETURN
      END
C      SUBROUTINE CARGRF(X,Y,N)
C
C
C        THIS PACKAGE PLCTS N PCINTS THE CARTESIAN CO-ORDINATES OF THE
C     JTH POINT BEING SPECIFIED AS X(J),Y(J).
C        THE PACKAGE USES THE CCMMON --
C
C     COMMON /GRFF/ TITLE(20), XMAX, XMIN, YMAX, YMIN, INDX, INDY, IND,
C    1IDOT, ANSTR1, IF, XLIMIT, YLIMIT, SCALX, SCALY
C
C       THE TITLE ARRAY CARRIES INFORMATICN FOR ANNOTATING THE OUTPUT
C     GRAPH. THIS ARRAY IS SET UP AS FOLLOWS -
C
C          TITLE(1)  -)
C            .        )CCNTAINS 24 HOLLERITH CHARACTERS GIVING THE UNITS
C          TITLE(3)  -)OF THE ABSCISSAE
C
C          TITLE(4)   )CCNTAINS 16 HOLLERITH CHARACTERS GIVING THE UNITS
C          TITLE(5)   )CF THE CRDINATE
C
C          TITLE(6)  -)
C            .        )CCNTAINS 80 HOLLERITH CHARACTERS GIVING A TITLE TO
C            .        )THE GRAPH
C          TITLE(15) -)
C
C          TITLE(16) -CONTAINS 8 HOLLERITH CHARACTERS GIVING DATE OF
C                     PROCESSING
C          TITLE(17) -CONTAINS 8 HOLLERITH CHARACTERS GIVING TIME OF
C                     PROCESSING
C          TITLE(18) -)
C            .        )UNUSED
C          TITLE(20) -)
C
C          XMAX )SET BOTH EQUAL IF PROGRAM TO CHOOSE THE ABSCISSAE
C          XMIN )SCALE. OTHERWISE SET TO CHOSEN LIMITS OF ABSCISSAE SCALE
C
C          YMAX )SET BOTH EQUAL IF PROGRAM TO CHOOSE THE ORDINATE SCALE.
C          YMIN )OTHERWISE SET TO CHOSEN VALUES OF ORDINATE SCALE
```

```
C
C       INDX IS AN INDICATOR FOR PLOTTING THE ABSCISSAE ON A LOG SCALE
C         INDX=1 ABSCISSAE ON LINEAR SCALE
C         INDX=2 ABSCISSAE ON LOG SCALE
C
C       INDY IS A SIMILAR INDICATOR FOR THE ORDINATE SCALE
C
C       N.B. CONTENTS OF ARRAYS ARE MODIFIED USING LOG SCALE.
C
C       IND IS AN INDICATOR FOR CONTROLLING FRAME CALLS -
C         IND=1 CARGRF CALLS ADVFLM AND ENDFME
C            =2 CARGRF CALLS ENDFME BUT NOT ADVFLM
C
C       IDOT IS THE SC4020 CODE OF THE REQUIRED PLOTTING SYMBOL
C
C       ANSTR1 INDICATES WHETHER THE PLOTTED POINTS HAVE TO BE JOINED UP
C         ANSTR1=1. POINTS NOT JOINED
C               =2. POINTS JOINED
C
C       IF SPECIFIES TYPE OF OUTPUT
C         IF=1 OUTPUT ON MICROFILM
C           =2 OUTPUT ON HARD COPY
C           =3 OUTPUT ON BOTH MICROFILM AND HARD COPY
C
C
C
      SUBROUTINE CARGRF(X,Y,N)
C
      DIMENSION X(N), Y(N)
C
      COMMON /GRFF/ TITLE(20), XMAX, XMIN, YMAX, YMIN, INDX, INDY, IND,
     1IDOT, ANSTR1, IF, XLIMIT, YLIMIT, SCALX, SCALY
C
      REAL*8 TITLE,AJOIN,BLANK,INSTR1,DATE,TIME
C
      INTEGER PLACEX, PLACEY, XPLOT1, XPLOT2, YPLOT1, YPLOT2
C
      DATA AJOIN/8HJOIN    /,BLANK/8H        /
C
C
      CALL DATIM(DATE,TIME)
      IF(IF)2,2,1
 1    IF(IF-4)3,3,2
 2    IF=3
 3    IF(IND.NE.2) IND=1
      IF(INDX.NE.2) INDX=1
      IF(INDY.NE.2) INDY=1
      IF(IDOT.GT.63) IDOT=48
      INSTR1=AJOIN
      IF(ANSTR1.EQ.1.)INSTR1=BLANK
C
C
      GO TO (55,60),INDX
   60 POSXT=POSMIN(X,N)
      POSX=ALOG10(POSXT)
      POSXT=POSXT*0.9999
      DO 201 I=1,N
      IF(X(I).LE.0.0)X(I)=POSXT
```

```
 201 CONTINUE
     CALL CLOG(X,N)
  55 GO TO (65,70),INDY
  70 POSYT=POSMIN(Y,N)
     POSY=ALOG10(POSYT)
     POSYT=POSYT*0.9999
     DO 202 I=1,N
     IF(Y(I).LE.0.0)Y(I)=POSYT
 202 CONTINUE
     CALL CLOG(Y,N)
 65  IF((XMAX-XMIN).GT.1.0E-7)GO TO 66
     CALL AMAX(X,N,XMX)
     CALL AMIN(X,N,XMN)
     IF((XMX-XMN).LT.1.0E-7)XMX=XMX+1.0E-7
     GO TO 67
 66  XMX=XMAX
     XMN=XMIN
 67  IF((YMAX-YMIN).GT.1.0E-7)GO TO 68
     CALL AMAX(Y,N,YMX)
     CALL AMIN(Y,N,YMN)
     IF((YMX-YMN).LT.1.0E-7)YMX=YMX+1.0E-7
     GO TO 200
 68  YMX=YMAX
     YMN=YMIN
 200 GO TO (888,889),IND
 888 CALL ADVFLM(IF)
 889 CALL EXPHVY(123,27,923)
     CALL SCALEN(X,XLIMIT,SCALX,PLACEX,XFACTR,N,XMX,XMN)
     CALL SCALEN(Y,YLIMIT,SCALY,PLACEY,YFACTR,N,YMX,YMN)
     GO TO (777,778),IND
 777 CALL VECTOR(115,923,1003,923)
     CALL VECTOR(123,931,123,43)
C
     DO 5 I=1,11
     FACTOR=FLOAT(I-1)*80.
     XSCAL=203.+FACTOR
     YSCAL=43.+FACTOR
     CALL VECTOR(XSCAL,923,XSCAL,931)
     CALL VECTOR(115,YSCAL,123,YSCAL)
 5   CONTINUE
C
 778 IGUIDE = 1
     IDRAW = 1
     IF(INDX.EQ.2.AND.X(1).LT.POSX)IGUIDE=2
     IF(INDY.EQ.2.AND.Y(1).LT.POSY)IGUIDE=2
     GO TO (998,999),IGUIDE
 998 XPLOT1=(X(1)-XLIMIT)*SCALX + 123.
     YPLOT1=923.-(Y(1)-YLIMIT)*SCALY
     CALL PLOT(XPLOT1,IDOT,YPLOT1)
     IDRAW=2
     IF(INSTR1.NE.AJOIN)IDRAW=1
 999 IGUIDE=1
C
     DO 10 I=2,N
     IF(INDY.EQ.2.AND.Y(I).LT.POSY)IGUIDE=2
     IF(INDX.EQ.2.AND.X(I).LT.POSX)IGUIDE=2
     GO TO (997,996),IGUIDE
 997 XPLOT2=(X(I)-XLIMIT)*SCALX + 123.
     YPLOT2=923.-((Y(I)-YLIMIT)*SCALY)
     CALL PLOT(XPLOT2,IDOT,YPLOT2)
     GO TO (995,994),IDRAW
```

```
  994 CALL VECTOR(XPLOT1,YPLOT1,XPLOT2,YPLOT2)
  995 YPLOT1=YPLOT2
      XPLOT1=XPLOT2
      IGUIDE=1
      IDRAW=2
      IF(INSTR1.NE.AJCIN)IDRAW=1
      GO TO 10
  996 IDRAW=1
      IGUIDE=1
 10   CONTINUE
C
C
      GO TO (779,780),IND
  779 Y4=4.*YFACTR
      X4 = 4.*XFACTR
C
      DO 30 I=1,3
      F=(I-1)
      YLIM=YLIMIT+F*Y4
      GO TO (21,31),INDY
   31 YLIM=10.**YLIM
   21 XLIM=XLIMIT+F*X4
      GO TO (22,32),INDX
   32 XLIM=10.**XLIM
   22 YPOS=915.-F*320.
      XPOS=52.+F*320.
      CALL TSP(12,48,YPOS)
      GO TO (23,33),INDY
   33 CALL C4020E(YLIM,11,2)
      GO TO 41
   23 CALL C4020F(YLIM,13,PLACEY)
   41 CALL TSP(XPOS,48,942)
      GO TO (24,34),INDX
   34 CALL C4020E(XLIM,11,2)
      GO TO 30
   24 CALL C4020F(XLIM,13,PLACEX)
 30   CONTINUE
C
C
      IF(TITLE(16).NE.DATE)GO TO 780
C
      CALL TSP(48,48,291)
      CALL VERAM(TITLE(4),16)
      CALL TSP(760,48,958)
      CALL HORAM(TITLE(1),24)
      CALL TSP(130,48,23)
      CALL HORAM(TITLE(6),80)
C
C
 780  CALL ENDFME
      RETURN
      END
      FUNCTION POSMIN(X,N)
C
C     FINDS MINIMUM POSITIVE VALUE OF ARRAY X
C
C
      DIMENSION X(N)
```

```
C
      IND = 0
      DO 10 I =1,N
      IF(X(I).LE.0.0)GO TO 10
      IND =I
      GO TO 1
   10 CONTINUE
    1 IF(IND.NE.0)GO TO 7
      PRINT 20
   20 FORMAT(132H1AN ARRAY FROM WHICH THE SMALLEST POSITIVE VALUE WAS RE
     1QUESTED FOR GRAPHING WAS ALL NEGATIVE  YOUR JOB HAS THEREFORE BEEN
     2 TERMINATED)
      CALL FINISH
      CALL EXIT
    7 KQ=IND
    5 KP=KQ
    2 IF(KQ-N)3,4,4
    3 KQ=KQ+1
      IF(X(KQ).LE.0.0)GO TO 2
      IF(X(KP)-X(KQ))2,5,5
    4 POSMIN=X(KP)
      RETURN
      END
      SUBROUTINE CLOG(X,N)
C
C     CONVERTS ARRAY X TO COMMON LOGS
C
C
      DIMENSION X(N)
C
      DO 1  I = 1,N
      X(I) = ALOG10(X(I))
    1 CONTINUE
      RETURN
      END
      SUBROUTINE SCALEN(X,XLIMIT,SCALX,IPLACE,FACTOR,N,XMAX,XMIN)
C
C     COMPUTES SCALING VALUES FOR CARGRF
C
C
      DIMENSION X(N)
      DOUBLE PRECISION XRG,R,FACT,S
C
      XRG =XMAX-XMIN
C
      R=0.0D0
    1 IF(XRG.LT.(10.0D0**R*.0000000001)) GO TO 2
      R =R+1.0D0
      GO TO 1
    2 IF(R.LT.1.0D0) GO TO 5
      FACT=(10.0D0**(R-1.0D0)*.000000000125)
      S=0.0D0
    3 IF(XRG.LE.FACT*(2.0D0**S)) GO TO 4
      S=S+1.0D0
      GO TO 3
    4 FACTOR=(FACT*(2.0D0**S))*10.0D-2
C
      XLIMIT=XMIN/FACTOR
      LIMITX=XLIMIT-.99999
      XLIMIT=FLOAT(LIMITX)*FACTOR
      IF(XMIN.LT.XLIMIT)XLIMIT=XLIMIT-FACTOR
      SCALX=80./FACTOR
```

```
      IPLACE=13.-R
      IF(IPLACE.LT.1)IPLACE=1
C
  5   RETURN
      END
      SUBROUTINE AMAX (X,N,XMAX)
C
C     FINDS MAXIMUM VALUE OF ARRAY X
C
      DIMENSION X(N)
      KQ = 1
    2 KP = KQ
    5 IF(KQ -N)3,4,4
    3 KQ = KQ + 1
      IF(X(KP) - X(KQ))2,5,5
    4 XMAX = X(KP)
      RETURN
      END
      SUBROUTINE AMIN (X,N,XMIN)
C
C     FINDS MINIMUM VALUE OF ARRAY X
C
      DIMENSION X(N)
      KQ = 1
    5 KP = KQ
    2 IF(KQ-N)3,4,4
    3 KQ = KQ + 1
      IF(X(KP) - X(KQ))2,5,5
    4 XMIN = X(KP)
      RETURN
      END
      SUBROUTINE CONTUR(A,NX,NY,N,CSTEP,CLOW,CHIGH,IF)
C
C
      DIMENSION A(N,N)
      CALL ADVFLM(IF)
      HX=10.2/FLOAT(NX)
      HY=10.2/FLOAT(NY)
      QX=0.02
      QY=0.02
      DC=CSTEP
      C3=CLOW
      C4=CHIGH
      C1=C4+DC
      C2=C1+DC
      CALL OBC7A(A,DC,C1,C2,C3,C4,NX,NY,HX,HY,QX,QY,0.,1,N)
      CALL ENDFME
      RETURN
      END
      SUBROUTINE CB07A(F,DC,C1,C2,C3,C4,NX,NY,HX,HY,QX,QY,COSS,NQ,IDF)
C
C
      DIMENSION F(IDF,IDF)
      COMMON /CONT/ OX,OY,COSG,SING,DX,DY,CX,CY,X,Y,A,B,C,D,CON,IHL,IHK
      IHL=1
      IHK=2
      IHO=3
      CEN=100.
      OX = QX
      OY = QY
```

```
      COSG = COSS
      DX = HX
      DY = HY
      IX = NX -1
      IY = NY -1
      AA = DX * FLOAT(IX)
      BB = DY * FLOAT(IY)
      CX = 0.5 * DX
      CY = 0.5 * DY
      SING = SQRT(1.-COSG*COSG)
      DELR = 1.0/DC
      IF (COSG) 101,102,102
101   OX = OX - DY*FLOAT(IY)*COSG
102   IF (NQ) 105,105,104
104   XD = CEN*(OX)
      YD = CEN*(OY)
      CALL QUACK(XD,YD,IHL)
      XD = CEN*(OX+AA)
      CALL QUACK(XD,YD,IHK)
      XD = CEN*(OX+AA+BB*COSG)
      YD = CEN*(OY+BB*SING)
      CALL QUACK(XD,YD,IHK)
      XD = CEN*(OX+BB*COSG)
      CALL QUACK(XD,YD,IHK)
      XD = CEN*(OX)
      YD = CEN*(OY)
      CALL QUACK(XD,YD,IHK)
      IF (NQ-1) 105,105,106
106   CONTINUE
      IX1=IX-1
      IY1=IY-1
      DO 107 J=1,IY1
      DO 108 I=1,IX1
      X = FLOAT(I) * DX
      Y = FLOAT(J) * DY
      XD = CEN*(OX+ X+ Y*COSG)
      YD = CEN*(OY+ Y*SING)
  108 CALL QUACK(XD,YD,IHC)
  107 CONTINUE
  105 CONTINUE
      SMALL=1.E-6
      DO 112 J=1,IY
      DO 113 I=1,IX
C
C
C     FOR REASONS WHICH WILL BECOME APPARENT, CONTOUR VALUES SHOULD NOT
C     EXACTLY COINCIDE WITH FIELD VALUES.  TO TAKE AN EXAMPLE, SUPPOSE
C     FIELD VALUES ARE READ IN AS  A=25.3  B=29.4  C=29.4  D=26.5  AND
C     THE CONTOURS ARE REQUESTED BY PUNCHING  C1=20.4  C2=38.4  DC=4.5 .
C     THERE IS THEN THE DANGER THAT CONTOUR 29.4 MIGHT BE IDENTIFIED AS
C     INTERSECTING SIDE BC  (SEE LINE OF EXECUT-
C     302  IF ((B-CCN)*(C-CCN).LT.0) 303,304     ).
C     IF BY CHANCE WE GO TO 303, WE WILL GET TO 402,404,410,OR 412 AND
C     GET OVERFLOW ON DIVIDING BY (C-B).
C         AS ANOTHER EXAMPLE, A MALFUNCTION CAN OCCUR WHEN ONLY ONE OF
C     THE 4 FIELD VALUES IS EQUAL TO A CONTOUR LEVEL.   SUPPOSE A=25.3,
```

```
3 PAUL.W.BURTON£ BLACKNEST£
9.    13.5 25.   42.   56.   71.50.8    .8    0.    30.   100. 43.100.320181.3.048040.00
8.    12.   24.   41.   58.   80.50.8    1.    0.    30.   100. 39.200.320161.0.048040.00
7.50011.5022.5042.0065.00103.00.8001.5000.00030.00100.032.000.320134.0.048040.00
6.50010.0020.0054.00109.0203.00.8003.0000.00030.00100.038.000.640149.00.09640.00
5.0007.50019.0088.00210.0420.00.8006.0000.00030.00100.020.200.640147.8.192040.00
8.50013.5026.0044.0059.0073.501.0000.8000.00030.00100.035.200.320148.8.048040.00
8.00013.5025.5045.0063.0087.501.0001.0000.00030.00100.036.000.320148.8.048040.00
7.50012.0024.0048.5078.00126.01.0001.5000.00030.00100.026.000.320148.5.064040.00
6.00010.0023.5067.00132.0243.01.0003.0000.00030.00100.015.000.320163.8.128040.00
5.0008.50024.00106.0243.0468.01.0006.0000.00030.00100.015.300.640130.5.192040.00
9.50015.5030.5050.5067.0084.001.5000.8000.00030.00100.048.200.640148.5.048040.00
8.50014.0028.5051.5072.0099.001.5001.0000.00030.00100.044.000.640172.0.064040.00
8.00013.0028.5059.0090.00140.01.5001.5000.00030.00100.035.000.640192.8.096040.00
7.50012.0032.0082.00147.0260.01.5003.0000.00030.00100.020.200.640146.3.128040.00
6.00011.0036.00127.0260.0484.01.5006.0000.00030.00100.021.001.280162.0.256040.00
10.5018.0036.0062.5084.00113.03.0000.8000.00030.00100.039.201.020149.5.064040.00
10.0017.5037.0068.5096.00133.03.0001.0000.00030.00100.035.701.020195.0.096040.00
8.50017.5049.00113.5184.0291.03.0003.0000.00030.00100.028.301.020147.8.096040.00
10.0017.0040.0080.50120.0175.03.0001.5000.00030.00100.016.701.020183.8.192040.00
8.50019.0061.00162.0292.0509.03.0006.0000.00030.00100.08.9001.020148.0.256040.00
9.00014.5028.5048.5067.0092.001.0001.0000.00035.00100.077.000.640196.4.048040.00
9.50016.0031.5056.0077.00105.01.5001.0000.00035.00100.052.000.640167.3.048040.00
10.0017.0035.5062.5086.00118.03.0001.0000.00035.00100.033.800.640198.4.064040.00
7.50011.5021.5035.5047.0058.501.0000.8000.00030.0075.0034.600.320161.5.064040.00
7.00011.5022.0037.5052.0070.001.0001.0000.00030.0075.0029.300.320139.0.064040.00
7.00010.5021.5040.5063.00100.01.0001.5000.00030.0075.0021.400.320156.8.096040.00
5.5009.50021.5056.00105.0187.01.0003.0000.00030.0075.0022.600.640176.2.192040.00
4.5008.00023.0086.50185.0357.01.0006.0000.00030.0075.0011.400.640127.3.256040.00
7.50012.5024.0040.0054.0069.001.5000.8000.00030.0075.0046.000.640204.0.096040.00
7.00011.5024.0043.0060.0081.001.5001.0000.00030.0075.0039.800.640176.2.096040.00
7.00011.5024.5050.0075.00113.01.5001.5000.00030.0075.0029.000.640176.3.128040.00
5.5009.50026.5068.00118.0201.01.5003.0000.00030.0075.0015.500.640154.8.192040.00
5.50010.5033.50103.0203.0375.01.5006.0000.00030.0075.0015.801.280116.1.256040.00
9.00015.0030.0052.5072.00101.03.0000.8000.00030.0075.0037.201.020144.3.096040.00
8.50015.0030.5057.0081.00117.03.0001.0000.00030.0075.0032.101.020169.0.128040.00
7.50014.0034.0069.00101.0148.03.0001.5000.00030.0075.0023.401.020196.6.192040.00
7.50015.5044.0098.00154.0237.03.0003.0000.00030.0075.0012.501.020165.0.256040.00
8.00017.5055.00141.0243.0414.03.0006.0000.00030.0075.0012.802.040149.5.384040.00
7.50011.5021.0034.0054.5056.000.8000.8000.00030.0075.0041.000.320173.0.064040.00
7.00011.0019.5034.0047.0065.000.8001.0000.00030.0075.0036.100.320153.0.064040.00
6.50010.0019.5036.0058.0096.000.8001.5000.00030.0075.0025.600.320170.7.096040.00
4.5008.50017.5047.5095.50176.00.8003.0000.00030.0075.0014.00.3200193.0.192040.00
4.0008.00018.5073.00172.0340.00.8006.0000.00030.0075.0014.000.640136.0.256040.00
8.0   12.5 24.5 44.5 62.5 87.001.0   1.0   0.0   25.   100. 50.200.640141.7.064040.00
8.0   13.0 27.5 49.0 57.5 92.001.5   1.0   0.0   25.   100. 35.800.640193.5.096040.00
9.5   17.   34.5 62.5 87.0 119.03.0   1.0   0.0   25.   100. 18.800.640150.0.096040.00
9.5   15.5 30.5 52.0 68.5 86.003.0   0.8   0.0   15.   100. 18.201.020146.2.192040.00
7.5   13.5 29.5 52.5 74.   102.03.0   1.0   0.0   15.   100. 16.801.020126.3.192040.00
7.0   13.   29.5 60.0 92.0 142.03.0   1.5   0.0   15.   100. 27.402.040188.0.384040.00
6.0   11.5 32.0 84.0 148.  255.03.0   3.0   0.0   15.   100. 15.302.040144.8.512040.00
4.5   10.0 37.5 125.5250.  468.03.0   6.0   0.0   15.   100. 8.3002.040166.81.02440.00
7.0   12.0 24.5 42.0 56.5 72.001.5   0.8   0.0   15.   100. 31.301.020173.8.192040.00
6.5   11.0 23.0 42.5 62.0 88.001.5   1.0   0.0   15.   100. 28.401.020150.1.192040.00
5.5   9.0  22.0 48.0 77.0 128.01.5   1.5   0.0   15.   100. 22.501.020148.8.256040.00
4.5   8.0  22.0 65.5 130.0237.01.5   3.0   0.0   15.   100. 26.002.040164.9.512040.00
3.0   6.5  23.   107.  239.  467.01.5   6.0   0.0   15.   100. 13.602.040175.71.02440.00
```

```
6.0   10.5 21.5 39.0 53.0 69.001.0  0.8  0.0   15.  100. 35.700.960182.2.192040.00
5.5   9.5  20.0 39.5 57.0 82.001.0  1.0  0.0   15.  100. 33.000.960160.0.192040.00
5.5   8.5  19.0 42.5 72.0 120.01.0  1.5  0.0   15.  100. 26.200.960159.8.256040.00
4.5   7.0  16.5 56.5 121. 233.01.0  3.0  0.0   15.  100. 17.001.020176.0.512040.00
5.0   9.0  20.0 37.0 52.0 68.000.8  0.8  0.0   15.  100. 39.300.960187.2.192040.00
5.0   8.0  18.0 37.0 55.0 80.000.8  1.0  0.0   15.  100. 35.500.960162.0.192040.00
4.5   7.5  16.5 39.5 69.0 120.00.8  1.5  0.0   15.  100. 28.000.960162.0.256040.00
4.5   6.5  14.5 53.0 117. 229.00.8  3.0  0.0   15.  100. 21.601.280180.0.512040.00
4.5   7.5  15.5 28.5 39.5 52.000.8  0.8  0.0   15.  75.  37.000.960187.2.256040.00
4.5   6.5  14.5 28.5 42.0 61.000.8  1.0  0.0   15.  75.0 32.200.960163.8.256040.00
4.5   6.5  13.5 30.0052.5 90.000.8  1.5  0.0   15.  75.  23.300.960181.5.384040.00
3.5   5.0  12.0 40.5 90.0 173.00.8  3.0  0.0   15.  75.  17.501.280199.0.768040.00
5.0   8.5  17.0 30.0 40.0 52.501.0  0.8  0.0   15.  75.  34.300.960180.0.256040.00
4.0   7.5  16.0 30.0 44.0 64.001.0  1.0  0.0   15.  75.  29.900.960155.0.256040.00
3.5   6.5  15.0 32.5 55.5 92.001.0  1.5  0.0   15.  75.  20.700.960172.7.384040.00
5.5   9.0  19.0 33.0 44.5 57.001.5  0.8  0.0   15.  75.  30.001.020166.0.256040.00
5.0   9.0  19.5 35.0 49.0 68.001.5  1.0  0.0   15.  75.  25.201.020142.6.256040.00
4.5   8.0  18.0 38.5 60.5 99.001.5  1.5  0.0   15.  75.  20.301.020159.7.384040.00
6.5   11.5 24.5 40.5 54.5 65.503.0  0.8  0.0   15.  75.  34.302.040200.0.384040.00
6.5   11.5 24.0 45.0 63.0 87.003.0  1.0  0.0   15.  75.  29.202.040165.8.384040.00
6.5   10.5 25.5 52.5 79.0 119.03.0  1.5  0.0   15.  75.  21.002.040165.8.512040.00
3.5   11.0 30.0 73.5 124. 209.03.0  3.0  0.0   15.  75.  11.502.040146.2.768040.00
 122362 1704 0055 04  INCREMENT=10 (AN EXAMPLE OF A COMPLETE DATA SET) 0126
KON/0055     22.7      111142.    1122000              300
  1.6    0    0    1   10    8   22    1    1   24   198   10  .2 10.     .04
111111111111111        11
      (12F5.0)
  122362 1704 0055 04  CALIBRATION PULSE OF SEISMO DATA NUMBER 0126
  41.  80. 170. 346. 557. 896. 11.2 .096 .08 942.                       0126   2
 5000 5001 5010 5011 5007 5005 5029 5032 4998 5000 5015 5015            01260001
 5013 5013 5040 5058 5052 5040 5029 5045 5053 5044 5027 5060            01260002
 5061 5047 5049 5048 5056 5032 5045 5037 4995 4989 5001 4966            01260003
 4934 4970 4985 4948 4955 4929 4956 4964 4944 4962 4981 4988            01260004
 5015 5046 5071 5085 5078 5076 5077 5082 5101 5106 5088 5085            01260005
 5064 5029 5020 4991 4970 4957 4936 4950 4955 4915 4959 4980            01260006
 4980 5002 5036 5069 5081 5073 5086 5135 5106 5072 5100 5096            01260007
 5066 5002 4978 4956 4931 4912 4890 4926 4936 4931 4991 5025            01260008
 5047 5064 5071 5100 5115 5129 5101 5072 5051 5032 5025 4986            01260009
 4937 4925 4956 4946 4929 4968 4990 5003 5040 5075 5105 5125            01260010
 5128 5094 5087 5058 5034 5001 4958 4938 4920 4918 4922 4936            01260011
 4993 5042 5049 5058 5085 5127 5132 5115 5091 5054 5036 4994            01260012
 4962 4946 4942 4925 4905 4992 5032 5029 5070 5095 5142 5140            01260013
 5089 5054 5032 5029 4995 4926 4920 4966 4959 4957 5036 5100            01260014
 5095 5062 5100 5107 5085 5040 4991 4985 4992 4961 4921 4973            01260015
 4980 4992 5029 5082 5085 5105 5135 5130 5087 5006 4974 4910            01260016
 4860 4824 4916 5021 5086 5124 5187 5215 5181 5107 5005 4936            01260017
 4856 4775 4828 4892 4988 5138 5315 5287 5162 5006 4960 4991            01260018
 4967 4866 4836 4896 4953 5062 5190 5187 5070 5121 5226 5140            01260019
 4992 4785 4600 4838 5225 5389 5362 5220 4986 4887 4895 4934            01260020
 4953 4984 5038 5083 5101 5112 5138 5132 5062 4955 4920 4996            01260021
 5008 5058 5078 5067 5058 5056 5062 5056 5047 5031 4958 4995            01260022
 5055 5054 4966 5011 5109 5103 5051 5026 5033 4992 4932 4962            01260023
 4996 5029 5057 5060 5049 5048 5042 5002 4956 4985 4987 4958            01260024
 5032 5057 5035 5060 5027 5020 5013 4981 4977 4978 4986 5000            01260025
```

REFERENCES

1. A Dziewonski, S Bloch and M Landisman: "A Technique for the Analysis of Transient Seismic Signals". BSSA, 59, 1, 427-444 (February 1969)

2. H H Inston, P D Marshall and C Blamey: "Optimisation of Filter Bandwidth in Spectral Analysis of Wavetrains". Geophys J Roy Astr Soc, 23, 243-250 (1971)

3. J B Young and A Douglas: "Map, Time Series and other Plotting Routines for Use with the Stromberg-Carlson 4020 Plotter". AWRE Report 041/68 (1968)

4. L D Enochson and R K Otnes: "Programming and Analysis for Digital Time Series Data". The Shock and Vibration Information Centre, United States Department of Defense (1968)

5. D W McCowan: "Finite Fourier Transform Theory and its Application to the Computation of Convolutions, Correlations and Spectra". Earth Sciences Division, Teledyne Industries Inc, Alexandria, Virginia. Memorandum No 8-66 (1966)

6. R Bracewell: "The Fourier Transform and its Applications". McGraw-Hill (1965)

7. J E W Kuye: "The Effect of Frequency Tapers on the Transfer Function of the Band Pass Filter". In preparation

8. A J Espinosa, J H Sutton and H J Miller: "A Transient Technique for Seismograph Calibration - Manual and Standard Set of Theoretical Transient Responses". Vesiac Special Report No 4410-106-X (October 1965)

The Source-Layering Function of Underground Explosions and Earthquakes—An Application of a 'Common Path' Method

P. D. Marshall and R. W. Burton

REPRINTED FROM

Geophys. J. R. astr. Soc. (1971) 24, 533–537

PUBLISHED BY

BLACKWELL SCIENTIFIC PUBLICATIONS

OXFORD AND EDINBURGH

PRINTED IN ENGLAND BY

C. F. HODGSON & SON LTD., LONDON

Geophys. J. R. astr. Soc. (1971) **24**, 533–537.

Letter to the Editors

The Source-Layering Function of Underground Explosions and Earthquakes—an Application of a 'Common Path' Method

P. D. Marshall and P. W. Burton

(Received 1971 August 10)

The vertical component of surface motion, $R(\omega)$, created by a Rayleigh wave in a layered medium, at a point distant r from a source, is given by the expression:

$$R(\omega) = \frac{\mathrm{K}}{r^{\frac{1}{2}}} \,.\, L(\omega, d) * I(\omega) * A(\omega) * S(\omega)$$

where K is a constant and $L(\omega, d)$, $I(\omega)$ and $S(\omega)$ represent the amplitude response of the layered medium as a function of frequency and source depth d. the amplitude response of the instrument, the absorption term and the source spectral function respectively. The Rayleigh wave amplitude $R(\omega)$ is expressed in the angular frequency domain (Toksöz, Ben-Menahem & Harkrider 1964).

For a closed system comprising a single epicentre, path and recording station:

$$\frac{S(\omega) * L(\omega, d)}{R(\omega)} = \frac{r^{\frac{1}{2}}}{\mathrm{K}.I(\omega) * A(\omega)} = \alpha(\omega)$$

is a function of frequency only, and constant at a given frequency; $\alpha(\omega)$ is a characteristic of the system and independent of the source. Any two events which occur at the same epicentre have a common path parameter $\alpha(\omega)$ and therefore are related by the expression

$$\frac{S_1(\omega) * L_1(\omega, d)}{R_1(\omega)} = \frac{S_2(\omega) * L_2(\omega, d)}{R_2(\omega)}. \qquad (1)$$

The terms $R_1(\omega)$ and $R_2(\omega)$ can be obtained by Fourier analysis of the Rayleigh wave trains. This gives a means of relating the spectral source-layering functions $S(\omega) * L(\omega, d)$ for two events; the terms for absorption, scattering and lateral refraction along the path and the instrument are eliminated.

It is usually difficult to assess the source-layering term. This paper suggests the comparison of a known with an unknown source, by means of the common path method to solve the problem.

The source spectrum for atmospheric explosions has been published by Carpenter & Marshall (1970) using data from the large explosions fired over Novaya Zemlya in 1962. Since 1964 large underground explosions have taken place very close to these epicentres. Rewriting relation (1) for these two types of event leads to:

$$S_u(\omega) * L_u(\omega, d) = \frac{R_u(\omega) * S_A(\omega) * L_A(\omega, 0)}{R_A(\omega)}. \qquad (2)$$

DURHAM UNIVERSITY SCIENCE 31 MAY 1973 SECTION

7

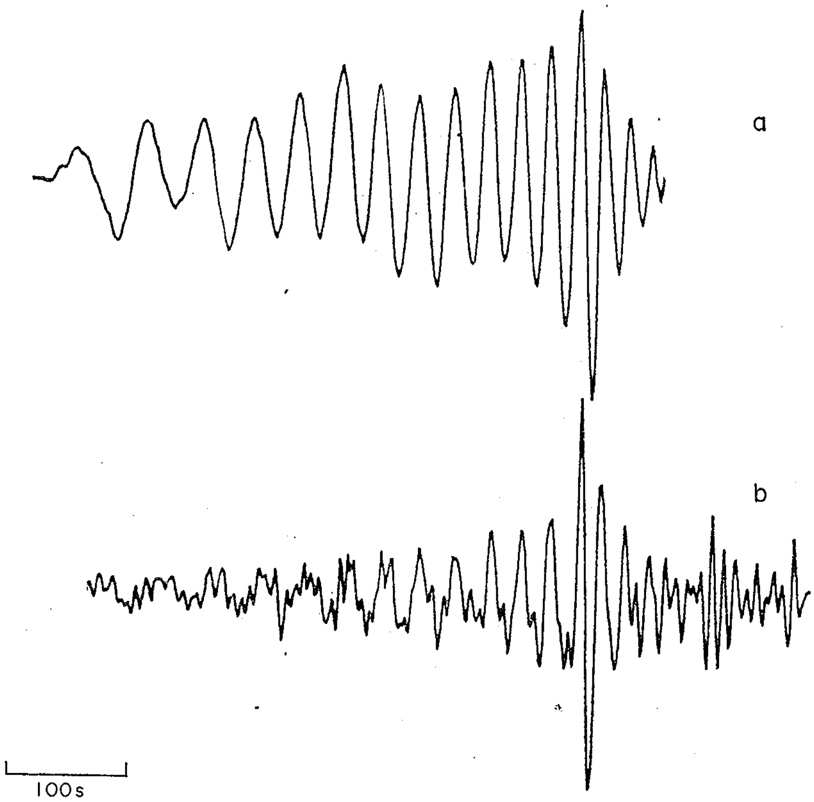

FIG. 1. Recordings at Quetta of (a) Atmospheric and (b) Underground explosions at Novaya Zemlya.

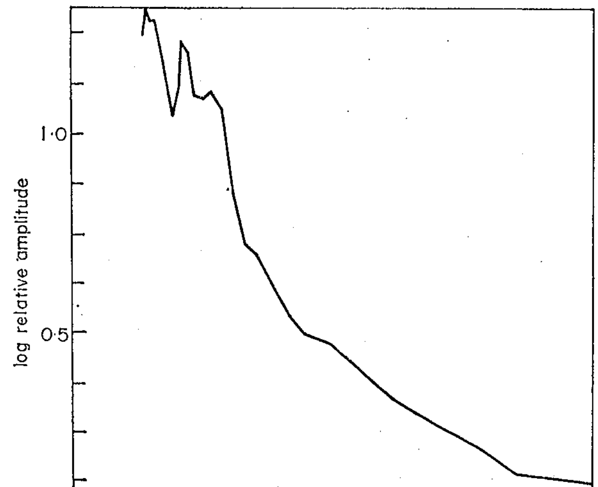

FIG. 2. The log source-layering function of an underground explosion (from the Quetta records).

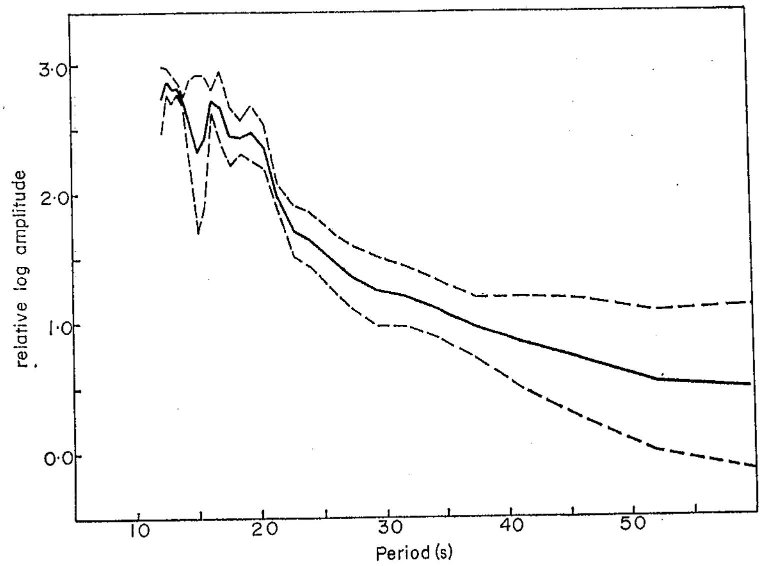

FIG. 3. The mean and one standard deviation variation of the log source-layering function of an underground explosion (from the summation of three sets of records).

The term $L_A(\omega, 0)$ can be considered as constant because it is a slowly varying function of ω in the range of interest (Carpenter & Marshall 1970). Rayleigh waves from two explosions at Novaya Zemlya and recorded at Quetta, Pakistan, were analysed (Fig. 1(a) and (b)) and their Fourier spectra obtained.

Atmospheric explosion:	27.9.62	0803 GMT	$h \simeq 0$ km
	74.3° N	52·4° E	
Underground explosion:	27.10.66	0558 GMT	$h \simeq 0$ km
	73·4° N	54·9° E.	

The spectral source-layering function (illustrated in Fig. 2) for this underground explosion was calculated for a set of discrete frequency points by substitution into equation (2) at each frequency point. The perturbations at the higher frequencies are probably due to differences in the background noise levels. There is more noise on the underground explosion record than on the atmospheric explosion record (Fig. 1(a) and (b)); ideally the signal-to-noise ratio would be the same for each seismogram.

Perturbations due to noise were reduced by the similar analysis of records from Albuquerque and Istanbul and then summing the individual spectra, the summed spectrum obtained is shown in Fig. 3. This process is valid for explosive sources because they are radially symmetric. The inclusion of one standard deviation from the mean in Fig. 3 illustrates the variation of the spectra which make up the average spectral values. The variation is reasonable although only a few records were analysed.

The ' Common Path ' method can be extended to earthquake investigation by using this known source-layering function. The assumption is that $L_u(\omega, d)$ does not vary significantly over many regions of the world because explosions are shallow events, and $L_u(\omega, d)$ depends mainly on gross crustal features. The large differences in crustal thickness between Kazakh S.S.R. and Nevada U.S.A. cause observable differences in $S_u(\omega) * L_u(\omega, d)$ (see Fig. 4, Marshall 1970). However, $S_u(\omega) * L_u(\omega, d)$ estimated in a region of normal crustal thickness may be applied in a region of similar crustal thickness.

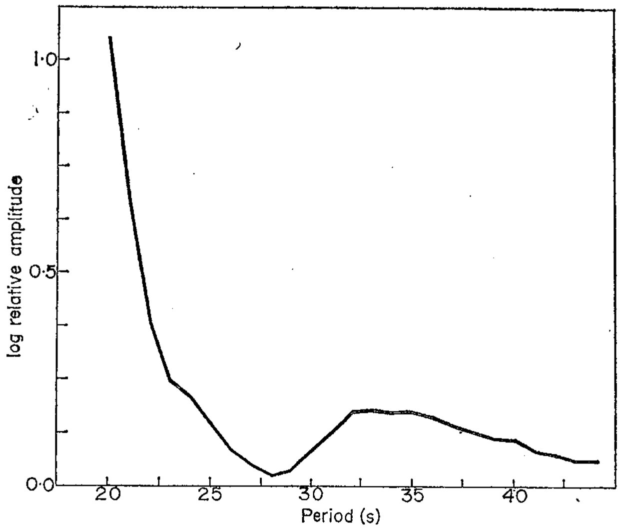

FIG. 4. The log source-layering function of an earthquake (from Milrow records).

The Rayleigh waves from an underground explosion and an earthquake which occurred in the same epicentral region were used to calculate the earthquake source-layering function:

$$S_E(\omega) * L_E(\omega, d) = \frac{S_u(\omega) * L_u(\omega, d) * R_E(\omega)}{R_u(\omega)} = R_E(\omega) * \alpha^1(\omega).$$

The events selected were:

Underground explosion:	2.10.69	2206 GMT	$h \simeq 0$ km
(MILROW)	57·4° N	179·2° E	
Earthquake:	18.9.69 52·5° N	0844 GMT 173·5° E.	$h \simeq 24$ km

and the resultant spectrum of the earthquake is shown in Fig. 4. The summation of several spectra cannot be applied to earthquakes because the source is radially asymmetric. This necessarily implies a study of the variation with azimuth.

As anticipated by other studies (SIPRI 1968; Marshall 1970) the source layering functions for the earthquake and explosion are significantly different, particularly at the longer periods. No further interpretation of the earthquake spectrum is attempted here except to say that the minimum at $T \simeq 28$ s in the earthquake spectrum is associated with the depth of the source (Douglas, Hudson & Kembhavi 1970).

To proceed further with the present analysis and obtain $S_u(\omega)$ we must eliminate $L_u(\omega, d)$. This can be done when the crustal structure is known in the region of Novaya Zemlya.

*U.K.A.E.A.,
Blacknest,
Brimpton,
Reading RG7 4RS*

*Department of Geology,
University of Durham,
Durham City,
Durham.*

References

Toksöz, M. N., Ben-Menahem, A. & Harkrider, D. G., 1964. Determination of source parameters by amplitude equilisation of seismic surface waves 1. Underground nuclear explosions, *J. geophys. Res.*, **69**, 4355–4366.

Carpenter, E. W. & Marshall, P. D., 1970. A.W.R.E. Report 0–88/70, H.M.S.O. *Surface waves generated by atmospheric nuclear explosions.*

SIPRI 1968. *Seismic methods for monitoring underground explosions*, Stockholm 1968, Rapporteur Dr. D. Davies.

Marshall, P. D., 1970. Aspects of the spectral differences between earthquakes and underground explosions, *Geophys. J. R. astr. Soc.*, **20**, 397–416.

Douglas, A., Hudson, J. A. & Kembhavi, V. K., 1970. The analysis of surface wave spectra using a reciprocity theorem for surface waves, *Geophys. J. R. astr. Soc.*, **23**, 207.

DURHAM UNIVERSITY
SCIENCE
31 MAY 1973
SECTION
LIBRARY

10 Anderson, D. L., Ben-Menahem, A., and Archambeau, C. B., *J. Geophys. Res.*, **70**, 6, 1441 (1965).
11 Anderson, D. L., and Archambeau, C. B., *J. Geophys. Res.*, **69**, 10, 2071 (1964).
12 Tsai, Y., and Aki, K., *BSSA*, **59**, 1275 (1969).
13 Backus, and Gilbert, *Phil. Trans.*, **266**, 123 (1970).
14 Solomon, S. C., Ward, R. W., and Toksoz, M. N., MIT, *Woods Hole Conference on Seismic Discrimination*, Mass. Inst. Tech., **1**, 71 (1971).

Printed in Great Britain by Flarepath Printers Ltd., St. Albans, Herts.

(*Reprinted from Nature Physical Science, Vol.* 238, *No.* 84, *pp.* 87–90, *August* 7, 1972)

Upper Mantle Zone of Low *Q*

SEISMOLOGISTS have great interest at present in delineating laterally varying properties of the upper mantle[1]. A quantity which is of great significance in this respect is the quality factor, Q, and the contrasting Q across the Benioff zones[2] and its many tectonic implications[3] have been discussed. Q is difficult to measure with reasonable accuracy, and even when this has been accomplished the inversion of Q obtained from surface waves into a depth distribution is difficult. However, the "Hedgehog" inversion technique[4,5] has greatly helped us to interpret some data of this type.

The specific attenuation factors, Q_γ^{-1}, were estimated as functions of frequency by one of us (P. W. B.), for teleseismic Rayleigh waves from a large nuclear explosion[6]. With the help of Hedgehog we show that these data are consistent with a region of low Q at the depth, about 120 km, of the Gutenberg low velocity zone.

Table 1 World Wide Standard Seismograph Network Recordings of the Event at Novaya Zemlya (73.6° N, 57.5° E) on December 24, 1962 (GMT: 11-11-42.0)

Addis Ababa	AAE	Godhavn	GOH	Madison	MDS
Albuquerque	ALQ	Golden	GOL	Quetta	QUE
Bermuda	BEC	Istanbul	IST	Toledo	TOL
Balboa Heights	BHP	Kongsberg	KON	Trinidad	TRN
Berkeley	BKS	Lahore	LAH	Valencia	VAL
Blacksburg	BLA	Longmire	LON	Windhoek	WIN
Caracas	CAR	La Palma	LPS		
Copenhagen	COP	Malaga	MAL		

The explosion used was the atmospheric nuclear test of about 20 Mtons[7] conducted at Novaya Zemlya on December 24, 1962. A spectral and dispersive analysis of the Rayleigh surface waves it generated was performed for the station recordings listed in Table 1. The records were digitized, Fourier analysed[8] and corrected for instrumental effects to yield spectral amplitude content. Group velocities were determined by using a multiple filtering technique similar to the method of Dziewonski *et al.*[9]. The radiation pattern from such an event was assumed to be circular for all frequencies of interest.

DURHAM UNIVERSITY SCIENCE 31 MAY 1973 SECTION

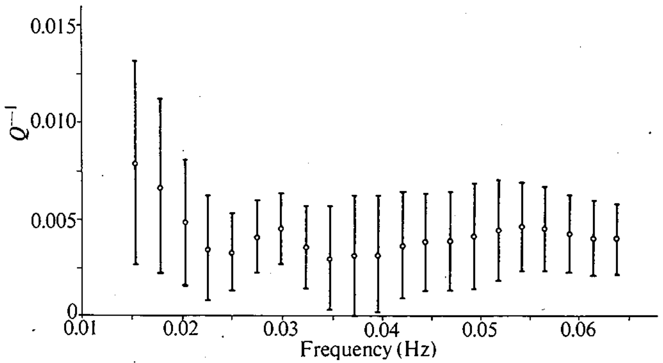

Fig. 1 Observational Q_γ^{-1} data for Rayleigh waves.

Values of Q_γ^{-1} were then obtained from the logarithmic form of the amplitude equation for a recording site

$$A = C(E\sin\Delta)^{-1/2}\, e^{-\left(\frac{\pi E \Delta f}{Q_\gamma U}\right)}$$

A = spectral amplitude (μs) at frequency f (Hz)
U = group velocity (km/s)
E = radius of the Earth
Δ = angular distance between epicentre and recording site
C = a constant.

Least squares values of Q_γ^{-1} for the frequency range 0.015–0.065 Hz (periods 65–15 s) and their 95% confidence limits are shown in Fig. 1.

Table 2 Velocity-Depth Model Assumed

P-wave velocity km s^{-1}	S-wave velocity km s^{-1}	Density g cm^{-3}	Thickness of layer km	$Q_{\alpha J}/Q_{\beta J}$
6.10	3.5	2.7	14.0	2.29
6.50	3.72	2.9	22.0	2.29
8.06	4.40	3.33	22.0	2.51
8.08	4.46	3.345	10.0	2.51
8.121	4.45	3.375	55.0	2.51
8.50	4.96	3.64	—	2.19

A velocity-depth model must be assumed to invert the Rayleigh wave $Q_\gamma(f)$ data into a variation with depth of Q_α, the Q for compressional waves, and Q_β, the Q for shear waves. Most of the propagation paths specified by Table 1 are of continental type, so that the simple, six layer, continental type, velocity-

the other for high frequencies. Our data do not show such a peak (although this does not exclude its possible existence within the 95% confidence limits). So we have been able to interpret our data with a frequency independent Q model, and have no reason to resort to any frequency dependence in our frequency interval.

Models of type II (Fig. 3), that is, moderate Q throughout the crust and uppermost mantle, do not seem to have been proposed before, but certainly cannot be eliminated by the present data. The difference between our interpretation and that of other authors is probably due to lateral variations of Q within the upper mantle for the different epicentral regions and propagation paths investigated. In using our data we did not assume the presence of a low velocity layer, yet all of our types of models show a low Q zone at depths below 70 kms, in an otherwise higher Q environment. This is in good agreement with Tsai and Aki, who assumed a Gutenberg-type continental Earth, and is further evidence for a zone of low Q, coinciding with this low velocity zone.

We thank V. P. Valus, Institute of Physics of the Earth, Moscow, for explaining the "Hedgehog" inversion technique and for the special programmes which he developed. The NERC provided the grant for Dr Valus's visit to Cambridge. B. L. N. K. thanks the British Petroleum Company for a research studentship.

P. W. Burton

UKAEA,
Blacknest, Brimpton,
Reading RG7 4RS,
and Department of Geology,
University of Durham

B. L. N. Kennett

Department of Applied Mathematics
and Theoretical Physics,
University of Cambridge,
Silver Street, Cambridge

Received June 29, 1972.

1. *Nature*, **236**, 259 (1972).
2. Barazangi, M., Isacks, B., and Oliver, J., *J. Geophys. Res.*, **77**, 5, 952 (1972).
3. Utsu, T., *Rev. Geophys. Space Phys.*, **9**, 4, 839 (1971).
4. Valus, V. P., *Vichislitelnaya Seismologiya*, **4**, 1 (1968).
5. Keilis-Borok, V. I., in *Proc. Fiftieth Enrico Fermi Summer School*, Varenna, 1969 (Academic Press, London, 1972).
6. Burton, P. W., thesis (University of Durham).
7. *Vela Uniform Periodic Information Digest Insert*, **3**, 1 (1963).
8. McCowan, D. W., *Earth Sci. Divis.*, Teledyne Industries Inc., Alexandria, Virginia, Memorandum No. 8–66 (1966).
9. Dziewonski, A., Bloch, S., and Landisman, M., *BSSA*, **59**, 427 (1969).

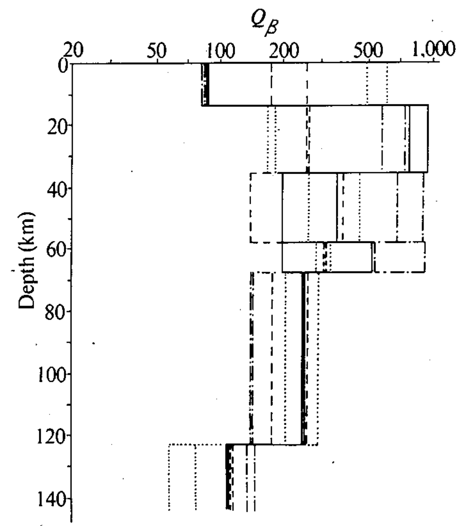

Fig. 3 Four types of inversion models. Model I, ═ : model II, ═ ═ ═; model III, : : : : : : model IV, ═ : ═ :.

indicative of lateral variations of Q between regions in the upper mantle[14].

The Rayleigh wave Q observed by Tsai and Aki shows a prominent peak at about 25 s period. To interpret this feature they required a Q model with a simple frequency dependence; they effectively combined two depth models, one for low and

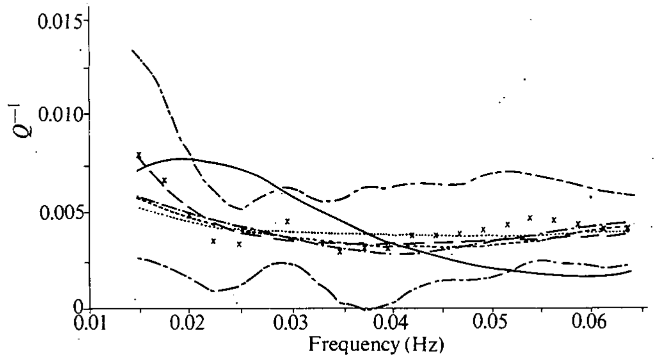

Fig. 4 Comparison between models and observations. ——, Anderson model; - - -, model 1; · · ·, model 2; — — —, model 3; — · — ·, model 4; x x x x, observed data with confidence limits.

depth model of Table 2 was chosen.

The Hedgehog inversion technique[4,5] was used to search for Q models consistent with the experimental data. Any N-layered model of the Earth's anelasticity may be specified by $2N$ parameters Q_j corresponding to the Qs in the individual layers $Q_{\alpha 1} \ldots Q_{\alpha N}$ and $Q_{\beta 1} \ldots Q_{\beta N}$. We define a region of search in the parameter space by requiring the Q_j to be positive and also imposing reasonable upper limits on their values. This search region is divided into a $2N$-dimensional network, with mesh lengths δQ_j^n between the nodal parameter values.

To start our search for suitable models we use the Monte-Carlo technique to generate a set $\{Q_j\}$ of values of the parameters. For each $\{Q_j\}$ a function $Q_\gamma(f_i)$ is calculated and compared with the observed value $Q_{\gamma 0}(f_i)$. The theoretical values for Rayleigh wave Q_γ are determined using Anderson's formula[10]. The observed values $Q_{\gamma 0}$ are obtained as a discrete function of frequency, $Q_{\gamma 0}(f_i)$ for M frequencies $f_1 \ldots f_m$.

We search for those regions where the match between $Q_\gamma(f_i)$ and $Q_{\gamma 0}(f_i)$ is good; that is, we require for the M frequencies considered, setting $Q_{\gamma i} = Q_\gamma(f_i)$, $Q_{\gamma 0i} = Q_{\gamma 0}(f_i)$

$$\left| \frac{Q_{\gamma i} - Q_{\gamma 0i}}{\Delta Q_{\gamma 0i}} \right| < a \qquad i = 1, \ldots, M \qquad (1)$$

$$\left[\frac{1}{M} \sum_{i=1}^{M} \left(\frac{Q_{\gamma i} - Q_{\gamma 0i}}{\Delta Q_{\gamma 0i}} \right)^2 \right]^{1/2} < \sigma$$

where $\Delta Q_{\gamma 0i}$ is a measure of the error in the observed measurement $Q_{\gamma 0i}$, and a, σ are precision measures on the fit.

Once we have found a good set of values $\{Q_j\}$ we move to the nearest node $\{Q_j^n\}$ on the network spanning the search region and test this against inequality (1). If these equations are satisfied we test the adjacent nodes $\{Q_j^n + \delta Q_j^n\}$ and continue until we have determined a connected region of acceptable Q models in the parameter space surrounded by nodes for which inequality (1) is no longer satisfied. Otherwise we return to the Monte-Carlo technique. Once a good region has been found we again invoke the Monte-Carlo technique and try to find another solution of inequality (1) outside this initial region. Thereafter the process is repeated until the region of search has been exhausted.

If independent values of Q_α and Q_β were attributed to each layer then we would be searching in a twelve-dimensional space. To reduce the region of search we made the assumption that there are no losses attributable to a bulk modulus[10], which leads to

$$Q_{\alpha j} = 3/4 \left(\frac{\alpha_j}{\beta_j} \right)^2 Q_{\beta j} \quad j = 1 \ldots 6$$

reducing the Hedgehog regional search to a six-dimensional parameter space. For a Poisson solid ($\alpha=\sqrt{3}\beta$) $Q_\alpha=2.25\ Q_\beta$, but for our velocity depth model the ratio $Q_{\alpha j}/Q_{\beta j}$ varies and is given in Table 2.

Postulated models were accepted if they fitted within the 75% confidence limits at all periods. Consistency was confirmed by repeating the search, but varying the mesh. The chosen region of search is shown in Fig. 2; Hedgehog yields two adequate solutions to the observed data—indicated by shading—but makes no geophysical distinction between them. Also shown are further good points but not connected regions found by the

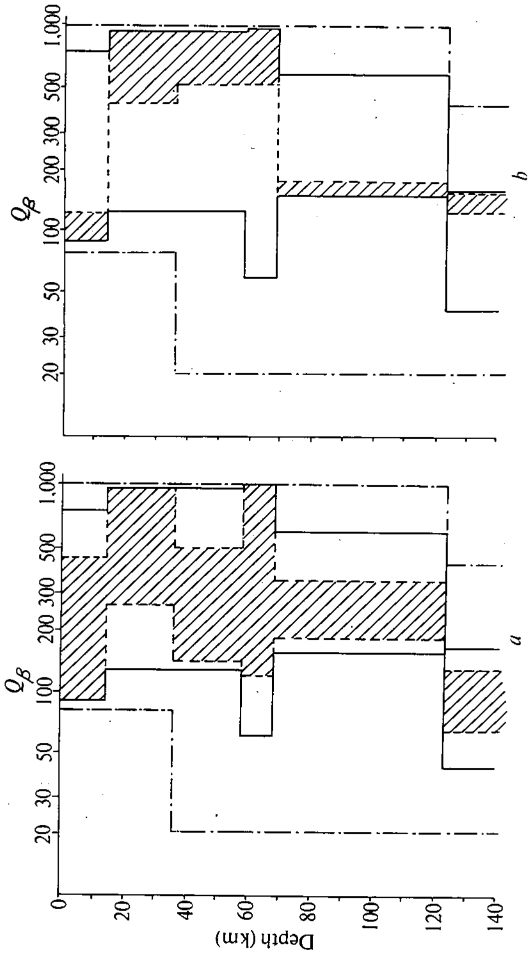

Fig. 2 *a* and *b*, Alternative Hedgehog solutions for attenuation data. Region of search; Monte-Carlo solutions; Hedgehog solutions.

Monte-Carlo technique.

The models fitting the data fall into four broad classes and examples of these are illustrated in Fig. 3. All the models obtained show a low Q zone in the upper mantle. In most cases this lies around and below a depth of 120 km. This low Q zone corresponds to the Gutenberg low velocity zone, but note that the Gutenberg low velocity zone was not assumed to exist during model fitting. The remaining models show low Q below about 70 km which tends to decrease slightly further below 120 km. This low Q zone is at a depth corresponding to the low velocity zone in tectonic regions of the continents. The range of models found probably reflects lateral variations in Q on the paths to the recording stations as well as the non-uniqueness of the inversion process.

Table 3 A Few Q-Depth Models

Layer	Anderson type model Q_α	Anderson type model Q_β	Model 1 Q_β	Model 2 Q_β	Model 3 Q_β	Model 4 Q_β
1	1,000	440	90	180	610	90
2	1,600	700	790	260	180	790
3	1,400	560	500	260	260	680
4	180	70	220	120	340	840
5	180	70	180	260	290	140
6	400	180	115	115	55	125

The Anderson type model has a low Q zone at about 50 km, and Q_α, Q_β are listed. Our models only list Q_β because this determines Q_α.

Table 3 lists four models representative of the classes found and an Anderson type Q model with a low Q zone at about 50 km. Theoretical values of Rayleigh wave Q for these models are shown in Fig. 4 along with the original observational data. Note that none of our models shows the low Q zone in the depth region 50–120 km with increasing Q below 120 km, found by Anderson[10,11]. Using short period Rayleigh waves, as in this report (15–65 s), Tsai and Aki found the Anderson model MM8 (ref. 10) to be unsatisfactory because it did not agree with their observed frequency dependence for Q[12]. More recently Backus and Gilbert found that their results did not establish a low Q zone in the upper mantle[13]. However, Anderson *et al.*[10] used two earthquakes, in Chile and Iran respectively, as their data source. Tsai and Aki used one earthquake in California while Backus and Gilbert used free oscillation studies. This study uses a source in Novaya Zemlya and continental paths—"a continental Q". These differences in the type, and more importantly the region, of the data source may lead to variations between the models. Such differences are observed and this is